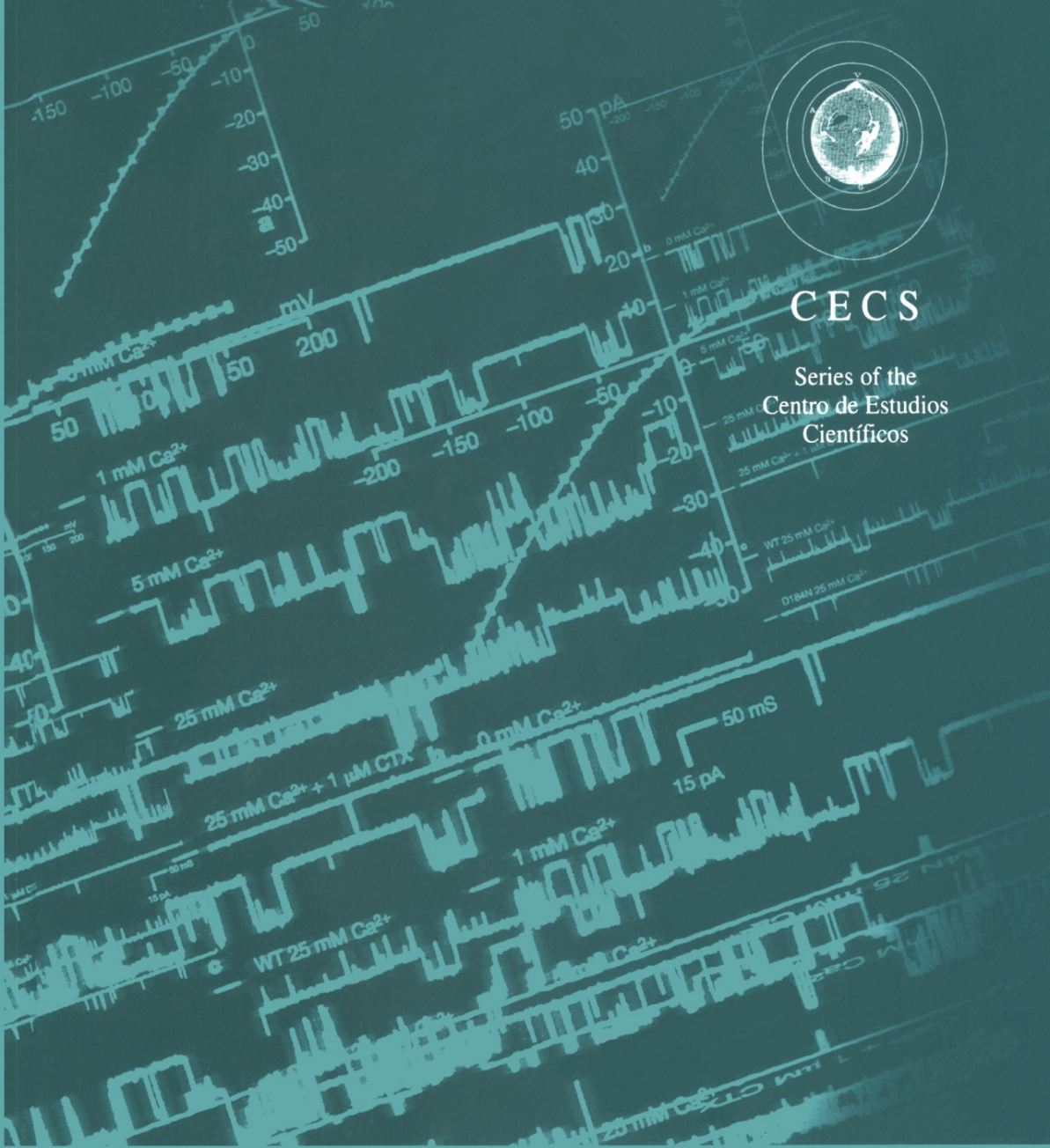


CECS

Series of the
Centro de Estudios
Científicos



PUMPS, TRANSPORTERS, AND ION CHANNELS

Studies on Their Structure,
Function, and Cell Biology

Edited by

Francisco V. Sepulveda and Francisco Bezanilla

**PUMPS, TRANSPORTERS,
AND ION CHANNELS**

Series of the Centro de Estudios Científicos

Series Editor: Claudio Teitelboim
Centro de Estudios Científicos
Valdivia, Chile

BLACK HOLES AND THE STRUCTURE OF THE UNIVERSE 2000
Edited by Claudio Teitelboim and Jorge Zanelli, World Scientific

THE BLACK HOLE 25 YEARS AFTER 1998
Edited by Claudio Teitelboim and Jorge Zanelli, World Scientific

FROM ION CHANNELS TO CELL-TO-CELL CONVERSATIONS 1997
Edited by Ramón Latorre

IONIC CHANNELS IN CELLS AND MODEL SYSTEMS 1986
Edited by Ramón Latorre

JOAQUIN LUCO: Dos Historias de Una Vida 1991
Ana Tironi and Pedro Labarca, Ediciones Pedagógicas Chilenas S.A.

LECTURES ON QUANTUM GRACITY 2004
Edited by Andrés Gomboroff and Donald Marolf

PHYSICAL PROPERTIES OF BIOLOGICAL MEMBRANES AND THEIR FUNCTIONAL
IMPLICATIONS 1988
Edited by Cecilia Hidalgo

PRINCIPLES OF STRING THEORY 1988
Lars Brink and Marc Henneaux

PUMPS, TRANSPORTERS, AND ION CHANNELS: Studies on Their Structure, Function, and Cell
Biology 2005
Edited by Francisco V. Sepúlveda and Francisco Bezanilla

QUANTIZATION OF GAUGE SYSTEMS 1992
Marc Henneaux and Claudio Teitelboim, Princeton University Press

QUANTUM MECHANICS OF FUNDAMENTAL SYSTEMS 1 1988
Edited by Claudio Teitelboim

QUANTUM MECHANICS OF FUNDAMENTAL SYSTEMS 2 1989
Edited by Claudio Teitelboim and Jorge Zanelli

QUANTUM MECHANICS OF FUNDAMENTAL SYSTEMS 3 1992
Edited by Claudio Teitelboim and Jorge Zanelli

THE PATAGONIAN ICEFIELDS: A Unique Natural Laboratory for Environmental and Climate Change
Studies 2002
Edited by Gino Casassa, Francisco V. Sepúlveda, and Rolf M. Sinclair

PHYSICAL PROPERTIES OF BIOLOGICAL MEMBRANES AND THEIR FUNCTIONAL
IMPLICATIONS 1986
Edited by Cecilia Hidalgo

PRINCIPLES OF STRING THEORY 1988
Lars Brink and Marc Henneaux

TRANSDUCTION IN BIOLOGICAL SYSTEMS 1990
Edited by Cecilia Hidalgo, Juan Bacigalupo, Enrique Jaimovich, and Julio Vergara

PUMPS, TRANSPORTERS, AND ION CHANNELS

Studies on Their Structure, Function, and Cell Biology

Edited by

Francisco V. Sepúlveda

*Centro de Estudios Científicos (CECS)
Valdivia, Chile*

and

Francisco Bezanilla

*David Geffen School of Medicine at UCLA
Los Angeles, California*

Kluwer Academic / Plenum Publishers
New York, Boston, Dordrecht, London, Moscow

ISSN: 1571-571X

ISBN: 0-306-48659-8; ISBN E-book: 0-306-48660-1

Centro de Estudios Científicos (CECS) series

Proceedings from the Symposium "Epithelia, pumps, transporters and ion channels: Structure and function at 60," held December, 2001, at the Centro de Estudios Científicos, Valdivia, Chile.

©2005 Kluwer Academic/Plenum Publishers, New York

All rights reserved. This work may not be translated or copied in whole or in part without the written permission of the publisher (Kluwer Academic/Plenum Publishers, 233 Spring Street, New York, NY 10013, USA), except for brief excerpts in connection with reviews or scholarly analysis. Use in connection with any form of information storage and retrieval, electronic adaptation, computer software, or by similar or dissimilar methodology now known or hereafter developed is forbidden.

The use in this publication of trade names, trademarks, service marks and similar terms, even if they are not identified as such, is not to be taken as an expression of opinion as to whether or not they are subject to proprietary rights.

Printed in the United States of America.

9 8 7 6 5 4 3 2 1

SPIN 11302995

springeronline.com

FOREWORD

This book is a compilation of articles based on some of the talks given at the Centro de Estudios Científicos (CECS) in Valdivia during the course of a celebration to mark the 60th birthdays of Ramón Latorre and Enrico Stefani.

Ramón Latorre is one of the most outstanding figures in channel Biophysics today. The first surprise is that he trained as a Biochemist! He soon, however, became a biophysicist through his work with Guayo (Eduardo) Rojas who guided him during his Ph.D thesis in the Laboratorio de Fisiología Celular in Montemar. His work at N.I.H with Gerald Eherenstein and Harold Lecar constitutes one of the milestones of single ion channel Biophysics. This classical work, done in planar bilayers, set the basis for understanding voltage-dependent conductances with single channel studies and predates, by many years, later studies using patch clamping techniques.

Ramón was one of the firsts to find and recognize the importance of calcium-activated potassium channels and to begin a detailed study of channel properties. He pioneered the ideas of voltage and calcium modulation of the open probability and he added detailed studies of gating and its modulation by other ions. Ramón is also interested in permeation and selectivity and he produced classical studies on the number of water molecules in the channel and sites occupied by barium. Results and concepts that have recently taken front page as the structure of KcSa has been described. His studies have not been limited to the biophysical aspects of channel function, because Ramón has extended his studies to complex systems and physiological phenomena.

All of those who were present at this meeting/birthday party will know about, and many have taken part in, his numerous scientific contributions in the field of biological membranes and ion channels. What is perhaps less well known, is that after coming back home after several years' exile in the USA, he created with Claudio Teitelboim the Centro de Estudios Científicos. This adds to his scientific work something that, in our view, is a most important contribution of Ramón to his country. This makes him a true patriot, to undertake this task for love to science and country with a unique passion and talent. The Centre was pivotal in the revival of Biophysics and Cell Physiology in Chile and, since 2000, has become a focal point for science growth in Chile with the setting up of new laboratories in the beautiful city of Valdivia.

Enrico Stefani is one of the brightest and most original minds of his generation and he is one of the few that can cut through the formalism and understand basic concepts in a simple fashion.

He is best known for his pioneering work on establishing a framework for the study of calcium channels in skeletal muscle and for his contribution to our understanding of the relationship between those currents and the process of excitation-contraction coupling. He was the first to study the calcium currents of skeletal muscle. In the era of cloned channels he was again the first to describe the gating currents of calcium channels in isolation and correlate them to the ionic conductance. These studies were done with his unequal experimental wizardry using the now established technique of cut-open oocyte that he himself developed. This technique also allowed him to study in detail gating currents of the potassium channel for the first time, to correlate them with ionic currents, develop models and more recently to discover even faster events preceding the main charge movement of gating: the "piquito". The studies on the piquito are unique because they represent the electrical expression of the intimate properties of the charges and their interaction with the microenvironment of the channel molecule. His work is marked by an intellectual breadth uncharacteristic of this technically specialized field. His wider studies on muscle re-innervation, cytoplasmic calcium regulation, and gating currents are recognized as "classic". Thus, recently, he has applied all his biophysical expertise in ion channels to the physiology of tissues such as uterine muscle.

In addition to his outstanding research, Enrico is a very active "citizen of science". He has fostered environments in which research can flourish; in Argentina, where together with Gerschenfeld and Chiarandini he started the field of quantitative membrane physiology; in México, where he placed the cornerstones of modern electrophysiology and attracted NIH and governmental funds in order to provide a unique home for young Mexican scientists; in Chile he has played a fundamental role in keeping our ion channel laboratory competitive worldwide.

The articles presented in this book concern interests of Ramón and Enrico during their careers. They span from considerations as to why bacteria need ion channels in their membranes to fine details of how conformational changes in the protein lead to ion channel opening and closing. The importance of water channels in tissue physiology to the control of excitability by ion channels and pumps. And from the cell biology of ion channel sorting to their failure in disease states.

The book is hereby dedicated to Ramón Latorre and Enrico Stefani, as homage as first class scientists, educators, innovators and, most importantly, best of friends.

ACKNOWLEDGMENTS

This book is the result of a Symposium celebrated at the Centro de Estudios Científicos, Valdivia, Chile, in December 2001. We would like to thank the contributors that decided to write articles based on their talks after the end of the meeting. The reunion itself was made possible through the generous funding of the Iniciativa Científica Milenio (ICM) that supports CECS as a Millenium Science Initiative Institute. The production of the volume was financed by the ICM, the Tinker Foundation, Empresas CMPC of Chile and Fundación Andes.

The editors are grateful to Karen Everett, Ana María Navia, Carolina Momberg and Margarita Cabrera for their help in organizing the meeting and their patient work in editing and compiling the present volume.

CONTENTS

List of Participants xv

CHAPTER 1. CHANNELS AND PUMPS EARLY IN EVOLUTION	1
Clay M. Armstrong	
1. INTRODUCTION	1
2. ION CHANNELS IN BACTERIA	1
3. ANIMAL CELLS	4
3.1 The Osmotic Dilemma	4
3.2 A Cell that is Too Simple	4
3.3 The Solution to the Dilemma	5
3.4 A Thought Experiment on Stopping the Na/K Pump	7
4. CONCLUSIONS	9
5. REFERENCES	10

CHAPTER 2. THE POSSIBLE ROLE OF AQUAPORIN 0 IN LENS PHYSIOLOGY	11
James E. Hall and Karin L. Németh-Cahalan	
1. INTRODUCTION	11
2. REGULATION OF WATER PERMEABILITY AND THE LENS	13
3. SINGLE-MOLECULE WATER PERMEABILITY OF AQP0 AND AQP1	13
4. REGULATION OF AQP0 WATER PERMEABILITY	14
5. CONCLUSIONS	17
6. ACKNOWLEDGMENTS	18
7. REFERENCES	18

CHAPTER 3. CENTRAL ROLE OF THE Ca^{2+}_i REGULATORY SITE IN IONIC AND METABOLIC MODULATION OF Na^+/Ca^{2+} EXCHANGER IN DIALYZED SQUID AXONS	21
Luis Beaugé and Reinaldo DiPolo	
1. INTRODUCTION	21
2. METHODS	23

3. RESULTS AND DISCUSSION	23
4. ACKNOWLEDGMENTS	29
5. REFERENCES	29

CHAPTER 4. CALCIUM DEPENDENCE OF CALCIUM RELEASE CHANNELS (RYANODINE RECEPTORS) FROM SKELETAL AND CARDIAC MUSCLE31

Cecilia Hidalgo, Paulina Donoso and Ricardo Bull

1. INTRODUCTION	31
2. METHODS	32
2.1 Membrane Preparations	32
2.2 Bilayer Experiments.....	33
3. RESULTS AND DISCUSSION	33
3.1 Calcium Dependence of Native Skeletal or Cardiac RyR Channels	33
3.1.1. Native RyR Channels in Bilayers.....	33
3.1.2. Release Experiments with Native RyR Channels	34
3.2 Calcium Dependence of Oxidized Skeletal or cardiac RyR Channels.....	36
3.2.1. Oxidized RyR Channels in Bilayers.....	36
3.2.2. Release Experiments with Oxidized RyR Channels	37
4. CONCLUSIONS	38
5. ACKNOWLEDGMENTS	38
6. REFERENCES	38

CHAPTER FIVE. MODULATION OF RYANODINE RECEPTOR CHANNELS FROM RAT BRAIN CORTEX IN LIPID BILAYERS41

María Isabel Behrens, Juan José Marengo, José Pablo Finkelstein and Ricardo Bull

1. INTRODUCTION	41
2. MATERIALS AND METHODS.....	43
2.1 Membrane Preparation.....	43
2.2 Channel Recording and Analysis.....	43
3. RESULTS AND DISCUSSION	45
3.1 Brain RyR Channels are Activated by Caffeine and Show the Characteristic Response to Ryanodine.....	45
3.2 Calcium Dependence of Native and Oxidized RyR-Channels	46
3.3 Activation by ATP	47
3.4 Effect of cADPR	48
4. CONCLUSIONS	49
5. ACKNOWLEDGMENT.....	50
6. REFERENCES	50

CHAPTER SIX. EXOCYTIC PATHWAY CHECK POINTS FOR FUNCTIONAL POTASSIUM CHANNELS IN THE PLASMA MEMBRANE53

Marcela Bravo-Zehnder

1. INTRODUCTION 53
2. THE EXOCYTIC PATHWAY..... 53
3. POTASSIUM CHANNELS AS SUBSTRATES OF THE EXOCYTIC PATHWAY 55
4. CONCLUDING REMARKS..... 58
5. REFERENCES 59

CHAPTER SEVEN. C-TERMINI REGION SHARED BY β_{2A} , β_{1B} AND β_3 SUBUNITS CONFER PREPULSE FACILITATION TO CARDIAC CALCIUM CHANNELS63

Igor Dzhura, Georgina Guerrero and Alan Neely

1. INTRODUCTION 63
2. METHODS 65
 - 2.1 RNA Synthesis and Preparation of Oocytes..... 65
 - 2.2 Construction fo Chimeras and Deletion Mutants 66
 - 2.3 Recording Techniques..... 66
3. RESULTS 67
4. DISCUSSION..... 70
5. ACKNOWLEDGMENTS 70
6. REFERENCES 71

CHAPTER EIGHT. DIFFERENTIAL EXPRESSION OF Ca CHANNELS AND SYNAPTIC TRANSMISSION IN NORMAL AND ATAXIC KNOCK-OUT MICE73

Francisco J. Urbano, Marcelo D. Rosato-Siri and Osvaldo D. Uchitel

1. INTRODUCTION 73
2. MOLECULAR SRUCTURE OF VDCC..... 73
3. CALCIUM CHANNELOPATHIES..... 74
4. CALCIUM CHANNELS AND NEUROTRANSMITTER RELEASE AT THE NEUROMUSCULAR JUNCTION 74
5. CONCLUSIONS 77
6. REFERENCES 77

CHAPTER NINE. INVESTIGATING THE MODULAR BASIS OF BK CHANNEL ACTIVATION BY CALCIUM..... 79

Edward Moczydlowski

1. INTRODUCTION 79
2. PROGRESS TOWARD BK(CA) CHANNEL STRUCTURE 80
3. PROGRESS TOWARD BK(CA) CHANNEL FUNCTION 84
4. REFERENCES 88

CHAPTER TEN. HELICAL NATURE OF THE VOLTAGE SENSOR 93

Osvaldo Alvarez, Eduardo Rosenmann, Francisco Bezanilla, Carlos González and Ramón Latorre

1. INTRODUCTION 93
2. *SHAKER* CHANNEL WORKS WITH S3-S4 SEGMENT DELETED..... 95
3. RESTORING THE S3-S4 LINKER FIVES CONFUSING RESULTS 97
4. UNDERSTANDING THESE RESULTS..... 99
5. CONCLUSIONS 101
6. REFERENCES 101

CHAPTER ELEVEN. PEPTIDE TOXINS AS CONFORMATIONAL PROBES FOR K-CHANNELS..... 103

David Naranjo

1. INTRODUCTION 103
2. PORE-SPECIFIC TOXINS FOR POTASSIUM CHANNELS 104
3. PEPTIDE TOXINS BIND TO OPEN AND CLOSED CHANNELS 105
 - 3.1 Binding the Open State 105
 - 3.2 Binding to the Closed State..... 106
4. POSSIBLE ORIGINS FOR THE CLOSED-OPEN STATE DEPENDENCY..... 106
 - 4.1 Pore Occupancy Modifies Toxin Binding..... 107
 - 4.2 The Voltage Sensor Interacts with the Toxin Bound to the Pore 108
 - 4.3 Ionic Strength Effects Could Distinguish Between Models..... 109
5. TOXINS BLOCK C-NACTIVATED AND CLOSED CHANNELS EQUALLY 109
 - 5.1 A Planar Rotation of the Vestibule During Slow Activation 111
6. CONCLUDING REMARKS 112
7. ACKNOWLEDGMENTS 112
8. REFERENCES 112

CHAPTER TWELVE. MOLECULAR PARTICIPANTS IN VOLTAGE-DEPENDENT GATING	115
Shinghua Ding, Thao P. Nguyen and Richard Horn	
1. INTRODUCTION	115
2. RESULTS	116
3. CONCLUSIONS	120
4. REFERENCES	120
CHAPTER THIRTEEN. Ca^{2+} DYNAMICS AT NERVE-TERMINAL ACTIVE ZONES MONITORED BY ENDOGENOUS K_{Ca} CHANNELS	121
Alan D. Grinnell, Bruce Yazejian, Xiaoping Sun and Bo-Ming Chen	
1. INTRODUCTION	121
2. METHODS	122
3. RESULTS	123
3.1 K_{Ca} Currents Track Ambient $[Ca^{2+}]_{AZ}$	123
3.2 K_{Ca} Channel Properties and $I_{K_{Ca}}$ Calibration	126
3.3 Titration of $[Ca^{2+}]_{AZ}$ for Study of Release	129
4. DISCUSSION	130
5. ACKNOWLEDGMENTS	131
6. REFERENCES	131
CHAPTER FOURTEEN. FINE TUNING OF EXCITABILITY BY K_{Ca} CHANNELS IN MUDPUPPY PARASYMPATHETIC NEURONS	133
Fabiana S. Scornik	
1. INTRODUCTION	133
2. RESULTS	134
2.1 Basic Characteristics of SMOCs and K_{Ca} Channels underlying SMOCs	134
2.2 SMOCs are Triggered by Calcium Released from Internal Stores	136
2.3 Calcium Influx Modulates SMOC Activity	138
2.4 Physiological Role of SMOCs in Mudpuppy Parasympathetic Neurons	139
3. CONCLUDING REMARKS	141
4. ACKNOWLEDGMENTS	142
5. REFERENCES	142
CHAPTER FIFTEEN. TWINKLE TWINKLE LITTLE SPARK: OUT OF TUNE POTASSIUM CHANNELS	145
Guillermo J. Pérez	
1. INTRODUCTION	145
1.1 Activation of K_{Ca} Channels by Ca^{2+} Sparks	146
2. RESULTS	147
2.1 Out of Tune	148

2.2 Twinkle Twinkle	150
3. CONCLUDING REMARKS	152
4. ACKNOWLEDGMENTS	153
5. REFERENCES	154

**CHAPTER SIXTEEN. A CLC-2-LIKE CHLORIDE
CONDUCTANCE IN *DROSOPHILA*
PHOTORECEPTORS.....**

157

Gonzalo Ugarte, Peter M. O'Day, Juan Bacigalupo and Cecilia Vergara

1. INTRODUCTION	157
2. OVERVIEW OF C1C CHANNELS WITH EMPHASIS ON C1C-2	157
3. RESULTS	159
4. ACKNOWLEDGMENTS	163
5. REFERENCES	163

EDITORS' NOTE

165

LIST OF PARTICIPANTS

Oswaldo Alvarez Universidad de Chile, Facultad de Ciencias, Departamento de Biología, Casilla 653, Santiago, Chile, email oalvarez@uchile.cl

Clay M. Armstrong Department of Physiology, University of Pennsylvania, Philadelphia, Pa, U.S.A, email carmstro@mail.med.upenn.edu

Felipe Barros Centro de Estudios Científicos (CECS), Avenida Arturo Prat 514, Casilla 1469, Valdivia, Chile, Tel +56 63 234500, Fax +56 63 234517, email fbarros@cecs.cl

Luis Beaugé Laboratorio de Biofísica, Instituto de Investigación Médica Mercedes y Martín Ferreyra, Casilla de Correo 389, 5000 Córdoba, Argentina, email lbeauge@immf.uncor.edu

María Isabel Behrens Departamento de Neurología y Neurocirugía, Facultad de Medicina, Universidad de Chile, Santiago, Chile

Francisco Bezanilla Departments of Physiology and Anesthesiology, UCLA School of Medicine, Los Angeles, California, U.S.A., email fbezani@ucla.edu

Marcela Bravo-Zehnder Laboratorio de Reumatología e Inmunología Clínica, Pontificia Universidad Católica de Chile, Marcoleta 367, Santiago, Chile, email mbravo@med.puc.cl

Luis Pablo Cid Centro de Estudios Científicos (CECS), Avenida Arturo Prat 514, Casilla 1469, Valdivia, Chile, Tel +56 63 234500, Fax + 56 63 234517, email pcid@cecs.cl

Ana María Correa Department of Anesthesiology, Brain Research Institute, University of California, Los Angeles, California, U.S.A., email nani@ucla.edu

- Leopoldo de Meis** Departamento de Bioquímica, Instituto de Ciencias Biomédicas, UFRJ, Rio de Janeiro, CEP 21941-590, Brasil, email demeis@server.bioqmed.ufrj.br
- Hersch M. Gerschenfeld** Laboratoire de Neurobiologie, Ecole Normale Supérieure, 46 rue de l'Ulm 75005, Paris, France, email gerschen@wotan.ens.fr
- Alan D. Grinnell** Department of Physiology, School of Medicine, University of California, Los Angeles, CA 90095, U.S.A., email adg@ucla.edu
- James E. Hall** Department of Physiology and Biophysics, University of California, Irvine, California, 92697-4560, Los Angeles, U.S.A., email jhall@uci.edu
- Cecilia Hidalgo** Centro de Estudios Científicos (CECS) and Instituto de Ciencias Biomédicas, Facultad de Medicina, Universidad de Chile, Casilla 70005, Santiago 7, Chile, chidalgo@med.uchile.cl
- Richard Horn** Department of Physiology, Institute of Hyperexcitability, Jefferson Medical College, 1020 Locust Street, Philadelphia, PA 19119, U.S.A., email richard.horn@tju.edu
- Pedro Labarca** Centro de Estudios Científicos (CECS), Avenida Arturo Prat 514, Casilla 1469, Valdivia, Chile, Tel +56 63 234500 Fax +56 63 234517, email plabarca@cecs.cl
- Ramón Latorre** Centro de Estudios Científicos (CECS), Avenida Arturo Prat 514, Casilla 1469, Valdivia, Chile, Tel +56 63 234500 Fax +56 63 234517, email ramon@cecs.cl
- Mario Luxoro** Universidad de Chile, Facultad de Ciencias, Departamento de Biología, Casilla 653, Santiago, Chile, email mluxoro@uchile.cl
- Edward Moczydlowski** Department of Pharmacology, Yale University School of Medicine, P.O. Box 208066, New Haven, CT 06520-8066, U.S.A., email edward.moczydlowski@yale.edu
- María Isabel Niemeyer** Centro de Estudios Científicos (CECS), Avenida Arturo Prat 514, Casilla 1469, Valdivia, Chile, Tel +56 63 234500, Fax +56 63 234517, email miniemeyer@cecs.cl
- Andrés Oberhauser** Department of Physiology and Biophysics, University of Texas Medical Branch, Galveston, Texas 77555-0437, U.S.A., email afoberha@utmb.edu
- David Naranjo** Centro de Neurociencia de Valparaíso, Universidad de Valparaíso, Gran Bretaña 1111, Playa Ancha, Valparaíso, Chile, email David.Naranjo@uv.cl

Alan Neely Centro de Neurociencia Celular y Molecular de Valparaíso, Universidad de Valparaíso, Gran Bretaña 1111, Playa Ancha, Valparaíso, Chile, email alan@cncv.cl

Guillermo J. Pérez Department of Experimental Cardiology, Masonic Medical Research Laboratory, 2150 Bleeker St. Utica, NY 13501, U.S.A, email gperez@mmrl.edu

Francisco V. Sepúlveda Centro de Estudios Científicos (CECS), Avenida Arturo Prat 514, Casilla 1469, Valdivia, Chile, Tel +56 63 234500, Fax +56 63 234517, email fsepulveda@cecs.cl

Fabiana Scornik Masonic Medical Research Laboratory, 2150 Blecker St. Utica, NY 13501, U.S.A, email fscornik@mmrl.edu

Enrico Stefani Division of Molecular Medicine, Department of Anesthesiology, University of California, Los Angeles, Basic Science Research Division, BH-509A CHS, Box 957115, Los Angeles, CA 90095-7115, U.S.A, email estefani@ucla.edu

Ligia Toro Department of Anesthesiology, University of California, Los Angeles, Division of Molecular Medicine, BH-509A CHS, Box 957115, Los Angeles, CA 90095-7115, U.S.A, email ltoro@ucla.edu

Oswaldo D. Uchitel Laboratorio de Fisiología y Biología Molecular, Departamento de Ciencias Biológicas, Facultad de Ciencias Exactas y Naturales, Universidad de Buenos Aires, Ciudad Universitaria, Pabellón II piso 2, Buenos Aires 1428, Argentina, Tel +54 11 4576 3368, Fax +54 11 4576 3321, email odu@bg.fcen.uba.ar

Cecilia Vergara Departamento de Biología, Facultad de Ciencias, Universidad de Chile, Santiago, Chile, email cvergara@uchile.cl

Miguel A. Valverde Cell Signalling Unit, Department Ciencias Experimentals, Universitat Pompeu Fabra, C/Dr. Aiguader 80, 08003, Barcelona, Spain, email miguel.valverde@cexs.upf.es

CHANNELS AND PUMPS EARLY IN EVOLUTION

Clay M. Armstrong^{1*}

1. INTRODUCTION

Ion channels and the electrical properties of cells are involved in every human characteristic that makes us interesting (at least to ourselves) and they distinguish us from the stones in a field. Ion channels are essential to every perception, every thought, every motion, every heartbeat. They are used in long-range communication, which allows the head to know within milliseconds what the feet are doing. But ion channels are very widespread, and are found even in bacteria, which do not have heartbeats or, so far as we know, thoughts. So, what primal necessity makes a bacterium require ion channels? And how did channels evolve from the performance of primal functions to form the basis for perception, thought, and motion? This short paper attempts to provide answers regarding the functions of ion channels early in their evolution.

2. ION CHANNELS IN BACTERIA

To those of us who work on nerve conduction, it came as a remarkable surprise that bacteria have highly-selective K channels. What function do these ions serve? Why must they be selective? An explanation for the existence of these channels in aerobic bacteria is relatively easy to guess (Epstein et. al., 1990). A major requirement of bacteria is a source of energy in the form of ATP, and for supplying ATP they rely on the metabolic machinery outlined in Figure 1. Near the top of the diagram is the citric acid cycle (Stryer, 1995) a complex set of enzymes present in aerobic bacteria as well as in the mitochondria of our own cells. The cycle uses many steps to metabolize acetyl-CoA, a substance provided to it by the break-down of sugars and fat in the metabolic steps that precede the cycle (Stryer, 1995). Simplifying greatly, the cycle has the function of providing electrons and protons, using acetyl-CoA as the source. The protons provided by the cycle initially enter the aqueous phase inside the bacterium. The electrons are carried by NADH to the first of the three stages of the electron transport chain. Each stage of this chain acts as a proton pump, to pump the protons provided by the citric acid cycle from

¹ Department of Physiology, University of Pennsylvania, Philadelphia, Pa, U.S.A

* corresponding author: carmstro@mail.med.upenn.edu

the inside into the space between the plasma membrane and the surrounding cell wall. The main function of the electron-transport chain is proton-pumping, and it might well be renamed the proton-pump chain. The energy for proton-pumping is provided by the electrons as they move downhill energetically through the stages of the chain, migrating in numerous steps to sites of progressively higher electron affinity (lower energy). On leaving the last of the three proton-pump stages, the electron is passed to oxygen, the bottom of the hill energetically.

The export of positively-charged protons makes the bacterial interior negative relative to the exterior, developing a membrane voltage estimated to be about -150 mV. A bacterium is thus strongly electrified, and it makes good use of its transmembrane voltage. The combination of a low internal proton concentration and a negative membrane voltage makes a large electrochemical driving force tending to force protons into the interior; the protons flow energetically downhill to the interior where the proton concentration is low and the voltage is negative. As they reenter the protons are channelled through an ATP-generating turbine, ATP synthase, which makes ATP from ADP. This amazing piece of molecular machinery actually spins as it produces ATP, reminiscent of a hydroelectric turbine.

As noted, the electron is handed off to atmospheric oxygen by the last proton-pump. The electron and the oxygen to which it is bound combine with the reentered protons to form water. Overall, the energy for driving ATP production comes from separating electrons from relatively low-affinity sites in acetyl-CoA and passing them through progressively higher affinity sites in the proton-pump chain, and finally to oxygen which binds them very tightly. Thanks to proton-pumping, the energy is stored temporarily as a strong electrochemical gradient of protons.

A membrane potential of -150 mV is thus essential for the production of energy by an aerobic bacterium. But why does the bacterium need ion channels? Plausible answers to this question have been provided by experts on bacterial transport (Epstein et. al., 1990). The bacterium lives in an aqueous medium containing ions, and, to maintain its turgor pressure, it needs ions inside. Turgor pressure keeps the bacterium expanded, by pressing its plasma membrane outward against the surrounding cell wall which is mechanically strong. Thus it is necessary that the pressure inside the bacterium be higher than outside, and this difference is the turgor pressure. Higher pressure internally is achieved by diluting the water inside the bacterium with ions and other solutes, making the water concentration inside lower than outside, and producing a tendency for water to migrate into the cell (in the usual way of stating this, the osmolarity inside the bacterium is higher than outside). The net inward movement of water stops when the pressure inside gets high enough to prevent further water movement. The external medium is imposed on the bacterium by nature. Consider three possibilities for the external environment: soil (*Streptomyces lividans*, a soil bacterium, is the source of the KcsA channel crystallized by Doyle et. al. 1998), the ocean, and our blood. Total ion concentration is very different in the three, but all are similar in that they have relatively a lot of Na^+ and Cl^- , a little K^+ , and a little Ca^{++} and Mg^{++} . All of the cations (Na^+ , K^+ , Ca^{2+} and Mg^{2+}) are attracted by the negative interior of the bacterium, and would gladly enter if given a chance. Which cation would it be logical to allow to enter? If a bacterium living in our blood were made freely permeable to Na^+ , that is if Na^+ were allowed to come to equilibrium (V_m -150 mV, Na^+ 145 mM externally) its internal concentration at equilibrium would be 46 M, as calculated from the Nernst equation (Figure 2). This is clearly impossible: the bacterium would turn into a salt crystal. Thus any sensible bacterium would prevent Na^+ entry by

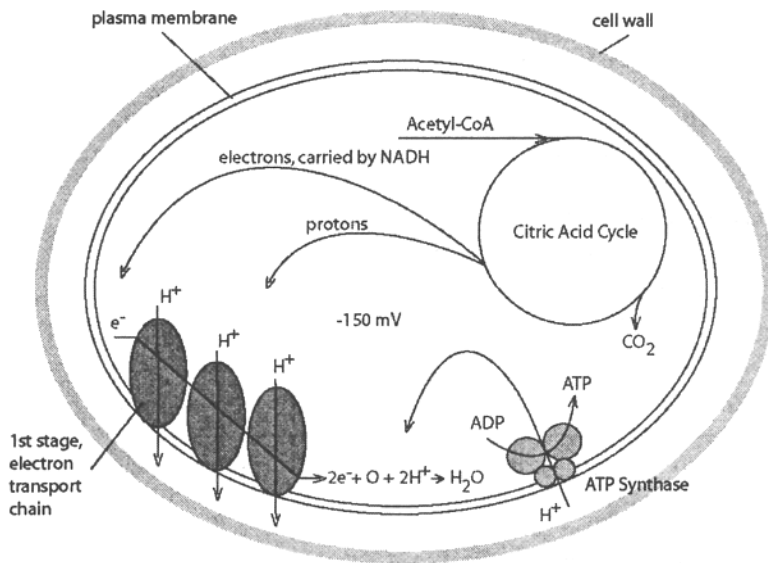


Figure 1. Energy production and membrane voltage in a bacterium. A central requirement for aerobic bacteria is the production of ATP from ADP using the citric acid cycle. Acetyl-CoA, a two carbon fragment from sugar metabolism, is complexed to coenzyme A and presented to the cycle. Using the acetyl fragment as a source, the cycle separates out protons, and relatively loosely-bound electrons. The protons combine with water in the bacterial interior, and are pumped out through the plasma membrane into the space enclosed by the cell wall. The electrons are carried by NADH to the first of three proton pumps that, by binding the electron to sites of progressively greater affinity, acquire the energy to pump the protons out. The result of proton pumping is negative internal voltage of about -150 mV and a deficit of protons inside. This strong electrochemical gradient of protons is used to drive protons inward through ATP synthase, which uses the energy of the gradient to make ATP from ADP. Maintenance of a strong membrane voltage is thus essential for energy production.

making its membrane impermeable to Na^+ . What about Ca^{2+} and Mg^{2+} ? Their equilibrium concentrations would be respectively ~ 130 M and 100 M internally (Figure 2), again clearly impossible. Ca^{2+} and Mg^{2+} must be very sparingly permeable at most. For K^+ the outcome is more favorable. With 4 mM external K^+ , the internal concentration would be 1.3 M at equilibrium, quite high and certainly sufficient to provide turgor pressure. It seems possible that bacteria in high millimolar K^+ might need to limit K^+ permeability, and perhaps even pump K^+ outward. For K^+ concentrations in the hundred μM range, an ATP-driven pump has been found necessary for growth of *E. Coli* (Dosch et. al., 1991), presumably because equilibrium with such low external concentrations does not supply enough internal K^+ . Anions would be repelled from the negative interior of a bacterium, making the equilibrium concentration of Cl^- only ~ 0.5 mM (for an external concentration of 150 mM).

In the accounting thus far, there is a clear deficit of negative charge inside the bacterium, which contains 1.3 M K^+ and only 0.5 mM Cl^- . The deficit in negative charge internally could be made good by the presence internally of negatively-charged species that are confined to the inside, e.g. anions containing phosphate, sulfate, and negatively-

charged amino acids. Also, proteins could provide a lot of negative charge, particularly since the internal proton concentration is low because of proton pumping to the outside. These questions are further considered below.

In summary then, the need to maintain a very negative interior (-150 mV) imposes on the bacterium the need to make Na^+ , Ca^{2+} , and Mg^{2+} essentially impermeant. K^+ permeability is permissible, and this ion enters to maintain turgor pressure. When external K^+ is in the millimolar range, internal K^+ concentration could remain high simply as a result of permeability through K channels and the membrane voltage: no pump is necessary.

3. ANIMAL CELLS

When we turn from bacteria to our own cells, there are many similarities: high internal K^+ , low internal Ca^{2+} , Mg^{2+} , and Cl^- , many impermeant intracellular anions, and a negative resting potential. In animal cells, however, energy production is performed by mitochondria, the descendants of symbiotic bacteria long ago incorporated inside the cell. Why then does an animal cell have a resting potential? The short answer is that it needs a negative membrane voltage because it does not have a cell wall: the membrane voltage is used not for energy production, but is used instead to stabilize the cell osmotically (Tosteson and Hoffman, 1960).

3.1. The Osmotic dilemma

Cells need to save inside themselves substances that are scarce in their surroundings, e.g. DNA, amino acids, sugars, proteins. All of these substances have osmotic activity, and if they are higher in concentration on the inside, they tend to make the osmotic activity higher inside than out. That is, the water inside is diluted by the solutes, lowering the water activity inside. This creates a gradient that drives water into the cell through the plasma membrane, leading to swelling. In a bacterium, this swelling tendency is resisted by the cell wall, with the result that the pressure inside the bacterium rises high enough to prevent further entry of water. The pressures generated are very large, and are in fact used to drive water up trees: an osmotic activity difference of 1M is sufficient to drive water well above the top of the tallest redwood tree. Animal cells have very fragile membranes, with the approximate mechanical strength of a soap bubble, completely unable to withstand even the smallest pressure, and with no supporting cell wall. And yet they are stable. The only conclusion is that the internal and external osmotic activities are equal, so that no osmotic pressure difference is created. How is this possible? How does the cell make 'osmotic room' on the inside for substances that must be concentrated internally?

3.2. A cell that is too simple

To make the argument clearer, consider a theoretical cell in a simplified external medium. The cell is freely permeable to all ions, and has no ion pumps in its membrane, so that all ion concentrations are the same inside and out. If the cell tries to save some nondissociable substance at concentration X on the inside, the osmolarity internally increases to $298+X$. Water activity is now lower internally than externally. Water enters

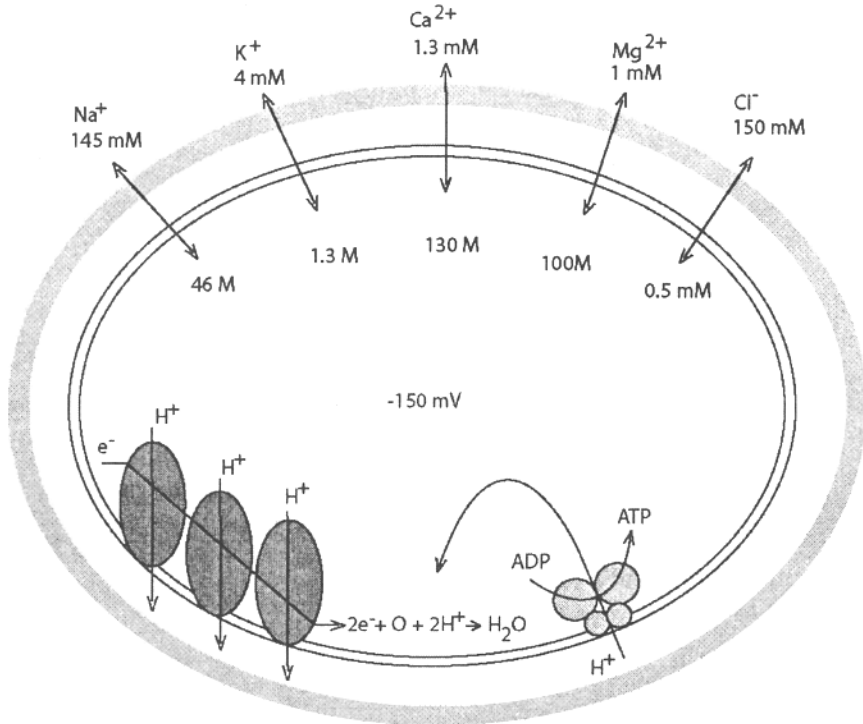


Figure 2. Why an aerobic bacterium needs highly selective K channels. The -150 mV membrane voltage that is essential for energy production tends to concentrate cations inside. The bacterium is shown in a medium with the ionic composition of our blood, a reasonable growth medium. The concentrations of cations inside the bacterium are the equilibrium concentrations that would hold if the ions were freely permeable and were not significantly ejected from the bacterium by a metabolically driven pump. For Na^+ , Ca^{2+} , and Mg^{2+} the equilibrium concentrations are impossibly high, and we can conclude that they must not be significantly permeable, or that the bacterium expends a large amount of energy to keep its internal concentrations of these ions low. K^+ at equilibrium would be about 1.3M , high enough to provide the turgor pressure necessary to expand the plasma membrane to the limit allowed by the rigid cell wall. Thus, it would be reasonable to have K channels in the plasma membrane, provided they were very selective for K^+ . Cl^- at equilibrium would be very low, and anionic charge would necessarily be provided by impermeant intracellular anions.

the cell, together with ions that remain in diffusional equilibrium on the two sides of the membrane. When the cell volume doubles, the internal osmolarity is $298 + X/2$. This is still higher than outside, and more water comes in. This will continue until the substance S is infinitely dilute, at infinite volume. Short of infinite volume, no equilibrium is possible.

3.3. The solution to the dilemma

Cells solve the osmotic dilemma by employing a clever strategy using pumps and ion channels, a strategy that evolved from pumps and channels in bacteria. The overall

solution is clear from a perusal of the known ion concentrations inside and outside of a typical cell.

Table I. Typical extra- and intracellular ion concentrations.

Substance	Outside	Inside
Na ⁺	145 mM	15 mM
K ⁺	4 mM	160 mM
Ca ²⁺	1.3 mM	10 ⁻⁷ M
Mg ²⁺	1 mM	2 mM
total identified cationic charge	154 meq/l	179 meq/l
Cl ⁻	110 mM	7 mM
HCO ₃ ⁻	28 mM	10 Mm
phosphates	2 mM	11 mM
misc	12 mM	
total identified anionic charge	154 meq/l	~30 meq/l
osmolarity of identified substances	~300 mosm/l	205 mosm/l
<i>anionic charge of essential substances</i>		<i>~124meq/l</i>
<i>osmolarity of essential substances</i>		<i>~95</i>

Internal ion concentrations are difficult to measure, and consequently are approximate. It is nonetheless clear that Na⁺ and Cl⁻ are low inside and K⁺ is high - the bacterial pattern. The accounting shows a big deficit of both internal anionic charge and internal osmolarity. We can be confident that these deficits do not really exist. First, it is certain on theoretical grounds that, within the accuracy specified, total anionic charge must equal total cationic charge (the small difference required for making a membrane voltage shows up after many decimal places). Second, internal and external osmolarity must be the same, for the reasons given above. The unidentified substances that make up the deficits are the material that the cell concentrates internally, substances essential for vital life processes. The essential point, and the solution to the osmotic dilemma, is that 'osmotic room' for these essential substances is available in the cell, because the Cl⁻ concentration is low. These essential substances carry a negative charge, so they simultaneously correct both of the deficits in internal osmolarity and internal negative charge. These very firm theoretical considerations allow us to add the two rows in italics to Table 1 above, making the anionic charge internally equal to the cationic charge, and making the internal osmolarity equal to the external.

Why is Cl⁻ low internally? One possibility is that Cl⁻ is pumped out by an ATP-driven pump. Nowhere in the animal kingdom, however, has a Cl⁻ pump driven by ATP been discovered (private communication, Dr. Robin Post). A better possibility is that Cl⁻ is permeable, and is in equilibrium at the normal resting potential. If this were the case, at a resting potential of -80 mV the internal concentration would be lower than external by a factor of 20, which is close to the ratio in Table 1. Also, within the accuracy available, Cl⁻ is in equilibrium in muscle fibers (Hodgkin and Horowicz, 1959). From the point of view of energy requirements, it would seem desirable to have Cl⁻ in equilibrium, for

reasons of economy. Resting Cl^- permeability is twice the resting K^+ permeability in muscle fibers. To push Cl^- significantly away from equilibrium would require a great deal of pumping by some indirect mechanism such as an exchange pump, and a great deal of energy.

Let us take a muscle fiber with Cl^- at equilibrium as our general model, bearing in mind that in cells with low Cl^- permeability, exchange pumps may push Cl^- away from equilibrium without excessive energy costs. 'Osmotic room' in a muscle fiber and in similar cells is thus provided by using the membrane voltage to lower the internal Cl^- concentration. The membrane potential is produced by the Na/K pump, which makes the K^+ difference between inside and out, in combination with a K^+ selective resting membrane. It seems highly probable that animal cells have a negative resting potential primarily for this reason, to stabilize themselves osmotically, a first necessity for a cell with a fragile membrane. All of the other activities that require a membrane voltage, e.g. Na^+ -driven transport processes and electrical signaling, are secondary uses that utilize a scenario developed for osmotic stabilization. A bacterium, on the other hand, though similar in ion content, uses its membrane voltage primarily for energy production.

3.4. A Thought Experiment on Stopping the Na/K Pump

From what has been said, it is not surprising that cells swell when their supply of metabolic energy is interrupted (Tosteson and Hoffman, 1960). To understand why this occurs, let us perform a thought experiment that allows us to observe, step by step, the events that follow stopping the Na/K pump. At each stage we can measure the cell electrolytes, solve for equilibrium potentials using the Nernst equation, and solve for V_m using the Goldman Hodgkin Katz (GHK) equation. Table 2 shows the quantities of interest in several situations, with normal conditions in the first row. Extracellular concentrations are fixed (imagine that the cell is in a very large bath) at the normal values given in Table 1. In each condition we will consider the various ions and the volume one by one.

Normal Conditions ("Normal" in Table 2)

K^+ is not in equilibrium, and E_K is negative to V_{rest} (resting potential). That is, V_{rest} is not sufficiently negative to prevent a net efflux of K^+ . Efflux through K channels is balanced by an influx of K^+ through the pump, making net flux equal to zero. K^+ is in a steady-state.

Na^+ is not in equilibrium, and E_{Na} is far positive to V_{rest} . That is, both the concentration gradient and V_{rest} tend to draw Na^+ into the cell. Influx through Na channels is balanced by efflux through the pump, so net efflux is zero. Na^+ is in a steady-state.

Cl^- is in equilibrium; i.e. $E_{\text{Cl}} = V_{\text{rest}}$. Cl^- is not pumped in any direction. The diffusion force that tends to drive Cl^- inwards, is just balanced by the electrical force pushing it out, keeping internal Cl^- relatively low.

A^- , the internal anions, are present in fixed quantity and confined to the inside.

Osmolarity inside equals the external osmolarity throughout the experiment: the cell shrinks and swells as necessary to keep this true.

Volume is constant.

V_{rest} is -72 mV, thanks to high internal K^+ and high K^+ permeability (P_K). V_{rest} , determined by the GHK equation, is near E_K , but kept positive to E_K by Na^+ permeability, P_{Na} .

Add a toxin that blocks chloride channels ("Toxin")

Now imagine that we add a toxin that makes Cl^- permeability (P_{Cl}) zero (no known agent is really this good).

V_{rest} is unchanged because chloride is in equilibrium ($E_{\text{Cl}} = V_{\text{rest}}$): the net flux through an open chloride channel is zero, so it does not matter in this special circumstance how many Cl channels are open.

K^+ , Na^+ , *Volume*: as under normal conditions.

Stop the pump ("ouabain + toxin, $t=0$ ")

Immediately after the pump is stopped by removing ATP or adding ouabain, ion concentrations have not had a chance to change, but we can predict the fluxes and the direction of change.

V_{rest} changes by about +2 mV with cessation of the small current generated by the pump, which in one cycle ejects three Na^+ ions while bringing in two K^+ ions.

K^+ : because $E_{\text{K}} < V_{\text{rest}}$ there is a net efflux of K^+ through K channels that is no longer balanced by the pump. $[\text{K}^+]_i$ is decreasing.

Na^+ : because $E_{\text{Na}} > V_{\text{rest}}$ there is a net efflux of Na^+ , no longer balanced by the pump. $[\text{Na}^+]_i$ is increasing.

Cl: P_{Cl} is zero, so there is no movement of Cl^- .

In the absence of pumping, these changes will continue as Na^+ and K^+ move toward equilibrium. Since there is no movement of anions through the membrane (P_{Cl} , when present, is the only anion permeability) we can be sure that the exchange of Na^+ and K^+ is one for one within measurable accuracy, as required by the equality (within measurable accuracy) of cationic and anionic charge internally.

Volume: There has been a 1:1 exchange of Na^+ for K^+ , and no movement of anions, so volume does not change.

Wait ("ouabain + toxin, $t=\infty$ ")

$V_{\text{rest}} = E_{\text{Na}} = E_{\text{K}} = 0$ at equilibrium.

Volume is unchanged.

Remove the chloride channel toxin ("ouabain only, $t=0$ and $t=\infty$ ")

V_{rest} is pulled toward E_{Cl} (still -72 mV) by restoring P_{Cl} . P_{Na} and P_{K} keep V_{rest} from reaching E_{Cl} . As a result, *none* of the ions are at equilibrium.

K^+ moves inward.

Na^+ moves inward.

Cl moves inward.

Volume increases as all three ions move inward. The only possible equilibrium is a Donnan equilibrium which requires that hydrostatic pressure inside be higher than outside, an impossibility for an animal cell because of its fragile membrane. The cell thus swells until it bursts.

Table 2. Results of a thought experiment on stopping the Na/K pump.

Conditions	$[K^+]_i$ E_K	$[Na^+]_i$ E_{Na}	$[Cl^-]_i$ E_{Cl}	P_K	P_{Na}	P_{Cl}	V_m	K^+ nFlux	Na^+ nFlux	Cl^- nFlux	Vol
normal	140 -93	15 59	7 -72	27	1	55	-72	0 ¹	0 ²	0 ³	V_0
toxin	140 -93	15 59	7 -72	27	1	0	-72	0	0	0	V_0
ouabain +toxin, $t=0$	140 -93	15 59	7 -72	27	1	0	-70	out	in		V_0
ouabain +toxin, $t=\infty$	-4 -0	-145 -0	7 -72	27	1	0	-0	-0	0		V_0
ouabain only, $t=0$	-4 -0	-145 -0		27	1	55	-60 ↑ ⁵	in	in	in	↑
ouabain only, $t=\infty$			7 -72	27	1	55		in	in	in	↑

¹ The efflux through K channels is balanced by K^+ influx driven by the Na/K pump.

² Influx through Na channels is balanced by Na^+ efflux driven by the Na/K pump.

³ Cl^- is in equilibrium: $E_{Cl} = V_m$.

⁴ The chloride channel toxin prevents Cl^- influx.

⁵ Cl^- enters the cell; as its concentration increases, V_m drifts positive.

4. CONCLUSIONS

Aerobic bacteria require a membrane potential of about -150 mV, inside negative in order to make ATP from ADP. Given this necessity, they must carefully limit the permeability of cations to avoid internal cation overload. The only acceptable cation permeability is to K^+ , because this cation is present at relatively low concentration in the environments that bacteria are likely to encounter. To avoid cation overload, aerobic bacteria had to develop ion channels highly selective for K^+ ions. Given selective K channels, K^+ ions could be concentrated inside simply as a result of attraction by the bacterium's negative interior, raising the internal osmolarity and providing the turgor pressure necessary to keep the bacterium's plasma membrane expanded and pressed against the surrounding cell wall. The membrane potential had the opposite effect on anions, making the concentration of permeant anions very low inside the bacterium. The dominant negatively charged species in the interior are impermeant, and confined to the interior of the bacterium. Among these species are the substances vital to the bacterium's ability to survive and reproduce.

The bacterial pattern of internally negative membrane voltage, high internal K^+ concentration, selective permeability to K^+ , and low internal concentration of other cations and of permeant anions was carried over to animal cells, where it fulfills a different purpose. In animal cells, ATP is made by the mitochondria, and the membrane voltage is thus not necessary for this purpose. Instead it is used to stabilize animal cells

osmotically. Animal cells are fluid and mobile because they lack the cell wall that is found in plants and bacteria. But the absence of a cell wall makes it necessary that the osmolarity inside and outside of an animal cell be equal. By driving permeant anions out of the negative interior, the membrane voltage makes “osmotic room” for the vital substances that the cell must save inside. The cell can thus save these vital substances internally and at the same time keep internal osmolarity from exceeding that outside. Concentration of K^+ in the animal cell interior is accomplished by an Na/K pump that drives K^+ inward and Na^+ out. In bacteria, K^+ is concentrated internally by the membrane voltage except when external K^+ concentration is very low, making it necessary for the bacterium to use a metabolically driven pump. The K channels that developed in bacteria to concentrate K^+ internally serve quite a different purpose in the animal cell, where their primary purpose is to establish a membrane voltage, in order to drive anions out.

Ion channels and membrane voltages thus developed in animal cells for the primal function of osmotic stabilization. This set the stage for the elaborate development of electrical properties that allows us to move, think, and perceive.

5. REFERENCES

- Dosch, D. C., G. L. Helmer, S. H. Sutton, F. F. Salvacion, and W. Epstein, 1991, Genetic analysis of potassium transport loci in *Escherichia coli*: evidence for three constitutive systems mediating uptake potassium. *J Bacteriol.*, **173**:687-96.
- Doyle, D. A., J. Morais Cabral, R. A. Pfuetzner, A. Kuo, J. M. Gulbis, S.L. Cohen, B. T. Chait, and R. MacKinnon. 1998. The structure of the potassium channel: molecular basis of K^+ conduction and selectivity. *Science*, **280**(5360):69-77.
- Epstein, W., M. O. Walderhaug, J. W. Polarek, J. E. Hesse, E. Dorus, and J. M. Daniel. 1990. The bacterial Kdp K^+ -ATPase and its relation to other transport ATPases, such as the Na^+/K^+ - and Ca^{2+} -ATPases in higher organisms. *Philos Trans R Soc Lond B Biol Sci.*, **326**:479-86.
- Hodgkin, A. L. and P. Horowicz. 1959. The influence of potassium and chloride ions on the membrane potential of single muscle fibres. *Journal of Physiology (London)*, **148**:127-160.
- Stryer, L. 1995. *Biochemistry*, 4th ed. W.H. Freeman, N.Y.
- Tosteson, D. C. and J. F. Hoffman. 1960. Regulation of cell volume by active cation transport in high and low potassium sheep red cells. *Journal of General Physiology*, **44**:169-194.

THE POSSIBLE ROLE OF AQUAPORIN 0 IN LENS PHYSIOLOGY

James E. Hall^{1*} and Karin L. Németh-Cahalan¹

1. INTRODUCTION

Water permeability is a crucial property of biological membranes and its regulation is a vital element of many physiological processes. But in the '70s and '80s biophysics took a wrong turn in assuming that variations in water permeability amongst biological membranes were primarily attributable to differences in lipid composition. When Peter Agre and colleagues showed that aquaporin 1, a member of a protein family, whose type member had been variously thought to be a species of gap junction or an ion channel (Gorin *et al.*, 1984; Girsch and Peracchia, 1985a; Peracchia *et al.*, 1985; Girsch and Peracchia, 1985b; Ehring and Hall, 1988; Ehring *et al.*, 1988), was actually the long-sought mercury-sensitive pathway for water movement across red blood cells (Preston *et al.*, 1992), biophysicists had to rethink and rediscover the whole notion of control of water permeability in biological systems.

In one such system, the crystalline lens of the eye, water permeability of is an emerging physiological puzzle. The lipid composition of the lens plasma membrane is rich in sphingomyelin and cholesterol, lipids which produce very low water permeability in lipid membrane systems (Finkelstein, 1976; Fettiplace and Haydon, 1980). But aquaporin 0 (AQP0), the major membrane protein of the lens and the type member of the aquaporin family, exhibits a much lower water permeability than AQP1 and was thought at one point not to be a water channel or aquaporin at all. Thus the question of how or even whether the water permeability of lens fiber cell membranes is regulated is one of increasing importance.

¹ From the Department of Physiology and Biophysics, University of California, Irvine, California, 92697-4560.

* corresponding author: jhall@uci.edu

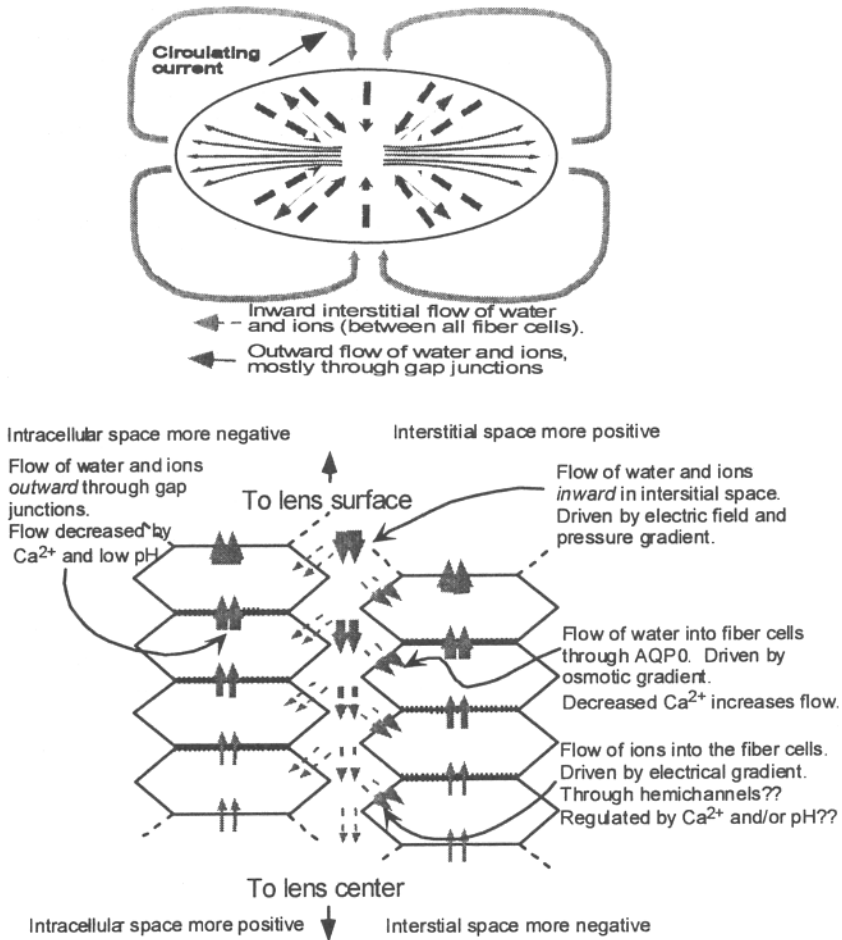


Figure 1. The intrinsic circulation of the lens. The upper panel shows the currents in a normal lens. The curved gray lines show the external current exiting the equator and entering at the poles. The internal arrows show the inward flows, thought to be between cells in the interstitial spaces, and the outward flows, thought to be through an intracellular pathway passing from cell to cell via gap junctions. The lower panel shows an exploded view of this process with the extracellular space greatly exaggerated in size. The arrows represent the fluxes of salt, water and other non-electrolytes such as glucose, which progressively decreases as material is lost by entering the cells through specialized, and presumably regulated, pathways. Inside the cells, the direction of the driving forces reverses and flow is outward from cell to cell via gap junctions. The permeability of the cells to water, and thus the coupling between osmotic gradient and water entry, is presumably controlled by AQP0.

2. REGULATION OF WATER PERMEABILITY AND THE LENS

In the kidney, the water permeability of the distal nephron is regulated by insertion of aquaporin 1 into the plasma membrane by ADH controlled vesicle fusion when high water permeability is required, and removal by recovery of the fused vesicle when high water permeability is no longer required. But such an energy-intensive mode of regulation clearly will not do for the lens which lacks a ready vascular supply of nutrients and must operate on a very limited energy budget. This lack of vascularization produces an immediate problem for the lens: how to overcome the limitations of diffusion, which, because of the large size of the lens, cannot supply the necessary nutrients. A clue as to how this might be accomplished is illustrated in Figure 1, based on the work of John Patterson and colleagues. Patterson found that the lens has a circulating current which exits the equator and enters at the poles. Mathias, Rae and Baldo (Mathias *et al.*, 1997) have constructed a model that suggests how internal currents of the lens might flow to give rise to the observed external circulating currents. These are shown schematically in the upper panel as inwardly directed arrows for currents flowing inward through extracellular space and as outwardly directed arrows for currents flowing through intracellular space. Water and non electrolyte fluxes follow the ionic currents, driven by small osmotic gradients generated by ion flow, and as material moves inward through extracellular space, a fraction enters the cells at each level and begins to flow in an outward direction (shown by arrows of decreasing size in the right-hand panel). Inside the cells, flow reverses direction and becomes outwardly directed.

The driving energy for all this activity is thought to be generated by the Na-K-ATPase of the mitochondria-rich regions near the surface of the lens. But the flows of ions, non-electrolytes and water in the interior of the lens are likely to be completely passive, using energy and gradients obtained by coupling fluxes to the membrane potential generated near the surface of the lens. How all these flows are regulated is thus a subject of some concern.

3. SINGLE-MOLECULE WATER PERMEABILITY OF AQP0 AND AQP1

By combining a physiological method, measuring the water permeability of oocytes expressing aquaporins, with a morphological method, electron microscopy freeze-fracture, Chandy et al (Chandy *et al.*, 1997) were able to compare the water permeability of aquaporin 1 and aquaporin 0 on a per molecule basis. Figure 2 illustrates the method. The top panel shows three freeze-fracture micrographs from three oocytes expressing (from left to right) increasing amounts of AQP0. Micrographs such as these give estimates of the number of particles per square micron. Measurements of the swelling rate and surface area of the corresponding oocytes give the permeability of the oocyte. Plotting the permeability as a function of the particle density gives permeability per particle and, since each particle (based on size) contains four molecules of aquaporin, dividing this value by four gives the permeability per molecule. AQP0 is about 1/40th as permeable as AQP1 on a per molecule basis.

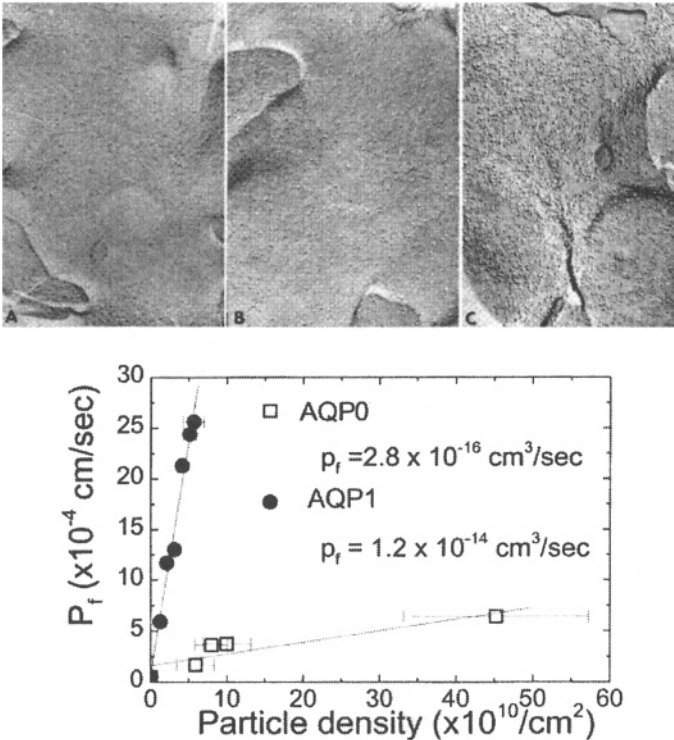
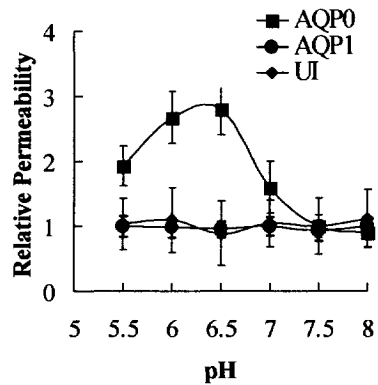


Figure 2. The single-molecule water permeabilities of AQP1 and AQP0. By combining physiology and morphology, one gets an estimate of the single particle and consequently the single molecule water permeability. In the upper panel are three freeze fracture electron micrographs from oocytes expressing increasing amounts of AQP0 (A, B, and C). By counting the number of particles one can estimate the surface density of aquaporin. The lower panel shows the water permeability of oocytes plotted against the particle density obtained from micrographs like A, B, and C in the upper panel for the same oocytes on which the permeability measurements were made. Note that each added particle of AQP1 increases the water permeability of the oocyte about 40 times more than an added particle of AQP0 (After Chandy *et al.*, 1997 with permission of Springer Verlag).

4. REGULATION OF AQP0 WATER PERMEABILITY

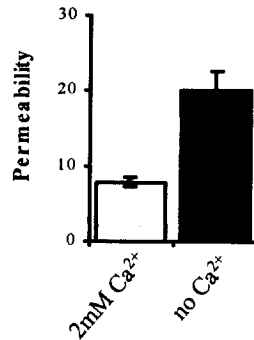
The low water permeability of AQP0 might be enough for a low-energy organ like the lens, but if water permeability of the lens is regulated via AQP0, it must be by a much less energy-hungry mechanism than that which regulates the AQP1 water permeability in the kidney. The pH of the lens increases toward the interior and acid products result from active metabolism. We thought, therefore, that pH might serve as a regulator for AQP0, and indeed that proved to be the case. Figure 3 (after Nemeth-Cahalan and Hall, (Nemeth-Cahalan and Hall, 2000)) shows the relative water permeability of oocytes expressing a constant amount of AQP0 as a function of pH.

Figure 3. Water permeability of AQP0 is pH-dependent. The water permeability of AQP0 peaks at about 6.5, the lowest pH observed in the lens, but the water permeability of AQP1 is pH independent as is the water permeability of uninjected oocytes (UI) (After Nemeth-Cahalan and Hall, 2000, with permission of the Journal of Biological Chemistry).



in water permeability with pH. And of greater significance, peak water permeability is at pH 6.5 and the range of regulation from pH 7.5 to pH 6.5 is very nearly the range of pH observed in the lens. Thus if the pH were to fall in a region of the lens performing more active metabolism than adjacent regions, and thus producing more acid metabolic products, the intrinsic circulation could be increased in that region by an increase in water permeability produced by the lowered local pH.

Figure 4. Dependence of AQP0 water permeability on Ca^{2+} . When the external Ca^{2+} is the standard value of 2 mM, the water permeability is low. When the external Ca^{2+} is lowered by not adding Ca^{2+} to the medium, the AQP0 water permeability more than doubles. (Units of permeability are 10^{-5} cm/sec)



AQP0 water permeability also depends on the external Ca^{2+} concentration. Figure 4 shows the water permeability of oocytes injected with AQP0 RNA when the external medium contains 2 mM Ca^{2+} or no added Ca^{2+} . Note that this is NO ADDED Ca^{2+} (approximately micromolar Ca^{2+}). With EGTA water permeability also increases, but to a lesser extent than with no added Ca^{2+} .

The results shown in Figures 3 and 4 led us to investigate both the structural features required for the regulation of the water permeability and any connections that there might be between Ca^{2+} regulation and pH regulation. Our first break was the discovery that DEPC (diethyl pyrocarbonate), a histidine modifying reagent, eliminated the regulatory effects of both Ca^{2+} and pH. Reversibility of the modification by hydroxyl amine confirmed that DEPC was indeed modifying a histidine and not acting by

minority side reaction with another amino acid residue. We thus began a search for possible candidate histidines which might be involved.

Figure 5 shows the folding of AQP0 deduced from the three dimensional structure of AQP1 (Murata et al., 2000; Sui et al., 2001). There are three histidines in external loops, H40, H122, and H201. Histidine 201 is found in AQP0, AQP1 and AQP4. Histidine 122 is found in AQP0 and AQP4, and Histidine 40 is found only in AQP0. Since only AQP0 exhibits the regulation by pH and Ca^{2+} described above, we decided to mutate H40 to three different amino acids with different charges and sizes, H40A, H40D and H40K.

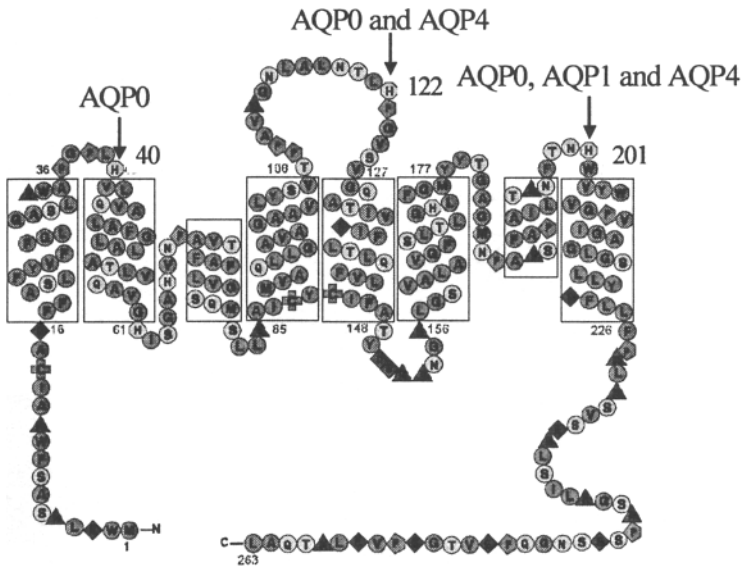


Figure 5. The folding of AQP0 showing the three external histidine candidates for possible involvement in regulation of water permeability by pH and Ca^{2+} . Only H40 is uniquely found in AQP0.

Figure 6 shows the functional results of these three mutants on the regulation of the water permeability of AQP0 by pH and Ca^{2+} . Note that both Ca^{2+} and pH regulation are eliminated by the three mutations alanine, lysine and aspartate. But the effect turns out to be more subtle than simply elimination. If we make the assumption (almost certain to be correct) that the expression levels of all the mutational constructs are fairly close, then the mutations not only eliminate regulation but seem to *lock* the protein into a *high permeability state*. This point of view is supported by the observation that the effects of pH and Ca^{2+} are not additive, but tend to elevate the water permeability to the same plateau value (Nemeth-Cahalan and Hall, 2000).

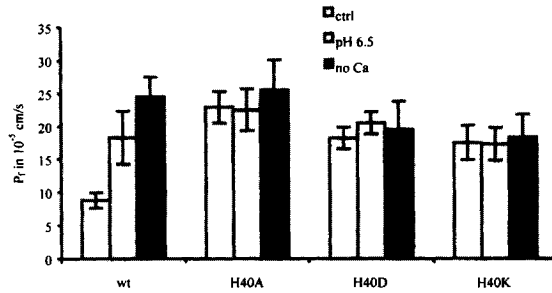


Figure 6. Mutation of H40 to alanine, aspartate or lysine eliminates both Ca^{2+} and pH dependence by locking the protein into a high permeability state. The same amount of RNA (10ng) was injected into the oocytes for all constructs. Thus if the expression levels for each construct are the same, likely a correct assumption for these point mutation constructs, the total permeabilities are proportional to the permeability per monomer.

A fourth histidine mutation confirms this view. Mutating histidine 40 to a cysteine eliminates pH dependence in the range from 7.5 to 6.5, but leaves the ability of low calcium to increase the water permeability intact. This result is shown in figure 7 and shows for the first time that the effects of pH and Ca^{2+} are completely separable.

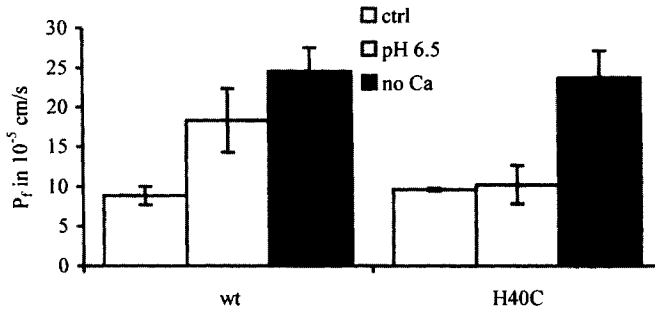


Figure 7. The independence of pH and Ca^{2+} is demonstrated by the mutant H40C. This figure compares the effects of low pH and low Ca^{2+} concentration on wild type aquaporin and the H40C mutant. The water permeability of the H40C at neutral pH 7.5 has the same permeability as wild type under the same conditions, a value we assign to the low permeability state. Lowering the pH to 6.5 has no effect on the permeability of the mutant, but lowering the Ca^{2+} concentration raises the permeability to the same high level seen for low Ca^{2+} for wild type AQP0. This experiment thus shows that pH modulation and Ca^{2+} are completely separable and it validates yet again the assumption of equal expression for equal amounts of RNA.

5. CONCLUSIONS

Our results clearly establish that the water permeability of AQP0, but not that of AQP1 and AQP4, is regulated by protons and calcium ions in the oocyte expression system. It remains to be seen if this regulation is of physiological importance in the living lens or if it proceeds in the manner we suggest. Mathias et al have shown that the water permeability of vesicles isolated from mouse lenses is proportional to the amount

of AQP0 present in the lens (Varadaraj et al., 1999). They have also demonstrated that the water permeability of isolated vesicles is altered by about the same factor as we find for AQP0 in oocytes for both pH and calcium. However the sign of the change is different for calcium (Mathias et al., 2002)! Where we find low calcium concentration increases the water permeability of AQP0 in oocytes, they find that high calcium increases the water permeability of vesicles isolated from mouse lenses. The reasons for these discrepancies are not known, but there are several intriguing possibilities. First AQP0 is a phosphoprotein (Johnson et al., 1986; Lampe and Johnson, 1991; Lampe and Johnson, 1989) and differences in the state of phosphorylation could alter the response to calcium. There is some experimental evidence that this idea is not entirely far-fetched. We have shown that the calcium regulation of AQP0 water permeability is likely due to the interaction of calmodulin with AQP0 (Nemeth-Cahalan and Hall, 2000), probably with the C-terminus of the protein (Louis et al., 1985; Peracchia and Girsch, 1985). Since the C-terminus is also the site of phosphorylation of AQP0 (Johnson et al., 1986; Lampe and Johnson, 1991; Lampe and Johnson, 1989) it is not unreasonable that phosphorylation could modify the Ca^{2+} -calmodulin dependent interaction with AQP0. Second, there could be auxiliary proteins present in the lens, but not in the oocyte, that alter the sign of the effect of low calcium.

In summary, there is clear evidence that the water permeability of AQP0 as expressed in oocytes and as found in lens vesicles varies by a factor of a little more than three at different pH and Ca^{2+} concentration. The water permeability of other aquaporins, notably AQP1, does not change with variation of pH or calcium concentration. Moreover the range of variation of pH and calcium concentration over which these changes take place lies comfortably within the range found in the living lens. It thus seems quite reasonable to posit a role for such regulation in the lens, possibly fitting into the scheme of circulating currents shown in Figure 1.

6. ACKNOWLEDGEMENTS

This work was supported by grant NIH EY 05661.

7. REFERENCES

- Bok, D., J. Dockstader, and J. Horwitz. 1982. Immunocytochemical localization of the lens main intrinsic polypeptide (MIP26) in communicating junctions. *J Cell Biol* **92**:213-220.
- Chandy, G., G.A.Zampighi, M.Kreman, and J.E.Hall. 1997. Comparison of the water transporting properties of MIP and AQP1. *J. Membrane Biol.* **159**:29-39.
- Ehring, G. R. and J. E. Hall. 1988. Single channel properties of lens MIP 28 reconstituted into planar lipid bilayers. *Proc. West. Pharmacol. Soc.* **31**:251-253.
- Ehring, G. R., G.A.Zampighi, and J.E.Hall. 1988. Properties of MIP 26 channels reconstituted into planar lipid bilayers. In *Gap Junctions*. R. G. Johnson and E. L. Hertzberg, editors. A.L. Liss, Inc., New York. 335-46.
- Fettiplace, R. and D. A. Haydon. 1980. Water permeability of lipid membranes. *Physiol Rev* **60**:510-550.
- Finkelstein, A. 1976. Water and nonelectrolyte permeability of lipid bilayer membranes. *J. Gen. Physiol.* **68**:127-135.
- Girsch, S. J. and C. Peracchia. 1985a. Lens cell-to-cell channel protein: I. Self-assembly into liposomes and permeability regulation by calmodulin. *J. Membrane Biol.* **83**:217-225.

- Girsch, S. J. and C.Peracchia. 1985b. Lens cell-to-cell channel protein: II. Conformational change in the presence of calmodulin. *J. Membrane Biol.* **83**:227-233.
- Gorin, M. B., S. B. Yancey, J. Cline, J. P. Revel, and J. Horwitz. 1984. The major intrinsic protein (MIP) of the bovine lens fiber membrane: characterization and structure based on cDNA cloning. *Cell* **39**:49-59.
- Johnson, K. R., P.D. Lampe, K. C. Hur, C. F. Louis, and R. G. Johnson. 1986. A lens intercellular junction protein, MP26 is a phosphoprotein. *J. Cell Biol.* **102**:1334-1343.
- Lampe, P. D. and R.G.Johnson. 1989. Phosphorylation of MP26, a lens junction protein, is enhanced by activators of protein kinase C. *J. Membrane Biol.* **107**:145-155.
- Lampe, P.D. and R.G.Johnson. 1991. Amino acid sequence of in vivo phosphorylation sites in the main intrinsic protein (MIP) of lens membrane. *Eur. J. Biochem.* **194**:541-547.
- Louis, C.F., R.G.Johnson, and J.Turnquist. 1985. Identification of the calmodulin-binding components in bovine lens plasma membranes. *Eur. J. Biochem.* **150**:271-278.
- Mathias, R.T., J.L.Rae, and G.J.Baldo. 1997. Physiological properties of the normal lens. *Physiol. Rev.* **77**:21-50.
- Mathias, R. T., Varadaraj, K., Kumari, S., Baldo, G. J., Shiels, A., and Bassnett, S. Water transport by Aquaporin 0 in the lens. *Association for research in vision and ophthalmology ARVO.* 2002.
- Murata, K., K.Mitsuoka, T.Hirai, T.Walz, P.Agre, J.B.Heymann, A.Engel, and Y.Fujiyoshi. 2000. Structural determinants of water permeation through aquaporin-1. *Nature.* **407**:599-605.
- Nemeth-Cahalan, K.L. and J.E.Hall. 2000. pH and calcium regulate the water permeability of aquaporin 0. *J. Biol. Chem.* **275**:6777-6782.
- Peracchia, C. and S.J.Girsch. 1985. Functional modulation of cell coupling: evidence for a calmodulin-driven channel gate. *Am. J. Physiol.* **248**:H765-H782.
- Peracchia, C., S.J.Girsch, G.Bernardini, and L.L.Peracchia. 1985. Lens junctions are communicating junctions. *Curr. Eye Res.* **4**:1155-1169.
- Preston, G.M., T.P.Carroll, W.B.Guggino, and P.Agre. 1992. Appearance of water channels in *Xenopus* oocytes expressing red cell CHIP28 protein. *Science* **256**:385-387.
- Sui, H., B.G.Han, J.K.Lee, P.Walian, and B.K.Jap. 2001. Structural basis of water-specific transport through the AQP1 water channel. *Nature* **414**:872-878.
- Varadaraj, K., C.Kushmerick, G.J.Baldo, S.Bassnett, A.Shiels, and R.T.Mathias. 1999. The role of MIP in lens fiber cell membrane transport. *J. Membr. Biol.* **170**:191-203.

3

CENTRAL ROLE OF THE Ca^{2+}_i REGULATORY SITE IN IONIC AND METABOLIC MODULATION OF $\text{Na}^+/\text{Ca}^{2+}$ EXCHANGER IN DIALYZED SQUID AXONS

Luis Beaugé^{1*} and Reinaldo DiPolo^{2*}

1. INTRODUCTION

The work presented below shows that in dialyzed squid axons the $\text{Na}^+/\text{Ca}^{2+}$ exchanger is completely insensitive to changes in extracellular pH in the range from 6 to 8.8, while in the same range it is largely affected by changes in the pH on the cytosolic side. Intracellular protons are powerful inhibitors of the exchanger; this inhibition is antagonized by Ca^{2+}_i , enhanced by Na^+_i and markedly diminished by MgATP. In addition, H^+_i increases inhibition by Na^+_i . Two sets of experimental data indicate that all these effects involve the Ca^{2+}_i regulatory site: (i) The apparent affinity for Ca^{2+}_i stimulation of the $\text{Na}^+_i/\text{Na}^+_o$ exchange is drastically reduced by H^+_i , an effect that is antagonized by MgATP; and (ii) the sulfhydryl group blocking agent pCMBS, that reduces the affinity for Ca^{2+}_i of the intracellular regulatory site and makes it insensitive to MgATP, also blocks the effects of intracellular H^+ on the $\text{Na}^+_i/\text{Na}^+_o$ and the $\text{Ca}^{2+}_i/\text{Na}^+_o$ exchange fluxes. Thus, the four cysteine residues found near the Ca^{2+} -binding region of the large intracellular loop are then likely to play an important role in H^+_i , Na^+_i , Ca^{2+}_i and MgATP regulation of the exchanger. Finally, these results are predicted by a model where the Ca^{2+}_i regulatory site, essential for binding of Na^+_i or Ca^{2+}_i to the transporting sites but not for cation translocation, becomes the center of all ionic and metabolic regulation of the squid nerve $\text{Na}^+/\text{Ca}^{2+}$ exchanger.

¹ Laboratorio de Biofísica, Instituto de Investigación Médica Mercedes y Martín Ferreyra, Casilla de Correo 389, 5000 Córdoba, Argentina.

² Laboratorio de Permeabilidad Iónica, Centro de Biofísica y Bioquímica, Instituto Venezolano de Investigaciones Científicas (IVIC), Apartado Postal 21287, Caracas 1020-A, Venezuela

* corresponding authors: lbeauge@immf.uncor.edu; rdipolo@ivic.ve

The $\text{Na}^+/\text{Ca}^{2+}$ exchanger comprises a family of plasma membrane component proteins that carry out a countertransport of Na^+ and Ca^{2+} ions between the intra and extracellular environments. The system works reversibly and is electrogenic in the sense that 1 Ca^{2+} is exchanged for 3 Na^+ ions (Blaustein and Lederer, 1999) or perhaps 4 (Fujioka *et al.*, 2000). In some groups of exchangers Na^+ and Ca^{2+} are the sole transported cations; this is the case in mammalian heart and squid nerve. In others, such as platelets and retinal rod cells, K^+ ions are transported together with Na^+ in exchange for Ca^{2+} (Blaustein and Lederer, 1999). Thermodynamic considerations indicate that the net flux of the transported species will depend on their relative concentrations and the affinities of the transporting sites at both membrane sides as well as the electrical transmembrane potential (Stein, 1986). This means that, depending on the conditions, one could observe net Ca^{2+} extrusion in exchange for external Na^+ (heterologous forward mode) or net Ca^{2+} uptake in exchange for internal Na^+ (heterologous reverse mode). Two additional homologous modalities of cation translocation have also been demonstrated: $\text{Ca}^{2+}_i/\text{Ca}^{2+}_o$ and $\text{Na}^+_i/\text{Na}^+_o$ exchange (DiPolo and Beaugé, 1990). For all these operative partial reactions it has been shown that Ca^{2+}_i binding to an intracellular regulatory non-transporting site is an essential requisite (DiPolo and Beaugé, 1999). Under physiological conditions the exchanger works almost exclusively in the Ca^{2+} extrusion mode, except perhaps during the plateau of the decaying phase of the action potential in the heart, where it has been suggested that a reverse $\text{Na}^+/\text{Ca}^{2+}$ exchange current plays an important role (McAlister and Noble, 1966; Mullins, 1981). This chapter describes data obtained mainly from the squid nerve exchanger but also refers to important aspects of the exchanger from the mammalian heart, two preparations that have given the most relevant information on the regulation of this countertransporter. There are two important aspects of these systems related to this work: structure and regulation. The structure of both exchangers is composed of a little less than one thousand amino acids with several transmembrane segments and a large intracellular loop between membrane segments 5 and 6. This loop, with a mass of about one half of the total protein, is the region where regulation, including splicing, takes place (Philipson and Nicoll, 2000). Taking aside splicing, the regulatory processes can be divided into two types: (i) ionic, among them Na^+_i inactivation, Ca^{2+}_i stimulation and H^+_i modulation, and (ii) metabolic, related mainly to ATP phosphorylations and, in the squid, also to the phosphorylation by the phosphagen phosphoarginine (Hilgemann, 1997; DiPolo and Beaugé, 1999; Blaustein and Lederer, 1999). However, this division among types of regulation is somehow arbitrary since, as will be pointed out later, both are closely interrelated. For instance, it is known that in both squid nerve and mammalian heart, intracellular Ca^{2+} and ATP antagonize Na^+_i inhibition (Requena, 1978; Hilgemann and Matsuoka, 1992). Interestingly, in the mammalian heart, H^+_i inhibition is enhanced by Na^+_i (Doering and Lederer, 1994). In this article we describe how ionic and metabolic interactions may be part of the same regulatory kinetic process.

2. METHODS

We performed internal dialysis of squid giant axon from *Loligo pealei* at the Marine Biological Laboratory, Woods Hole, MA, USA, and *Loligo plei*, at the Instituto Venezolano de Investigaciones Científicas. Once dissected, the axons were mounted into the dialysis chamber and dialyzed using capillary fibers of regenerated cellulose (210 μm OD; 200 μm ID; Spectrapor Number 132226; Spectrum, Houston, Texas) (DiPolo and Beaugé, 1999) that allow permeation of solutes up to a MW cutoff of 18 kD but have practically no water permeability. The usual dialysis solution contained (mM): Tris-Mops, 385; NaCl, 40; ionized Mg^{2+} , 1; Glycine, 285; Tris-EGTA, 1 or 1-3 mM BAPTA or Dibromo BAPTA when intracellular pH varied (a pH of 7.3 is considered normal for these cells). The standard external solution had (mM); NaCl, 440; CaCl_2 , 0.3; MgCl_2 , 60; Tris-Cl (pH 7.6), 10. Osmolarity was adjusted to 940 mosmols per liter. The concentrations of ionized Ca^{2+} were estimated with the WinMaxc computer program (Version 2.00, 1999; Chris Patton Hopkins Marine Station, CA, USA). Concentrations of Ca^{2+}_i from 0.3 to 0.7 μM were buffered with BAPTA and from 1.2 μM to 10 μM with Dibromo BAPTA. Concentrations of Ca^{2+}_i higher than 10 μM were taken as equal to the CaCl_2 added in excess to that required to obtain 10 μM . Removal of extracellular Na^+ was compensated with Li^+ . ATP production was minimized by adding 1 mM NaCN to the external media. Sodium channels were blocked with 100 nM TTX. The Ca^{2+} and the Na^+/K^+ pumps were inhibited by including 100 μM vanadate into the dialysis media. In a typical experiment the axon was pre-dialyzed for about 45 minutes with the standard medium containing 0.2 mM EGTA and no calcium or ATP. The addition of ATP (3 mM) to the dialysis solution was done at a constant free $[\text{Mg}^{2+}]_i$ of 1 mM. Steady-state $^{45}\text{Ca}^{2+}$ or $^{22}\text{Na}^+$ effluxes were measured before and after changing the experimental conditions; in this way, each axon served as its own control. BAPTA and Dibromo BAPTA were from Molecular Probes (Molecular Probes, Eugene, OR). All other reagents were from SIGMA (St Louis, MO). Temperature was 17-18°C.

3. RESULTS AND DISCUSSION

Some old, but important results in dialyzed squid axons, are summarized in Figure 1. They show that while intracellular acidification inhibits the $\text{Na}^+/\text{Ca}^{2+}$ exchanger, changing the extracellular proton concentration over the same range (about two orders of magnitude) has no influence on these fluxes. This is indeed quite relevant because it means that the effect of protons are asymmetric. In turn, it implies that H^+_i inhibition does not represent simple competition with the cations for their transporting sites because, if that were the case, one would expect to see at least some effect on both membrane sides.

We are analyzing here the intracellular interactions between ionic (H^+ , Na^+ and Ca^{2+}) and metabolic (ATP) regulations of the $\text{Na}^+/\text{Ca}^{2+}$ exchanger in squid nerves under steady-state conditions. To do this we have, in some way, dissected individual interactions, and then tried to build a consistent overall picture. The first step deals with the inhibition by H^+_i of the forward-exchange mode in the absence of Na^+_i . Without MgATP the results will reflect solely the interactions between H^+_i and Ca^{2+}_i . Upon addition of ATP, results will show how these ion concentrations are influenced by metabolic regulation.

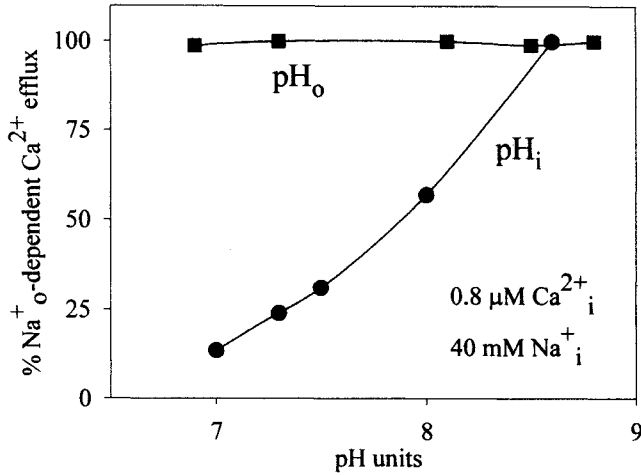


Figure 1. Forward $\text{Na}^+/\text{Ca}^{2+}$ exchange in squid axons dialyzed with standard solutions containing $0.8 \mu\text{M Ca}^{2+}$ and no ATP at different pH_i and pH_o . Note that pH_o is ineffective while intracellular acidification inhibits the exchanger. Recalculated from data of DiPolo, R., and Beaugé, L., 1982, The effect of pH on Ca extrusion mechanisms in dialyzed squid axons, *Biochim. Biophys. Acta*, 688:237-245. Reprinted in modified form with permission from Elsevier Science.

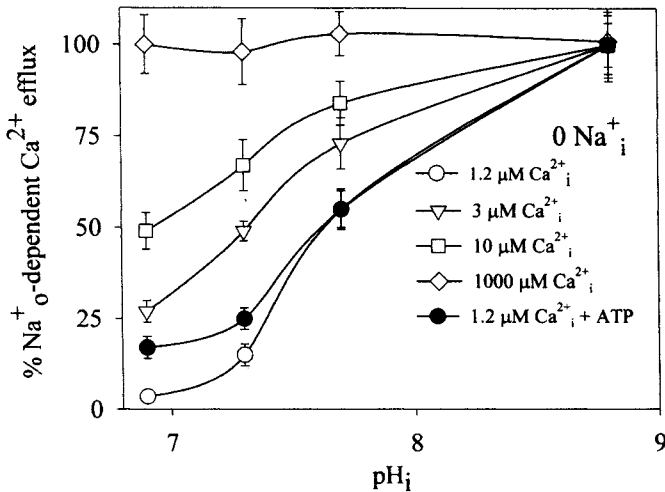


Figure 2. Effect of pH_i on the forward $\text{Na}^+/\text{Ca}^{2+}$ exchange in dialyzed squid axons, at four different $[\text{Ca}^{2+}]_i$, 1.2 μM , 3 μM , 10 μM and 1,000 μM in the absence of Na^+_i . The graph is a plot of the percentage inhibition as a function of pH_i , taking as 100 percent the values of the Na^+_o -dependent Ca^{2+} efflux obtained for each $[\text{Ca}^{2+}]_i$ at a pH_i of 8.8. Open symbols represent axons dialyzed without ATP. Filled circles are axons dialyzed with 3 mM MgATP. Error bars indicate S.E.M. Recalculated from data of DiPolo R., and Beaugé L., 2002, MgATP counteracts intracellular proton inhibition of the Sodium Calcium exchanger in dialyzed squid axons, *J. Physiol.*, 539:791-803. Reprinted in modified form with permission from The Journal of Physiology.

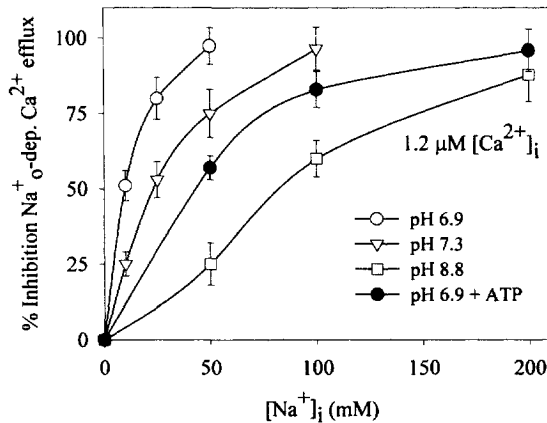


Figure 3. Effect of $[\text{Na}^+]_i$ on the forward $\text{Na}^+/\text{Ca}^{2+}$ exchange at three different pH_i values: 6.9, 7.3 and 8.8 in dialyzed squid axons. The graph is a plot of the percentage inhibition as a function of $[\text{Na}^+]_i$ compared to the fluxes obtained in the absence of Na^+ at each pH_i . Open symbols represent axons dialyzed without ATP; filled circles are axons dialyzed with 3 mM MgATP. Error bars indicate S.E.M. Recalculated from data of DiPolo R., and Beaugé L., 2002, MgATP counteracts intracellular proton inhibition of the Sodium Calcium exchanger in dialyzed squid axons, *J. Physiol.*, 539:791-803. Reprinted in modified form with permission from The Journal of Physiology.

In Figure 2 the steady-state Na^+ -dependent Ca^{2+} efflux, obtained at $[\text{Ca}^{2+}]_i$, from 1.2 μM to 1000 μM , is plotted as a function of intracellular pH . For each $[\text{Ca}^{2+}]_i$ we arbitrarily took as 100 percent the values of the fluxes at a pH_i of 8.8. In the absence of MgATP (open symbols) and a $[\text{Ca}^{2+}]_i$ of 1.2 μM , 3 μM and 10 μM , protons inhibit the forward $\text{Na}^+/\text{Ca}^{2+}$ exchange. However, the fractional inhibition is reduced as $[\text{Ca}^{2+}]_i$ increases. At 1000 μM $[\text{Ca}^{2+}]_i$ protons have no effect on the exchanger. Taken altogether, these results show (i) that H^+ inhibits the $\text{Na}^+/\text{Ca}^{2+}$ exchanger in the absence of Na^+ , and (ii) antagonism between H^+ and Ca^{2+} at the intracellular side of the exchanger. In cardiac myocytes under patch-clamp conditions in the absence of Na^+ , Doering and Lederer (1994) also found that H^+ inhibits the exchanger. However, they could not find conclusive evidence that Ca^{2+} antagonizes H^+ in that preparation. The filled circles in Figure 2 reflect the effects of H^+ at 1.2 μM Ca^{2+} in the presence of 3 mM MgATP. Interestingly, above pH_i 7.7 MgATP is completely ineffective. Below this pH_i the nucleotide counteracts proton inhibition, an effect that is more noticeable at the physiological pH of 7.3 and below. Actually, between pH_i 7.3 and pH_i 6.9 inhibition is substantial (75 %) in the absence of MgATP, and is less marked (32 %) in its presence.

In guinea-pig cardiac sarcolemma subjected to patch clamp there is a synergism between Na^+ and H^+ in the inhibition of the $\text{Na}^+/\text{Ca}^{2+}$ exchanger (Doering and Lederer, 1994). The existence of this $\text{Na}^+ - \text{H}^+$ interaction was explored in dialyzed squid axons. In these experiments the steady-state forward $\text{Na}^+/\text{Ca}^{2+}$ exchange was followed at three different pH_i 's: 6.9, 7.3 and 8.8, as a function of $[\text{Na}^+]_i$, from zero up to 200 mM and at a constant $[\text{Ca}^{2+}]_i$ of 1.2 μM . Figure 3 is a plot of the percentage of Na^+ inhibition at each pH . In addition, the effect of 3 mM MgATP was also investigated at pH 6.9 (filled

symbols). The figure shows that as $[Na^+]_i$ increases, a progressive inhibition of the forward Na^+_o/Na^+_i exchange occurs, and this is the case at every pH_i investigated. An additional important result is that Na^+_i became a more powerful inhibitor as pH_i was reduced. The $K_{0.5}$ for this effect of Na^+_i was 90 mM at pH 8.8, 40 mM at the physiological pH of 7.3 and 10 mM at pH 6.9. Therefore, in squid axons, H^+_i and Na^+_i inhibit the Na^+_o/Na^+_i exchanger synergistically. Moreover, the concentration-response curves suggest that at pH 8.8, more than one Na^+ is involved, whereas a single Na^+ ion kinetics can account for the data at pH_i 7.3 and 6.9. The filled circles in Figure 3 indicate that 3 mM MgATP strongly antagonizes Na^+_i inhibition at pH 6.9. Notice that inhibition is almost non-existent at 10 mM Na^+_i whereas 50% inhibition requires 100 mM Na^+_i ; i.e. MgATP has increased tenfold the apparent affinity for Na^+_i inhibition at pH 6.9. Other experiments not presented here show that at an alkaline pH of 8.8, inhibition by Na^+_i was markedly reduced while the addition of ATP barely modified it. In other words, Na^+_i inhibition of the Na^+_o/Na^+_i is antagonized by both ATP and alkalization. This favors the hypothesis that MgATP modulation occurs by counteracting H^+_i inhibition.

The experiments described so far provide evidence for a H^+_i inhibition of the Na^+_o/Na^+_i exchanger, which is antagonized by Ca^{2+}_i and MgATP and is enhanced in a mutual synergistic way, by Na^+_i . What is not yet known is at which sites all these interactions take place. For instance, there are two intracellular loci in the Na^+_o/Na^+_i exchanger where Ca^{2+} ions can bind: transport and regulatory. It is already known that MgATP stimulates the exchanger by increasing the affinity for the Ca^{2+}_i regulatory site. As MgATP also antagonizes Na^+_i - H^+_i inhibition (see Hilgemann, 1977; DiPolo and Beaugé, 1999; Blaustein and Lederer, 1999), the Ca^{2+}_i regulatory site appears as a likely candidate. To investigate this possibility we looked at the effects of pH_i on the homologous Na^+_o/Na^+_i exchange mode through the Na^+_o/Na^+_i exchanger which requires the binding of Ca^{2+}_i to its regulatory site but, obviously, not to the transporting sites. The actual experiment consisted in measuring the Ca^{2+}_i stimulation of a Na^+_o -dependent $[^{22}Na]Na^+$ efflux under different conditions at a constant physiological $[Na^+]_i$ of 40 mM. The results are illustrated in Figure 4 where open symbols correspond to axons dialyzed with ATP-free solutions and filled circles to those with 3 mM MgATP. Without ATP and at pH_i 6.9, Ca^{2+}_i activates Na^+_o/Na^+_i exchange with a $K_{0.5}$ around 20 μ M; the value of this $K_{0.5}$ decreases to 2 μ M at the physiological pH_i of 7.3 and to 0.4 μ M at pH_i 8.8. The conclusion is that H^+_i reduces the apparent affinity of the Ca^{2+}_i regulatory site for Ca^{2+}_i . These results concur with those of Hilgemann and Matsuoka (1992) who found that alkalization of the cytoplasmic side of guinea-pig cardiac cells increases the affinity for Ca^{2+}_i stimulation of the Na^+_o/Na^+_i exchanger outward current. Although not shown in this figure, the levels of the Na^+_o -dependent Na^+ efflux attained at saturating $[Ca^{2+}]_i$ were almost the same at pH_i 6.9 or 8.8, indicating that protons have no effect on the rate of Na^+ translocation. The role of ATP in these processes can also be deduced from the results in Figure 4. At pH_i 6.9, the $K_{0.5}$ for Ca^{2+}_i stimulation of Na^+_o/Na^+_i exchange is reduced from 20 μ M to about 3 μ M by the addition of 3 mM MgATP; i.e., ATP counteracts H^+_i inhibition by increasing the affinity of the Ca^{2+}_i regulatory site for Ca^{2+}_i . Here again, alkalization and addition of MgATP have similar effects.

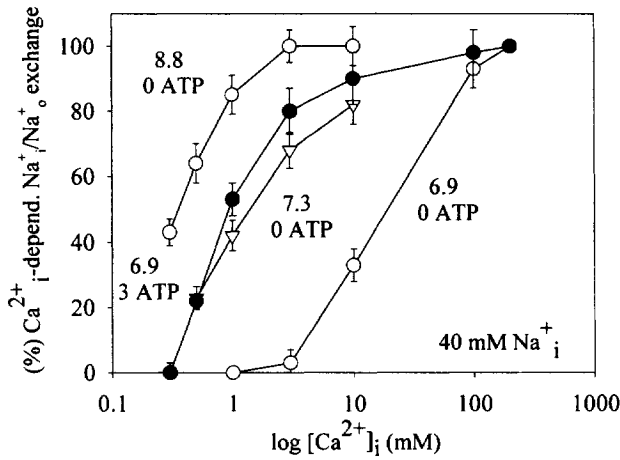


Figure 4. Stimulation by Ca^{2+}_i of the Na^+_o/Na^+_i exchange through the Na^+/Ca^{2+} exchanger in dialyzed squid axons at pH_i values of 6.9, 7.3 and 8.8. The graph is a plot of the percentage stimulation of the $(Ca^{2+}_i + Na^+_o)$ -dependent $[^{22}Na]Na^+$ efflux as a function of $[Ca^{2+}]_i$. A value of 100 percent was given to the maximal efflux obtained in each condition. Open symbols represent axons dialyzed without ATP; filled circles are axons dialyzed with 3 mM MgATP. Error bars indicate S.E.M. Reproduced from DiPolo R., and Beaugé L., 2002, MgATP counteracts intracellular proton inhibition of the Sodium Calcium exchanger in dialyzed squid axons, *J. Physiol.*, 539:791-803, with permission from The Journal of Physiology.

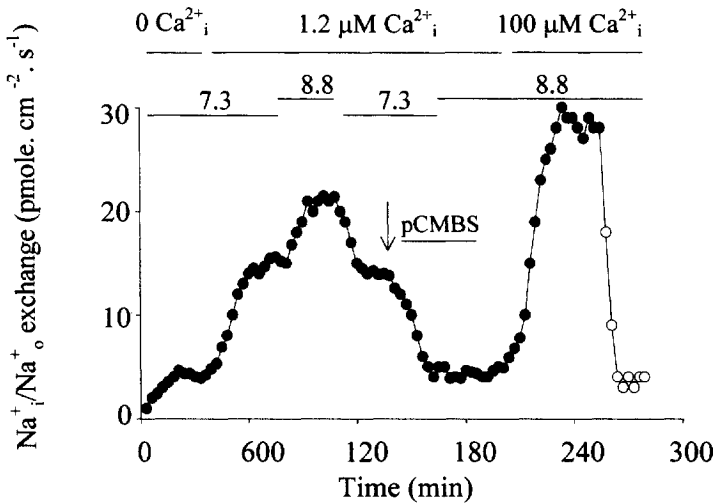


Figure 5. Effect of pCMBS on the alkalization-induced increase in the Na^+_o -dependent Na^+ efflux (Na^+_o/Na^+_i exchange) catalyzed by the Na^+/Ca^{2+} exchanger in an axon dialyzed without ATP. The numbers above the lines represent the values of $[Ca^{2+}]_i$ and pH_i . The arrow indicates the beginning, and the line the duration, of exposure to 1 mM pCMBS in the cytosol. At the end of the experiment the $[Ca^{2+}]_i$ was increased to saturating values to reactivate the flux to its normal levels. Reproduced from DiPolo R., and Beaugé L., 2002, MgATP counteracts intracellular proton inhibition of the Sodium Calcium exchanger in dialyzed squid axons, *J. Physiol.*, 539:791-803, with permission from The Journal of Physiology.

There is more experimental evidence indicating that the H^+_i - Ca^{2+}_i and H^+_i - ATP antagonisms occur at or by modifying the affinity of the Ca^{2+}_i regulatory site. The sulfhydryl blocking reagent p-chloromercuriphenylsulfonic acid (pCMBS) changes the reactivity of the Ca^{2+}_i regulatory site preventing the MgATP-dependent increase in its affinity for Ca^{2+}_i but without altering the V_{max} of the Na^+/Ca^{2+} exchange fluxes (DiPolo and Beaugé, 1993). Therefore, the expectation would be that after pCMBS treatment the exchanger will not respond to changes in pH_i . These expectations were borne out. Figure 5 describes one of these experiments where the Na^+_i/Na^+_o exchange reaction was used as a tool. The experiment started measuring a steady-state Na^+ efflux in the absence of Ca^{2+}_i and ATP at pH_i 7.3. Upon addition of $1.2 \mu M Ca^{2+}_i$, the anticipated activation of the Na^+_o -dependent Na^+ efflux is observed. This efflux of Na^+ increased further at pH_i 8.8 and returned back to its pH_i 7.3 level. The inclusion of 1 mM pCMBS fully inhibits the Ca^{2+}_i -activated Na^+_o -dependent Na^+ efflux and under this condition, alkalinization to pH_i 8.8 does not modify the levels of the Na^+_o/Na^+_i exchange. As shown before (DiPolo and Beaugé, 1993), pCMBS does not induce a non-specific inhibition of the exchanger because when $[Ca^{2+}_i]$ is raised to $100 \mu M$ the levels of fluxes are similar to those obtained without pCMBS and all are Na^+_o -dependent (open circles represent Na^+_o -free, lithium sea water). Similar results were found for the forward Na^+_o -dependent Ca^{2+} efflux (DiPolo and Beaugé, 2002).

240	D R R L L N K Y L S K K Y R A S K Q K G V I V Q C	C-264
265	E G Q D A E A G E G K S E D G A L K E G G D D V E	
290	V R E F E Q H R K E Y I E I L R E M R K K N P T L	
305	D M K T L E D M A E S E A V N R G P K S R A F Y R	
330	I Q A T R K L T G S G N I I K K A K A Q A G V A Q	
355	P I V I D Q K P E D E I T R V S F D P G H Y T V M	
380	<u>E N V G T F Y G T V T R E G G D L T K T L Y V D Y</u>	
405	<u>K T E D G T A N A G S D Y V Y A E G T L V F Y P M</u>	
430	<u>E T H K Q F P I S I I D D D I F E E D E H F Y I R</u>	
455	<u>L S N L R V G D S N G L F E S G Q A E A K A Q L A</u>	
480	<u>N P F L A T V M I L D D D H P G I F Q I D E K E M</u>	
505	<u>S V T E S S G E V E V R I I R T S G A R G C V K V</u>	C-536
530	P F H S V D G T A T Y G K D Y E L V D K D V I F D	
555	N D E T E K F L R V R V V D D E E Y E K N E T F F	
580	I W L D E P Y L V K K P T G S S S G S V V E D D D	
605	P V L A E L G K P R R G E N I K I T V H I I E S T	
630	E F K S V V D K L L K K A N L S L V V G T S S W R	
655	E Q F I E A I T V N A E G D D D D E E G E E E K L	
680	P S C M D Y I M H F V C L F W K V L F A F V P P T	C-692
705	D Y W G	C-701

Figure 6. Amino acid composition of the large intracellular loop of the squid Na^+/Ca^{2+} exchanger. The XIP region is indicated in cursive and the Ca^{2+} -binding domain is underlined. The regulatory Ca^{2+} -binding sites are the two groups, of three aspartyl residues each represented in bold cursive. Cysteine residues (C263, C532, C690 and C699) are in regular bold. Constructed from data of He et al. (1998) based on the work of Levitsky et al. (1994).

Therefore, these data strongly suggest that intracellular proton inhibition and MgATP stimulation of the Na^+/Ca^{2+} exchanger involve interaction/s with the Ca^{2+}_i regulatory site

without significantly affecting the affinities of the Na^+ or Ca^{2+} transporting sites or the translocation rates of these cations.

We have recently proposed an integrated model that can account for intracellular H^+ - Na^+ - Ca^{2+} - MgATP steady-state modulation of the squid $\text{Na}^+/\text{Ca}^{2+}$ exchanger (DiPolo and Beaugé, 2002), where the intracellular Ca^{2+} regulatory site plays a central role. Adequate fitting to the experimental results required that two H^+ bind sequentially with association constants of 10^9 for the first proton binding and 10^8 for the proton binding second. There are several amino acid residues that can fulfill these requirements, among them cysteine (pKa's 1.8, 8.3 and 10.8) that strongly reacts with pCMBS. As mentioned in the introduction, it is now known that all ionic and metabolic (ATP) regulation of the $\text{Na}^+/\text{Ca}^{2+}$ exchanger take place at the large intracellular loop (Philipson and Nicoll, 2000). Figure 6, constructed from data of He *et al.* (1998), gives the amino acid composition of this loop in the squid exchanger. It has a high degree of homology with that of the mammalian heart, particularly in the regulatory regions (Philipson and Nicoll, 2000). The Ca^{2+} binding domain (underlined) has two consensus regions of three aspartyl residues each (bold cursive). In what is relevant to this work, there are four cysteine residues in the loop: C264 (near the end of the XIP region), C536 (21 residues after the end of the Ca^{2+} -binding region), and further down, C692 and C701. Levitsky *et al.*, (1994) have identified the high-affinity Ca^{2+} -binding sites of the cardiac $\text{Na}^+/\text{Ca}^{2+}$ exchanger, and have also shown that binding of Ca^{2+} to those sites markedly modifies the electrophoretic mobility of the isolated expressed loop. As the authors concluded, it is quite likely that those changes in mobility represent conformational changes of the protein. Using a similar approach we will continue our studies of ionic and metabolic regulation of the squid $\text{Na}^+/\text{Ca}^{2+}$ exchanger looking for conformational changes in the isolated loop as influenced by H^+ , Na^+ , Ca^{2+} , MgATP , pCMBS and mutation of the cysteine residues.

4. ACKNOWLEDGMENTS

Supported by Grants from NSF, USA (IBN-01309962), FONCYT, Argentina (PICT99 05-5118) and CONICIT, Venezuela (S1- 99000946)

5. REFERENCES

- Blaustein, M. P., and Lederer, W. J., 1999, Sodium/Calcium Exchange: its physiological implications, *Physiol. Rev.*, **79**:764-830.
- DiPolo, R., and Beaugé, L., 1982, The effect of pH on Ca extrusion mechanisms in dialyzed squid axons, *Biochim. Biophys. Acta*, **688**:237-245.
- DiPolo, R., and Beaugé, L., 1993, In squid axons the Ca(i) regulatory site of the Na/Ca exchanger is drastically modified by sulphhydryl blocking agents. Evidences that intracellular regulatory and transport sites are different, *Biochim. Biophys. Acta*, **1145**:75-84.
- DiPolo, R., and Beaugé, L., 1990, Calcium Transport in Excitable Cells. In *Intracellular Calcium Regulation*, F. Bronner, ed., Alan R. Liss, New York, pp. 381-413.
- DiPolo, R., and Beaugé, L., 1999, Metabolic pathways in the regulation of invertebrate and vertebrate $\text{Na}^+/\text{Ca}^{2+}$ exchange, *Biochim. Biophys. Acta*, **1422**:57-71.
- DiPolo, R., and Beaugé, L., 2002, MgATP counteracts intracellular proton inhibition of the Sodium Calcium exchanger in dialyzed squid axons, *J. Physiol.*, **539**:791-803.
- Doering, A.E. and Lederer, W.J., 1994, The action of Na^+ as a cofactor in the inhibition by cytoplasmic protons of the cardiac $\text{Na}^+/\text{Ca}^{2+}$ exchanger in the guinea-pig. *J. Physiol.*, **480**:9-20.

- Fujioka, Y., Hiroe, K. and Matsuoka, S., 2000, Regulation kinetics of the Na^+ - Ca^{2+} exchange in guine-pig ventricular myocytes, *J. Physiol.*, **529**:611-623.
- He, Z., Tong, Q., Quednau, B.D., Philipson, K.D., Hilgemann, D.W., 1998, Cloning, expression, and characterization of the squid Na^+ - Ca^{2+} exchanger (NCX-SQ1), *J. Gen. Physiol.*, **111**:857-873.
- Hilgemann, D.W., 1997, Cytoplasmic ATP-dependent regulation of ion transporters and channels: Mechanism and messenger, *Ann. Rev. Physiol.*, **59**:193-220.
- Hilgemann, D.W and Matsuoka, S., 1992, Steady-state and dynamic properties of cardiac sodium-calcium exchanger. Secondary modulation by cytoplasm calcium and ATP, *J. Gen. Physiol.*, **100**:933-961.
- Levitsky, D.O., Nicoll, D.A., Philipson, K.D., 1994. Identification of the high affinity Ca^{2+} -binding domain of the cardiac Na^+ - Ca^{2+} exchanger. *J. Biol. Chem.* **269**:22847-22852.
- McAlister, R., and Noble, D., 1966, The time and voltage dependence of the slow outward current in cardiac Purkinje fibres, *J. Physiol.*, **186**:632-662.
- Mullins, L.J., 1981, Ion Transport In Heart, Raven Press Books, Ltd., New York.
- Philipson, K.D., and Nicoll, D.A., 2000, Sodium-calcium exchange: a molecular perspective, *Ann. Rev. Physiol.*, **62**:111-133.
- Requena, J. 1978. Calcium efflux from squid axons under constant sodium electrochemical gradient, *J. Gen. Physiol.*, **72**:443-470.
- Stein, W.D., 1986, Transport and diffusion across cell membranes, Academic Press Inc., San Diego.

CALCIUM DEPENDENCE OF CALCIUM RELEASE CHANNELS (RYANODINE RECEPTORS) FROM SKELETAL AND CARDIAC MUSCLE

Cecilia Hidalgo^{1,2*}, Paulina Donoso¹ and Ricardo Bull¹

1. INTRODUCTION

In this work, we compare the effects of free $[Ca^{2+}]$ on the activity of the Ryanodine receptors, the intracellular calcium channels responsible for calcium release in mammalian skeletal and cardiac muscle. In lipid bilayer experiments, all native channels displayed more than one calcium dependence, albeit with different frequencies depending on channel origin. Following incubation with oxidizing agents, skeletal and cardiac channels modified their calcium dependencies sequentially, and displayed a significant increase in activity. We also studied the effects of Ca^{2+} on the kinetics of Ca^{2+} release from sarcoplasmic reticulum vesicles isolated from skeletal or cardiac mammalian muscle. Native skeletal vesicles exhibited maximal stimulation of release kinetics by 10-20 μM $[Ca^{2+}]$, whereas in native cardiac vesicles, maximal stimulation of release required only 1 μM $[Ca^{2+}]$. At pCa 5, the oxidant thimerosal increased the stimulation of release kinetics in skeletal or cardiac vesicles. We propose that channel redox state controls the high affinity sites responsible for calcium activation of channel activity, and we discuss the possible physiological and pathological implications of these results.

¹ Instituto de Ciencias Biomédicas, Facultad de Medicina, Universidad de Chile, Casilla 70005, Santiago 7, Chile.

² Centro de Estudios Científicos, Valdivia, Chile.

* corresponding autor: chidalgo@machi.med.uchile.cl

The cytosolic free Ca^{2+} concentration, which is precisely regulated in all cells, can increase rapidly and transiently in response to various types of stimuli (Berridge *et al.*, 1997). Two different receptors mediate the fast release of Ca^{2+} from intracellular stores, the IP_3 -gated calcium channels and the Ryanodine receptors/calcium release channels (RyR channels) that mediate calcium release in skeletal and cardiac muscle.

The physiological mechanisms of activation of RyR channels differ in skeletal and cardiac muscle (Lamb, 2000). The RyR2 channels of cardiac muscle are activated directly by Ca^{2+} entering the cells through voltage-activated L-type Ca^{2+} channels (Bers, 2002). This process is a classical example of Ca^{2+} -induced Ca^{2+} release (CICR), an amplification mechanism by means of which a localized $[\text{Ca}^{2+}]$ increase generated by Ca^{2+} entry induces Ca^{2+} release from the stores, significantly increasing the first signal. In skeletal muscle, in contrast, Ca^{2+} release from the SR does not require Ca^{2+} entry into cells. The RyR1 channels of skeletal muscle open following membrane depolarization, presumably by direct coupling with plasma membrane voltage sensors (Ríos and Pizarro, 1991). In fact, CICR in mammalian skeletal muscle has been questioned because this tissue does not present spontaneous Ca^{2+} sparks (Shirokova *et al.*, 1998). The drastic inhibition of skeletal RyR1 channels by Mg^{2+} observed *in vitro* may be responsible for the lack of CICR observed in this tissue (Meissner *et al.*, 1986; Moutin and Dupont, 1988; Donoso *et al.*, 2000).

Multiple cellular components and reactions regulate RyR channels (Meissner, 1994; Coronado *et al.* 1994; Franzini-Armstrong and Protasi, 1997; Zucchi and Ronca-Testoni, 1997). These include ions such as Ca^{2+} , Mg^{2+} and protons, cyclic ADP-ribose, ATP and other adenine nucleotides, interaction with several proteins, and metabolic reactions including phosphorylation and oxidation. Due to its central role as a channel agonist, it is important to characterize how Ca^{2+} affects RyR channel activity and how other ions or metabolic reactions normally occurring in cells modulate the effects of Ca^{2+} on the channels.

In the present work, we will present experiments showing the different calcium dependencies of native skeletal and cardiac RyR channels. We also show how oxidation modified the calcium dependence of RyR channels incorporated in planar bilayers as well as CICR kinetics from SR vesicles isolated from skeletal or cardiac mammalian muscle.

2. METHODS

2.1. Membrane Preparations

SR vesicles enriched in triads were isolated from rabbit fast skeletal muscle in the presence of a combination of protease inhibitors, as described previously (Hidalgo *et al.*, 1993). Cardiac sarcoplasmic reticulum vesicles were isolated from rabbit or canine hearts as described (Marengo *et al.*, 1998, Inui *et al.*, 1998). All procedures were done according to the "Position of the American Heart Association on Research and Animal Use" and the guidelines of the Animal Care Committee of the Faculty of Medicine, University of Chile. SR vesicles were stored at $-80\text{ }^\circ\text{C}$ for up to one month. The protein content of membrane fractions was determined according to Hartree (1972) using bovine serum albumin as standard.

2.2. Bilayer Experiments

Channel recording and analysis was performed as described in detail previously (Bull and Marengo, 1994; Marengo *et al.*, 1996). All experiments were carried out at room temperature (22 - 24°C). Open probability values (P_o) were calculated from single channel records lasting at least 180 s. The recording conditions were: 40 mM Ca^{2+} -HEPES, 15 mM HEPES/Tris, pH 7.4 in the *trans* compartment; 225 mM HEPES/Tris, pH 7.4 and variable $[\text{Ca}^{2+}]$ in the *cis* compartment. To set the desired *cis* $[\text{Ca}^{2+}]$, 0.5 mM total Ca^{2+} and sufficient N-(2-hydroxyethyl)-ethylenediamine-triacetic acid (HEDTA) or ethyleneglycol-bis(β -aminoethyl ether) N, N, N', N'-tetraacetic acid (EGTA) were added to the *cis* compartment. Resulting *cis* $[\text{Ca}^{2+}]$ values were routinely checked with a calcium electrode. After channel incorporation into the bilayer and establishment of recording conditions (Bull and Marengo, 1994), oxidation was carried out as detailed previously (Marengo *et al.*, 1998).

Calcium release kinetics. Ca^{2+} release kinetics were determined in a SX.18MV stopped-flow spectrofluorometer from Applied Photophysics Ltd. (Leatherhead, U.K.) following the procedures described in detail elsewhere (Donoso *et al.*, 2000). Before inducing release, vesicles were actively or passively loaded with Ca^{2+} as described (Donoso *et al.*, 2000). The increase in extravesicular $[\text{Ca}^{2+}]$ produced by release was determined by measuring the fluorescence of a Ca^{2+} indicator (1 μM) selected according to the $[\text{Ca}^{2+}]$ range of the release solution (Donoso *et al.*, 2000). Release solutions contained (final concentrations): 1.2 mM free ATP, variable free $[\text{Ca}^{2+}]$ and $[\text{Mg}^{2+}]$, 20 mM Mops/Tris, pH 7.2.

Materials. All reagents used were of analytical grade. Lipids were obtained from Avanti Polar Lipids, Inc., Birmingham, AL. Thimerosal, dithiothreitol and protease inhibitors (Leupeptin, Pepstatin A, benzamidin and phenylmethylsulfonyl fluoride) were obtained from Sigma Chemical Co. All fluorescent calcium indicators used in this work were from Molecular Probes, Inc.

3. RESULTS AND DISCUSSION

3.1. Calcium Dependence of Native Skeletal or Cardiac RyR Channels

3.1.1. Native RyR channels in bilayers.

The activity of all channels studied in this work was modulated by *cis* $[\text{Ca}^{2+}]$. As illustrated in Figure 1, RyR channels from mammalian skeletal or cardiac muscle showed more than one calcium dependence, as reported previously (Marengo *et al.*, 1998). In skeletal RyR channels, the most frequently observed calcium dependence was bell-shaped, with activation by μM $[\text{Ca}^{2+}]$ and inhibition by 0.5 mM $[\text{Ca}^{2+}]$. Most often, skeletal channels presented hyperbolic activation by μM $[\text{Ca}^{2+}]$ to P_o values > 0.2 , with $K_a = 1.4 \mu\text{M}$. Increasing $[\text{Ca}^{2+}]$ to 0.5 mM produced inhibition of channel activity, with $K_i = 130 \mu\text{M}$. Less frequently, we observed channels which never attained P_o values > 0.1 in the entire $[\text{Ca}^{2+}]$ range studied. Only occasionally, skeletal RyR1 channels displayed a third calcium dependence: they presented activation by μM $[\text{Ca}^{2+}]$ and kept increasing their activity on increasing $[\text{Ca}^{2+}]$ to 0.5 mM, reaching P_o values close to unity. This third calcium

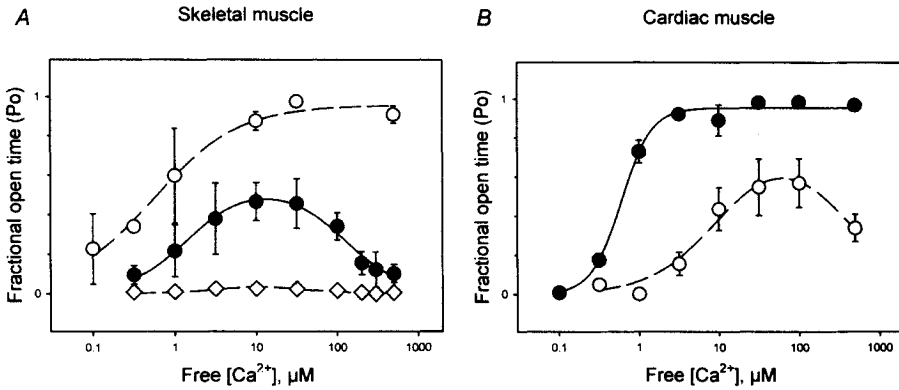


Figure 1. Effect of *cis* $[Ca^{2+}]$ on the activity of RyR-channels derived from skeletal (A) or cardiac (B) muscle SR vesicles. The panels show the changes in P_o as a function of *cis* $[Ca^{2+}]$. The solid lines indicate the calcium dependence most frequently observed. Values are given as Mean \pm S.E.

dependence, in contrast, was the most frequently observed behavior displayed by cardiac RyR2 channels. The activation of cardiac channels with this calcium dependence was sigmoidal ($n = 2$), with $K_a = 0.6 \mu M$. Less frequently, RyR2 channels presented bell-shaped calcium dependence with P_o values > 0.2 in the $\mu M [Ca^{2+}]$ range (Figure 1).

3.1.2. Release experiments with native RyR channels.

The bilayer experiments described above were done under steady state conditions. To collect data in a time domain compatible with physiological release rates, we measured Ca^{2+} release kinetics in a stopped flow fluorescence spectrophotometer. All vesicular preparations displayed Ca^{2+} release time courses that followed either single or double exponential functions; each exponential function was characterized by its rate constant k , that is directly linked to channel activity (Donoso *et al.*, 1995). The k values of double exponential functions differed in magnitude by at least 5-fold. Accordingly, when release followed a double exponential time course we selected only the higher k values as an indication of the channel response to a sudden $[Ca^{2+}]$ jump. We measured the Ca^{2+} dependence of release through RyR channels at a constant free [ATP] of 1.2 mM to induce maximal channel activation (Bull, R. and Behrens, M.I., unpublished observations). Figure 2 illustrates how changing free $[Ca^{2+}]$ modifies the relative values of k in cardiac and skeletal SR vesicles. In both cases, a bell shaped curve characterized the Ca^{2+} dependence of the rate constant k .

Skeletal SR vesicles displayed a Ca^{2+} dependence with maximal relative values of k in the $[Ca^{2+}]$ range 10-20 μM (Figure 2, A). The absolute values of k varied from 40 to 50 s^{-1} in this $[Ca^{2+}]$ range. Decreasing or increasing free $[Ca^{2+}]$ beyond this range produced a significant decrease in release rate constants, to values $< 3 s^{-1}$. These results indicate that 10-20 $\mu M [Ca^{2+}]$ enhanced markedly Ca^{2+} release from native skeletal SR vesicles. The most frequently observed calcium dependence of RyR1 channels in bilayers was comparable to the calcium dependence of the release rate constants bilayers

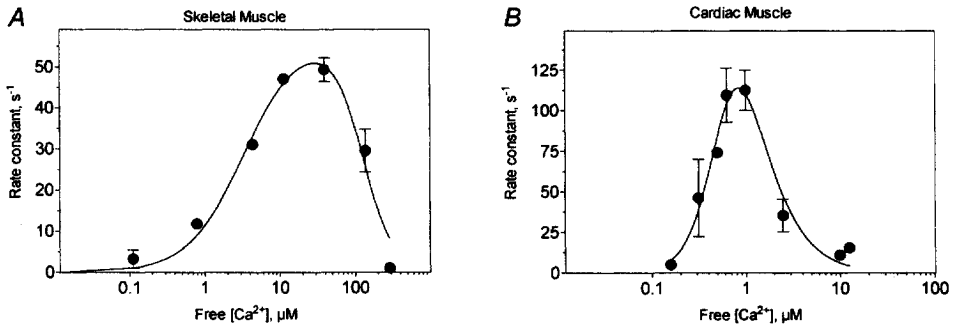


Figure 2. Calcium dependence of Ca²⁺ release rate constants from SR vesicles isolated from skeletal (A) and cardiac (B) muscle. Release kinetics were measured as described in the text. Fluo 3 was used for determinations at pCa 6.8 and 6.5, Calcium Green 2 for pCa 6.3 and 6.2 and Calcium Green 5N for pCa ≤ 6.. Release rate constant values were obtained from non-linear fits of exponential Ca²⁺ release records. Data represent Mean ± S.E. from independent determinations in 2-6 different preparations.

was comparable to the calcium dependence of the release rate constants measured in skeletal SR vesicles.

In cardiac SR vesicles the highest k values, which varied around 110 s^{-1} , were obtained in $1 \mu\text{M}$ free $[\text{Ca}^{2+}]$ (Figure 2, B). We observed a marked decrease in release rate constants at lower or higher $[\text{Ca}^{2+}]$ values. Thus k had an average value of 5.1 s^{-1} at $0.1 \mu\text{M}$ $[\text{Ca}^{2+}]$, whereas at $10 \mu\text{M}$ $[\text{Ca}^{2+}]$ k was 11.0 s^{-1} .

In contrast to the behavior of RyR1 channels, the two types of calcium dependencies displayed by RyR2 channels were very different to the dependence of k values. A similar finding was described by Chu *et al.* (1993), who found that free $[\text{Ca}^{2+}]$ which did not affect RyR2 channels in bilayers inhibited Ca²⁺ release from cardiac vesicles. These results suggest that RyR2 channels behave differently when exposed to sudden $[\text{Ca}^{2+}]$ changes than when exposed to the same $[\text{Ca}^{2+}]$ for a sustained period. Previous findings (Fabiato, 1985) indicate that the rate of calcium release in skinned cardiac Purkinje fibers depends not only on the trigger $[\text{Ca}^{2+}]$ but also on the time taken to reach that trigger $[\text{Ca}^{2+}]$. A model was proposed whereby the RyR2 channels inactivation sites bind Ca²⁺ with higher affinity but with lower association rates than activating sites (Fabiato, 1985). Additionally, it is possible that other vesicular proteins affect RyR2 channel function when the channels are forming part of the SR than when incorporated into the lipid bilayer.

These combined results show that even in the constant presence of 1.2 mM free $[\text{ATP}]$, μM free $[\text{Ca}^{2+}]$ enhanced markedly Ca²⁺ release kinetics from both skeletal and cardiac SR vesicles. However, activation and inhibition of release by Ca²⁺ was significantly shifted to the left in cardiac SR when compared to skeletal SR vesicles. Furthermore, the maximal absolute values of k were about two-fold higher in cardiac than in skeletal SR. Assuming these results reflect the behavior of RyR channels *in vivo*, cardiac muscle release would be most efficient in $1 \mu\text{M}$ free $[\text{Ca}^{2+}]$. However, Ca²⁺ release *in vivo* occurs in the presence of $0.7\text{-}1 \text{ mM}$ free $[\text{Mg}^{2+}]$. We have found recently

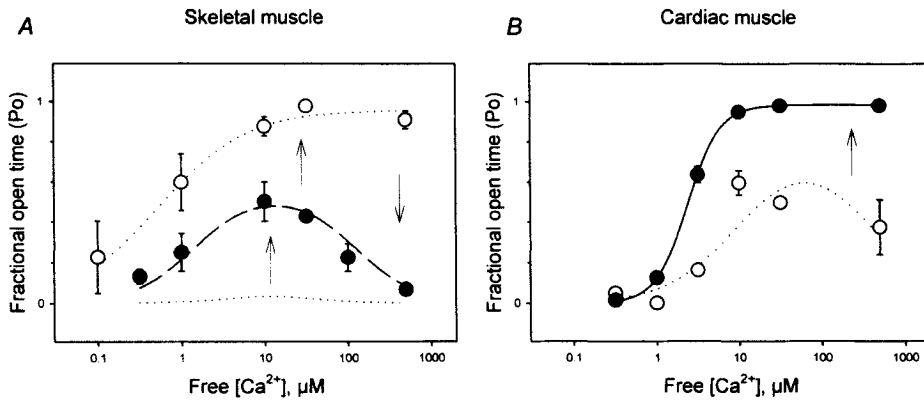


Figure 3. Effect of *cis* $[Ca^{2+}]$ on the activity of RyR-channels derived from skeletal (A) or cardiac (B) SR vesicles after oxidation. The panels show the changes in P_o as a function of *cis* $[Ca^{2+}]$ for RyR-channels from A: rabbit skeletal muscle or B: rabbit cardiac muscle. Values are given as Mean \pm S.E.

that at these concentrations Mg^{2+} is a very effective inhibitor of CICR from cardiac muscle at pCa 6 but not at pCa 5. In the presence of 0.8 mM free $[Mg^{2+}]$, k values at 1 μM and 10 μM free $[Ca^{2+}]$ were undistinguishable (Hidalgo *et al.*, 2002).

3.2. Calcium dependence of oxidized skeletal or cardiac RyR channels

The redox status of the channel protein affects RyR channel activity, as determined with different experimental approaches. Changes in redox state of RyR channels from skeletal or cardiac muscle modifies single channel P_o (Abramson *et al.*, 1995; Favero *et al.*, 1995; Eager *et al.*, 1997; Marengo *et al.*, 1998). Changes in redox state also affect Ryanodine binding (Abramson *et al.*, 1995; Favero *et al.*, 1995; Aghdasi *et al.*, 1997; Suko and Hellman, 1998) and Ca^{2+} release from SR vesicles (Trimm *et al.*, 1986; Zaidi *et al.*, 1989; Prabhu and Salama, 1990; Salama *et al.*, 1992; Abramson *et al.*, 1995).

3.2.1. Oxidized RyR channels in bilayers.

As illustrated in Figure 3, oxidation of skeletal or cardiac RyR channels produced a sequential increase in channel activity, and modified the calcium dependence of all channels studied. Skeletal RyR1 channels that exhibited bell-shaped calcium dependence with maximal $P_o < 0.1$ changed in two steps following oxidation (Marengo *et al.*, 1998). Likewise, following incubation with thimerosal, cardiac channels with a bell-shaped calcium dependence increased their activity and were no longer inhibited by 0.5 mM $[Ca^{2+}]$ (Marengo *et al.*, 1998).

We investigated next whether SH-reducing agents modified the calcium dependencies of native channels and reversed the changes in channel response to *cis* $[Ca^{2+}]$ produced by oxidation. Native or oxidized RyR channels from cardiac muscle, which displayed high

Table 1. Effect of oxidation on the rate constants of CICR^a

Rate constant, s ⁻¹	
Skeletal SR vesicles	
Control	19.3 ± 7.7 (7)
+ 0.25 mM Thimerosal	40.9 ± 2.1 (3)
Cardiac SR vesicles	
Native vesicles	11.0 ± 4.1 (8)
+ 0.25 mM Thimerosal	34.9 ± 6.3 (3)

^aRelease was measured at pCa 5, as described in the text. Values represent Mean ± SD. In parentheses, number of determinations.

addition of SH-reducing agents, as reported previously (Marengo *et al.*, 1998). We observed the same behavior in RyR channels from amphibian skeletal muscle (data not shown). However, after incubation with SH reducing reagents muscle RyR channels never changed to the lowest activity bell-shaped calcium dependence (Marengo *et al.*, 1998).

3.2.2. Release experiments with oxidized RyR channels.

We have reported previously that thimerosal stimulates CICR kinetics from skeletal SR vesicles (Donoso *et al.*, 2000). In the absence of Mg²⁺, skeletal SR vesicles incubated with either 250 μM or 500 μM thimerosal displayed at pCa 5 release rate constant values significantly higher than native vesicles, as illustrated in Table 1. Likewise, we found that incubation with 250 μM thimerosal produced a significant increase in k values in cardiac SR vesicles (Table 1). In contrast, incubation of skeletal SR vesicles with 10 mM glutathione (GSH) for up to 30 min at 25 °C had no effect on CICR kinetics (data not shown).

These combined results indicate that CICR in skeletal and cardiac SR vesicles is stimulated by thimerosal. It remains to be tested *in vivo* if oxidation of RyR channels with endogenous redox agents stimulates CICR in mammalian skeletal muscle.

We propose that the oxidation state of the channel protein is a decisive factor in determining the calcium dependence of the activity exhibited by the RyR1 and RyR2 channel isoforms. If *in vivo* these channel isoforms behaved as *in vitro*, oxidative stress should enhance CICR in skeletal and cardiac muscle cells. The changes in calcium dependence may involve molecular rearrangement of channel protein segments produced by oxidation of critical SH residues, which somehow increase the Ca²⁺ affinity of cytoplasmic activating sites and hinder Ca²⁺ binding to low affinity inhibitory sites.

4. CONCLUSIONS

Tissue specific RyR channel isoforms mediate skeletal and cardiac muscle contraction. Consequently, redox modifications of RyR channel activity should have important consequences regarding the function of muscle cells. A concomitant increase in reactive oxygen species and cytoplasmic free $[Ca^{2+}]$ has been observed in muscle in conditions such as hypoxia and reperfusion following ischemia (Kaneko *et al.*, 1994). The present results suggest that, through the resulting enhancement of CICR, oxidation of RyR channels may contribute to the increase in cytoplasmic $[Ca^{2+}]$ observed in these pathological conditions.

In summary, the results shown in this work suggest that redox modifications of RyR channels will affect Ca^{2+} signaling in mammalian cardiac and skeletal muscle cells. In both cases, oxidation produced a significant increase in RyR single channel activity and Ca^{2+} release. It remains to be tested *in vivo* whether Ca^{2+} release through the skeletal RyR channels – activated by the voltage sensors - is further amplified through CICR when the muscle is exposed to an increase in ROS or to other oxidative conditions. Likewise, whether channel oxidation enhances CICR through cardiac RyR channels *in vivo* remains an open question. Reversible activation of cardiac RyR channels by oxidation could be of relevance in the heart, especially when there is an increase in free radical production such as in ischemia/reperfusion situations (Menshikova and Salama, 2000). In any case, the present results suggest that sustained or uncontrolled oxidation of RyR channels may elicit an imbalance in Ca^{2+} homeostasis. If not compensated, this imbalance may trigger cell death through apoptosis or necrosis.

5. ACKNOWLEDGMENTS

The contributions of Gina Sánchez and Paula Aracena in some of the experiments are gratefully acknowledged. This study was supported by the Chilean Fondo Nacional de Investigación Científica y Tecnológica grant 8980009. We also acknowledge the institutional support to the Centro de Estudios Científicos by Empresas CMPC. The Centro de Estudios Científicos is a Millennium Institute funded in part by Fundación Andes and the Tinker Foundation.

6. REFERENCES

- Abramson J. J., A. C. Zable, T. G. Favero and G. Salama. 1995. Thimerosal interacts with the Ca^{2+} release channel ryanodine receptor from skeletal muscle sarcoplasmic reticulum. *J. Biol. Chem.* **270**: 29644-29647.
- Aghdasi, B., M. B. Reid and S.L. Hamilton. 1997. Nitric oxide protects the skeletal muscle Ca^{2+} release channel from oxidation induced activation. *J. Biol. Chem.* **272**:25462-25467.
- Berridge M. J., Lipp, P. and Bootman, M. D. 2000. The versatility and universality of calcium signalling. *Nat Rev Mol Cell Biol*, **1**: 11-21.
- Bers, D. M. 2002. Cardiac excitation-contraction coupling. *Nature* **415**:198-205.
- Bull, R., and J. J. Marengo. 1994. Calcium-dependent halothane activation of sarcoplasmic reticulum calcium channels from frog skeletal muscle. *Am. J. Physiol.* **266** (Cell Physiol. 35): C391-C396.
- Chu, A., M. Fill, E. Stefani and M. L. Entman. 1993. Cytoplasmic Ca^{2+} does not inhibit the cardiac muscle sarcoplasmic reticulum ryanodine receptor Ca^{2+} channel, although Ca^{2+} -induced Ca^{2+} inactivation of Ca^{2+} release is observed in native vesicles. *J. Membr. Biol.* **135**:49-59.

- Coronado, R., J. Morrisette, M. Sukhareva, and D. N. Vaughan. 1994. Structure and function of ryanodine receptors. *Am. J. Physiol.* **266** (Cell Physiol. 35): C1485-C1504.
- Donoso, P., H. Prieto and C. Hidalgo. 1995. Luminal calcium regulates calcium release in triads isolated from frog and rabbit skeletal muscle. *Biophys. J.* **68**: 507-515.
- Donoso, P., P. Aracena and C. Hidalgo. 2000. SH oxidation overrides Mg^{2+} inhibition of calcium induced calcium release in skeletal muscle triads. *Biophys. J.* **79**:279-286.
- Eager, K. R., L. D. Roden, and A. F. Dulhunty. 1997. Actions of sulfhydryl reagents on single ryanodine receptor Ca^{2+} -release channels from sheep myocardium. *Am. J. Physiol.* **272** (Cell Physiol. 41): C1908-C1918.
- Fabiato, A. 1985. Time and calcium dependence of activation and inactivation of calcium-induced release of calcium from the sarcoplasmic reticulum of a skinned canine cardiac Purkinje cell. *J. Gen. Physiol.* **85**:247-289.
- Favero, T. G., A. C. Zable, and J. J. Abramson. 1995. Hydrogen peroxide stimulates the Ca release channel from skeletal muscle sarcoplasmic reticulum. *J. Biol. Chem.* **270**: 25557-25563.
- Franzini-Armstrong C. and F. Protasi. 1997. Ryanodine receptors of striated muscles: a complex channel capable of multiple interactions. *Physiol. Rev.* **77**: 699-729.
- Hartree, E. F. 1972. Determination of protein: a modification of the Lowry method that gives a linear photometric response. *Analytical Biochem.* **48**, 422-427.
- Hidalgo, C., J. Jorquera, V. Tapia, and P. Donoso. 1993. Triads and transverse tubules isolated from frog skeletal muscle contain high levels of inositol 1,4,5-trisphosphate. *J. Biol. Chem.* **268**: 15111-15117.
- Hidalgo, C., P. Aracena, G. Sánchez and P. Donoso. 2002. Redox regulation of calcium release in skeletal and cardiac muscle. *Biol. Res.*, in press.
- Inui, M., S. Wang, A., Saito and S. Fleischer. 1988. Characterization of junctional and longitudinal sarcoplasmic reticulum from heart muscle. *J. Biol. Chem.* **263**:10843-10850.
- Kaneko, M., Y. Matsumoto, H. Hayashi, A. Kobayashi, and N. Yamazaki. 1994. Oxygen free radicals and calcium homeostasis in the heart. *Mol. Cell Biochem.* **139**: 91-100.
- Lamb G. D. 2000. Excitation-contraction coupling in skeletal muscle: comparisons with cardiac muscle. *Clin Exp Pharmacol Physiol.* **27**:216-224.
- Menshikova, E. V. and G. Salama. 2000. Cardiac ischemia oxidizes regulatory thiols on ryanodine receptors: captopril acts as a reducing agent to improve Ca^{2+} uptake by ischemic sarcoplasmic reticulum. *J. Cardiovasc. Pharmacol.* **36**:656-668.
- Meissner, G. 1994. Ryanodine receptor/ Ca^{2+} release channels and their regulation by endogenous effectors. *Annu. Rev. Physiol.* **56**: 485-508.
- Meissner, G., E. Darling and J. Eveleth. 1986. Kinetics of rapid Ca^{2+} release by sarcoplasmic reticulum. Effects of Ca^{2+} , Mg^{2+} , and adenine nucleotides. *Biochemistry* **25**: 236-244.
- Moutin M. J. and Y. Dupont. 1988. Rapid filtration studies of Ca^{2+} -induced Ca^{2+} release from skeletal sarcoplasmic reticulum. Role of monovalent ions. *J Biol Chem*, **263**: 4228-4235.
- Prabhu, S.D. and G. Salama. 1990. Reactive disulfide compounds induce Ca^{2+} release from cardiac sarcoplasmic reticulum. *Arch Biochem Biophys*, **282**: 275-283.
- Ríos, E. and G. Pizarro. 1991. Voltage sensor of excitation-contraction coupling in skeletal muscle. *Physiol. Rev.* **71**: 849-908.
- Salama, G., J. J. Abramson, and G. K. Pike. 1992. Sulfhydryl reagents trigger Ca^{2+} release from the sarcoplasmic reticulum of skinned rabbit psoas fibres. *J Physiol*, **454**: 389-420.
- Shirokova N., J.Garcia and E. Ríos. 1998. Local calcium release in mammalian skeletal muscle. *J Physiol*, **512** (Pt 2): 377-384.
- Suko, J. and G. Hellman. 1998. Modification of sulfhydryls of the skeletal muscle calcium release channel by organic mercurial compounds alters Ca^{2+} affinity of regulatory Ca^{2+} sites in single channel recordings and [3H]ryanodine binding. *Biochem. Biophys. Acta* **1404**:435-450.
- Trimm, J. L., G.Salama and J. J. Aramson. 1986. Sulfhydryl oxidation induces rapid calcium release from sarcoplasmic reticulum vesicles. *J Biol Chem*, **261**: 16092-16098.
- Zaidi, N. F., C. F. Lagenaur, J. J. Abramson, I Pessah and G. Salama. 1989. Reactive disulfides trigger Ca^{2+} release from sarcoplasmic reticulum via an oxidation reaction. *J Biol Chem*, **264**: 21725-21736.
- Zucchi R., and S. Ronca-Testoni. 1997. The sarcoplasmic reticulum Ca^{2+} channel/ryanodine receptor: modulation by endogenous effectors, drugs and disease states. *Pharmacol. Rev.* **49**: 1-51.

MODULATION OF RYANODINE RECEPTOR CHANNELS FROM RAT BRAIN CORTEX IN LIPID BILAYERS

María Isabel Behrens¹, Juan José Marengo², José Pablo Finkelstein³, and Ricardo Bull^{3,*}

1. INTRODUCTION

Endoplasmic reticulum RyR channels from rat brain cortex were studied at the single channel level in planar lipid bilayers. The channels were activated by caffeine and locked by ryanodine at the characteristic subconductance state. RyR channels displayed either poor activation by Ca^{2+} (low P_o channels), moderate, bell-shaped Ca^{2+} activation (moderate P_o channels) or high, sigmoid Ca^{2+} activation (high P_o channels). Oxidation of RyR channels with thimerosal or 2,2'-dithiodipyridine changed the calcium dependence sequentially, from low to moderate to high P_o , and the action of reducing agents restored the original behavior. At 10 μM cytoplasmic $[\text{Ca}^{2+}]$, ATP activated RyR low, moderate, and high P_o channels, but with different affinity; low P_o channels required higher $[\text{ATP}]$ for activation than moderate P_o channels, and these required higher $[\text{ATP}]$ than high P_o . Addition of cADPR (in the presence of 100 nM calmodulin) increased 2-fold the activity of channels with moderate Ca^{2+} activation, when measured at 10 μM cytoplasmic $[\text{Ca}^{2+}]$. In contrast, cADPR had no effect on the activity of low P_o channels. These combined results suggest that the redox state of RyR channels from brain modulates their response to calcium, ATP, and cADPR, which may have important physiological implications.

The release of calcium through ryanodine receptor (RyR) channels of endo/sarcoplasmic reticulum is a highly regulated process that underlies many cellular responses (Berridge, 2000; Futatsugi *et al.*, 1999; Carafoli, 2002). Several agonists/modulators, such as caffeine, Ca^{2+} , and ATP, are known to activate RyR channels of cardiac and skeletal muscle (Meissner, 1994; Zucchi and Ronca-Testoni, 1997). On the

¹ Departamento de Neurología y Neurocirugía, Facultad de Medicina, Universidad de Chile.

² Programa de Patología, ICBM, Facultad de Medicina, Universidad de Chile, Santiago, Chile.

³ Programa de Fisiología y Biofísica, ICBM, Facultad de Medicina, Universidad de Chile, Santiago, Chile.

* corresponding autor: rbull@med.uchile.cl

other hand, RyR channels from brain tissue have been less well studied.

The first studies describing channel properties of brain ryanodine receptors in planar lipid bilayers show that these channels are activated by millimolar [ATP] (Ashley, 1989; McPherson *et al.*, 1991; Lai *et al.*, 1992) and caffeine (McPherson *et al.*, 1991). Ryanodine receptors purified from bovine brain are activated by calcium at micromolar concentrations (Lai *et al.*, 1992). Moreover, rat brain RyR channels present three different calcium dependencies (Marengo *et al.*, 1996). Cyclic ADPR (cADPR) is a naturally occurring metabolite of NADP, which has been shown to activate Ca^{2+} release from intracellular stores in different tissues (Lee *et al.*, 1994; Lee, 2001; Li *et al.*, 2001; Mészáros *et al.*, 1993; Iino *et al.*, 1997). The response to cADPR is known to require the presence of calmodulin (Lee, 2001). There is much controversy on whether the increase in intracellular $[\text{Ca}^{2+}]$ induced by cADPR occurs by the activation of RyR channels or through a different route (Morrisette *et al.*, 1993; Fruen *et al.*, 1994; Copello *et al.*, 2001). Calcium flux studies in brain microsomes show that cADPR induces ryanodine-sensitive Ca^{2+} release (Mészáros *et al.*, 1993; White *et al.*, 1993). However, the effect of cADPR at the level of single RyR channels in brain has not yet been reported.

The RyR channel protein possesses many SH residues (Takeshima *et al.*, 1989; Otsu *et al.*, 1990; Nakashima *et al.*, 1997). Oxidation, alkylation or S-nitrosylation of some highly reactive SH residues has been shown to increase vesicular Ca^{2+} release and to activate RyR-channels in bilayers (Eager *et al.*, 1997; Abramson *et al.*, 1995; Favero *et al.*, 1995; Donoso *et al.*, 1997, 2000, Feng *et al.*, 2000, Sun *et al.*, 2001; Liu *et al.*, 1994). It has been proposed that RyR-channels may function as intracellular redox sensors (Xia *et al.*, 2000; Eu *et al.*, 2000; Feng *et al.*, 2000). SH oxidation also modifies channel modulation by agonists and inhibitors (Marengo *et al.*, 1998; Suko *et al.*, 2000; Donoso *et al.*, 2000; Xia *et al.*, 2000, Oba *et al.*, 2002). In particular, we have shown that the oxidation state of SH residues of the channel molecule play a central role in determining the calcium dependence of RyR-channels from different tissues (Marengo *et al.*, 1998). Here we summarize our work on the effects of various agonists/modulators on RyR-channels present in the endoplasmic reticulum (ER) from rat brain cortex.

2. MATERIALS AND METHODS

2.1. Membrane Preparation

ER vesicles enriched in RyR were obtained from rat (Sprague-Dawley) brain cortex as described previously using dithiothreitol (DTT) as SH reducing agent during all stages of the preparation (Marengo *et al.*, 1996).

2.2. Channel Recording and Analysis

Planar phospholipid membranes were painted with a mixture of palmitoyloleoyl phosphatidylethanolamine (POPE), phosphatidylserine (PS), and phosphatidylcholine (PC) in the proportion POPE:PS:PC = 5:3:2. Lipids were dissolved in decane to a final concentration of 33 mg/ml. ER vesicles were fused with the bilayer as described previously (Bull and Marengo, 1994; Marengo *et al.*, 1996). After fusion, the cis (cytoplasmic) compartment, where the vesicles were added, was perfused with 5-10 times the compartment volume of a solution containing 225 mM HEPES/Tris, pH 7.4. To obtain the desired cytoplasmic free calcium at least 0.5 mM Ca-HEPES plus enough N-(2-hydroxyethyl)-ethylenediamine-triacetic acid (HEDTA) or ethyleneglycol-bis(β -aminoethyl ether) N, N, N', N'-tetraacetic acid (EGTA) were added to this compartment. In the experiments where activation by ATP was studied, 10 mM HEDTA was used. The amount of calcium, calcium buffer, and/or ATP required were calculated with the program WinMAXC (www.stanford.edu/~cpatton/wmaxc.zip) using the parameters provided in the file bers.tcm. The trans (intrareticular) compartment was replaced with 40 mM Ca-HEPES, 10 mM Tris-HEPES, pH 7.4. The experiments were carried out at room temperature (22 - 24°C), with membranes held at 0 mV. Voltage was applied to the cis compartment, and the trans compartment was held at virtual ground through an operational amplifier in a current-to-voltage configuration. Current signals were both recorded on tape and acquired online. For analysis, data were filtered at 400 Hz (-3 dB) using an eight-pole low-pass Bessel type filter (902 LPF, Frequency Devices Inc., Haverhill, MA) and digitized at 2 kHz with a 12 bit A/D converter (Labmaster DMA interface, Scientific Solutions, Inc., Solon, OH) using Axotape software (Axon Instruments, Inc., Burlingame, CA). Fractional open time (P_o) was computed from records of 60 s or longer using pClamp software (Axon Instruments, Inc., Burlingame, CA). SH oxidizing agents thimerosal or 2,2'-dithiodipyridine (DTDP) or the reducing agent glutathione (GSH) were added to the cytoplasmic compartment. The reaction was stopped by removal of the non-reacted reagent through extensive perfusion of the compartment (5-10 times the compartment volume) with a solution containing 225 mM HEPES/Tris, pH 7.4 (Marengo *et al.*, 1998).

Materials. Lipids were obtained from Avanti Polar Lipids, Inc., Birmingham, AL. cADPR was purchased from Calbiochem, San Diego, CA. Protease inhibitors and all other reagents were obtained from SIGMA Chemical Co., St. Louis, MO.

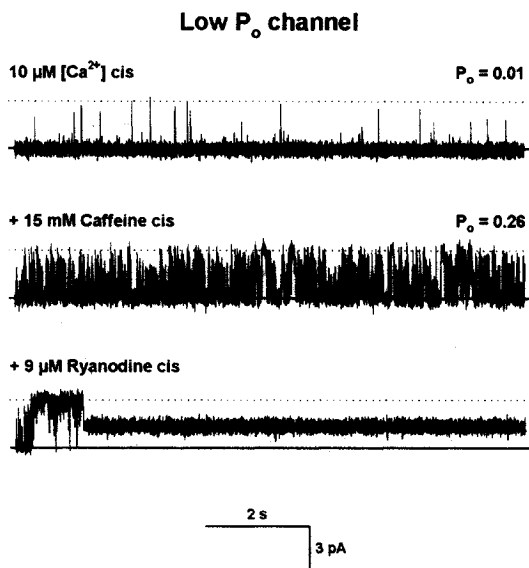


Figure 1. RyR channels from rat brain cortex are activated by caffeine and locked by ryanodine at a subconductance state. Representative current records of a low P_o channel were obtained at 10 μM cytoplasmic free $[\text{Ca}^{2+}]$ before (upper trace) and after addition of caffeine (middle trace). Subsequent addition of ryanodine (lower trace) locked the channel at the typical subconductance level.

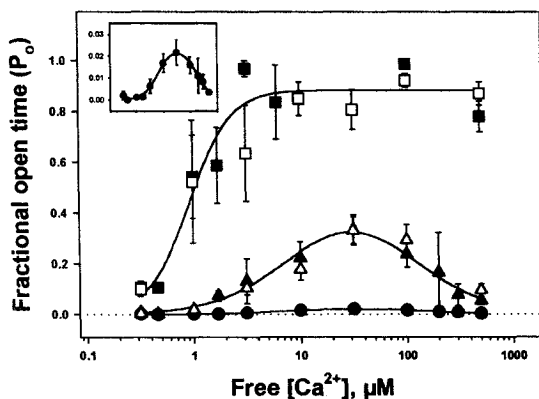


Figure 2. Calcium dependence of native and oxidized RyR channels. Fractional open times of low (circles), moderate (triangles) and high (squares) P_o channels as a function of cytoplasmic $[\text{Ca}^{2+}]$. Mean P_o values \pm S.E.M of native channels (filled symbols) and oxidized channels (open symbols) are given. Solid lines represent the best nonlinear fits of native channel data. Insert: activity of low P_o channels is shown in an amplified vertical scale.

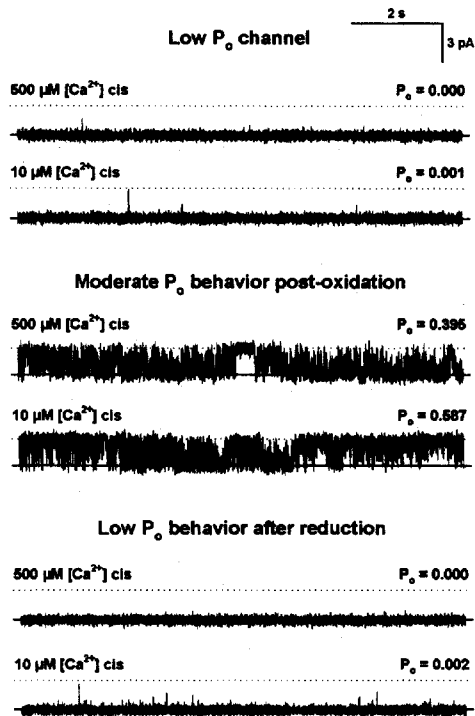


Figure 3. Reversibility of the change in calcium dependence induced by SH oxidation. The upper two current records show a native channel displaying low P_o calcium dependence. Following oxidation with 7 μM thimerosal the channel showed moderate P_o behavior (middle set of current records). After reduction with 8 mM GSH the channel presented again the low P_o response (lower set of records).

3. RESULTS AND DISCUSSION

3.1. Brain RyR Channels are Activated by Caffeine and Show the Characteristic Response to Ryanodine

RyR channels from rat brain were activated by mM concentrations of caffeine, a characteristic of all RyR channels studied to date (Rousseau *et al.*, 1988; Coronado *et al.*, 1994; Herrmann-Frank *et al.*, 1999). Fig. 1 (upper trace) shows the activity of a channel that was poorly activated by 10 μM free cytoplasmic $[\text{Ca}^{2+}]$. This type of behavior was the most frequent response to cytoplasmic calcium (low P_o) of brain RyR channels incorporated in a lipid bilayer (see below). Addition of 15 mM caffeine activated the channel increasing P_o from 0.01 to 0.26 (Fig.1). Activation of RyR channels by caffeine in the millimolar range has been described in brain channels (McPherson *et al.*, 1991).

The channels studied in this work were modified by ryanodine. Fig. 1 (lower trace) shows the effect of 9 μM ryanodine added to the cytoplasmic compartment. Ryanodine

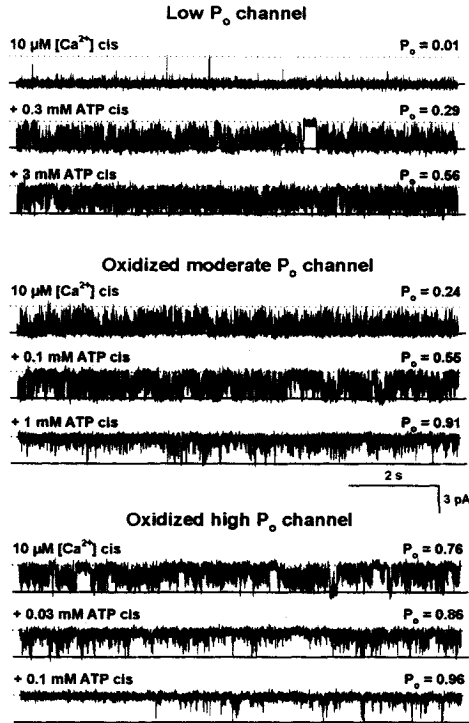


Figure 4. Activation by ATP of single RyR-channels that displayed different responses to cytoplasmic $[Ca^{2+}]$. Representative current traces obtained with a channel that spontaneously displayed low P_o behavior (upper panel) and with channels that after treatment with thimerosal acquired moderate (middle panel) or high (lower panel) P_o behavior are depicted. Records were obtained at $10 \mu M$ cytoplasmic free $[Ca^{2+}]$ using $10 mM$ HEDTA as calcium buffer, before and after addition of ATP to the cytoplasmic compartment. Free $[ATP]$ values and average P_o values, calculated from at least 120 s of continuous records, are given at the upper left and right of each trace, respectively. Membrane was held at $0 mV$. Channels open upwards. Data were filtered at $200 Hz$ ($-3 dB$) with a low-pass digital Gaussian filter for display.

locked the channel in the characteristic subconductance level with $\sim 40\%$ conductance and P_o near unity (Rousseau *et al.*, 1987).

3.2. Calcium Dependence of Native and Oxidized RyR-channels

All channels recorded in this work were activated by cytoplasmic $[Ca^{2+}]$, however three different responses to changes in free $[Ca^{2+}]$ were observed, in agreement with our previous report (Marengo *et al.*, 1996). The most frequently encountered behavior (Fig. 2, filled circles), displayed poor activation by calcium with P_o less than 0.1 at all $[Ca^{2+}]$ tested (low P_o channels) (Marengo, 1996; Copello *et al.*, 1997). A less frequent behavior observed with brain RyR channels (moderate P_o channel; Fig. 2 filled triangles) is characterized by a moderate, bell-shaped activation by calcium, with inhibition at $[Ca^{2+}] \geq 0.1 mM$ (Smith *et al.*, 1986; Fill *et al.*, 1990; Chu *et al.*, 1993). An even less frequently observed behavior is the

high P_o type of calcium dependence (high P_o channel; Fig 2, filled squares), characterized by sigmoid activation and absence of inhibition up to 0.5 mM $[Ca^{2+}]$ (Marengo *et al.*, 1996; Chu *et al.*, 1993). These 3 types of calcium dependence are also observed in skeletal muscle from rabbit and frog (Marengo 1998, Copello *et al.*, 1997, Oba *et al.*, 2002). Cardiac muscle, on the other hand, displays at least 2 calcium dependencies, namely moderate and high P_o (Marengo *et al.*, 1998). These behaviors of RyR channels from cardiac and skeletal muscle are further analyzed in another chapter of this book (Hidalgo *et al.*).

Oxidation of SH residues of single low P_o channels with 2,2'-dithiodipyridine (DTDP) or thimerosal, changed their calcium dependence sequentially from low to moderate P_o (see Fig. 2, open triangles and 3) and from moderate to high P_o as shown in Fig. 2 (open squares). The activity of channels that attained moderate or high P_o behavior after oxidation was comparable to that shown by native moderate or high P_o channels (compare open and filled symbols in Fig. 2). Reduction of SH groups of high P_o channels with β -mercaptoethanol reversed the effect, inducing again a moderate P_o behavior (Marengo *et al.*, 1998). Furthermore, Fig. 3 shows an experiment where a low P_o channel (upper panel) was oxidized with 7 μ M thimerosal to acquire moderate P_o behavior (middle panel), and subsequently reduced with 8 mM GSH to obtain again the low P_o behavior (lower panel).

The three known mammalian RyR genes are expressed in rat brain (Coronado *et al.*, 1994; Furuichi *et al.*, 1994). The most abundant isoform in brain cortex is RyR-2 (McPherson and Campbell, 1993). We do not know which isoform was incorporated in the lipid bilayer. However, considering that RyR-2 is by far the most abundant isoform present in the brain ER vesicle preparation used in our experiments (Hidalgo C and Humeres A, personal communication) it is likely that RyR-2 is the isoform most commonly incorporated. In any case, the three different responses to cytoplasmic calcium (low, moderate or high P_o) could be successively obtained in the same single channel (i.e. the same isoform) through SH oxidation (see Fig. 5 in Marengo *et al.*, 1998).

Taken together, these results indicate that RyR channels from brain change their response to calcium reversibly, acquiring low, moderate, or high P_o behavior, depending on their redox state.

3.3. Activation by ATP

ATP added at the cytoplasmic compartment activated all brain RyR channels, regardless of their calcium dependence, but with different apparent affinities (Fig. 4). Representative current traces, obtained in the presence of 10 μ M cytosolic free $[Ca^{2+}]$ (upper trace in each panel), and after addition of ATP at the concentrations necessary to attain about half-maximal (middle traces) and near maximal activation (lower traces), respectively, are depicted for the three channels. The upper panel displays a channel with spontaneous low P_o response. The middle and lower panels show channels that after oxidation with thimerosal displayed moderate or high P_o behavior, respectively. Near half-maximal activation was obtained with 0.3, 0.1 or 0.03 mM ATP for the low, moderate, or high P_o channel, respectively. Moreover, two different responses to ATP could be observed in the same single RyR channel, before and after oxidation (see Fig. 3 in Bull *et al.*, 2003).

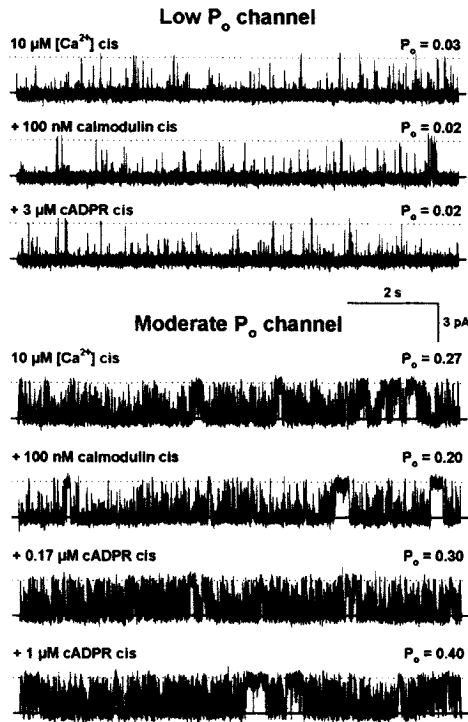


Figure 5. Differential activation of native brain RyR-channels by cADPR. Upper panel: Absence of activation of a spontaneous low P_o channel. Lower panel: activation of a spontaneous moderate P_o channel.

Therefore oxidation is able to induce a change in calcium dependence and also an increase in apparent affinity to ATP. This differential response to ATP is in agreement with a recent report performed with purified RyR-channels from skeletal muscle, that shows activation by an ATP analog of “high- P_o ”, but not of “low- P_o ” channels (Oba *et al.*, 2002). The activity level of their “high- P_o ” and “low- P_o ” channels is similar to our moderate and low P_o channels, respectively. The causes underlying the absence of activation by ATP of low P_o channels in their experiments, besides the difference in the tissue studied remain to be investigated.

3.4. Effect of cADPR

Fig. 5 shows the effect of cADPR in a spontaneous low and in a spontaneous moderate P_o channel studied at 10 μM free $[\text{Ca}^{2+}]$ in the presence of 100 nM calmodulin. Addition of 1 μM cADPR to the cytoplasmic compartment induced a 2-fold increase in P_o of the moderate P_o channel. Addition of 3 μM cADPR induced a further slight increase in P_o (not shown). Instead, up to 3 μM cADPR had no effect on the low P_o channel. High P_o type RyR channels

were not included in this study due to their low frequency of appearance in bilayer experiments. The fact that cADPR had an activating effect on moderate P_o channels and not on low P_o channels suggests that the redox state of the channels has a modulatory action on the effect of this agonist.

Activation of single brain RyR-channels by cADPR is in accordance with calcium flux studies in brain microsomes, which show an increase in Ca^{2+} release rates induced by cADPR that was blocked by ryanodine (Mészáros *et al.*, 1993, White *et al.*, 1993). Moreover, using calcium sensitive dyes and patch-clamp techniques to deliver cADPR, ryanodine-sensitive release of calcium from intracellular stores has been reported in bullfrog sympathetic neurons and neuroblastoma cells (Hua *et al.*, 1994; Empson and Galione, 1997). There are conflicting reports regarding the effect of cADPR on cardiac (Mészáros *et al.*, 1993; Fruen *et al.*, 1994; Sitsapesan *et al.*, 1994; Copello *et al.*, 2001) and skeletal single RyR-channels (Mészáros *et al.*, 1993; Morrisette *et al.*, 1993; Copello *et al.*, 2001). If the redox state of the channel modulates the response to cADPR, the lack of effect of cADPR reported by some authors could be explained, at least partially by different degrees of channel oxidation in the different studies. However, Copello *et al.*, (2001) report that in skeletal and cardiac muscle, they did not observe activation by cADPR neither in the absence nor presence of DTT.

4. CONCLUSIONS

In this work it is shown that caffeine, calcium, ATP, and cADPR activated RyR channels from rat brain cortex. The results also show that oxidation of SH groups induced an increase in the apparent affinity for agonists such as calcium (Marengo *et al.*, 1998) and ATP (Bull *et al.*, 2003). Furthermore, our results show that reduction of the channels reversed the effects induced by oxidation in agreement with previous data (Marengo *et al.*, 1998). In addition, it is shown that cADPR activates RyR channels with the moderate P_o behavior, the channel with a higher degree of SH oxidation, but not the low P_o channel. Oxidation or reduction of critical hyperreactive SH groups could induce molecular rearrangements of channel-protein segments, producing the low, moderate, and high P_o channel states, changing the apparent affinity for different agonists (calcium, ATP, cADPR). These changes could occur *in vivo* leading to the possibility that channel oxidation-reduction is a physiologically relevant mechanism of regulation of Ca^{2+} release from neuronal ER. Changes in intracellular redox potential could modify neuronal processes that depend on calcium release from the ER, including LTP and LTD, and presumably learning and memory (Alkon *et al.*, 1998; Berridge, 2000; Futatsugi *et al.*, 1999). On the other hand oxidative stress may enhance CICR in neurons, since oxidation not only increases RyR-channel response to calcium and ATP, but also suppresses the inhibition of skeletal RyR channels exerted by Mg^{2+} (Donoso *et al.*, 2000).

5. ACKNOWLEDGMENTS

This study was supported by Fondo Nacional de Investigación Científica y Tecnológica (FONDECYT) grant 8980009. The authors thank Marco A. Córdova for his skillful help with the experiments, and Dr. Cecilia Hidalgo for her helpful criticism of the manuscript.

6. REFERENCES

- Abramson JJ, Zable AC, Favero TG, and Salama G. Thimerosal interacts with the Ca^{2+} release channel ryanodine receptor from skeletal muscle sarcoplasmic reticulum. *J Biol Chem* **270**: 29644-29647, 1995.
- Alkon DL, Nelson TJ, Zhao W, and Cavallaro S. Time domains of neuronal Ca^{2+} signaling and associative memory: steps through a calyculin, ryanodine receptor, K^+ channel cascade. *Trends Neurosci* **21**: 529-537, 1998.
- Ashley RH. Activation and conductance properties of Ryanodine-sensitive calcium channels from brain microsomal membranes incorporated into planar lipid bilayers. *J Membrane Biol* **111**: 179-189, 1989.
- Berridge MJ, Lipp P, Bootman MD. The versatility and universality of calcium signaling. *Nat Rev Mol Cell Biol* **1**: 11-21, 2000.
- Bull R, and Marengo JJ. Calcium-dependent halothane activation of sarcoplasmic reticulum calcium channels from frog skeletal muscle. *Am J Physiol Cell Physiol* **266**: C391-C396, 1994.
- Bull R, Marengo JJ, Finkelstein JP, Behrens MI, and Alvarez O. SH oxidation coordinates subunits of rat brain ryanodine receptor channels activated by calcium and ATP. *Am J Physiol Cell Physiol* **285**: C119-C128, 2003.
- Carafoli E. Calcium signaling: A tale for all seasons. *Proc Natl Acad Sci* **99**: 1115-1122, 2002.
- Chu A, Fill M, Stefani E, and Entmann ML. Cytoplasmic Ca^{2+} does not inhibit the cardiac muscle sarcoplasmic reticulum ryanodine receptor Ca^{2+} channel, although Ca^{2+} -induced Ca^{2+} inactivation of Ca^{2+} release is observed in native vesicles. *J Membr Biol* **135**: 49-59, 1993.
- Copello JA, Barg S, Onoue H, and Fleischer S. Heterogeneity of Ca^{2+} gating of skeletal muscle and cardiac ryanodine receptors. *Biophys J* **73**: 141-156, 1997.
- Copello JA, Qi Y, Jeyakumar LH, Ogunbunmi E, Fleischer S. Lack of effect of cADP-ribose and NAADP on the activity of skeletal muscle and heart ryanodine receptors. *Cell Calcium* **30**: 269-284, 2001.
- Coronado R, Morrisette J, Sukhareva M, and Vaughan D. N. Structure and function of ryanodine receptors. *Am J Physiol Cell Physiol* **266**: C1485-C1504, 1994.
- Donoso P, Rodríguez P, and Marambio P. Rapid kinetic studies of SH-oxidation induced calcium release from sarcoplasmic reticulum vesicles. *Arch Biochem Biophys* **341**: 295-299, 1997.
- Donoso P, Aracena P, and Hidalgo C. Sulphydryl oxidation overrides Mg^{2+} inhibition of calcium-induced calcium release in skeletal muscle triads. *Biophys J* **79**: 279-286, 2000.
- Eager KR, Roden LD, and Dulhunty AG. Actions of sulphydryl reagents on single ryanodine receptor Ca^{2+} -release channels from sheep myocardium. *Am J Physiol Cell Physiol* **272**: C1908-C1918, 1997.
- Empson RM, Galione A. Cyclic ADP-ribose enhances coupling between voltage-gated Ca^{2+} entry and intracellular Ca^{2+} release. *J Biol Chem* **272**: 20967-20970, 1997.
- Eu JP, Sun J, Xu L, Stamler JS, and Meissner G. The skeletal muscle calcium release channel: coupled O_2 sensor and NO signaling functions. *Cell* **102**: 499-509, 2000.
- Favero TG, Zable AC, and Abramson JJ. Hydrogen peroxide stimulates the Ca^{2+} release channels from skeletal sarcoplasmic reticulum. *J Biol Chem* **270**: 2557-2563, 1995.
- Feng W, Liu G, Allen PD, and Pessah IN. Transmembrane redox sensor of ryanodine receptor complex. *J Biol Chem* **275**: 35902-35907, 2000.
- Fill M, Coronado R, Mickelson JR, Vilveen J, Ma J, Jacobson BA, and Louis CF. Abnormal ryanodine receptor channels in malignant hyperthermia. *Biophys J* **50**: 471-475, 1990.
- Fruen BR, Mickelson JR, Shomer NH, Vélez P, Louis CF. Cyclic ADP-ribose does not affect cardiac or skeletal muscle ryanodine receptors. *FEBS Lett* **352**: 123-126, 1994.
- Furuichi T, Khoda K, Miyawaki A, and Mikoshiba K. Intracellular channels. *Curr Opin Neurobiol* **4**: 294-303, 1994.
- Futatsugi A, Kato K, Ogura H, Li ST, Nagata E, Kuwajima G, Tanaka K, Itohara S, and Mikoshiba K. Facilitation of

- NMDA_R-independent LTP and spatial learning in mutant mice lacking ryanodine receptor type 3. *Neuron* **24**: 701-713, 1999.
- Herrmann-Frank A, Lüttgau HC, and Stephenson DG. Caffeine and excitation-contraction coupling in skeletal muscle: a stimulating story. *J Muscle Res Cell Motil* **20**: 223-237, 1999.
- Hua SY, Tokimasa T, Takasawa S, Furuya Y, Nohmi M, Okamoto H, Kuba K. Cyclic ADP-Ribose modulates Ca²⁺ release channels for activation by physiological Ca²⁺ entry in bullfrog sympathetic neurons. *Neuron* **12**: 1073-1079, 1994.
- Iino S, Cui Y, Galione A, Terrar DA. Actions of cADP-ribose and its antagonist on contraction in guinea pig isolated ventricular myocytes. *Circ Res* **81**: 879-884, 1997.
- Lai AF, Dent M, Wickenden C, Xu L, Kumari G, Misra M, Lee HB, Sar M, and Meissner G. Expression of a cardiac Ca²⁺-release channel isoform in mammalian brain. *Biochem J* **288**: 553-564, 1992.
- Lee HC. Physiological functions of cyclic ADP-ribose and NAADP as calcium messengers. *Annu Rev Pharmacol Toxicol* **41**: 317-345, 2001.
- Lee HC, Aarhus R, Graeff R, Gurnack ME, Walseth TF. Cyclic ADP-ribose activation of the ryanodine receptor is mediated by calmodulin. *Nature* **370**: 307-309, 1994.
- Li PL, Tang WX, Valdivia HH, Zou AP, Campbell WB. cADP-ribose activates reconstituted ryanodine receptors from coronary arterial smooth muscle. *Am J Physiol Heart Circ Physiol* **280**: H208-H215, 2001.
- Liu G, Abramson JJ, Zable AC, and Pessah IN. Direct evidence for the existence and functional role of hyperactive sulfhydryls on the ryanodine receptor-triadin complex selectively labeled by the coumarin maleimide 7-diethylamino-3'-4'-maleimidylphenyl)-4-methylcoumarin. *Mol Pharmacol* **45**: 189-200, 1994.
- Marengo JJ, Bull R, and Hidalgo C. Calcium dependence of ryanodine-sensitive calcium channels from brain cortex endoplasmic reticulum. *FEBS Lett* **383**: 59-62, 1996.
- Marengo JJ, Hidalgo C, and Bull R. Sulfhydryl oxidation modifies the calcium dependence of ryanodine-sensitive calcium channels. *Biophys J* **74**: 1263-1277, 1998.
- McPherson PS, Kim YK, Valdivia H, Knudson CM, Takekura H, Franzini-Armstrong C, Coronado R, and Campbell KP. The brain ryanodine receptor: A caffeine-sensitive calcium release channel. *Neuron* **7**: 17-25, 1991.
- McPherson PS, and Campbell KP. Characterization of the major brain form of the ryanodine receptor/Ca²⁺ release channel. *J Biol Chem* **268**: 19785-19790, 1993.
- Mészáros LG, Bak J, Chu A. Cyclic ADP-ribose as an endogenous regulator of the non-skeletal type ryanodine receptor Ca²⁺ channel. *Nature* **364**: 76-79, 1993.
- Meissner G. Ryanodine receptor/Ca²⁺ release channels and their regulation by endogenous effectors. *Annu Rev Physiol* **56**: 485-508, 1994.
- Morrisette J, Heisermann G, Cleary J, Ruoho A, Coronado R. Cyclic ADP-ribose induced Ca²⁺ release in rabbit skeletal muscle sarcoplasmic reticulum. *FEBS Lett* **330**: 270-74, 1993.
- Nakashima Y, Nishimura S, Maeda A, Barsoumian EL, Hakamata Y, Nakai J, Allen PD, Imoto K, Kita T. Molecular cloning and characterization of a human brain ryanodine receptor. *FEBS Lett* **417**: 157-162, 1997.
- Oba T, Murayama T, and Ogawa Y. Redox states of type 1 ryanodine receptor alter Ca²⁺ release channel response to modulators. *Am J Physiol Cell Physiol* **282**: C684-C692, 2002.
- Otsu K, Willard HF, Khanna VK, Zorzato F, Green NM, MacLennan DH. Molecular cloning of cDNA encoding the Ca²⁺ release channel (ryanodine receptor) of rabbit cardiac muscle sarcoplasmic reticulum. *J Biol Chem* **265**: 13472-13483, 1990.
- Rousseau E, Smith JS, and Meissner G. Ryanodine modifies conductance and gating behavior of single Ca²⁺ release channel. *Am J Physiol Cell Physiol* **253**: C364-C368, 1987.
- Rousseau E, LaDine J, Liu Q, Meissner G. Activation of the calcium release channel of skeletal muscle sarcoplasmic reticulum by caffeine and related compounds. *Arch Biochem Biophys* **267**: 75-86, 1988.
- Sitsapesan R, McGarry SJ, Williams AJ. Cyclic ADP-ribose competes with ATP for the adenine nucleotide binding site on the cardiac ryanodine receptor Ca²⁺ release channel. *Circ Res* **75**: 596-600, 1994.
- Smith JS, Coronado R, and Meissner G. Single channel measurements of the calcium release channel from skeletal muscle sarcoplasmic reticulum. *J Gen Physiol* **88**: 573-588, 1986.
- Suko J, Hellmann G, and Drobny H. Modulation of the calmodulin-induced inhibition of sarcoplasmic reticulum calcium release channel (ryanodine receptor) by sulfhydryl oxidation in single channel current recordings and [³H]ryanodine binding. *J Membr Biol* **174**: 105-120, 2000.
- Sun J, Xu L, Eu JP, Stamler JS, and Meissner G. Classes of thiols that influence the activity of the skeletal muscle

- calcium release channel. *J Biol Chem* **276**: 15625-15630, 2001.
- Takeshima H, Nishimura S, Matsumoto T, Ishida H, Kangawa K, Minamino N, Matsuo H, Ueda M, Hanaoka M, Hirose T, and Numa S. Primary structure and expression from complementary DNA of skeletal muscle ryanodine receptor. *Nature* **339**: 439-45, 1989.
- White AM, Watson SP, Galione A. Cyclic ADP-ribose-induced Ca^{+2} release from rat brain microsomes. *FEBS Lett* **318**: 259-63, 1993.
- Xia R, Stangler T, Abramson JJ. Skeletal muscle ryanodine receptor is a redox sensor with a well-defined redox potential, which is sensitive to channel modulators. *J Biol Chem* **275**: 36556-36561, 2000.
- Zucchi R, and Ronca-Testoni S. The sarcoplasmic reticulum Ca^{2+} channel/ryanodine receptor: Modulation by endogenous effectors, drugs and disease states. *Pharmacol Rev* **49**: 1-51, 1997.

EXOCYTTIC PATHWAY CHECK POINTS FOR FUNCTIONAL POTASSIUM CHANNELS IN THE PLASMA MEMBRANE

Marcela Bravo-Zehnder^{1*}

1. INTRODUCTION

Potassium channels play a pivotal role in cell physiology since their precise activation and inactivation at the cell surface determines particular characteristics of cellular excitability. Most studies approaching the mechanisms that regulate their cell surface expression levels have been restricted to the contribution made by gene expression. Recent studies revealed that the number of potassium channels that reach the cell surface from their site of synthesis could be also subjected to control by events, both during their assembly in the endoplasmic reticulum and their subsequent transport to the cell surface along the exocytic pathway. Furthermore, sorting events occurring during this traffic determine in certain kind of cells, such as polarized epithelial cells and neurons, a specific regionalization within discrete domains of the cell surface. Alterations in transport and regionalization processes can lead to severe pathological disorders. This review is focused on the different strategies that regulate the number and location of insertion of potassium channels at the cell surface.

2. THE EXOCYTTIC PATHWAY

Plasma membrane proteins are first co-translationally inserted in the ER membrane where their topology respect to the bilayer is defined. Glycosylation in specific residues also occurs co-translationally and, together with chaperone and auxiliary proteins, plays a

¹ Laboratorio de Reumatología e Inmunología Clínica. Pontificia Universidad Católica de Chile. Marcoleta 367, Santiago, Chile.

* corresponding author: mbravo@med.puc.cl

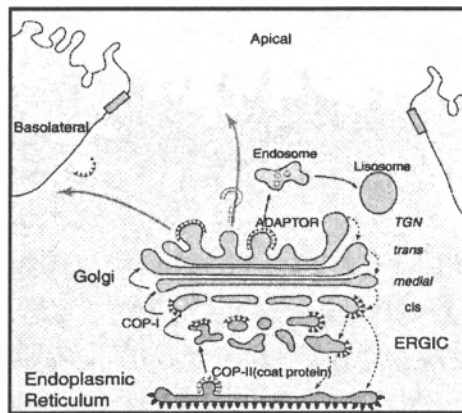


Figure 1. Schematic representation of the exocytic pathway in polarized epithelial cells. Membrane glycoproteins are synthesized on polyribosomes and translocated to the endoplasmic reticulum (ER) where they undergo cotranslational and postranslational processing. They exit the ER via coated vesicles (COPII), which serve to shuttle them to the ER-Golgi intermediate compartment (ERGIC). From there, they can be transported to the cis-Golgi network. Subsequently, either the proteins traverse the Golgi cisternae one by one via vesicular carriers or transport occurs by cisternal maturation. Sorting occurs in the trans Golgi network (TGN), where adaptor proteins play an important role in the formation and cargo selection of the vesicle. In polarized epithelial cells, separate pathways exist for delivery of vesicles to the basolateral or apical domain. Recently, two adaptor complexes, AP-1B and AP-4, have been described that recognize basolateral sorting signals.

pivotal role in protein folding, oligomerization, quality control, sorting and transport (Hurtley and Helenius, 1989; Klausner and Sitia, 1990; Helenius, 2001). While improperly folded or assembled proteins are retained and degraded by the ER quality control system, transport-competent proteins are exported in vesicles to the Golgi complex for further processing. This postranslational modification in certain cases can modulate the targeting or activity of the protein.

Once proteins are completed, they are localized to transport vesicles that fuse with the plasma membrane. This process occurs in the most distal cisternae of the Golgi complex, the trans-Golgi network (TGN). Here distinct plasma membrane proteins are segregated into different vesicular pathways directed to the cell surface in both non-polarized (Musch *et al.*, 1996) and polarized cells (Rodríguez-Boulán *et al.*, 1989). This is more evident in polarized epithelial cells since their surface is divided into apical and basolateral domains which are morphologically and functionally different by virtue of their distinct lipid and protein composition, kept separate by tight junctions (Rodríguez-Boulán *et al.*, 1989). Yet, the mechanisms accounting for polarized protein sorting are still poorly understood. A general model for intracellular protein sorting and vesicular transport between organelles and the plasma membrane, involves stepwise events of cargo selection coupled to vesicle formation at donor membranous compartments, and then targeting and fusion of the resulting transport vesicle with a specific acceptor organelle. Control elements of the transport device, which should undergo transient and recurrent modifications, are necessary to ensure an ordered orchestration at each step and vectoriality in the overall process (Sollner and Rothman, 1996). A budding device

consists in cytosolic enzymes and structural proteins, which are recruited to the donor membrane in a process regulated by small GTPases, forming a coat, which presumably molds the membrane into a bud followed by fission. Docking and fusion with the appropriate target membrane require the inclusion in the vesicle of additional elements, called v-SNARES, which in concert with t-SNARES at the target membrane specify destination (Sollner and Rothman, 1996). GTPases of the rab family probably provide further elements important for vectoriality and specificity (Zerial and Stenmark, 1993). Trimeric GTPases and diverse kinases seem to also participate in yet undefined manners (Mostov *et al.*, 2000).

Figure 1 schematizes the exocytic pathway in a polarized epithelial cell indicating some of the proteins that participate in this process.

3. POTASSIUM CHANNELS AS SUBSTRATES OF THE EXOCYTIC PATHWAY

Potassium channels are integral membrane proteins and therefore they are substrates of all the machinery involved in the synthesis, folding and transport processes experienced by other integral membrane proteins through the exocytic pathways. The following paragraphs review our current knowledge of the different transport check points along the various compartments involved, as indicated in some cases by pathologies associated to failure of the channels to reach the plasma membrane.

One of the most studied genetic disease involving potassium channels is the cardiac "long Q-T" syndrome (Zhou *et al.*, 1999). Here the HERG gen, which encodes the pore-forming subunit of the cardiac rapidly-activating delayed rectifier potassium channel, has a mutation that renders the channels location temperature sensitive. At restrictive temperature (37°C) the channel is located in the ER while at 27°C its trafficking to the plasma membrane is markedly improved. The antiarrhythmic drug E-4031, that selectively binds to the channel, also improves its traffic to the plasma membrane. It is possible that both, lower temperature and binding of the drug, facilitate channel folding either by stabilizing hydrogen bonds or by acting as chemical chaperones, respectively (Zhou *et al.*, 1999). A relationship between folding and transport is also suggested by the finding that a high concentration of glycerol (1M) restores traffic of a mutated CFTR chloride channel to the cell surface (Sato *et al.*, 1996).

It has been described that β -subunits of the Kv potassium channel, in addition to modulating the channel activity at the cell surface, could control the surface expression of the α -subunit (Shi *et al.*, 1996) presumably by assisting its folding in the ER (Shi *et al.*, 1996). In the same line, the chaperon KChAP enhances the functional cell surface expression of specific Kv channels without changing their channel properties (Kuryshv *et al.*, 2000; Kuryshv *et al.*, 2001). KChAP belongs to a newly described multigene family of transcription factor-interacting proteins that inactivate transcription. Besides this function, KChAP interacts transiently with the channels facilitating their folding. In contrast with the Kv β -subunits, KChAP does not remain attached to the mature channel complex (Wible *et al.*, 1998). The folding effect could be reproduced by only a 98-residue fragment of full-length KChAP that binds to the amino termini of the Kv1.3, Kv2.1 and Kv4.3 channels (Kuryshv *et al.*, 2000).

Proteins that regulate channel function could also modulate the surface expression of the SK4/IK1 Ca^{2+} -activated K^+ channels. In this case Calmodulin (CaM) not only opens the channels in the presence of elevated intracellular Ca^{2+} , but also participates in the assembly and trafficking of the channels to the cell surface (Joiner *et al.*, 2001).

Other channels, like the inwardly rectifying Kir potassium channel, contain ER export signals in their structure. Kir 2.1 and Kir 1.1. have on their carboxyl terminus two different short sequences containing a diacidic EXE or EXD motif (Ma *et al.*, 2001; Stockklauser *et al.*, 2001), similar to the DXE motif required for ER to Golgi transport of the vesicular stomatitis virus glycoprotein (Nishimura and Balch, 1997; Sevier *et al.*, 2000). Lack of this sequence results in ER retention and degradation of the protein. The voltage-gated Kv potassium channels, Kv1.2, 1.4 and 1.5 also contain forward signals, that differ from the diacidic motif. The Kv 1.4 channel has a VXXSL motif that is more efficient than the LXXSL motif borne by the Kv1.5 channel (Li *et al.*, 2000). These two motifs are functionally interchangeable, but the relative efficacy of cell surface targeting is determined by the amino acid at position one of the motif. The Kv 1.2 has the motif VXXSN and requires Kv β for surface expression (Li *et al.*, 2000).

The number of inward rectifier ATP-sensitive potassium channels (KATP Channels) in the plasma membrane could be controlled by retention in the ER. Its two subunits, SUR1 and Kir 6.2 or Kir 6.1 (Clement *et al.*, 1997), have a retention or retrograde signal in their C terminus (Zerangue *et al.*, 1999). In the ER, only properly assembled channels mask their retention signal and proceed to the cell surface. Additionally SUR1 has an anterograde signal required for surface expression of KATP channels. In congenital or neonatal hyperinsulinism disease this channel is practically absent in the cell surface because its forward signal is deleted or mutated (Sharma *et al.*, 1999).

Surface expression of both α and β subunits of the human Maxi-K channel could be regulated by a splice variant of the α -subunit (Zarei *et al.*, 2001). This mechanism of regulation is novel and its physiological relevance has still to be resolved. These channels are unique in that they are modulated not only by voltage but also by calcium in the micromolar range. The α subunit has seven transmembrane domains (S0-S6) and seems to be the product of a single gene (Meera *et al.*, 1997). In contrast, modulatory β subunits are products of several genes and contribute largely to the functional diversity of Maxi K channels (Toro *et al.*, 1998). This diversity is further enhanced by alternative splicing of its α and β subunits (Wallner *et al.*, 1999; Uebele *et al.*, 2000). The α subunit splice variant SV-1 contains a 33 amino acid insert between the S0 and S1 transmembrane domains and specifically traps wild-type α and β 1 subunits in the ER (Zarei *et al.*, 2001). Therefore, it is possible that modulation of the expression levels of the SV-1 splice variant may affect transport of Maxi-K channel complexes from the ER to the cell surface.

As it was mentioned before, glycans have a common role in promoting protein folding in the early secretory pathway. For the Shaker K^+ channel the two glycosylation sites increase stability and cell surface expression, by allowing a more rapid exit of the protein from the ER rather than affecting the acquisition of the native structure (Khanna *et al.*, 2001). Timely exit from the ER may be a key factor in protecting the wild-type but not the unglycosylated protein from degradation (Khanna *et al.*, 2001).

For other channels such as the Maxi-K channel, *N*-glycosylation does not influence the trafficking of the protein towards the plasma membrane of mammalian cells (Bravo-

Zehnder *et al.*, 2000). In this case mutation of the only possible glycosylation site does not alter its apical localization in polarized epithelia. This observation is remarkable, because the participation of *N*-glycans as specific sorting signals in polarized epithelia has been subject of debate. One group supports that *N*-glycosylation is a sorting signal *per se* (Scheiffele *et al.*, 1995; Gut *et al.*, 1998; Alfalah *et al.*, 1999). However, a balanced consideration of the evidence led others to suggest, as an alternative, that the role of *N*-glycans could be indirect, providing either structural support for the functional expression of proteinaceous sorting signals or facilitating association with lipid rafts involved in apical sorting review in (Rodríguez-Boulan and González, 1999).

Potassium channels are located in different plasma membrane domains in polarized epithelial cells where vectorial ion transport is their major function. In this case, trafficking checkpoints of the channels are crucial. Nevertheless, little is known about the sorting mechanism involved in the traffic of the different potassium channels.

Recently, Kir 2.3 has been reported to have a basolateral expression in polarized epithelial cells and, like other basolateral proteins, this sorting signal is located in the carboxy terminal domain of the channel. Nevertheless at the amino acid level, it seems to be novel, since it does not share any resemblance to previously described basolateral sorting signals. In addition, the basolateral sorting signal contains nearby a protein-protein interaction PDZ binding motif (Le Maout *et al.*, 2001). The PDZ-domains engage PDZ-containing proteins to facilitate multiprotein complex formation and to localize expression in particular membrane domains (Gomperts, 1996). Interestingly deletion of the PDZ binding motif, but not of the basolateral sorting signal, causes channels to accumulate in an endosomal compartment (Olsen *et al.*, 2002). Furthermore this PDZ domain could interact with hLin-7b as part of a multimeric complex on the basolateral membrane, similar to the basolateral membrane complex in *C. elegans* vulva progenitor cells (Olsen *et al.*, 2002). Recently two adaptor protein complexes, AP-1B and AP-4, that recognize basolateral sorting signals have been found at the TGN (Figure 1)(Folsch *et al.*, 1999; Ohno *et al.*, 1999; Simmen *et al.*, 1999). Nevertheless, an adaptor protein recognizing specifically a potassium channel sorting signal has not yet described. It would be interesting to study if these new adaptor complexes would recognize any described potassium channel basolateral sorting signal.

The final targeting of the trans Golgi-derived transport vesicles to the plasma membrane is highly regulated and helps to determine the subcellular distribution of the proteins (Griffiths and Simons, 1986; Reaves *et al.*, 1998a; Reaves *et al.*, 1998b). It has been described that ion channels are located in discrete plasma membrane microdomains (Burke *et al.*, 1999). This kind of regionalization can prevent free diffusion of the proteins throughout the lipid bilayer and facilitate their regulation through protein-protein or protein-lipid interactions. The channels can become clustered by MAGUK proteins (Membrane-Associated Guanylate Kinases) or associated with specific lipid microdomains, enriched in glycosphingolipids and cholesterol, called rafts. MAGUK proteins are concentrated in tight junctions of epithelial cells and synapses of neurons (Ponting *et al.*, 1997). Among the most widely studied MAGUKs is the PSD-95 subfamily, whose members (PDS-95 and SAP-97) induce clustering of Kv 1.4 channels (El-Husseini *et al.*, 2000). These protein could interact directly, by binding of PSD-95 to a PDZ domain in the protein, or indirectly by self-association of PDS-95 domains between two proteins (Burke *et al.*, 1999). PSD-95 domains could also stabilize

potassium channels at the cell-surface by suppressing the internalization of the channel from the plasma membrane (Jugloff *et al.*, 2000).

On the other hand, lipid rafts can include or exclude proteins to variable extents (Roper *et al.*, 2000). The presence or absence of proteins is used to define different types of lipid rafts. Caveolae represent one well studied subpopulation of lipid rafts that contain the scaffolding protein caveolin (Roper *et al.*, 2000). Caveolin can bind, organize, and sometimes functionally regulate proteins within lipid rafts (Okamoto *et al.*, 1998). A common idea that has emerged is that the clustering of separate rafts exposes proteins to a new membrane environment, enriched in specific enzymes, such as kinases, phosphatases and perhaps palmitoylases. A small change of partitioning of a protein into a lipid raft can, through amplification, initiate signaling cascades (Simons and Toomre, 2000).

Specific isoforms of voltage-gated K⁺ channels have been recently described to locate into distinct lipid rafts. Kv1.5 was found associated with caveolar lipid rafts (Martens *et al.*, 2001), whereas Kv2.1 was found in non-caveolar lipid rafts (Martens *et al.*, 2000). It was proposed that this different compartmentalization in the plasma membrane might permit isoform-specific modulation of K⁺ channel function.

The α -subunit of the Maxi-K channel also floats in lipid rafts (Bravo-Zehnder *et al.*, 2000). It has been shown that the apical sorting of some proteins in polarized epithelial cells includes association with lipid raft microdomains (Simons and Ikonen, 1997; Rodríguez-Boulan and González, 1999). But this association is not a unique requirement, since this property *per se* does not ensure apical sorting in other proteins (González *et al.*, 1987; Marzolo *et al.*, 1997; Yeaman *et al.*, 1997; Lin *et al.*, 1998; Benting *et al.*, 1999; Lipardi *et al.*, 2000; Marmorstein *et al.*, 2000). For this reason, the role of raft association of the α -subunit of the Maxi-K channel in the apical pole remains to be elucidated. Probably, the α -subunit of the Maxi-K channel possesses structural information for both raft-association and apical sorting (Bravo-Zehnder *et al.*, 2000).

4. CONCLUDING REMARKS

In summary, the process of assembly and transport of ion channels from the endoplasmic reticulum (ER) to the Golgi complex and then to the plasma membrane provides multiple opportunities to control the number of functional channel molecules that reach the cell surface. First, in the ER there is a quality control system that eliminates misfolded or unassembled proteins. In the folding process, chaperones and auxiliary proteins play an important role and for some potassium channels a specific chaperone, KChAP, is also crucial. The exposure and/or masking of export or sorting signals from potassium channels constitute additional strategies for regulating transport toward the plasma membrane. Finally, an α -subunit of a potassium channel could be retained in the ER by a particular splice variant. Once at the plasma membrane, at least two different mechanisms of regulation based on spatial organization have been described, one involving clustering by the MAGUK proteins and the other based on inclusion or exclusion within lipid rafts. All these regulatory mechanisms play a crucial role in cellular physiology and are potential loci for dysfunctions leading to human disease.

5. REFERENCES

- Alfalah, M., Jacob, R., Preuss, U., Zimmer, K. P., Naim, H. and Naim, H. Y., 1999, O-linked glycans mediate apical sorting of human intestinal sucrase- isomaltase through association with lipid rafts, *Curr Biol* **9**(11): 593-6.
- Benting, J. H., Rietveld, A. G. and Simons, K., 1999, N-Glycans mediate the apical sorting of a GPI-anchored, raft-associated protein in madin-darby canine kidney cells, *J Cell Biol* **146**(2): 313-20.
- Bravo-Zehnder, M., Orío, P., Norambuena, A., Wallner, M., Meera, P., Toro, L., Latorre, R. and González, A., 2000, Apical sorting of a voltage- and Ca²⁺-activated K⁺ channel alpha - subunit in Madin-Darby canine kidney cells is independent of N- glycosylation, *Proc Natl Acad Sci U S A* **97**(24): 13114-9.
- Burke, N. A., Takimoto, K., Li, D., Han, W., Watkins, S. C. and Levitan, E. S., 1999, Distinct structural requirements for clustering and immobilization of K⁺ channels by PSD-95, *J Gen Physiol* **113**(1): 71-80.
- Clement, J. P. T., Kunjilwar, K., González, G., Schwanstecher, M., Panten, U., Aguilar-Bryan, L. and Bryan, J., 1997, Association and stoichiometry of K(ATP) channel subunits, *Neuron* **18**(5): 827-38.
- El-Husseini, A. E., Craven, S. E., Chetkovich, D. M., Firestein, B. L., Schnell, E., Aoki, C. and Brecht, D. S., 2000, Dual palmitoylation of PSD-95 mediates its vesiculotubular sorting, postsynaptic targeting, and ion channel clustering, *J Cell Biol* **148**(1): 159-72.
- Folsch, H., Ohno, H., Bonifacino, J. S. and Mellman, I., 1999, A novel clathrin adaptor complex mediates basolateral targeting in polarized epithelial cells [In Process Citation], *Cell* **99**(2): 189-98.
- Gomperts, S. N., 1996, Clustering membrane proteins: It's all coming together with the PSD- 95/SAP90 protein family, *Cell* **84**(5): 659-62.
- González, A., Rizzolo, L., Rindler, M., Adesnik, M., Sabatini, D. D. and Gottlieb, T., 1987, Nonpolarized secretion of truncated forms of the influenza hemagglutinin and the vesicular stomatitis virus G protein from MDCK cells, *Proc Natl Acad Sci U S A* **84**(11): 3738-42.
- Griffiths, G. and Simons, K., 1986, The trans Golgi network: sorting at the exit site of the Golgi complex, *Science* **234**(4775): 438-43.
- Gut, A., Kappeler, F., Hyka, N., Balda, M. S., Hauri, H. P. and Matter, K., 1998, Carbohydrate-mediated Golgi to cell surface transport and apical targeting of membrane proteins, *Embo J* **17**(7): 1919-29.
- Helenius, A., 2001, Quality control in the secretory assembly line, *Philos Trans R Soc Lond B Biol Sci* **356**(1406): 147-50.
- Hurtley, S. M. and Helenius, A., 1989, Protein oligomerization in the endoplasmic reticulum, *Annu Rev Cell Biol* **5**: 277-307.
- Joiner, W. J., Khanna, R., Schlichter, L. C. and Kaczmarek, L. K., 2001, Calmodulin regulates assembly and trafficking of SK4/IK1 Ca²⁺-activated K⁺ channels, *J Biol Chem* **276**(41): 37980-5.
- Jugloff, D. G., Khanna, R., Schlichter, L. C. and Jones, O. T., 2000, Internalization of the Kv1.4 potassium channel is suppressed by clustering interactions with PSD-95, *J Biol Chem* **275**(2): 1357-64.
- Khanna, R., Myers, M. P., Laine, M. and Papazian, D. M., 2001, Glycosylation increases potassium channel stability and surface expression in mammalian cells, *J Biol Chem* **276**(36): 34028-34.
- Klausner, R. D. and Sitia, R., 1990, Protein degradation in the endoplasmic reticulum, *Cell* **62**(4): 611-4.
- Kuryshv, Y. A., Gudz, T. I., Brown, A. M. and Wible, B. A., 2000, KChAP as a chaperone for specific K⁺ channels, *Am J Physiol Cell Physiol* **278**(5): C931-41.
- Kuryshv, Y. A., Wible, B. A., Gudz, T. I., Ramirez, A. N. and Brown, A. M., 2001, KChAP/Kvbeta1.2 interactions and their effects on cardiac Kv channel expression, *Am J Physiol Cell Physiol* **281**(1): C290-9.
- Le Maout, S., Welling, P. A., Brejon, M., Olsen, O. and Merot, J., 2001, Basolateral membrane expression of a K⁺ channel, Kir 2.3, is directed by a cytoplasmic COOH-terminal domain, *Proc Natl Acad Sci U S A* **98**(18): 10475-80.
- Li, D., Takimoto, K. and Levitan, E. S., 2000, Surface expression of Kv1 channels is governed by a C-terminal motif, *J Biol Chem* **275**(16): 11597-602.
- Lin, S., Naim, H. Y., Chapin Rodriguez, A. and Roth, M. G., 1998, Mutations in the middle of the transmembrane domain reverse the polarity of transport of the influenza virus hemagglutinin in MDCK epithelial cells [In Process Citation], *J Cell Biol* **142**(1): 51-7.
- Lipardi, C., Nitsch, L. and Zurzolo, C., 2000, Detergent-insoluble GPI-anchored proteins are apically sorted in fischer rat thyroid cells, but interference with cholesterol or sphingolipids differentially affects detergent insolubility and apical sorting, *Mol Biol Cell* **11**(2): 531-42.

- Ma, D., Zerangue, N., Lin, Y. F., Collins, A., Yu, M., Jan, Y. N. and Jan, L. Y., 2001, Role of ER export signals in controlling surface potassium channel numbers, *Science* **291**(5502): 316-9.
- Marmorstein, A. D., Csaky, K. G., Baffi, J., Lam, L., Rahaal, F. and Rodriguez-Boulau, E., 2000, Saturation of, and competition for entry into, the apical secretory pathway, *Proc Natl Acad Sci U S A* **97**(7): 3248-53.
- Martens, J. R., Navarro-Polanco, R., Coppock, E. A., Nishiyama, A., Parshley, L., Grobaski, T. D. and Tamkun, M. M., 2000, Differential targeting of Shaker-like potassium channels to lipid rafts, *J Biol Chem* **275**(11): 7443-6.
- Martens, J. R., Sakamoto, N., Sullivan, S. A., Grobaski, T. D. and Tamkun, M. M., 2001, Isoform-specific localization of voltage-gated K⁺ channels to distinct lipid raft populations. Targeting of Kv1.5 to caveolae, *J Biol Chem* **276**(11): 8409-14.
- Marzolo, M. P., Bull, P. and González, A., 1997, Apical sorting of hepatitis B surface antigen (HBsAg) is independent of N-glycosylation and glycosylphosphatidylinositol-anchored protein segregation, *Proc Natl Acad Sci U S A* **94**(5): 1834-9.
- Meera, P., Wallner, M., Song, M. and Toro, L., 1997, Large conductance voltage- and calcium-dependent K⁺ channel, a distinct member of voltage-dependent ion channels with seven N-terminal transmembrane segments (S0-S6), an extracellular N terminus, and an intracellular (S9-S10) C terminus, *Proc Natl Acad Sci U S A* **94**(25): 14066-71.
- Mostov, K. E., Verges, M. and Altschuler, Y., 2000, Membrane traffic in polarized epithelial cells, *Curr Opin Cell Biol* **12**(4): 483-90.
- Musch, A., Xu, H., Shields, D. and Rodríguez-Boulau, E., 1996, Transport of vesicular stomatitis virus G protein to the cell surface is signal mediated in polarized and nonpolarized cells, *J Cell Biol* **133**(3): 543-58.
- Nishimura, N. and Balch, W. E., 1997, A di-acidic signal required for selective export from the endoplasmic reticulum, *Science* **277**(5325): 556-8.
- Ohno, H., Tomemori, T., Nakatsu, F., Okazaki, Y., Aguilar, R. C., Foelsch, H., Mellman, I., Saito, T., Shirasawa, T. and Bonifacino, J. S., 1999, Mu1B, a novel adaptor medium chain expressed in polarized epithelial cells, *FEBS Lett* **449**(2-3): 215-20.
- Okamoto, T., Schlegel, A., Scherer, P. E. and Lisanti, M. P., 1998, Caveolins, a family of scaffolding proteins for organizing "preassembled signaling complexes" at the plasma membrane, *J Biol Chem* **273**(10): 5419-22.
- Olsen, O., Liu, H., Wade, J. B., Merot, J. and Welling, P. A., 2002, Basolateral membrane expression of the Kir 2.3 channel is coordinated by PDZ interaction with Lin-7/CASK complex, *Am J Physiol Cell Physiol* **282**(1): C183-95.
- Ponting, C. P., Phillips, C., Davies, K. E. and Blake, D. J., 1997, PDZ domains: targeting signalling molecules to sub-membranous sites, *Bioessays* **19**(6): 469-79.
- Reaves, B. J., Banting, G. and Luzio, J. P., 1998a, Lumenal and transmembrane domains play a role in sorting type I membrane proteins on endocytic pathways, *Mol Biol Cell* **9**(5): 1107-22.
- Reaves, B. J., Roquemore, E. P., Luzio, J. P. and Banting, G., 1998b, TGN38 cycles via the basolateral membrane of polarized Caco-2 cells, *Mol Membr Biol* **15**(3): 133-9.
- Rodriguez-Boulau, E. and González, A., 1999, Glycans in post-golgi apical targeting: sorting signals or structural props? [In Process Citation], *Trends Cell Biol* **9**(8): 291-4.
- Rodriguez-Boulau, E., Salas, P. J., Sargiacomo, M., Lisanti, M., Lebivic, A., Sambuy, Y., Vega-Salas, D. and Graeve, L., 1989, Methods to estimate the polarized distribution of surface antigens in cultured epithelial cells, *Methods Cell Biol* **32**: 37-56.
- Roper, K., Corbeil, D. and Huttner, W. B., 2000, Retention of prominin in microvilli reveals distinct cholesterol-based lipid micro-domains in the apical plasma membrane, *Nat Cell Biol* **2**(9): 582-92.
- Sato, S., Ward, C. L., Krouse, M. E., Wine, J. J. and Kopito, R. R., 1996, Glycerol reverses the misfolding phenotype of the most common cystic fibrosis mutation, *J Biol Chem* **271**(2): 635-8.
- Scheiffele, P., Peranen, J. and Simons, K., 1995, N-glycans as apical sorting signals in epithelial cells, *Nature* **378**(6552): 96-8.
- Sevier, C. S., Weisz, O. A., Davis, M. and Machamer, C. E., 2000, Efficient export of the vesicular stomatitis virus G protein from the endoplasmic reticulum requires a signal in the cytoplasmic tail that includes both tyrosine-based and di-acidic motifs, *Mol Biol Cell* **11**(1): 13-22.
- Sharma, N., Crane, A., Clement, J. P. T., González, G., Babenko, A. P., Bryan, J. and Aguilar-Bryan, L., 1999, The C terminus of SUR1 is required for trafficking of KATP channels, *J Biol Chem* **274**(29): 20628-32.
- Shi, G., Nakahira, K., Hammond, S., Rhodes, K. J., Schechter, L. E. and Trimmer, J. S., 1996, Beta subunits promote K⁺ channel surface expression through effects early in biosynthesis, *Neuron* **16**(4): 843-52.

- Simmen, T., Nobile, M., Bonifacino, J. S. and Hunziker, W., 1999, Basolateral sorting of furin in MDCK cells requires a phenylalanine- isoleucine motif together with an acidic amino acid cluster, *Mol Cell Biol* **19**(4): 3136-44.
- Simons, K. and Ikonen, E., 1997, Functional rafts in cell membranes, *Nature* **387**(6633): 569-72.
- Simons, K. and Toomre, D., 2000, Lipid rafts and signal transduction, *Nat Rev Mol Cell Biol* **1**(1): 31-9.
- Sollner, T. H. and Rothman, J. E., 1996, Molecular machinery mediating vesicle budding, docking and fusion, *Experientia* **52**(12): 1021-5.
- Stockklauser, C., Ludwig, J., Ruppertsberg, J. P. and Klocker, N., 2001, A sequence motif responsible for ER export and surface expression of Kir2.0 inward rectifier K(+) channels, *FEBS Lett* **493**(2-3): 129-33.
- Toro, L., Wallner, M., Meera, P. and Tanaka, Y., 1998, Maxi-Kca, a unique member of the voltage gated K channel superfamily., *News Physiol Sci* **13**: 112-117.
- Uebele, V. N., Lagrutta, A., Wade, T., Figueroa, D. J., Liu, Y., Mckenna, E., Austin, C. P., Bennett, P. B. and Swanson, R., 2000, Cloning and functional expression of two families of beta-subunits of the large conductance calcium-activated K+ channel, *J Biol Chem* **275**(30): 23211-8.
- Wallner, M., Meera, P. and Toro, L., 1999, Molecular basis of fast inactivation in voltage and Ca²⁺-activated K+ channels: a transmembrane beta-subunit homolog, *Proc Natl Acad Sci U S A* **96**(7): 4137-42.
- Wible, B. A., Yang, Q., Kuryshv, Y. A., Accili, E. A. and Brown, A. M., 1998, Cloning and expression of a novel K+ channel regulatory protein, KChAP, *J Biol Chem* **273**(19): 11745-51.
- Yeaman, C., Le Gall, A. H., Baldwin, A. N., Monlauzeur, L., Le Bivic, A. and Rodriguez-Boulan, E., 1997, The O-glycosylated stalk domain is required for apical sorting of neurotrophin receptors in polarized MDCK cells, *J Cell Biol* **139**(4): 929-40.
- Zarei, M. M., Zhu, N., Alioua, A., Eghbali, M., Stefani, E. and Toro, L., 2001, A novel MaxiK splice variant exhibits dominant-negative properties for surface expression, *J Biol Chem* **276**(19): 16232-9.
- Zerangue, N., Schwappach, B., Jan, Y. N. and Jan, L. Y., 1999, A new ER trafficking signal regulates the subunit stoichiometry of plasma membrane K(ATP) channels, *Neuron* **22**(3): 537-48.
- Zerial, M. and Stenmark, H., 1993, Rab GTPases in vesicular transport, *Curr Opin Cell Biol* **5**(4): 613-20.
- Zhou, Z., Gong, Q. and January, C. T., 1999, Correction of defective protein trafficking of a mutant HERG potassium channel in human long QT syndrome. Pharmacological and temperature effects, *J Biol Chem* **274**(44): 31123-6.

C-TERMINI REGION SHARED BY β_{2A} , β_{1B} AND β_3 SUBUNITS CONFER PREPULSE FACILITATION TO CARDIAC CALCIUM CHANNELS

Igor Dzhura¹, Georgina Guerro¹ and Alan Neely^{1,2*}

1. INTRODUCTION

Facilitation of calcium currents by depolarizing prepulses has been observed in many different cells including heterologous expression systems such as *Xenopus* oocytes. The mechanisms mediating this modulation appear to differ among calcium channels and to depend on the type of auxiliary subunits associated with the pore-forming subunit. In the case of L-type calcium channels, prepulse-induced current facilitation is recorded when the α_{1C} subunit ($Ca_v1.2$) is co-expressed with the auxiliary subunits β_{1b} , β_3 , or β_4 but not with neuronal β_{2a} . A palmitolation site, unique to the N-terminus of β_{2a} , was shown to inhibit prepulse facilitation (Quin *et al.*, 1998) suggesting that all structural elements to support facilitation are shared by all β subunits. Here we report that β_{1a} co-expressed in *Xenopus* oocytes with $Ca_v1.2$ yields channels that cannot be facilitated by strong depolarization. Through the construction of chimeras between β_{1a} and β_{2a} we also show that transferring to β_{1a} - a structure encoded in the C-termini of β_{2a} - restores prepulse facilitation and we discuss the potential role of two motifs shared by β_{2a} , β_{1b} and β_3 subunits.

A number of processes such as muscle contraction and neurotransmitter release are tightly coupled to the influx of calcium through high voltage-activated calcium channels (VACC). Hormones and neurotransmitters also regulate these channels through mechanisms that are often voltage dependent giving rise to complex time-dependent behaviors that confer memory and frequency dependency to calcium-mediated responses.

One common manifestation of the conjugation between voltage and hormonal regulation is the so-called prepulse facilitation described for several types of VACC.

¹ Department of Physiology. Texas Tech University Health Sciences Center, 3601 4th Street, Lubbock, Texas 79430, USA.

² Centro de Neurociencias Celular y Molecular de Valparaíso, Universidad de Valparaíso, Gran Bretaña 111, Valparaíso, Chile.

* corresponding author: alan@cnv.cl

This prepulse facilitation appears to involve different mechanisms depending on the type of channel. In L-type calcium channels, found in skeletal, cardiac and smooth muscle, facilitation appears to be dependent on phosphorylation when studied in native cells (Zygmunt and Maylie, 1990). However, in N-type channels, found in neurons, the removal of tonic inhibition mediated by the $G_{\beta\gamma}$ subunit of G-proteins is thought to be the dominant mechanism in native cells (Pollo *et al.*, 1991) as well as in heterologous expression systems (Meir *et al.*, 2000; Herlitze *et al.*, 2001).

VACC are heteromultimeric proteins composed of a channel forming subunit (α_1) and up to three auxiliary subunits, termed β , γ and α_2/δ that have regulatory functions. The α_1 subunit, which by itself supports voltage dependent Ca^{2+} influx, is composed of four repeats; each resembling monomers of voltage-activated K^+ channels. To date, ten different genes have been identified that code for different forms of α_1 , three genes for α_2/δ (Catterall, 2000), four for β (Birnbaumer *et al.*, 1998) and seven for γ (Moss *et al.*, 2002). Initial studies in heterologous expression systems have shown that prepulse facilitation depends on the subunit composition of the channel. Prepulse facilitation in N-type Ca-currents underlying expression of $Ca_v2.1$ (α_{1B}), is greatly enhanced by the presence of GTP γ S and reduced by co-expression of β but is not affected by α_2/δ (Stephens *et al.*, 1998). These observations are consistent with the view that for $Ca_v2.1$, prepulse facilitation reflects a voltage-dependent relief of block $G_{\beta\gamma}$ that binds primarily to the intracellular loop joining domains I and II of α_1 (Stephens *et al.*, 1998; Canti *et al.*, 2000; Page *et al.*, 1997; De Waard *et al.*, 1997). This loop also includes the main interaction site with the β -subunit (De Waard *et al.*, 1996). Prepulse facilitation in L-type currents underlying the expression of $Ca_v1.2$ (α_{1C}) requires the presence of certain isoforms of the β -subunit (Cens *et al.*, 1998) and is suppressed by α_2/δ (Platano *et al.*, 2000). There is also experimental evidence ruling out phosphorylation or G-protein-dependent modulation when expressed in mammalian cell lines (Dai *et al.*, 1999). In contrast to β_{1b} and β_3 , the brain isoform of β_{2a} does not support facilitation. This isoform of β_{2a} is unique in that it contains a palmitolation site in its N-terminus and Quin and co-workers (1998) showed that destroying this site restores the ability of β_{2a} to support prepulse facilitation. The latter suggests that the structures required for depolarization-induced potentiation may be common to all β -subunits and that palmitolation of β_{2a} would chronically facilitate Ca-channels.

Amino-acid sequence alignments of β -subunits reveal five domains (Figure 1). Among them, domains II and IV, of 120 and 210 amino acids respectively, are highly conserved, with over 55% identity. Domain IV starts with a highly conserved segment of 40 amino acids that interact with the loop joining repeats I and II of the pore-forming α_1 subunit. This segment is referred to as BID (Beta Interaction Domain; De Waard *et al.*, 1994). The other domains vary in length and composition and often diverge among splice variants. Domain III of β_{1b} , for example, is only 7 amino acids long, whilst the same domain in β_{1a} encompasses more than 50 amino acids (Hogan *et al.*, 1999). Domains I and V also vary greatly in length and composition between the different types and splice variants. This variability means there is a possibility that some untested splice variants of β_1 or β_3 may differ in their ability to modulate calcium channels. Here, we report that the splice variant of β_1 expressed in skeletal muscle, β_{1a} , which also lacks palmitolation sites in its N-terminus, does not support facilitation. To sort out the structural component that could be responsible for this difference in function we

between β_{1a} and β_{2a} . We report here that transferring the last 35 amino acids of β_{2a} into β_{1a} restored prepulse facilitation and we discuss potential motifs in domain V shared by β_{2a} , β_{1b} and β_3 that may be required for depolarization-induced potentiation of L-type calcium channels.

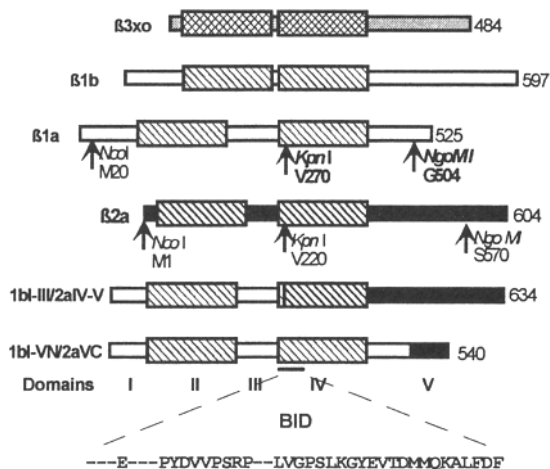


Figure 1. Schematic representation of β subunits highlighting conserved domains II and IV as hatched boxes. Restriction sites used to construct chimeras 1bI-III/2aIV-V and 1bI-VN/2aVC are shown with the amino acid position of the cut. Restriction sites inserted in β_{1a} are shown in bold. The sequence encompassing the β Interaction Domain (BID) is shown at the bottom.

2. METHODS

2.1. RNA Synthesis and Preparation of Oocytes

The cardiac calcium channel α_1 subunit used here was an amino-terminal deletion mutant of the rabbit $\text{Ca}_v1.2$ (DN60) that yields larger ionic and gating currents without changes in kinetics or sensitivity to the modulation by the β subunits (Wei *et al.*, 1996). The β_{2a} (Wei *et al.*, 1991) and β_{1b} (Pragnell *et al.*, 1991) subunits were from rat, the β_{1a} was from rabbit (Ruth *et al.*, 1989) and β_{3xo} is a β_3 -like subunit cloned from *Xenopus* oocytes (Tareilus *et al.*, 1997). DN60, β_{2a} and β_{3xo} subunits were subcloned into pAGA2 (Sanford *et al.*, 1991), β_{1a} into pGEM-3 and β_{1b} into pBS. PAGA-DN60, pAGAB β_{2a} and pAGAB β_{3xo} cDNA were linearized with Hind III; pBS β_{1b} with Not I and pGEM β_{1a} with Xba I (New England Biolabs Inc., Beverly, MA, U.S.A.). RNAs were synthesized *in vitro* with the Message Machine™ (AMBION, Austin TX USA) according to the manufacturer's instructions and resuspended in 10 μl water at 4-6 $\mu\text{g}/\mu\text{l}$. Stock solutions were diluted from 10- to 100-fold and those dilutions yielding larger expression and maximal functional changes were chosen for subsequent experiments. 50nl of cRNA were injected per oocyte using an automatic injector (Drummond Sci., Broomall, PA, U.S.A.).

Large *Xenopus* females (Nasco, Modesto, CA, U.S.A.) were anaesthetized by immersion in 0.15% tricaine for 15 minutes. One or two lobes of an ovary were removed through a 10-12 mm abdominal incision under sterile conditions. Oocytes were harvested from the same frog up to five times, allowing at least six weeks recovery between harvests. This procedure and the general care and handling of *Xenopus* frogs were carried out according to a protocol approved by the Institutional Animal Care Committee of Texas Technical University Health Sciences Center. Oocytes were defolliculated by collagenase treatment (2 mg/ml, type II; Worthington Biochemical Co., Lakewood, NJ, U.S.A.) for 30 minutes in Ca^{+2} -free solution (82.5 mM NaCl, 2.5 mM KCl, 1 mM MgCl_2 and 5 mM HEPES titrated to pH 7.6 with NaOH). Collagenase treatment was stopped by repeated rinses with Ca^{+2} -free media that was then replaced by SOS (100 mM NaCl, 2 mM KCl, 1.8 mM CaCl_2 , 1 mM MgCl_2 and 5 mM HEPES titrated to pH 7.6 with NaOH) in several partial dilution steps over a period of one hour. Oocytes were maintained at 19.5 °C in SOS supplemented with Na-pyruvate (2.5 mM), gentamycin (50 or 200 $\mu\text{g/ml}$) and **Verapamil** (10 μM). The latter appears to increase survival of oocytes expressing large calcium currents, although a systematic survey was not carried out.

2.2. Construction of Chimeras and Deletion Mutants

All point mutations were carried out by the Quick ChangeTM method (Stratagene Inc., Austin, TX, U.S.A.) and ligation, with the Rapid DNA Ligation Kit (Roche Diagnostic Corp., Indianapolis, IN, U.S.A.) according to the manufacturer's instructions. To construct 1bI-III/2aIV-V, a Kpn I site was introduced into β_{1a} by substituting G968 by an adenine and obtaining pGEM- β_{1a} mut. Using an endogenous NcoI site, a fragment encompassing M20 to V270 was obtained by digesting pGEM- β_{1a} mut with NcoI and KpnI. This segment was then inserted into pAGA- β_{2a} after NcoI/KpnI digestion to remove from M1 to V220 and obtain 1bI-III/2aIV-V. To construct 1bI-VN/2aVC, a Ngo MI site was inserted by substituting G1668 with a cytosine. This yields pGEM- β_{1a} mut2 with a G504K mutation. pGEM- β_{1a} mut2 was then digested with Kpn I/Ngo MI to yield a 705 base pairs fragment encompassing from V270 to K504, which was isolated from a 0.8% agarose gel. This fragment was used to replace a homologue in 1bI-III/2aIV-V to obtain 1bI-VN/2aVC, which includes M20 to G503 from β_{1a} followed by the C-terminus of β_{2a} starting at S570 (Figure 1).

2.3. Recording Techniques

Macroscopic currents were recorded using the cut-open oocyte voltage-clamp technique (Tagliatalata *et al.*, 1992) with a CA-1 amplifier (Dagan Corp., Minneapolis, MN, U.S.A.). Oocyte membrane exposed to the bottom chamber was permeabilized by a brief treatment with 0.1% saponin. The voltage pipettes were filled with 2 M tetramethylammonium-methanesulfonate, 50 mM NaCl and 10 mM EGTA and had a tip resistance from 600 to 1,200 k Ω . Data acquisition and analysis were performed using the pCLAMP6 system (Axon Instruments Inc., Foster City, CA, U.S.A.). The external solution contained 10 mM Ba^{2+} , 96 mM n-Methylglucamine, and 10 mM HEPES, and

tetramethylammonium-methanesulfonate, 50 mM NaCl and 10 mM EGTA and had a tip resistance from 600 to 1,200 Ω . Data acquisition and analysis were performed using the pCLAMP6 system (Axon Instruments Inc., Foster City, CA, U.S.A.). The external solution contained 10 mM Ba^{2+} , 96 mM n-Methylglucamine, and 10 mM HEPES, and the pH was adjusted to 7.0 with methanesulfonic acid. The internal solution contained 120 mM n-Methylglucamine, 10 mM EGTA, and 10 mM HEPES, pH adjusted to 7.0 with methanesulfonic acid. To eliminate Cl^- currents through endogenous calcium-activated channels, we injected the oocytes with 50 nl of 50mM BAPTA [1,2-bis(2-aminophenoxy)-ethane-N,N,N',N'-tetraacetic K_4 hydrate] before recordings; there were no differences in prepulse facilitation when compared to non-injected oocytes.

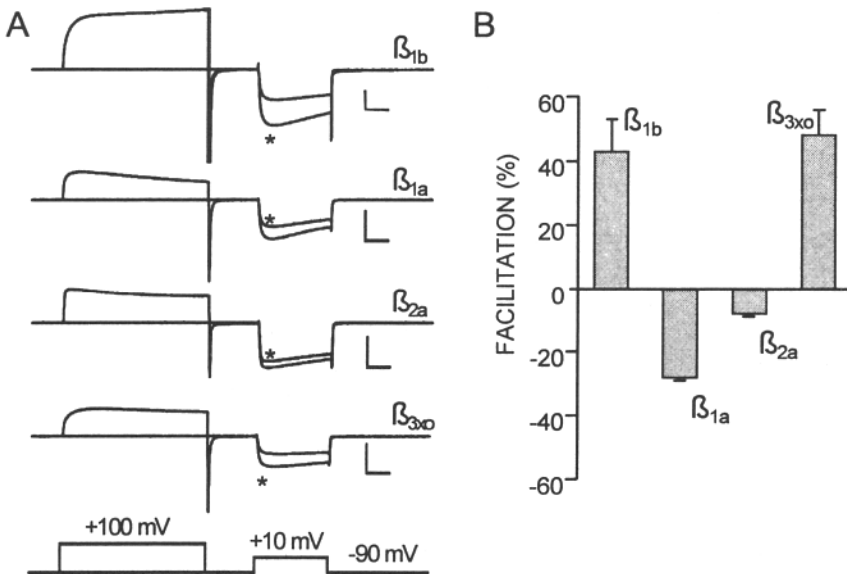


Figure 2. Prepulse modulation of $Ca_v1.2$ co-expressed with different α subunits. A) Ba^{2+} currents from *Xenopus* oocytes expressing different subunit combinations with (*) and without a 300 ms prepulse to +100 mV. Facilitation was measured during a 150ms pulse to +10 mV after a 100 ms gap. Calibration bars are 1 μA and 50 ms for all traces. B) Average facilitation measured as the ratio of peak current at +10 mV, with and without prepulse. For oocytes expressing β_{1b} or β_{3xo} , facilitation was 43% \pm 10% (n=10) and 48% \pm 8% (n=9) respectively while for β_{2a} and β_{1a} there was inhibition of 8% \pm 1% (n=9) and 28% \pm 1% (n=9) respectively.

3. RESULTS

We confirmed that currents through L-type calcium channels could be stimulated by strong depolarizations in heterologous expression systems for certain subunit combinations (Figure 2). When $Ca_v1.2$ was co-expressed with β_{1b} , Ba^{2+} currents recorded during a 150 ms pulse to +10 mV were increased by 43% \pm 10% (n=10) by a 300 ms prepulse to 100 mV after a 100 ms gap to the holding potential (-90 mV). Under

similar conditions, a comparable stimulation was observed for β_{3x0} ($48\% \pm 8\%$; $n=9$). Also in agreement with previous work (Qin *et al.*, 1998), we found that combining the rabbit neuronal β_{2a} with $Ca_v1.2$, yields channels that could not be potentiated by similar treatment. In fact, we observed a small inhibition with the stimulation protocol used here ($8\% \pm 1\%$, $n=9$). The novel finding we report here, is that we identified another subunit (β_{1a}) that yields calcium channels that are inhibited rather than potentiated by prepulses ($28\% \pm 1\%$; $n=9$). This inhibition is likely to be a consequence of partial inactivation during the prepulse that is expected to be smaller with β_{2a} known to inhibit voltage-dependent inactivation (Olcese *et al.*, 1994)

The β_{1a} subunit, normally expressed in skeletal muscle, differs from the neuronal β_{1b} in domains III and V, while it shares identical domains I, II and IV. It also lacks the palmitolation sites identified in the N-terminus of β_{2a} that need to be removed to observe prepulse facilitation. Together, this information lead us to conclude that some structural elements absent in the β_{1a} but present in β_{1b} , β_{2a} , and β_3 , are required for this type of modulation. To investigate whether domain III was the culprit, we constructed a chimera combining the first 250 amino acids of β_{1a} with the last 334 amino acids of β_{2a} . As shown in Figure 1, this chimera, named 1bI-III/2aIV-V, carries domains IV and V from β_{2a} and domains I to III from β_{1a} . Domain I in 1bI-III/2aIV-V lacks the first 20 amino acids of the N-terminus for the use of an endogenous Nco I restriction site at Met₂₀. Since these amino acids are also present in β_{1b} they should not interfere with facilitation. However, the short domain I characteristic of β_{3x0} and β_{2a} , as long as palmitolation is removed, is compatible with prepulse facilitation suggesting that the first 20 amino acids of β_{1a} (or β_{1b}) are not necessary for this type of modulation.

Top traces in Figure 3A, show Ba^{2+} currents arising from co-expression of 1bI-III/2aIV-V with $Ca_v1.2$, with and without a 300 ms depolarization to +100 mV. Ba^{+2} currents from eight oocytes of three different batches increased $41\% \pm 6\%$ when preceded by depolarization (Figure 3B).

Thus, domain III of β_{1a} does not interfere with prepulse facilitation. From this result we also confirm that the first 20 N-terminal amino acids are not required, nor do they inhibit depolarization-induced potentiation. The other alternative that thus arises, is that the short C-terminus (domain V) of the skeletal muscle splice variant of β_1 lacks some of the structural elements required for prepulse-induced facilitation.

Alignment of multiple sequences of the β subunits supporting prepulse facilitation, reveal that a series of conserved charged and aromatic amino acids in the C-terminus are missing in β_{1a} (Figure 4). To examine the role of these amino acids, we constructed a new chimera in which the last 18 amino acids of β_{1a} C-terminus were replaced by the last 34 amino acids of β_{2a} . This new chimera (1bI-VN/2aVC) was constructed from 1bI-III/2aIV-V and thus also lacks the first 20 amino acids. As shown in Figure 3, prepulses to +100 mV potentiate channels resulting from the combination of $Ca_v1.2$ with 1bI-VN/2aVC.

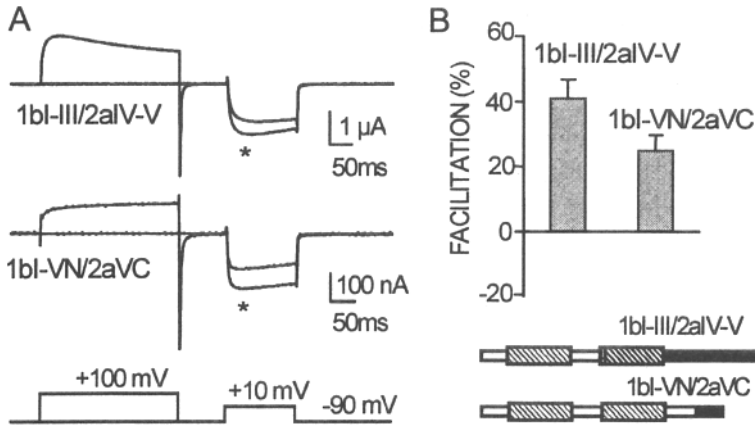


Figure 3. Prepulse facilitation modulation of $Ca_v1.2$ co-expressed with chimeras 1bI-III/2aIV-V and 1bI-VN/2aVC. **A)** Representative traces of Ba^{2+} currents recorded from *Xenopus* oocytes expressing two different chimeras of β_{1a} and β_{2a} as indicated next to each trace. (*) points to the current during the test pulse preceded by a 300 ms pulse to +100 mV. **B)** Bar plot showing average facilitation measured as in Figure 2. With 1bI-III/2aIV-V, facilitation was $41\% \pm 6\%$ ($n=8$) and for 1bI-VN/2aVN it reaches $25\% \pm 5\%$ ($n=9$). A schematic representation of the chimeras is shown at the bottom of panel B.

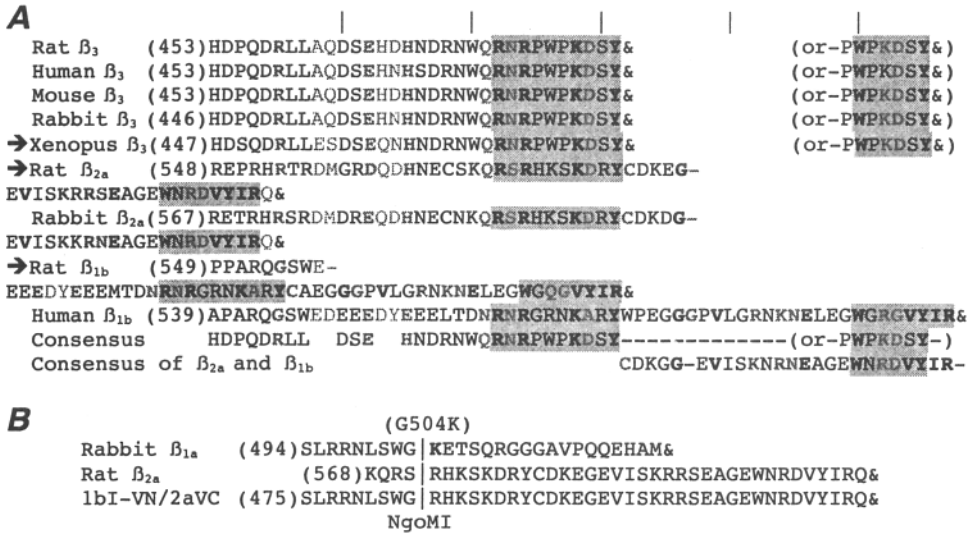


Figure 4. A. C-terminus sequence alignment of different β subunits; those tested in this work are indicated by arrows. The complete protein sequences were used for the alignments 'ANTHERPROT' 5.2. Conserved residues are highlighted as bold for 100% identity; as gray for $\geq 75\%$ identity; regular characters indicate $\geq 50\%$ identity; and light gray, non-conserved residues. Shaded boxes highlight regions of high sequence homology. The C-terminus of β_3 shows two possible alignments. **B.** Description of 1bI-VN/2aVC showing C-terminus sequences of parental β_{1a} and β_{2a} around de Ngo MI native to β_{2a} and inserted in β_{1b} . Note that the G504K mutation introduced with the insertion of Ngo MI is not carried to 1bI-VN/2aVC.

Average facilitation measured from nine oocytes from three different batches was $25\% \pm 5\%$. Although smaller than that with 1bI-III/2aIV-V, this increase in current amplitude contrasts strongly with the 28% percent reduction observed with the native β_{1a} . From these results we propose that the last 34 amino acids of β_{2a} encode some structural elements necessary for depolarization-induced facilitation of $\text{Ca}_v1.2$ channels.

4. DISCUSSION

From previous work, the emerging picture is one in which the structural elements supporting prepulse facilitation are shared by all β subunits (Cens *et al.*, 1998; Dai *et al.*, 1999) and that with β_{2a} , this phenomenon is suppressed due to an additional interaction with the plasma membrane through palmitoylation by a specific site at N-terminal (Qin *et al.*, 1998). However, prepulse facilitation in neuronal channels is interpreted as relief of G-protein-mediated inhibition that involves the main interaction surface of α_1 and β i., i.e. BID in β and twelve amino acids within the loop-joining repeats I and II of the α_1 subunit (De Waard *et al.*, 1997). Thus, it appeared reasonable to assume that this same interaction surface may also participate in G-protein-independent facilitation.

One may speculate that the interaction of α_1 and β at this site is itself voltage dependent and the depolarization increases the interaction and thus promotes channel opening (Neely *et al.*, 1993). However, this picture is no longer sustainable given the observations reported here, that is, that $\text{Ca}_v1.2$ combined with β_{1a} does not show facilitation, as domain III, encompassing BID, is exactly the same as in β_{1b} , which supports facilitation. But, here we restored facilitation by transferring the C-terminus of β_{2a} indicating that some additional structural feature required for prepulse facilitation is missing in β_{1a} . Sequence alignment of the C-terminus of several β_3 , β_{2a} and β_{1b} subunits suggests two potential motifs shown as shaded areas in Figure 4, which may play an important role in potentiation. The first appears to be determined by two arginines separated by a polar residue followed by a more distant lysine and perhaps ending with the aromatic residue tyrosine. Alternatively, the motif may encompass a fully conserved tryptophane two residues upstream from a positively charged amino acid (Lys or Arg) and terminating in a tyrosine. Another possibility that we have not yet ruled out, is that the eighteen amino acids of β_{1a} that were replaced in 1bI-VN/2aVC, suppress prepulse facilitation. To evaluate these possibilities, additional experiments mutating potentially critical amino acids will be required.

5. ACKNOWLEDGMENTS

We thank Vicky Prado for the preparation, injection and maintenance of *Xenopus* oocytes and David Naranjo for helpful comments on this manuscript. This work was supported by grants from NIH (GM53196), FONDECYT (1991016) and ICM (P99-037-F) to Alan Neely.

6. REFERENCES

- Birbaumer, L., Qin, N., Olcese, R., Tareilus, E., Platano, D., Costantin, J., & Stefani, E. 1998, Structures and functions of calcium channel beta subunits, *Journal of Bioenergetics and Biomembranes* **30**(4): 357-375.
- Canti, C., Bogdanov, Y., & Dolphin, A. C. 2000, Interaction between G proteins and accessory subunits in the regulation of α_{1B} calcium channels in *Xenopus* oocytes, *Journal of Physiology (London)* **527 Pt 3**: 419-432.
- Catterall, W. A. 2000, Structure and regulation of voltage-gated Ca^{2+} channels, *Annual Review of Cell and Developmental Biology* **16**: 521-555.
- Cens, T., Restituito, S., Vallentin, A., & Charnet, P. 1998, Promotion and inhibition of L-type Ca^{2+} channel facilitation by distinct domains of the β subunit, *Journal of Biological Chemistry* **273** (29): 18308-18315.
- Dai, S., Klugbauer, N., Zong, X., Seisenberger, C., & Hofmann, F. 1999, The role of subunit composition on prepulse facilitation of the cardiac L-type calcium channel, *FEBS Letter*. **442**(1): 70-74.
- De Waard, M., Liu, H. Y., Walker, D., Scott, V. E. S., Gurnett, C. A., & Campbell, K. P. 1997, Direct binding of G-protein β complex to voltage-dependent calcium channels, *Nature* **385**(6615): 446-450.
- De Waard, M., Pragnell, M., & Campbell, K. P. 1994, Ca^{2+} channel regulation by a conserve β subunit domain, *Neuron* **13**: 495-530.
- De Waard, M., Scott, V. E., Pragnell, M., & Campbell, K. P. 1996, Identification of critical amino acids involved in alpha-beta interaction in voltage-dependent Ca^{2+} channels, *FEBS Letter* **380**(3): 272-276.
- Herlitz, S., Zhong, H., Scheuer, T., & Catterall, W. A. 2001, Allosteric modulation of Ca^{2+} channels by G proteins, voltage-dependent facilitation, protein kinase C, and Ca(v) beta subunits, *Proceedings of the National Academy of Sciences of the United States of America* **98**(8): 4699-4704.
- Hogan, K., Greg, R. G., & Powers, P. A. 1999, Structure and alternative splicing of the gene encoding the human $\beta 1$ subunit of voltage dependent calcium channels, *Neuroscience Letters* **277**(2): 111-114.
- Meir, A., Bell, D. C., Stephens, G. J., Page, K. M., & Dolphin, A. C. 2000, Calcium channel beta subunit promotes voltage-dependent modulation of alpha 1 B by G beta gamma, *Biophysical Journal* **79**(2): 731-746.
- Moss, F. J., Viard, P., Davies, A., Bertaso, F., Page, K. M., Graham, A., Canti, C., Plumpton, M., Plumpton, C., Clare, J. J., & Dolphin, A. C. 2002, The novel product of a five-exon stargazin-related gene abolishes $\text{Ca(V)}_{2.2}$ calcium channel expression, *EMBO Journal* **21**(7): 1514-1523.
- Neely, A., Wei, X., Olcese, R., Birbaumer, L., & Stefani, E. 1993, Potentiation by the β subunit of the ratio of the ionic current to the charge movement in the cardiac calcium channel, *Science* **262**: 575-578.
- Olcese, R., Qin, N., Schneider, T., Neely, A., Wei, X., Stefani, E., & Birbaumer, L. 1994, The amino termini of calcium channel β subunits set rates of inactivation independently of their effect on activation, *Neuron* **13**: 1433-1438.
- Page, K. M., Stephens, G. J., Berrow, N. S., & Dolphin, A. C. 1997, The intracellular loop between domains I and II of the B-type calcium channel confers aspects of G-protein sensitivity to the E- type calcium channel, *Journal of Neuroscience* **17**(4): 1330-1338.
- Platano, D., Qin, N., Noceti, F., Birbaumer, L., Stefani, E., & Olcese, R. 2000, Expression of the alpha(2)delta subunit interferes with prepulse facilitation in cardiac L-type calcium channels, *Biophysical Journal* **78**(6): 2959-2972.
- Pollo, A., Tagliatalata, M., & Carbone, E. 1991, Voltage-dependent inhibition and facilitation of Ca channel activation by GTP-gamma-S and Ca-agonists in adult rat sensory neurons, *Neuroscience Letters* **123**: 203-207.
- Pragnell, M., Sakamoto, J., Jay, S. D., & Campbell, K. P. 1991, Cloning and tissue-specific expression of the brain calcium channel beta-subunit, *FEBS Letter*. **291**: 253-258.
- Qin, N., Platano, D., Olcese, R., Costantin, J. L., Stefani, E., & Birbaumer, L. 1998, Unique regulatory properties of the type 2a Ca^{2+} channel beta subunit caused by palmitoylation, *Proceedings of the National Academy of Sciences of the United States of America* **95**(8): 4690-4695.
- Ruth, P., Rohrkasten, A., Biel, M., Bosse, E., Regulla, S., Meyer, H. E., Flockerzi, V., & Hofmann, F. 1989, Primary structure of the beta subunit of the DHP-sensitive calcium channel from skeletal muscle, *Science* **245**: 1115-1118.
- Sanford, J., Codina, J., & Birbaumer, L. 1991, Gama-subunit of G-Proteins, but not their α - or β -subunits, are polyisoprenylated, *Journal of Biological Chemistry*. **266**(15): 9570-9579.
- Stephens, G. J., Brice, N. L., Berrow, N. S., & Dolphin, A. C. 1998, Facilitation of rabbit alpha1B calcium channels: involvement of endogenous Gbetagamma subunits, *Journal of Physiology (London)* **509**: 15-27.

- Tagliatela, M., Toro, L., & Stefani, E. 1992, Novel voltage clamp to record small, fast currents from ion channels expressed in *Xenopus* oocytes, *Biophysical Journal* **61**: 78-82.
- Tareilus, E., Roux, M., Qin, N., Olcese, R., Zhou, J. M., Stefani, E., & Birnbaumer, L. 1997, A *Xenopus* oocyte β subunit: Evidence for a role in the assembly/expression of voltage-gated calcium channels that is separate from its role as a regulatory subunit, *Proceedings of the National Academy of Sciences of the United States of America* **94**(5): 1703-1708.
- Wei, X., Neely, A., Olcese, R., Lang, W., Stefani, E., & Birnbaumer, L. 1996, Increase in Ca^{2+} channel expression by deletions at the amino terminus of the cardiac $\alpha 1C$ subunit, *Receptors and Channels*. **4**: 205-215.
- Wei, X. Y., Pérez Reyes, E., Lacerda, A. E., Schuster, G., Brown, A. M., & Birnbaumer, L. 1991, Heterologous regulation of the cardiac Ca^{2+} channel $\alpha 1$ subunit by skeletal muscle β and γ subunits, Implications for the structure of cardiac L-type Ca^{2+} channels, *Journal of Biological Chemistry*. **266**: 21943-21947.
- Zygmunt, A. C. and Maylie, J. 1990, Stimulation-dependent facilitation of the high threshold calcium current in guinea-pig ventricular myocytes, *Journal of Physiology (London)* **428**: 653-671.

8

DIFFERENTIAL EXPRESSION OF Ca CHANNELS AND SYNAPTIC TRANSMISSION IN NORMAL AND ATAXIC KNOCK-OUT MICE

Francisco J. Urbano¹, Marcelo D. Rosato-Siri¹ and Osvaldo D. Uchitel^{1*}.

1. INTRODUCTION

Voltage dependent calcium channels (VDCC) play a key role in neuronal signaling as mediators of Ca^{2+} entry during the process of neurotransmitter release (Katz, 1969; Llinás *et al.*, 1976). Ca^{2+} influx through VDCCs is considered to increase intracellular Ca^{2+} concentration in a bell shape microdomain close to the channel mouth (Llinás and Moreno, 1998). This means that intracellular Ca^{2+} constitutes a complex signal, which can be modulated by factors that alter Ca^{2+} buffering and/or diffusion, with a large effect on Ca^{2+} triggered cellular events like synaptic neurotransmitter release.

2. MOLECULAR STRUCTURE OF VDCC

VDCC are transmembrane proteins that open in response to membrane depolarization and allow Ca^{2+} ions to enter the cell from extracellular space. Neuronal VDCC have been subdivided on the bases of their electrophysiological and pharmacological properties into low voltage activated or T type channels and high voltage activated (HVA) channels a class that includes the L, N, P/Q and R types. The HVA types have mainly been characterized by their different sensitivity to pharmacological modulators and inhibitory toxins (Uchitel, 1997)

High voltage-activated Ca^{2+} channels consist of an α_1 subunit that forms the core of the channel, in addition to β , α_2 - δ , and possibly γ subunits that modulate the functional properties of the α_1 subunit. Molecular cloning has identified ten different genes (Cav 1.1 to Cav 3.3) encoding α_1 subunit genes (called α_{1A} - α_{1B} - α_{1S}), which are the main subunit of many of the previously characterized native Ca^{2+} channel subtypes. Four different

¹ Laboratorio de Fisiología y Biología Molecular, Departamento de Ciencias Biológicas, Facultad de Ciencias Exactas y Naturales, Universidad de Buenos Aires, Ciudad Universitaria, Pabellón II piso 2, Buenos Aires 1428, Argentina, TE 54 11 4576 3368, FAX 54 11 4576 3321.

* corresponding author: odu@bg.fcen.uba.ar

genes encoding β subunits (i.e. $\beta_1 - \beta_4$), three genes encoding the $\alpha_2 - \delta$ complex, and five genes encoding neuronal γ subunits have also been identified (Ertel *et al.*, 2000).

Structurally, the Ca^{2+} channel α_1 subunit is comprised of four highly homologous domains that are connected via cytoplasmically oriented linker regions. Each of these four domains contains six transmembrane helices (termed S1–S6), plus a non-helical P-loop motif linking the S5 and S6 segments. Molecular biological studies have identified many of the structural determinants that govern the functional pharmacological properties of the α_1 subunit, and its sites of interaction with modulatory proteins (Birnbaumer *et al.*, 1998).

The four known Ca^{2+} channel β subunits are cytoplasmic proteins that share a similar structural arrangement. The consequences of the β subunit expression on the function of the α_1 subunit include an increase in current density, modulation of activation and inactivation kinetics, effects on pharmacological properties, and interactions with second-messenger regulation. The $\alpha_2 - \delta$ complex is derived from a single gene that is post-translationally cleaved and re-linked via disulfide bonds. The precise role of the $\alpha_2 - \delta$ subunit in the function of the channel remains poorly understood. By contrast, the γ subunit spans the plasma membrane via four transmembrane segments and might affect activation and inactivation properties of voltage-dependent Ca^{2+} channels.

3. CALCIUM CHANNELOPATHIES

Although different Ca^{2+} channel subunits have been implicated in several CNS diseases, mutations of the $\text{Ca}_v2.1$ gene that encodes the α_{1A} subunit of the P/Q channel are perhaps the best known (Jen, 1999). Mutations in the $\text{Ca}_v2.1$ gene have been found to be responsible for the human episodic neurological disorders Familial Hemiplegic Migraine (FHM), Episodic Ataxia type 2 and Spinocerebellar Ataxia type 6 (Zhuchenko *et al.*, 1997; Ophoff *et al.*, 1998). The $\text{Ca}_v2.1$ gene is likely to be also involved in (non-hemiplegic) typical migraine (Terwindt *et al.*, 1998; Nyholt *et al.*, 1998; Ambrosini *et al.*, 1999). Likewise, natural $\text{Ca}_v2.1$ mutations have been reported for the tottering (tg) and leaner (tg^{la}) mice, of which the homozygous animals exhibit symptoms of ataxia and epilepsy (Fletcher *et al.*, 1996; Doyle *et al.*, 1997).

Mutations in Ca^{2+} channel genes lead to channel dysfunction and altered channel properties. These disturbances may cause abnormally increased or decreased Ca^{2+} entry that could have profound influence on various Ca^{2+} signaling pathways including neurotransmitter release (Kraus *et al.*, 1998; Hans *et al.*, 1999; Toru *et al.*, 2000).

4. CALCIUM CHANNELS AND NEUROTRANSMITTER RELEASE AT THE NEUROMUSCULAR JUNCTION

Different types of VDCC support neurotransmitter release at many synapses (Reuter, 1996; Catterall, 1998). At mature mammalian neuromuscular junctions, neurotransmitter release is blocked completely by the P/Q-type channel blocker ω -Agatoxin IVA indicating that neurotransmitter release is mediated almost exclusively by this type of channel (Uchitel *et al.*, 1992; Protti and Uchitel, 1993; Katz *et al.*, 1997). In contrast at neonatal rat neuromuscular junctions, both Ca^{2+} channel blockers, ω -Agatoxin IVA and

the N-type blocker ω -Conotoxin GVIA, are capable of inhibiting neurotransmitter release being ω -Agatoxin IVA more effective (see Figure; Rosato Siri and Uchitel, 1999). Therefore at the neonatal neuromuscular junction there is a differential participation of these channels at individual release sites with different efficacy.

Fast neurotransmitter release strongly depends on the extracellular concentration of Ca^{2+} in a non-linear relationship where the amplitude of the end-plate potentials varies as the 4th power of Ca^{2+} concentration at low concentrations. This has been interpreted as the co-operative action of four Ca^{2+} ions in the release of each neurotransmitter vesicle (Dodge and Rahamimoff, 1967). In mammals, this relationship has also been described as non-linear, with a slope close to 3.0 (Cull-Candy *et al.*, 1980).

At adult neuromuscular junctions some VDCCs are involved in neurotransmitter release only when intracellular Ca^{2+} -concentration was reduced. Indeed, fast cell-permeant calcium chelators such as BAPTA-AM, but not slow ones as EGTA-AM, are capable of unmasking a L-type component of the perineurial presynaptic calcium current. Interestingly, only when protein phosphatases are inhibited (using the inhibitor of serine/threonine phosphatase okadaic acid), in the presence of BAPTA-AM, this component also mediate neurotransmitter release (Urbano *et al.*, 2001). L-type-mediated EPPs presented both higher latency onset and slower rise time than the P/Q-type-mediated ones. In conclusion, L-type VDCC can mediate neurotransmitter release under experimental conditions that allow both intracellular $[\text{Ca}^{2+}]$ buffered by fast chelators and the presence of OA. Finally, the presence of the $\alpha 1D$ subunit for L-type VDCCs has been recently found at adult neuromuscular junctions using immunohistochemical techniques (Pagani and Uchitel, unpublished results), reinforcing our point of view about the important role these channels may be playing on the normal neuromuscular junction physiology and also making of this Bapta/OA preincubated neuromuscular preparation a useful model to understand the process of neurotransmitter release by multiple types of VDCC during development.

On the other hand, at neonatal neuromuscular the Ca^{2+} dependence of nerve-evoked neurotransmitter release studied by changing the external Ca^{2+} concentration produces a supralinear relationship in quantal content of neurotransmitter release with a higher exponential when release is mediated by P/Q than N-type channels. This difference could be accounted for by the presence of both channels at every release site but with the P/Q-type VDCCs closer to the Ca^{2+} sensor than the N-type (Rosato Siri and Uchitel, unpublished results). Furthermore, one prediction of this hypothesis is that the Ca^{2+} entering via N-type Ca^{2+} channels will diffuse along a greater distance before reaching the Ca^{2+} sensor. This increases the probability of Ca^{2+} being bound by a Ca^{2+} buffer, particularly by a fast one like BAPTA (Adler *et al.*, 1991). Indeed, at the adult and late neonatal mouse neuromuscular junction loading the nerve terminal with 10 μM BAPTA-AM did not affect neurotransmitter release, which, in those cases, is only mediated by P/Q-type channels (Urbano and Uchitel, 1999). On the other hand, at early stages of development (0-4 postnatal days), BAPTA-AM loaded nerve terminals strongly reduces synaptic output. The effect is related to the capacity of buffering Ca^{2+} influx specifically through N-type VDCCs (Rosato-Siri) and Uchitel, unpublished results).

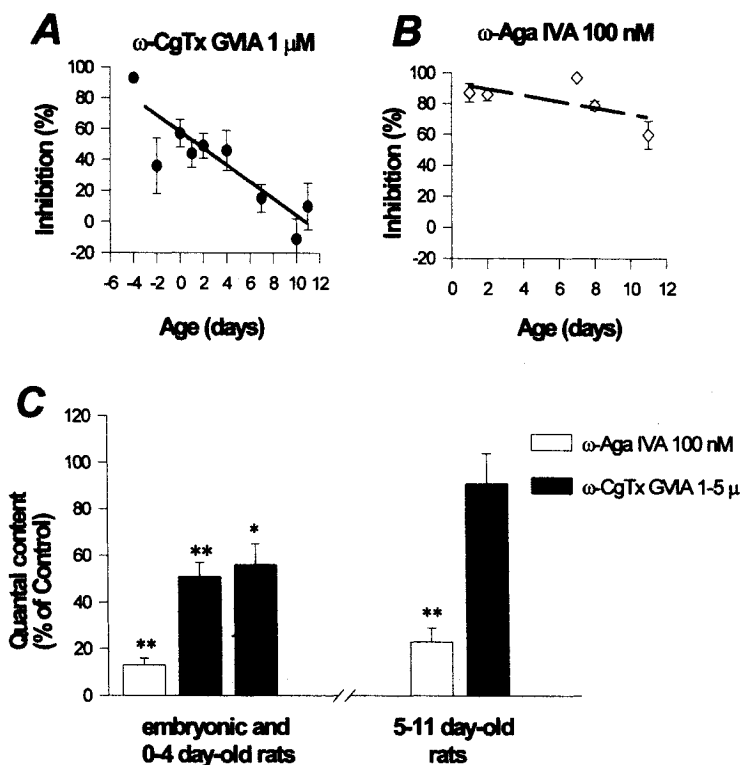


Figure 1. Plots show the correlation between the percentage of inhibition (of quantal content) and the time of development (age of the animals) in *A*, ω -CgTx GVIA (1 μ M); *B*, ω -Aga IVA (100 nM) treated preparations. Each value represents a mean \pm s.e.mean of the data pooled from a nerve-muscle preparation (at least 12 endplates per muscle). The lines represent the best linear fit of the data of ω -CgTx GVIA (solid line, $r^2 = 0.8$, $P < 0.01$), ω -Aga IVA (dashed line, $r^2 = 0.37$, $P = 0.27$). *C*. The bar diagrams show the effect of the drugs on quantal content (m) expressed as a percentage of the control value. The toxins ω -Aga IVA (100nM) and ω -CgTx GVIA (1-5 μ M) significantly reduced the evoked response in embryonic and 0-4 day-old rats. In control fibres, $m = 0.85 \pm 0.08$ (mean \pm s.e.mean, $n = 64$ endplates from 16 muscles). On the other hand, in 5-11 day-old rats ω -Aga IVA (100nM) maintained its strong effect on the evoked response shown at early stages while ω -CgTx GVIA (1 μ M) lacked any effect. In control fibres, $m = 1.27 \pm 0.16$ (mean \pm s.e.mean, $n = 43$ endplates from 13 muscles).

Control fibres were assayed in a 0.7-1 mM Ca^{2+} and 5-8 mM Mg^{2+} saline solution. Treated fibres were assayed in the same muscles after 1-hour incubation with the respective drug. Each column represents the mean \pm s.e.mean of data pooled from 2-5 nerve-muscle preparations (at least 12 endplates per muscle). m was calculated by the failure method. Stimulation frequency 0.5 Hz. ** $P < 0.0001$; * $P < 0.05$ compared with the values obtained in the same muscles before addition of the calcium channel blockers.

Further insight into synaptic alterations due to Ca^{2+} channel mutation came studying synaptic transmission at the neuromuscular junctions from a P/Q deficient mouse. Elimination of P/Q Ca^{2+} currents in the $\text{Ca}_v2.1$ null mutant mice induces a neurological deficit characterized by progressive ataxia and dystonia until the mice are unable to walk and die (\sim P20) (Jun *et al.*, 1999). We also explored the status of short-term plasticity at

NMJ of Ca_v2.1 null mutant mice. In mutant mice, neurotransmitter release is reduced and paired-pulse facilitation is absent. Neurotransmitter release is mediated by N-type and R-type Ca²⁺ channels but with a different dependence of extracellular Ca²⁺ chelators suggesting that they were located far from the release site (Urbano *et al.*, 2001).

5. CONCLUSIONS

At neuromuscular junction as well as at Central Nervous System synapses, multiple types of VDCCs are involved in neurotransmitter release. Interestingly, at neuromuscular junctions a "switch" on the VDCCs coupled to neurotransmitter release can be modified by development, intracellular Ca²⁺ buffering as well as by phosphorylation. The fact that Ca_v2.1, including certain forms of migraine, epilepsy and ataxia. Clinical and experimental studies of neuromuscular transmission might provide with important clues for unravelling neuropathological mechanisms of these human diseases.

6. REFERENCES

- Adler, E.M., Augustine, G.J., Duffy, S.N., and Charlton, M.P., 1991, Alien intracellular calcium chelators attenuate neurotransmitter release at the squid giant synapse, *Journal of Neuroscience* **11**(6): 1496-1507.
- Ambrosini, A., Maertens de Noordhout, A., Alagona, G., Dalpozzo, F., and Schoenen, J., 1999, Impairment of neuromuscular transmission in a subgroup of migraine patients, *Neuroscience Letters* **276**: 201-203.
- Birnbaumer, L., Qin, N., Olcese, R., Tareilus, E., Platano, D., Costantin, J., and Stefani, E., 1998, Structures and functions of calcium channel beta subunits, *Journal of Bioenergetics Biomembranes* **4**: 357-375.
- Catterall, W.A., 1998, Structure and function of neuronal Ca²⁺ channels and their role in neurotransmitter release, *Cell Calcium* **24** (5/6): 307-323
- Cull-Candy, S.G., Miledi, R., Trautmann, A., and Uchitel, O.D., 1980, On the release of transmitter at normal, myasthenia gravis and myasthenic syndrome affected human end-plates, *Journal of Physiology (London)* **299**: 621-638.
- Dodge, F.A., and Rahamimoff, R., 1967, Co-operative action a calcium ions in transmitter release at the neuromuscular junction, *Journal of Physiology (London)* **193**: 419-432.
- Doyle, J., Ren, X., Lennon, G., and Stubbs, L., 1997, Mutations in the Cacn1a4 calcium channel gene are associated with seizures, cerebellar degeneration, and ataxia in tottering and leaner mutant mice, *Mammalian Genome* **8**: 113-120.
- Ertel, E.A., Campbell, K.P., Harpold, M.M., Hofmann, F., Mori, Y., Perez-Reyes, E., Schwartz, A., Snutch, T.P., Tanabe, T., Birnbaumer, L., Tsien, R.W., and Catterall, W.A., 2000, Nomenclature of voltage-gated calcium channels, *Neuron* **25**: 533-535
- Fletcher, C.F., Lutz, C.M., O'Sullivan, T.N., Shaughnessy, J.D., Jr., Hawkes, R., Frankel, W.N., Copeland, N.G., and Jenkins, N.A., 1996, Absence epilepsy in tottering mutant mice is associated with calcium channel defects, *Cell* **87**(4): 607-617.
- Hans, M., Luvisetto, S., Williams, M.E., Spagnolo, M., Urrutia, A., Tottene, A., Brust, P.F., Jhonson, E.C., Harpold, M.M., Staurderman, K.A., and Pietrobon, D., 1999, Functional consequences of mutations in the human alpha1A calcium channel subunit linked to familial hemiplegic migraine, *Journal of Neuroscience* **19**: 1610-1619.
- Jen, J., 1999, Calcium channelopathies in the central nervous system, *Current Opinion in Neurobiology* **9**(3): 274-280.
- Jun, K., Piedras-Renteria, E.S., Smith, S.M., Wheeler, D.B., Lee, S.B., Lee, T.G., Chin, H., Adams, M.E., Scheller, R.H., Tsien, R.W., and Shin, H.-S., 1999, Ablation of P/Q-type Ca²⁺ channel currents, altered synaptic transmission, and progressive ataxia in mice lacking the ω_{1A} -subunit, *Proceedings of the National Academy of Sciences U.S.A.*, **96**(26): 15245-15250,
- Katz, B., 1969, The release of neural transmitter substances, Sherrington lectures, N° 10, Liverpool University Press.
- Katz, E., Protti, D.A., Ferro, P.A., Rosato-Siri, M.D., and Uchitel, O.D., 1997, Effects of Ca²⁺ channel blocker neurotoxins on transmitter release and presynaptic currents at the mouse neuromuscular junction, *British*

- Journal of Pharmacology* **121**: 1531-1540.
- Kraus, R.L., Sinnegger, M.J., Glossmann, H., Hering, S., and Striessnig, J., 1998, Familial hemiplegic migraine mutations change alpha 1A Ca²⁺ channel kinetics, *Journal of Biological Chemistry* **273(10)**: 5586-5590.
- Llinás, R., and Moreno H., 1998, Local Ca²⁺ signaling in neurons, *Cell Calcium* **2**: 359-366.
- Llinás, R., Steinberg, I.Z., and Walton, K., 1976, Presynaptic calcium currents and their relation to synaptic transmission: Voltage clamp study in squid giant synapse and theoretical model for the calcium gate, *Proceedings of the National Academy of Sciences U.S.A.*, **73**: 2918-2922.
- Nyholt, D.R., Dawkins, J.L., Brimage, P.J., Goadsby, P.J., Nicholson, G.A., and Griffiths, L.R., 1998, Evidence for an X-linked genetic component in familial typical migraine, *Human Molecular Genetics* **7**: 459-463.
- Ophoff, R.A., Terwindt, G.M., Frants, R.R., and Ferrari, M.D., 1998, P/Q-type Ca²⁺ channel defects in migraine, ataxia and epilepsy, *Trends in Pharmacological Sciences* **19**: 121-127.
- Protti, D.A., and Uchitel, O.D., 1993, Transmitter release and presynaptic Ca²⁺ currents blocked by the spider toxin ω -Aga-IVA, *NeuroReport* **5**: 333-336
- Reuter, H., 1996, Diversity and function of presynaptic calcium channels in the brain, *Current Opinion in Neurobiology* **6**: 331-337.
- Rosato-Siri, M.D., and Uchitel, O.D., 1999, Calcium channels coupled to neurotransmitter release at neonatal rat neuromuscular junctions, *Journal of Physiology (London)* **514**: 533-540.
- Terwindt, G.M., Ophoff, R.A., Haan, J., Sandkuijl, L.A., Frants, R.R., and Ferrari, M.D., 1998, Migraine, ataxia and epilepsy: a challenging spectrum of genetically determined calcium channelopathies, *European Journal of Human Genetics* **6**: 297-307.
- Toru, S., Murakoshi, T., Ishikawa, K., Saegusa, H., Fujigasaki, H., Uchihara, T., Nagayama, S., Osanai, M., Mizusawa, H., and Tanabe, T., 1999, Spinocerebellar ataxia type 6 mutation alters P-type calcium channel function, *Journal of Biological Chemistry* **275(15)**: 10893-10898.
- Uchitel, O.D., 1997, Toxins affecting calcium channels in neurons, *Toxicon* **35(8)**: 1161-1191.
- Urbano, F.J., Depetris, R.S., and Uchitel, O.D., 2001, Coupling of L-type calcium channels to neurotransmitter release at mouse motor nerve terminals, *Pflugers Archiv* **441(6)**: 824-831.
- Uchitel, O.D., Protti, D.A., Sánchez, V., Cherksey, B.D., Sugimori, M., and Llinás, R., 1992, P-type voltage-dependent calcium channel mediates presynaptic calcium influx and transmitter release in mammalian synapses, *Proceedings of the National Academy of Sciences U.S.A.*, **89**: 3330-3333.
- Urbano, F.J., Piedras-Rentería, E., Tsien, R.W., and Uchitel, O.D., 2001, Short term facilitation and Ca²⁺ dependence of transmitter release are altered at the neuromuscular junction of P/Q Ca²⁺ channel knock out mice, *Biophysical Journal* **80(1)**:234a.
- Urbano, F.J., and Uchitel, O.D., 1999, L-type calcium channels unmasked by cell-permeant Ca²⁺ buffer at mouse motor nerve terminals, *Pflugers Archiv* **437(4)**: 523-528.
- Zhuchenko, O., Bailey, J., Bonnen, P., Ashizawa, T., Stockton, D.W., Amos, C., Dobyns, W.B., Subramony, S.H., Zoghbi, H.Y., and Lee, C.C., 1997, Autosomal dominant cerebellar ataxia (SCA6) associated with small polyglutamine expansions in the alpha 1A-voltage-dependent calcium channel, *Nature Genetics* **15(1)**:62-69.

INVESTIGATING THE MODULAR BASIS OF BK CHANNEL ACTIVATION BY CALCIUM

Edward Moczydlowski^{1*}

1. INTRODUCTION

Potassium channels are biomolecular devices that mediate the genesis and regulation of membrane voltage, a physiochemical process that is essential to many forms of life. The key to understanding K-channel function lies in understanding the evolution of channel proteins. K-channels exist in nature as a multitude of related modular constructs with unique functional specialties. Analysis of the structural relationships among diverse members of the K-channel family has led to important deductions concerning the function of these modular structural elements. The purpose of this article is to illustrate how identification and analysis of separate domains of the BK(Ca) channel is leading to an emerging picture of its function and mechanism.

BK(Ca) channel refers to a large-conductance (200-300 pS) Ca^{2+} - and voltage-activated potassium channel that is found in numerous types of cells. The gene encoding BK(Ca) was first identified as the product of the *Slowpoke* gene locus of *Drosophila* (Atkinson *et al.*, 1991; Butler *et al.*, 1993) and is often referred to as DSlo, HSlo, etc., to specify *Drosophila* and human orthologs, respectively. As two examples of physiological function, BK(Ca) is particularly important in regulating electrical excitability of neurons and smooth muscle cells (Toro *et al.*, 1998). In neurons, BK(Ca) is co-localized with voltage-gated calcium channels (CaV) in the presynaptic nerve terminal membrane. Much evidence indicates that neuronal BK(Ca) channels open in response to Ca^{2+} entry through CaV channels and are responsible for attenuating release of neurotransmitter by hyperpolarization. On the other hand, opening of BK(Ca) channels in the smooth muscle plasma membrane appears to be triggered by release of intracellular Ca^{2+} stores mediated by the ryanodine receptor calcium-release channel. In both of these systems, the BK(Ca) channel can be viewed as an important negative feedback element that modulates the strength of synaptic coupling in neuronal networks and sets the level of contractile tone in smooth muscle.

¹ Department of Pharmacology, Yale University School of Medicine, P.O. Box 208066, New Haven, CT 06520-8066

* corresponding author: edward.moczydlowski@yale.edu

The pivotal role of BK(Ca) as a cellular control element can also be gauged by the multitude of regulatory pathways that impinge upon it. Aside from intrinsic activation of the channel protein α -subunit by depolarizing voltage and binding of intracellular Ca^{2+} , BK(Ca) is further regulated by steroid hormones (Valverde *et al.*, 1999), arachidonic acid metabolites (Lu *et al.*, 2001), nitric oxide/protein kinase G (Swayze and Braun, 2001), protein kinase A (Esguerra *et al.*, 1994), protein kinase C (Reinhart and Levitan, 1995), protein phosphatases, tyrosine kinases (Wang *et al.*, 1999; Ling *et al.*, 2000), and a family of accessory β -subunits (Meera *et al.*, 2000). In addition, expression of numerous protein isoforms of BK(Ca) is predicted to occur from the complex pattern of alternative exon splicing at the transcriptional level (Tseng-Crank *et al.*, 1994). An enlightened view of the significance of BK(Ca) to the life of the cell ultimately depends upon a detailed understanding the molecular mechanism that lies at the heart of its unique Ca^{2+} - and voltage-dependence.

2. PROGRESS TOWARD BK(CA) CHANNEL STRUCTURE

Genome sequencing efforts have largely revealed the evolutionary basis of the extensive diversity of potassium channels (Coetzee *et al.*, 1999; Hille, 2001). The basic picture is that all potassium-selective channels contain a ~100-residue protein module homologous to KcsA, a homo-tetrameric membrane protein from *Streptomyces lividans*, whose crystal structure has been described in intricate detail (Doyle *et al.*, 1998; Zhou *et al.*, 2001a). The structural diversity of potassium channels arises from various types of embellishments or modular additions to this basic core structure.

The essential KcsA-like module (Fig. 1) is also referred to as the Pore Domain since it contains the ion selectivity filter. This latter filter is the narrowest cylindrical part of the channel with approximate dimensions of 3 Å in diameter and 12 Å in length. The filter region avidly binds multiple K^+ ions, giving rise to the process of single-file, multi-ion conduction that underlies the extraordinary ion permeation properties of K^+ channels. Individual monomer subunits of the tetrameric Pore Domain consist of three consecutive α -helical regions called S5 (or M1), the Pore Helix, and S6 (or M2). The S5 and S6 helices span the whole length of the lipid bilayer. S5 forms the outer lipid-facing surface and S6 forms part of the inner surface that lines the aqueous channel. The short Pore Helix is tilted at about 45° relative to the plane of the membrane and is situated near the outer third of the bilayer. The Pore Helix is oriented with the negative end of its helix dipole pointed toward a spherical aqueous cavity (~10 Å in diameter) located in the center of the pore. The Pore Helix is connected to the S6 helix by a short strand containing a highly conserved sequence motif (TVGYG) that forms the selectivity filter. The Pore Domain also includes specific binding sites for numerous blockers of K^+ channels that include scorpion toxins such as charybdotoxin, small organic cations such as tetraethylammonium, and inorganic cations such as Ba^{2+} (MacKinnon *et al.*, 1998; Jiang and MacKinnon, 2000; Zhou *et al.*, 2001b).

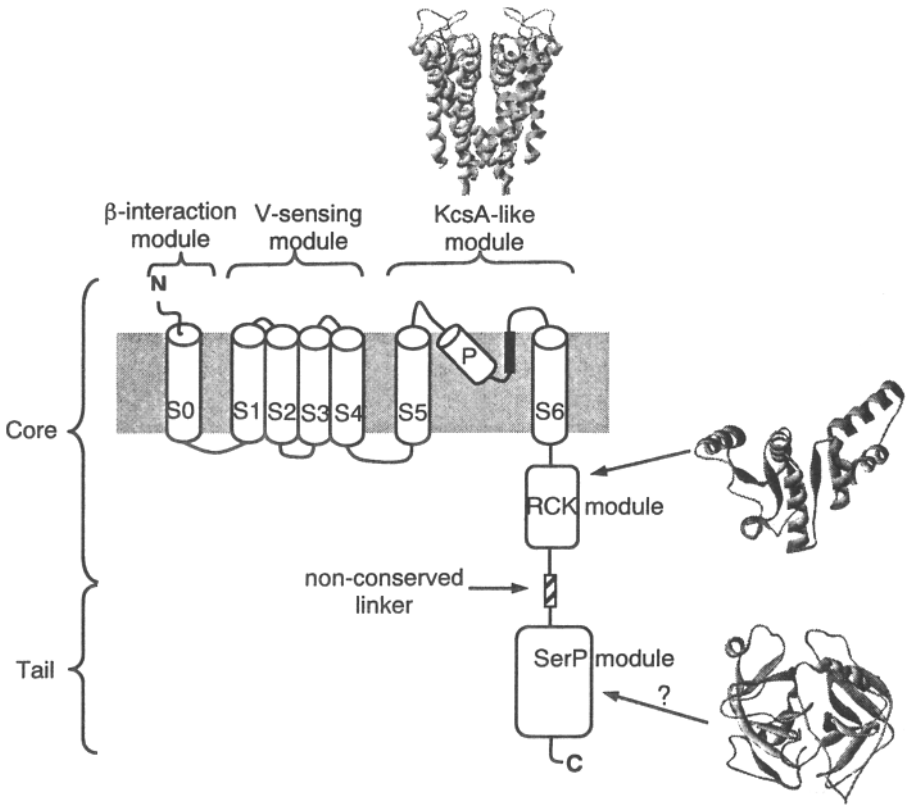


Figure 1. Schematic diagram showing the domain architecture of BK (Ca) channels. The channel forming α -subunit appears to consist of distinct structural domains or modules associated with different functions.

In contrast to the ~100-residue KcsA-like module and proteins that belong to the structurally similar family of inward rectifier potassium channels, the α -subunit monomer of the BK(Ca) channel is about ten-fold larger in mass, comprising 1113 residues for one common splice variant of human BK(Ca). What is the basis for this extra protein mass?

Why does a BK(Ca) channel require so much more protein content to transport K^+ down an electrochemical gradient than its primordial potassium channel relatives? The answer to this question must be related to the intricate gating mechanism of BK(Ca) and the nature of the structural elements that give rise to its unique Ca^{2+} - and voltage-dependence. It now is fairly clear that voltage-dependence and Ca^{2+} -dependence of the BK (Ca) channel are physically separable processes that are allosterically linked.

The first inkling that this might be the case, came from the recognition that the primary sequence of BK(Ca) α -subunit from many animals is highly conserved at both the N-terminal ~640 residues and at the C-terminal ~430 residues. However, the short intervening segment between these two conserved regions is poorly conserved (<10% identity) and varies in length from 50-100 residues in different species. In fact, it is

possible to functionally express BK(Ca) channels from two separate genes coding for the conserved N-terminal and C-terminal halves by engineering a stop codon and a new methionine initiation site within the non-conserved linker (Wei *et al.*, 1994; Meera *et al.*, 1997). Such experiments demonstrated that the N-terminal Core Domain of the channel can recognize and interact with an independently folded C-terminal Tail Domain to form an active BK(Ca) channel in two parts that exhibits relatively normal voltage- and Ca^{2+} -dependence. Analysis of the gating properties of such chimeric channels formed from a Core Domain of one species (e.g., mouse) and a Tail domain of another species (e.g., fruit fly) suggested that the voltage-dependence of the channel is specified by the Core whereas the Ca^{2+} -dependence is associated with the Tail (Wei *et al.*, 1994). The validity of this approach has been subsequently reinforced by studies that utilize Tail domains from a more distant homolog of *Slowpoke*, a Ca^{2+} -insensitive potassium channel gene called Slo3 (Schreiber *et al.*, 1998; Schreiber *et al.*, 1999). These latter experiments further implicated the Tail domain as a major locus of Ca^{2+} -sensitivity within the BK(Ca) α -subunit and identified a highly conserved segment called the “Ca-bowl” (Schreiber and Salkoff, 1997) as a possible site of Ca^{2+} -binding.

The location of the voltage-sensing mechanism within the Core domain of BK(Ca) nicely fits with studies of other voltage-gated potassium channels, such as the Shaker K^+ channel of *Drosophila* and its close relatives, Kv1-Kv4, in mammals. In such voltage-gated channels, a domain comprising four membrane spanning regions N-terminal to the Pore Domain, S1-S4, is known to be involved in sensing voltage and coupling membrane depolarization to channel opening. For example, it has been found that the pore-forming domain of KcsA can be appropriately linked to the S1-S4 domain of Shaker to produce a chimeric but functional voltage-gated channel (Lu *et al.*, 2001). This latter experiment strongly supports the idea that the S1-S4 voltage sensing domain and the pore domain are separate modular elements that interact to form the basic structure of a voltage-gated channel.

In particular, voltage-dependence in steeply voltage-dependent channels is known to be associated with ~ 7 conserved Arg/Lys residues that occur at every third position in S4 segments (Yellen, 1998). In contrast, the S4 region of the BK(Ca) channel contains only 3-4 Arg residues in the S4 region. Mutational analysis of these latter Arg residues of BK(Ca) generally supports their role in the voltage sensing process; however, the quantitative effects of such mutations on the slope and midpoint of the conductance-voltage activation curve are quite complex (Díaz *et al.*, 1998). BK(Ca) channels also exhibit voltage-dependent gating currents due to intra-membrane charge movement that occurs in response to depolarizing and repolarizing voltage pulses (Stefani *et al.*, 1997; Horrigan and Aldrich, 1999). Such gating currents are consistent with the idea that the BK(Ca) channel is an intrinsically voltage-gated channel that consists of an S1-S4 voltage-sensing domain coupled to a separate Ca^{2+} -binding domain. Indeed, BK(Ca) channels can be activated by voltage in the virtual absence of Ca^{2+} ; however, a voltage close to +200 mV is required to achieve 50% channel opening under these conditions (Horrigan *et al.*, 1999).

Apart from the pore domain and the S1-S4 module, BK(Ca) channels contain a unique structural element located at the N-terminus of the α -subunit. It has been shown that there is an extra N-terminal hydrophobic transmembrane segment in BK(Ca) channels called, S0, that precedes the typical S1 segment (Wallner *et al.*, 1996; Meera *et al.*, 1997). The presence of S0 at this location results in an extracellular orientation of the

N-terminus of the BK(Ca) α -subunit. This topology is opposite to all other members of the K^+ channel family where an intracellular location of the N-terminus prevails. In mammalian BK(Ca) channels, a 41-residue segment consisting of the extracellular N-terminus and S0 is known to have a unique functional role. This role involves coupling to β -subunits, a family of 200-300 residue glycosylated membrane proteins containing two transmembrane spans (Wallner *et al.*, 1999; Uebele *et al.*, 2000; Behrens *et al.*, 2000; Xia *et al.*, 2000; Brenner *et al.*, 2000). These β -subunits co-associate with the α -subunit tetramer and modulate BK(Ca) channels by a variety of mechanisms including changes in Ca^{2+} -dependence, inactivation kinetics, and toxin pharmacology. It has been shown that the S0 domain of the mammalian BK(Ca) channel is essential for enhancement of Ca^{2+} -sensitivity that occurs upon co-expression with the $\beta 1$ subunit (Wallner *et al.*, 1996). The modular nature of S0 leads to the hypothesis that this small N-terminal segment of the channel constitutes an independent functional domain that regulates channel opening by interaction with accessory β -subunits.

Analysis of the evolutionary relationships among divergent K-channels has yielded another interesting finding concerning a ~ 177 -residue region located C-terminal to the S6 transmembrane span. This region (called RCK for regulator of conductance K^+) has been identified as a conserved sequence motif found in numerous 6-transmembrane K-channels of prokaryotes, including the *E. coli* K-channel (Jiang *et al.*, 2001). It is also found in a peripheral membrane subunit (called TrkA) of the Trk family of prokaryotic K^+ transport systems (Durell *et al.*, 1999). Remarkably, this RCK motif is also present in mammalian and *Drosophila* BK(Ca) channels as demonstrated by multiple sequence alignment. The structure of the soluble RCK domain of the *E. coli* K-channel has been solved to 3.2 Å resolution by X-ray crystallography (Jiang *et al.*, 2001). The RCK structure is described as an α/β protein containing a Rossmann fold, a structural motif that is typically associated with binding of certain small molecule ligands such as the nucleotide cofactor, NAD. The exact function of the RCK domain of the BK(Ca) channel has not yet been established. However, one interesting possibility is that it may contain a binding site for Mg^{2+} . Despite the fact that Mg^{2+} alone is rather ineffective as an activator of BK(Ca) channel opening, a physiological concentration of Mg^{2+} (1-3 mM) is known to enhance channel activation by increasing the apparent Hill coefficient for activation by Ca^{2+} (Golowasch *et al.*, 1986; Oberhauser *et al.*, 1988; Shi and Cui, 2001; Zhang *et al.*, 2001). Thus, the RCK domain, situated close to the C-terminal end of S6 on the cytoplasmic side of the membrane, may be responsible for mediating the binding of Mg^{2+} or another cytoplasmic ligand that regulates BK(Ca) channel gating. Mutations that disrupt a conserved Lys-Asp salt bridge in the RCK domain of the human BK(Ca) channel have been found to shift the midpoint voltage for channel opening toward a more positive voltage range at a given Ca^{2+} concentration (Jiang *et al.*, 2001). Such results support the idea that the RCK domain plays a role in the Ca^{2+} - and voltage-dependent gating reaction.

As described above, the highly conserved Tail region of the BK(Ca) channel can itself be considered as a separate modular domain. Our laboratory has introduced the hypothesis that a region of ~ 250 residues near the C-terminus of the Tail structurally resembles the protein fold of serine proteinase enzymes such as trypsin and chymotrypsin. This proposal is based on structure-activity relationships between certain serine proteinase inhibitors such as BPTI that induce a unique type of substate behavior when added to the intracellular side of single BK(Ca) channels from mammals and

Drosophila (Moss *et al.*, 1996a). In support of this hypothesis, we presented a plausible sequence alignment between known members of the serine proteinase family and a C-terminal region of the BK(Ca) α -subunit (Moss *et al.*, 1996b). In summary, Figure 1 illustrates various lines of evidence suggesting that the large BK(Ca) channel protein has a modular architecture consisting of at least five distinct structural domains that interact via protein conformational changes to produce its characteristic voltage and Ca^{2+} -dependent gating behavior.

3. PROGRESS TOWARD BK(CA) CHANNEL FUNCTION

BK (Ca) channels exhibit a single-channel conductance in the range of 200-300 pS in symmetrical 150 mM KCl. This is the highest unitary conductance of any known, highly K^+ -selective, channel. Electrophysiological measurements of BK(Ca) current provide a direct readout of kinetic transitions between closed and open states of the channel. When patch-clamp recording techniques were first perfected in the mid 1980's, it was hoped that the high resolution afforded by such a large conductance would allow the mechanism of BK(Ca) channel gating to be solved by analyzing the voltage- and Ca^{2+} -dependence of its single-channel current. However, the early optimism of this naive hope has since been dampened by the sheer complexity of BK(Ca) gating as viewed from single-channel activity. A major problem is heterogeneity of the kinetics of any given channel and heterogeneity of individual behavior from channel to channel. For example, there is considerable channel-to-channel variation in the probability of the open state for different channels recorded under exactly the same conditions (Moczydlowski *et al.*, 1985; McManus and Magleby, 1991). In addition, the gating behavior of an individual BK(Ca) channel is difficult to describe by a single cluster of kinetic states in equilibrium. Many BK(Ca) channels exhibit large spontaneous shifts in open state probability. Such non-stationary or unstable gating behavior has been described as mode shifting (McManus and Magleby, 1988) or "Wanderlust" behavior (Silberberg *et al.*, 1996). Another complexity is the tendency of BK(Ca) channels to exhibit decreased open state probability at high positive voltage and high Ca^{2+} . This behavior, reflected by long-lived closed states, has been variously suggested to arise from a Ca^{2+} -blocked state (Vergara and Latorre, 1983), a Ba^{2+} -blocked state due to contaminant Ba^{2+} in KCl solutions (Neyton, 1996; Cox *et al.*, 1997), and an intrinsic gating mode distinct from the predominant activation gating kinetics (Rothberg *et al.*, 1996). These and other complex phenomena make it difficult to analyze BK(Ca) channel gating within the framework of conventional equilibrium kinetics.

Despite this caveat, careful analysis of single-channel and macroscopic currents has recently led to a "simplified" 50-state structural/kinetic model that is consistent with many features of BK(Ca) gating (Cox and Aldrich, 2000; Rothberg and Magleby, 2000). Inherent in this model, is the recognition of the channel as a homotetramer of monomeric subunits. Each monomer contains one dynamic voltage-sensor domain and one Ca^{2+} binding site. Outward movement (or activation triggered by depolarization) of 0 to 4 voltage sensors coupled to binding of 0 to 4 Ca^{2+} ions in a tetrameric complex gives rise to a scheme with 25 closed and 25 open states. The 25 states are elements of a 5 x 5 matrix that arises from consecutive but independent movement of 0-4 voltage sensors and binding of 0-4 Ca^{2+} ions. These two tiers of 25 closed and 25 open states are connected

together by 25 closed-open transitions between the corresponding voltage/occupancy states. In this model, the voltage-dependence of activation is solely attributed to the voltage domain. Ca^{2+} binding is assumed to be intrinsically voltage-independent. The apparent increase in affinity for activation by Ca^{2+} as a function of positive voltage is thus derived from allosteric coupling within the cyclic transitions of the scheme. This model is able to simulate many features of BK(Ca) channel activation that include: voltage-dependent gating currents, Ca^{2+} -dependence of the midpoint ($V_{0.5}$) for voltage-activation, and Hill coefficients in the range of 1-4 for Ca^{2+} -dependent activation at fixed voltage (Cox and Aldrich, 2000; Rothberg and Magleby, 2000). The allosteric 50-state model has recently been expanded to describe the enhancing effect of intracellular Mg^{2+} on BK(Ca) activation, by allowing each state of the 50-state model to bind 0 to 4 Mg^{2+} ions (Shi and Cui, 2001; Zhang *et al.*, 2001). This leads to a 250-state model that is unwieldy, but provides a consistent framework for representing a tetrameric channel that is both voltage- and ligand-gated (Ca^{2+} , Mg^{2+}) (Magleby, 2001).

The extraordinary complexity of BK(Ca) channel gating and the “simplified” models devised to describe it, has led to a yearning for experimental approaches that provide more direct information on channel structure and function. As noted above, one such approach is the use of X-ray crystallography to obtain high-resolution structural information on subdomains of the channel that can be expressed in soluble form using a recombinant expression system. Such approaches may ultimately allow one to “visualize” state changes in channel conformation. The validity of this approach has already been demonstrated by X-ray structural analysis of the RCK domain of the *E. coli* K⁺ channel (Jiang *et al.*, 2001). Based on sequence similarity, this latter structure is expected to resemble the homologous region of BK(Ca) located on the C-terminal side of S6.

Our laboratory is pursuing a similar strategy for investigation of modular intracellular domains of the BK(Ca) channel that are involved in gating and Ca^{2+} -binding. This project originally began with the discovery that certain serine proteinase inhibitors called Kunitz inhibitors and structurally related dendrotoxins from mamba snake venom produce a unique type of subconductance phenomenon when present on the intracellular side of the BK(Ca) channel (Luchessi and Moczydlowski, 1991). Small protein toxins such as the charybdotoxin family of K-channel toxins from scorpion venom have proven to be invaluable for elucidating the structure-activity basis of pore block due by toxin binding in the outer vestibule of the BK(Ca) channel (Miller, 1995). Although the intercellular site of interaction of Kunitz inhibitors and dendrotoxins with the BK(Ca) channel may not necessarily represent a “physiological target” for these inhibitors, a fortuitous but specific protein-protein interaction on the cytoplasmic side of the channel may nevertheless be valuable in characterizing structural domains that bind and recognize such small protein molecules.

Figure 2 shows a sequence alignment of the 58-residue BPTI (bovine pancreatic trypsin inhibitor) and the 60-residue DTX-I, or Toxin I from the black mamba snake, *Dendroaspis polylepis*. Despite the fact that these two small homologous proteins have only 19 identical residues, they share a common fold (figure 2) that is highly constrained by virtue of 3 disulfide bonds that are absolutely conserved in all members this protein family.

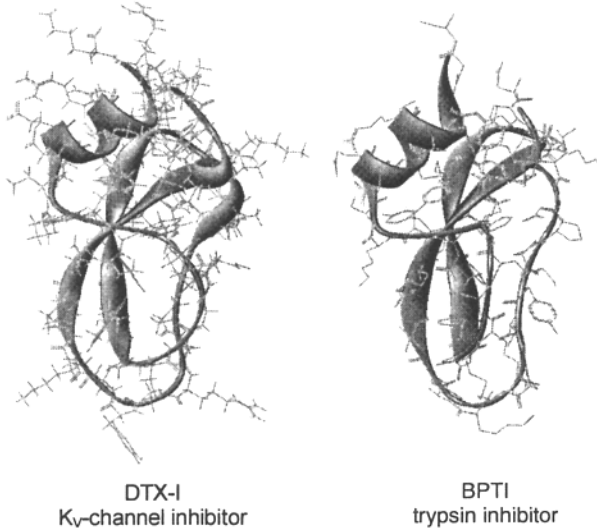


Figure 2. Sequence alignment and structural comparison of dendrotoxin I (DTX-I) and bovine pancreatic trypsin inhibitor (BPTI), a class of molecules that induce discrete substate events by binding at an intracellular site on BK(Ca) channels.

BPTI is most commonly known as a specific inhibitor of various serine proteinases (SerP) such as trypsin and chymotrypsin. In contrast, DTX-I is a potent blocker of certain voltage-gated K-channels from the intracellular side. Despite these two different activities, Figure 3 shows that both BPTI and DTX-I mediate a distinct type of substate behavior of the BK(Ca) channel from the intracellular side. Our studies indicate that substate events produced by such inhibitors are due to reversible binding at a single site or kinetically homogeneous class of sites on the cytoplasmic side of the channel (Favre and Moczydlowski, 1999).

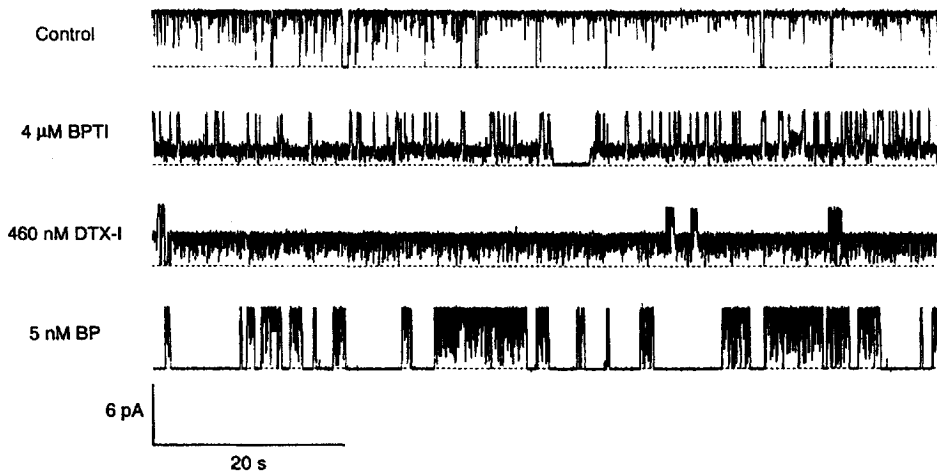


Figure 3. Effect of three different peptide inhibitors on the intracellular side of single BK(Ca) channels from rat muscle in planar lipid bilayers: BPTI, DTX-I and BP, a Shaker ball peptide homolog (MAAVAVLYVLGKKRQHRKKQ). Experimental details are described in Favre and Moczydlowski (1999).

The apparent substate events produced by BPTI and DTX-I may be contrasted with the effect of other peptide blockers such as homologs of the Shaker inactivating ball peptide (BP) (Fig. 3) that produce discrete blocking events by binding to a separate intracellular site on the BK(Ca) channel that is competitive with block by intracellular TEA, a known pore blocking agent (Toro *et al.*, 1994). Biophysical analysis and competition experiments between various intracellular inhibitors (BPTI, DTX-I, Ba^{2+} , TEA, BP) have led to the following conclusions (Favre and Moczydlowski, 1999): The binding site for BPTI and DTX-I does not physically overlap the intracellular ion conduction pathway accessible to Ba^{2+} , TEA and BP. However, there is a negative allosteric interaction between BP and DTX-I since the binding affinity for BP is lowered by 8-fold in the DTX-I bound state. BPTI and DTX-I preferentially bind to a common high affinity site that lies outside the intracellular pore. When these latter inhibitors are bound to the channel, the apparent “subconductance” event is actually produced by rapid flickering of the channel on a time scale that is much faster than the filtering frequency (1 kHz) routinely used to record single-channel activity (Moss and Moczydlowski, 1996).

An important piece of evidence that the BPTI/DTX-I binding site may be structurally related to a SerP fold is the finding that ovoinhibitor, a 449-residue protein from chicken egg white, also produces substate events that are competitive with BPTI binding (Moss *et al.*, 1996a). Ovoinhibitor consists of seven tandemly linked Kazal domains that exhibit a different protein fold from BPTI but also inhibit SerP's by binding in the active site cleft. Such evidence has led us to search for a SerP-like domain localized on the cytoplasmic side of the BK(Ca) channel. We currently believe that the best candidate for such a domain is a ~250 residue sequence at C-terminus of BK(Ca). Sequence analysis of this region supports this hypothesis (Moss *et al.*, 1996b). However, this analysis also suggests that this SerP-like domain is unlikely to be catalytically active since it lacks Asp

and His residues that are part of the conserved Asp/His/Ser catalytic triad of active SerP's.

What is the functional significance of a SerP-like domain in the BK(Ca) channel? To address this question, some speculations may be offered. When the BK(Ca) channel is purified from native tissues, the α -subunit is often found to be proteolytically cleaved at several sites in the C-terminal region (García-Calvo *et al.*, 1994; Knaus *et al.*, 1995). One might postulate that under certain conditions the BK(Ca) channel is capable of self-proteolysis mediated by an intrinsic proteinase domain (García *et al.*, 1999). (Alternatively, such proteolysis may be due to distinct cellular proteases.) Many SerP enzymes such as trypsin, elastase, and certain members coagulation cascade factors are regulated by Ca^{2+} , and contain a known Ca^{2+} -binding site that consists of a self-contained loop between two adjacent β -strands (Sabharwal *et al.*, 1995). In the course of molecular evolution, it is possible that the BK(Ca) channel appropriated a Ca^{2+} -binding SerP-like domain for use as a Ca^{2+} -sensing domain in activation gating. In support of this idea, we recently demonstrated that a recombinant SerP-like fragment of the *Drosophila* BK(Ca) channel exhibits $^{45}\text{Ca}^{2+}$ -binding activity using a protein blot assay (Bian *et al.*, 2001). We hope that further studies along these lines will provide more information on the biochemical basis of Ca^{2+} binding and the nature of the domain-domain interactions that underly Ca^{2+} -dependent activation of the BK(Ca) channel.

4. REFERENCES

- Atkinson, N. S., Robertson, G. A., and Ganetzky, B., 1991, A component of calcium-activated potassium channels encoded by the *Drosophila* slo locus, *Science*, **253**:551-555.
- Behrens, R., Nolting, A., Reimann, F., Schwarz, M., Waldshütz, R., and Pongs, O., 2000, hKCNMB3 and hKCNMB4, cloning and characterization of two members of the large conductance calcium activated potassium channel β subunit family, *FEBS Letters*, **474**:99-106.
- Bian, S., Favre, I., and Moczydlowski, E., 2001, Ca^{2+} -binding activity of a COOH-terminal fragment of the *Drosophila* BK channel involved in Ca^{2+} -dependent activation, *Proceedings of the National Academy of Science USA*, **98**:4776-4781.
- Brenner, R., Jegla, T. J., Wickenden, A., Liu, Y., and Aldrich, R. W., 2000, Cloning and functional characterization of novel large conductance calcium-activated potassium channel β subunits, hKCNMB3 and hKCNMB4, *Journal of Biological Chemistry*, **275**: 6453-6461.
- Butler, A., Tsunoda, S., McCobb, D. P., Wei, A., and Salkoff, L., 1993, mSlo, a complex mouse gene encoding "maxi" calcium-activated potassium channels, *Science*, **261**:221-224.
- Coetzee, W. A., Amarillo, Y., Chiu, J., Chow, A., Lau, D., McCormack, T., Morena, H., Nadal, M. S., Ozaita, A., Pountney, D., Saganich, M., Vega-Saenz de Miera, E., and Rudy, B., 1999, Molecular Diversity of K^+ Channels, *Annals NY Academy of Science*, **868**:233-255.
- Cox, D. H., and Aldrich, R. W., 2000, Role of $\beta 1$ subunit in large conductance Ca^{2+} -activated K^+ channel gating energetics: mechanisms of enhanced Ca^{2+} sensitivity, *Journal General Physiology*, **116**:411-432.
- Cox, D. H., Cui, J., and Aldrich, R. W., 1997, Separation of gating properties from permeation and block in mslo large conductance Ca-activated K^+ channels, *Journal of General Physiology*, **109**:633-646.
- Díaz, L., Meera, P., Amigo, J., Sefani, E., Alvarez, O., Toro, L., and Latorre, R., 1998, Role of the S4 segment in a voltage-dependent calcium-sensitive potassium (hSlo) channel, *Journal of Biological Chemistry*, **273**:32430-32436.
- Doyle, D. A., Morais-Cabral, J., Pfuetzner, R. A., Kuo, A., Gulbis, J. M., Cohen, S. L., Chait, B. T., and MacKinnon, R. 1998, The structure of the potassium channel: molecular basis of K^+ conduction and selectivity, *Science*, **280**: 69-77.
- Durell, S. R., Hao, Y., Nakamura, T., Bakker, E. P., and Guy, H. R., 1999, Evolutionary relationship between K^+ channels and symporters, *Biophysical Journal*, **77**:775-788.
- Esguerra, M., Wang, J., Foster, C. D., Adelman, J. P., North, R. A., and Levitan, I. B. 1994, Cloned Ca^{2+} -dependent K^+ channel modulated by a functionally associated protein kinase, *Nature*, **369**:563-565.

- Favre, I., and Moczydlowski, E., 1999, Simultaneous binding of basic peptides at intracellular sites on a large conductance Ca^{2+} -activated K^+ channel: equilibrium and kinetic basis of negatively coupled ligand interactions, *Journal of General Physiology*, **113**:295-320.
- García, M. L., Giangiacomo, K. M., Hanner, M., Knaus, H.-G., McManus, O. B., Schmalhofer, W. A., and Kaczorowski, G. J., 1999, Purification and functional reconstitution of high-conductance calcium-activated potassium channel from smooth muscle, *Methods in Enzymology*, **294**:274-287.
- García-Calvo, M., Knaus, H.-G., McManus, O. B., Giangiacomo, K. M., Kaczorowski, G. J., and García, M. L., 1994, Purification and reconstitution of the high-conductance, calcium-activated potassium channel from tracheal smooth muscle, *Journal of Biological Chemistry*, **269**:676-682.
- Golowasch, J., Kirkwood, A., and Miller, C., 1986, Allosteric effects of Mg^{2+} on the gating of Ca^{2+} -activated K^+ channels from mammalian skeletal muscle, *Journal of Experimental Biology*, **124**:5-13.
- Hille, B., 2001, Potassium channels and chloride channels, in: *Ion Channels of Excitable Membranes*, Sinauer Assoc. Inc., Sunderland, MA, pp. 131-167.
- Horrigan, F T., Cui, J., and Aldrich, R. W., 1999, Allosteric gating of potassium channels I: mSlo ionic currents in the absence of Ca^{2+} , *Journal of General Physiology*, **114**:277-304.
- Horrigan, F T., and Aldrich, R. W., 1999, Allosteric gating of potassium channels II: mSlo channel gating charge movement in the absence of Ca^{2+} , *Journal of General Physiology*, **114**:305-336.
- Jiang, Y., and MacKinnon, R., 2000, The barium site in a potassium channel by X-ray crystallography, *Journal of General Physiology*, **115**:269-272.
- Jiang, Y., Pico, A., Cadene, M., Chait, B. T., and MacKinnon, R., 2001, Structure of the RCK domain from the *E. coli* K^+ channel and the demonstration of its presence in the human BK channel, *Neuron*, **29**:593-601.
- Knaus, H.-G., Eberhart, A., Koch, R. O. A., Munujos, P., Schmalhofer, W. A., Warmke, J. W., Kaczorowski, G. J., and García, M. L., 1995, Characterization of tissue-expressed α subunits of the high conductance Ca^{2+} -activated K^+ channel, *Journal of Biological Chemistry*, **270**:22434-22439.
- Ling, S., Woronuk, G., Sy, L., Lev, S., and Braun, A. P., 2000, Enhanced activity of a large conductance, calcium-sensitive K^+ channel in the presence of Src tyrosine kinase, *Journal of Biological Chemistry*, **275**:30683-30689.
- Lu, T., Katakam, P. V. G., VanRollins, M., Weintraub, N. L., Spector, A. A., and Lee, H.-C., 2001, Dihydroeicosatrienoic acids are potent activators of Ca^{2+} -activated K^+ channels in isolated rat coronary arterial myocytes, *Journal of Physiology (London)*, **534**:3:651-667.
- Lu, Z., Klem, A. M., and Ramu, Y., 2001, Ion conduction pore is conserved among potassium channels. *Nature*, **413**:809-813.
- Lucchesi, K. J., and Moczydlowski, E. 1991, On the interaction of bovine pancreatic trypsin inhibitor with maxi Ca^{2+} -activated K^+ channels: a model system for analysis of peptide-induced subconductance states, *Journal of General Physiology*, **97**:1295-1319.
- MacKinnon, R., Cohen, S. L., Kuo, A., Lee, A., and Chait, B. T., 1998, Structural conservation in prokaryotic and eukaryotic potassium channels, *Science*, **280**:106-109.
- Magleby, K. L., 2001, Kinetic gating mechanisms for BK channels: when complexity leads to simplicity. *Journal of General Physiology*, **118**: 583-587.
- McManus, O. B., and Magleby, K. L., 1988, Kinetic states and modes of single large conductance calcium activated potassium channels in cultured rat skeletal muscle, *Journal of Physiology (London)*, **402**:79-120.
- McManus, O. B., and Magleby, K. L., 1991, Accounting for the Ca^{2+} -dependent kinetics of single large conductance Ca^{2+} -activated K^+ channels in rat skeletal muscle, *Journal of Physiology (London)*, **443**:739-777.
- Meera, P., Wallner, M., Song, M., and Toro, L., 1997, Large conductance voltage- and calcium-dependent K^+ channel, a distinct member of voltage-dependent ion channels with seven N-terminal transmembrane segments (S0-S6), an extracellular N terminus, and an intracellular (S9-S10) C-terminus, *Proceedings of the National Academy of Science USA*, **94**:14066-14071.
- Meera, P., Wallner, M., and Toro, L., 2000, A neuronal β subunit (KCNMB4) makes the large conductance, voltage- and Ca^{2+} -activated K^+ channel resistant to charybdotoxin and iberiotoxin, *Proceedings of the National Academy of Science USA*, **97**:5562-5567.
- Miller, C. 1995, The charybdotoxin family of K^+ channel-blocking peptides, *Neuron*, **15**:5-10.
- Moczydlowski, E., Alvarez, O., Vergara, C., and Latorre, R., 1985, Effect of phospholipid surface charge on the conductance and gating of a Ca^{2+} -activated K^+ channel in planar lipid bilayers, *Journal of Membrane Biology*, **83**:273-282.
- Moss, G. W. J., Marshall, J., Morabito, M. Howe, J. R., and Moczydlowski, E., 1996a, An evolutionary conserved binding site for serine proteinase inhibitors in large conductance calcium activated potassium channels, *Biochemistry*, **35**:16024-16035.

- Moss, G. W. J., Marshall, and Moczydlowski, E., 1996b, Hypothesis for a serine proteinase-like domain at the COOH terminus of Slowpoke calcium-activated potassium channels, *Journal of General Physiology*, **108**:473-484.
- Moss, G. W. J., and Moczydlowski, E., 1996, Rectifying conductance substates in a large conductance Ca^{2+} -activated K^+ channel: evidence for a fluctuating barrier mechanism, *Journal of General Physiology*, **107**: 47-68.
- Neyton, J., 1996, A Ba^{2+} -chelator suppresses long shut events in fully activated high-conductance Ca^{2+} -dependent K^+ channels, *Biophysical Journal*, **71**:220-226.
- Oberhauser, A., Alvarez, O., and Latorre, R., 1988, Activation by divalent cations of a Ca^{2+} -activated K^+ channel from skeletal muscle membrane, *Journal of General Physiology*, **92**:67-86.
- Rothberg, B. S., Bello, R. A., Song, L., and Magleby, K. L., 1996, High Ca^{2+} concentrations induce a low activity mode and reveal Ca^{2+} -independent long shut intervals in BK channels from rat muscle, *Journal of Physiology (London)*, **493**:3:673-689.
- Rothberg, B. S., and Magleby, K. L., 2000, Voltage and Ca^{2+} activation of single large-conductance Ca^{2+} -activated K^+ channels described by a two-tiered allosteric gating mechanism, *Journal of General Physiology*, **116**:75-99.
- Reinhart, P. H., and Levitan, I. B., 1995, Kinase and phosphatase activities intimately associated with a reconstituted calcium-dependent potassium channel, *Journal of Neuroscience*, **15**: 4572-4579.
- Sabharwal, A. K., Birktoft, J. J., Gorka, J., Wildgoose, P., Petersen, L. C., and Bajaj, S. P., 1995, High affinity Ca^{2+} -binding site in the serine protease domain of human factor VIIa and its role in tissue factor binding and development of catalytic activity, *Journal of Biological Chemistry*, **270**:15523-15530.
- Schreiber, M., and Salkoff, L., 1997, A novel calcium-sensing domain in the BK channel, *Biophysical Journal*, **73**:1355-1363.
- Schreiber, M., Wei, A., Yuan, A., Gaut, J., Saito, M., and Salkoff, L., 1998, Slo3, a novel pH-sensitive K^+ channel from mammalian spermatocytes, *Journal of Biological Chemistry*, **273**:3509-3516.
- Schreiber, M., Yuan, A., and Salkoff, L., 1999, Transplantable sites confer calcium sensitivity to BK channels. *Nature Neuroscience*, **2**:416-421.
- Shi, J., and Cui, J., 2001, Intracellular Mg^{2+} enhances the function of BK-type Ca^{2+} -activated K^+ channels, *Journal of General Physiology*, **118**:589-605.
- Siberberg, S. D., Lagrutta, A., Adelman, J. P., and Magleby, K. L., 1996, Wanderlust kinetics and variable Ca^{2+} -sensitivity of dSlo, a large conductance Ca^{2+} -activated K^+ channel, expressed in oocytes, *Biophysical Journal*, **70**:2640-2651.
- Stefani, E., Ottolia, M., Noceti, F., Oclase, R., Wallner, M., Latorre, R., and Toro, L., 1997, Voltage-controlled gating in a large conductance Ca^{2+} -sensitive K^+ channel (hSlo), *Proceedings of the National Academy of Science USA*, **94**:5427-5431.
- Swayze, R. D., and Braun A. P., 2001, A catalytically inactive mutant of type I cGMP-dependent protein kinase prevents enhancement of large conductance, calcium-sensitive K^+ channels by sodium nitroprusside and Cgmp, *Journal of Biological Chemistry*, **276**:19729-19737.
- Toro, L., Ottolia, M., Stefani, E., and Latorre, R., 1994, Structural determinants in the interaction of *Shaker* inactivating peptide and a Ca^{2+} -activated K^+ channel, *Biochemistry*, **33**:7220-7228.
- Toro, L., Wallner, M., Meera, P., and Tanaka, Y., 1998, Maxi- K_{Ca} , a unique member of the voltage-gated K^+ channel superfamily, *News Physiological Science*, **13**:112-117.
- Tseng-Crank, J., Foster, C. D., Krause, J. D., Mertz, R., Godinot, N., DiChiara, T. J., and Reinhart, P. H., 1994, Cloning, expression, and distribution of functionally distinct Ca^{2+} -activated K^+ channel isoforms from human brain, *Neuron*, **13**:1315-1330.
- Uebele, V. N., Larutta, A., Wade, T., Figueroa, D. J., Liu, Y., McKenna, E., Austin, C. P., Bennet, P. B., and Swanson, R., 2000, Cloning and functional expression of two families of β -subunits of the large conductance calcium-activated K^+ channel, *Journal of Biological Chemistry*, **275**:23211-23218.
- Valverde, M. A., Rojas, P., Amigo, J., Cosmelli, D., Orío, P., Bahamonde, M. I., Mann, G. E., Vergara, C., and Latorre, R., 1999, Acute activation of maxi- K channels (hSlo) by estradiol binding to the beta subunit, *Science*, **285**:1929-1931.
- Vergara, C., and Latorre, R., 1983, Kinetics of Ca^{2+} -activated K^+ channels from rabbit muscle incorporated into planar bilayers: evidence for a Ca^{2+} and Ba^{2+} blockade, *Journal of General Physiology*, **82**:543-568.
- Wallner, M., Meera, P., and Toro, L., 1996, Determinant for β -subunit regulation in high conductance voltage-activated and Ca^{2+} -sensitive K^+ channels: an additional transmembrane region in the N terminus, *Proceedings of the National Academy of Science USA*, **93**:14922-14927.
- Wallner, M., Meera, P., and Toro, L., 1999, Molecular basis of fast inactivation in voltage and Ca^{2+} -activated K^+ channels: a transmembrane β -subunit homolog, *Proceedings of the National Academy of Science USA*, **96**:4137-4142.

- Wang, J., Zhou, Y., and Levitan, I. B., 1999, Simultaneous binding of two protein kinases to a calcium-dependent potassium channel, *Journal of Neuroscience*, **19**:RCA4:1-7.
- Wei, A., Solaro, C., Lingle, C., and Salkoff, L., 1994, Calcium sensitivity of BK-type K_{Ca} channel determined by a separable domain, *Neuron*, **13**: 671-681.
- Xia, X.-M., Ding, J.-P., Zeng, X.-H., Duan, K.-L., and Lingle, C., 2000, Rectification and rapid activation at low Ca^{2+} of Ca^{2+} -activated, voltage-dependent BK currents: consequences of rapid inactivation by a novel β subunit, *Journal of Neuroscience*, **20**:4890-4903.
- Yellen, G., 1998, The moving parts of voltage-gated ion channels, *Quarterly Reviews of Biophysics*, **31**:239-295.
- Zhang, X., Solaro, C. R., and Lingle, C. J., 2001, Allosteric regulation of BK channel gating by Ca^{2+} and Mg^{2+} through a nonselective, low affinity divalent cation site, *Journal of General Physiology*, **118**:607-635.
- Zhou, Y., Morais-Cabral, J. H., Kaufman, A., and MacKinnon, R., 2001a, Chemistry of ion coordination and hydration revealed by a K^+ channel-Fab complex at 2.0 Å resolution, *Nature*, **414**:43-48.
- Zhou, M., Morais-Cabral, J. H., Mann, S., and MacKinnon, R., 2001b, Potassium channel receptor site for the inactivation gate and quaternary amine inhibitors, *Nature*, **411**:657-661.

HELICAL NATURE OF THE VOLTAGE SENSOR

Oswaldo Álvarez^{1*}, Eduardo Rosenmann², Francisco Bezanilla^{2,3}, Carlos González², and Ramón Latorre^{1,2,3}

1. INTRODUCTION

The Shaker K⁺ channel is a tetramer, with each monomer having six transmembrane segments. The channel is voltage-activated and the positively charged fourth segment, S4, is an important part of the voltage sensor. Voltage activation involves the displacement of ten amino acid residues of S4 from the intracellular to the extracellular side of the structure, therefore some flexibility of the S3-S4 linker segment is required. By systematically altering the length of the S3-S4 linker, we have found periodic perturbations of the voltage-dependent activation kinetics. The periodicity has an angular frequency consistent with an alpha-helical structure of S4. As explained below, based on this structure we develop a molecular model for the voltage-sensor operation where a displacement as small as 3Å accounts for the experimental observations.

I (Oswaldo Álvarez) was invited to give a talk during the symposium “Epithelia, Pumps, Transporters and Ion Channels: Structure and Function at 60” organized by CECS, Valdivia, to celebrate the 60th birthday of Ramón and Enrico. I was very happy to prepare a presentation about my collaboration with Ramón during the last years gathering material from our papers and lectures (e.g., González *et al.*, 2000; González *et al.*, 2001). During a great barbecue party held in the countryside, the participants of the symposium agreed to contribute to a book of the Meeting Proceedings and during that banquet this chapter was conceived. What follows is a rearrangement of the material following the history of developments from my point of view.

¹ Universidad de Chile Facultad de Ciencias, Departamento de Biología, Casilla 653, Santiago, Chile.

² Centro de Estudios Científicos, Arturo Prat 514, Valdivia, Chile

³ UCLA School of Medicine, Los Angeles, California, USA.

* Corresponding autor: oalvarez@uchile.cl.

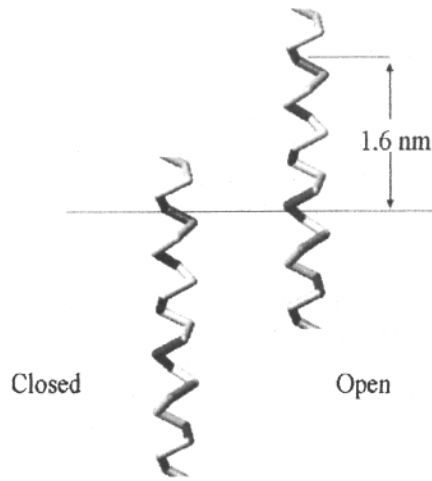


Figure 1. Hypothetical S4-segment displacement.

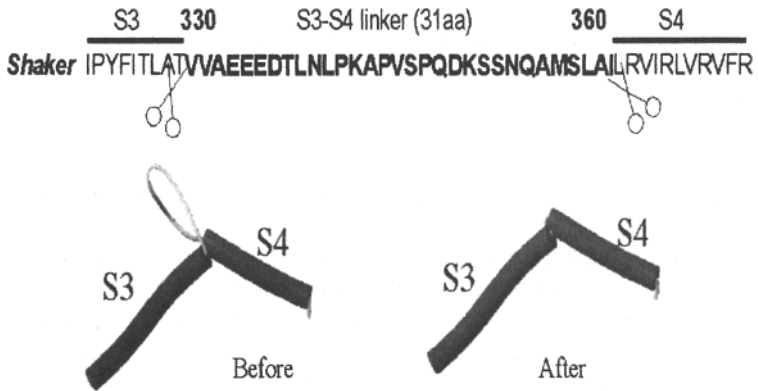


Figure 2. The Oaa Shaker deletion mutant

My participation in this project began when I was invited to join the weekly seminars of Ramón's laboratory while he was still at the Facultad de Ciencias, Universidad de Chile in Santiago. At that time Carlos González was a fresh arrival from Cuba and he was assigned a project involving deletions of the S3-S4 linker segment of the *Shaker* K⁺ channel. The rationale of the project was based on the emerging evidence of the involvement of the S4 transmembrane segment as a voltage sensor. At that time the current hypothesis was that the S4 segment would move normal to the membrane surface when the membrane was depolarized (Catterall, 1986; Guy and Seetharamulu, 1986). In particular, Catterall based on the pioneering ideas of Armstrong (1981) proposed that the S4 helix displacement consisted of a rotation and a movement normal to the membrane plane (sliding helix model). This idea was a direct consequence of the primary structure of the S4 segment that has repetitions of the sequence arginine-X-X-arginine where X is a hydrophobic amino acid. The detailed studies performed with the *Shaker* K⁺ channel (Aggarwal and MacKinnon, 1996; Seoh *et al.*, 1996) revealed that four of the positive charges contained in S4 were important in determining the total number of gating charges per channel involved in activation. More recently, histidine-scanning mutagenesis, a methodology in which, one by one, the arginines contained in the S4 are replaced by histidines, demonstrated that these four charges move the entire electric field upon channel opening (Starace and Bezanilla, 2001)³. This is illustrated in Figure 1, in which the lipid bilayer is represented by the horizontal line. If the model shown in Figure 1 is correct, then deleting the S3-S4 segment would have a dramatic impact on the ability of S4 to move, which might be revealed as a large modification in the position of the activation curve along the voltage axis and profound alterations to the channel opening kinetics. In our laboratory, Eduardo Rosemann was brave enough to suggest the construction of a mutant lacking the whole S3-S4 linker and this is how the short linker project started (more details of this fascinating story can be found in Bezanilla, 2000; Yellen, 1998; Horn, 2000).

2. SHAKER CHANNEL WORKS WITH S3-S4 SEGMENT DELETED.

Our molecular biology laboratory produced the RNA of a short linker *Shaker* K⁺ channel with the S3-S4 linker deleted and S3 and S4 segments connected directly (Figure 2).

The RNA was injected into oocytes and the cell-attached patch-clamp determinations revealed the expression of *Shaker*-like currents. The currents were clearly voltage-dependent, though the activation curve was displaced 45 mV to the right, the activation time constant was nearly 50 times longer, and the limiting slope charge was one half that of the wild type. Representative families of currents elicited by depolarizations under symmetric K⁺ concentrations are shown in Figure 3.

This observation was the starting point of a series of deletion mutants in which the amino acid residues were restored systematically to find what was the minimum length of the linker that would recover the characteristics of the wild type. The interpretation of the intriguing electrophysiology of these mutants produced long discussions that had my mind in turmoil for sometime. Here I show the history of its development.

³ In a pH gradient some of these histidines were able to grab a proton from the low pH side producing a measurable proton transport!

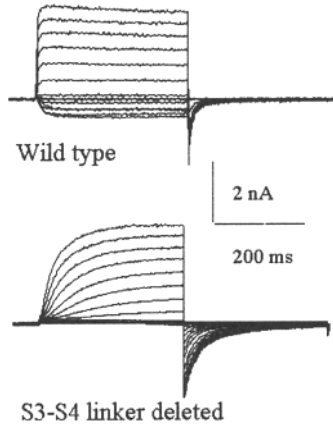


Figure 3. Shaker currents recorded under cell-attached patch-clamp using symmetric K^+ concentration.

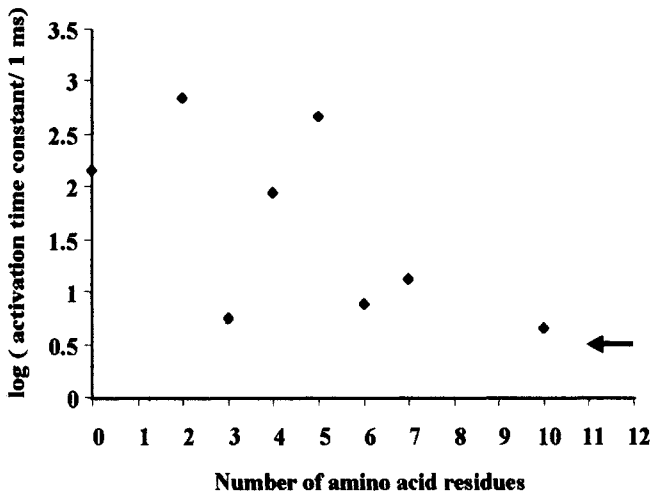


Figure 4. Plot of log of the activation time constant as a function of the number of residues restored. Arrow marks the wild type time constant.

3. RESTORING THE S3-S4 LINKER GIVES CONFUSING RESULTS

Figure 2 shows where the scissors severed the S3-S4 linker. At that time the S3-S4 linker segment was proposed to be the 31-amino acid residue stretch running from valine 330 to isoleucine 360 (Wallner *et al.*, 1996). The mutant with the complete deletion of the so defined linker was called 0aa for zero amino acid. The mutants with some of the amino acid residues restored, were named after the one-letter code of the amino acids as seen in Table I. Later, we found it more convenient to name the mutants after the number of amino acid restored, as seen also in Table I.

Table I. Deletion Mutants.			Name	N
<i>Shaker</i> H4Δ (6-46)	Δ(330-360)		0aa	0
<i>Shaker</i> H4Δ (6-46)	Δ(330-358)		AI	2
<i>Shaker</i> H4Δ (6-46)	Δ(330-357)		LAI	3
<i>Shaker</i> H4Δ (6-46)	Δ(330-356)		SLAI	4
<i>Shaker</i> H4Δ (6-46)	Δ(330-355)		MSLAI	5
<i>Shaker</i> H4Δ (6-46)	Δ(330-354)		AMSLAI	6
<i>Shaker</i> H4Δ (6-46)	Δ(330-353)		QAMSLAI	7
<i>Shaker</i> H4Δ (6-46)	Δ(330-350)		SSNQAMSLAI	10

For all the mutants described we measured: the conductance as a function of voltage using tail current analysis; activation-time constant at large depolarizations; gating charge using the limiting slope method (Almers, 1978); and the maximum probability of finding the channel open using mean-variance analysis.

The results were as follows:

- All channel mutants open to a maximum probability of 0.75 which is comparable to that of the wild type.
- Gating charge was $6e^-$ for the 0aa mutant but close to $13e^-$ for all others as well as for the wild type.
- Activation time constants were voltage-dependent. A plot of the 0 mV activation time constant gave a scattered plot as seen in Figure 4.
- Conductance vs. potential curves were all displaced to the right with respect to the wild type. A plot of the half activation voltage gave a scattered plot similar to that drawn for the activation time constant.

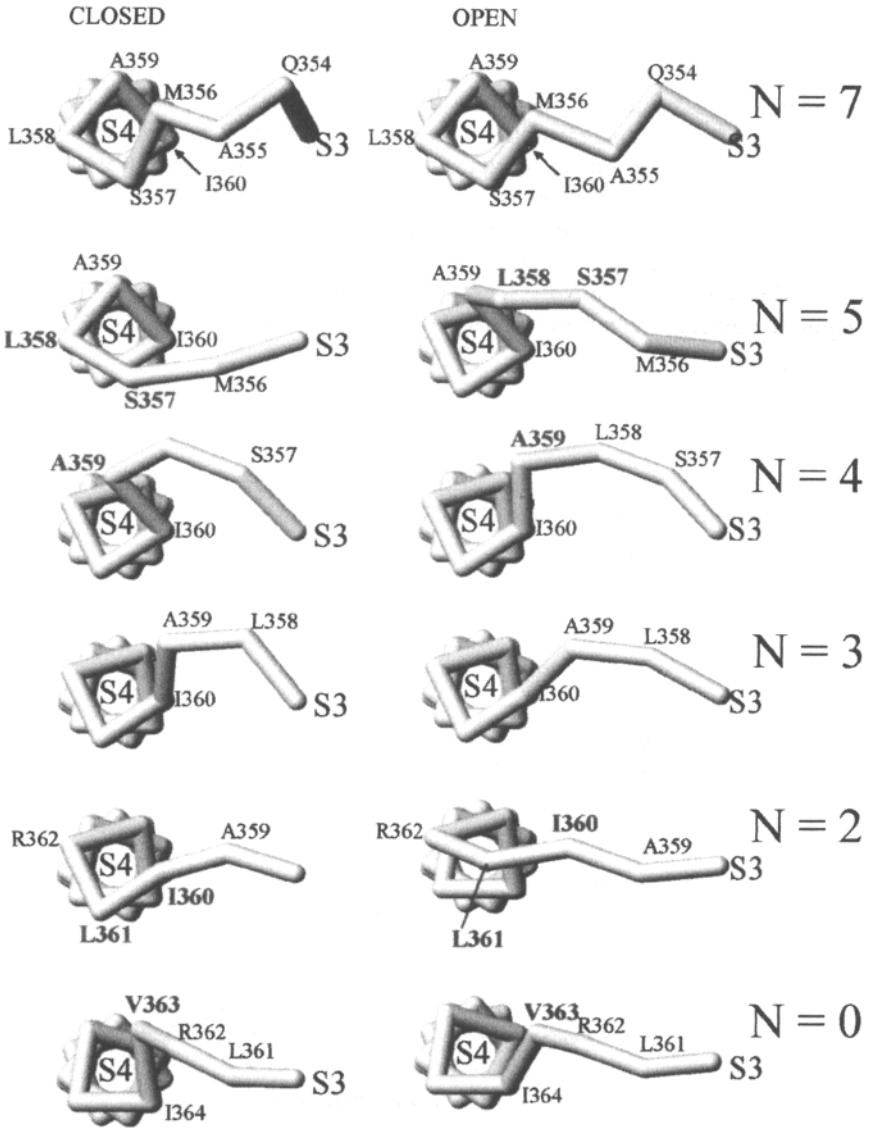


Figure 5. Mechanical model of voltage sensor. Closed to open transition is represented as a 3 Å displacement of S4 with respect to S3. Amino acids dissociated from the helix during the transition are labeled in red.

4. UNDERSTANDING THESE RESULTS

The results for the activation time constant and the half-activation voltage were unexpected. We expected a smooth transition in characteristics from the 0aa to the wild type. Our first step to understanding the experiments was to make a mechanical model that was able to reproduce these results and that would allow us to find some clues about the underlying molecular structure of the S4 domain. The mechanical model is restricted to the motion of S4 with respect to S3 since we expected this movement to be hindered by a short S3-S4 linker. In this model the motion of S4 with respect to S3 was set to be only 3 Å. For long S3-S4 linkers, the motion of S4 with respect to S3 can take place by changing the dihedral angles of the backbone of the linker as shown for N = 7 in Figure 5.

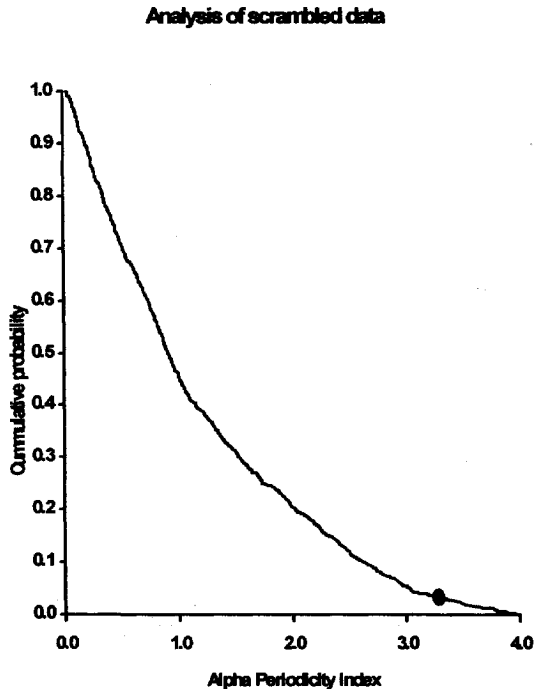


Figure 6. The vertical axis is the probability of finding by chance an α PI better than the corresponding value of horizontal axis.

This involves a small amount of energy and therefore a fast activation rate constant. For N = 5 the motion is no longer possible by changing the dihedral angles. In this case, two amino acid residues have to dissociate from the S4 alpha helical structure. The residues dissociated are leu358 and ser357, labeled in bold face red characters. This takes a larger amount of energy and therefore a slow activation constant is expected. For N = 4, some amino acid residues are already dissociated in the closed state. For the

closed to open transition only one extra residue has to dissociate from the S4 alpha helix. The extra energy for this mutant is less than that for $N = 5$ and therefore the activation constant is predicted to be faster than $N = 5$ mutant but slower than $N = 7$ mutant. For $N = 3$ there are enough amino acids dissociated from the alpha helix for the motion to occur without further dissociation. According to the model, the activation would be as fast as the $N = 7$ mutant. For $N = 2$, again two amino acid residues have to dissociate to allow the S4 motion and the activation is expected to be as slow as it is for $N = 5$. Finally for $N = 0$ only one amino acid has to dissociate and the activation rate constant must be comparable to that of $N = 3$ mutant. The model reproduces the periodic behavior for the activation constant observed experimentally and shown in Figure 4. In addition, the model explain the smaller gating valence found for $N = 0$, since arginine 362 is placed on the S3-S4 linker for this mutant.

The mechanical model was a useful introduction to the idea of partial dissociation of the S4 alpha helical structure. However it calls for too many *ad hoc* assumptions to reproduce the experimental results to be convincing. Our next step was to perform a simple curve-fitting exercise. We calculated the free energy of activation, ΔG^* , and the free energy of the closed to open transition, ΔG_0 . We compared the energies of the mutants with that of the wild type and searched for the best cosine function describing the two data sets, $\Delta \Delta G^*$ and $\Delta \Delta G_0$ as a function of N , the number of amino acids restored on the 0aa mutant. We were pleased to find that cosine functions with an angular period of 3.6 amino acid residues per revolution described our results well. This was a welcome independent analysis informing us that dissociation of amino acids from an alpha helix was involved in the activation of the short S3-S4 linker mutants.

We presented the mechanical model and the cosine curve fitting during a symposium held at CECS in Valdivia in the year 2000. During the discussion period it was pointed out that the significance of the curve fitting was weak because of the small number of data points and the large number of adjustable parameters involved. Use of a Fourier power spectrum analysis to evaluate the periodicity was also suggested. Stimulated by this discussion we returned to the laboratory to fill in the gaps to complete a series of mutants from one containing no amino acids to a mutant having 10 amino acid residues in the S3-S4 linker ($N = 0$ to $N = 10$). We were pleased to find that $\Delta \Delta G^*$ and $\Delta \Delta G_0$ data for $N = 1$ to $N = 6$ were, as expected, well described by a sine function. Moreover, as predicted by the mechanical model of Figure 5, mutants with 8 and 9 amino acids in the linker showed fast kinetics. We computed the Fourier power spectrum to find a nice peak at 100 degrees, a result clearly consistent with the proposed α helical nature of the amino terminus of the S4 segment ($360^\circ/3.6$ residues per turn). We also evaluated the Alpha Periodicity Index, αPI , (Cornette *et al.*, 1987) and found values of 3.0 and 3.4 for $\Delta \Delta G^*$ and $\Delta \Delta G_0$ respectively. Since values larger than 2.0 are considered good indications of alpha helical structures, the mechanical model was on solid grounds. However, it can be argued that the number of data points included in the analysis is too small and a more robust test was needed to determine whether or not the amino acid segment we analyzed was an α helix. As suggested by Dr. Richard Horn, we tested the probability of finding such αPI values just by chance. To do so, we scrambled the experimental results and computed the αPI for 1000 random permutations of the data. We observed that the probability of finding, by chance, the experimentally observed αPI values is 0.06 for the activation energy and 0.03 for the equilibrium constant. The arrow

in Figure 6 shows the probability of finding, by chance, the experimental α PI of $\Delta\Delta G_0$. These results indicate that the periodicity we found is true with a margin of error of 3 to 6%.

5. CONCLUSIONS

We developed a deletion methodology to determine the structural nature of the N-terminus of S4, determining that the S4 α helix extends up to amino acid residue M355. In other words, we added four amino acids to the N terminus of S4: the sequence MSLAI. The periodic energy perturbations observed here can be accounted for by a movement of the voltage sensor with respect to S3 as small as 3 Å.

A note added in proof: Using biotin and streptavidin labeling in KvAP channel, Jiang et al (Nature 423:42-48, 2003) proposed that the S4 and part of S3 move together as a paddle a total of 20 Å across the bilayer. We did not consider the simultaneous movement of S3 of S4 in the discussion of our results. Our conclusion about the relative movement of S4 with respect to S3 is still valid.

6. REFERENCES

- Aggarwal, S. K., and MacKinnon R., 1996, Contribution of the S4 segment to gating charge in the *Shaker* K⁺ channel, *Neuron*, **16**:1169-1177.
- Almers, W., 1978, Gating currents and charge movements in excitatory membranes, *Reviews of Physiology, Biochemistry and Pharmacology*, **82**:96-190.
- Bezanilla, F., 2000, The voltage sensor in voltage-dependent ion channels, *Physiological Reviews*, **80**:555-592.
- Catterall, W. A., 1986, Molecular properties of voltage-sensitive sodium channels, *Annual Review of Biochemistry*, **55**:953-985.
- Cornette, J. L., Cease, K. B., Margalit, H., Spouge, J.L., Berzofsky, J.A., and DeLisi, C., 1987, Hydrophobicity scales and computational techniques for detecting amphipathic structures in proteins, *Journal of Molecular Biology*, **95**:659-685.
- González, C., Rosenmann, E., Bezanilla, F., Alvarez, O., and Latorre, R, 2000, Modulation of the Shaker channel gating by the S3-S4, *Journal of General Physiology*, **115**:193-207.
- Gonzalez, C., Rosenmann, E., Bezanilla, F., Alvarez, O., and Latorre, R., 2001, Periodic perturbations in Shaker channel kinetics by deletions in the S3-S4 linker, *Proceedings of the National Academy of Sciences of the United States of America*, **98**: 9617-9623.
- Guy, H. R., and Seetharamulu, P., 1986, Molecular model of the action potential sodium channel, *Proceedings of the National Academy of Sciences of the United States of America*, **508**:508-512.
- Horn, R., 2000, Conversation between voltage sensors and gates of ion channels, *Biochemistry*, **39**:15653-15658.
- Seoh, S. A., Sigg, D., Papazian, D. M., and Bezanilla, F., 1996, Voltage-sensing residues in the S2 and S4 segments of the *Shaker* K channel, *Neuron*, **16**:1159-1167.
- Starace, D. M., and Bezanilla F., 2001, Histidine Scanning Mutagenesis of Basic Residues of the S4 Segment of the Shaker K⁺ Channel, *Journal of General Physiology*, **117**: 469-490.
- Wallner, M., Meera, P., and Toro, L., 1996, Determinant for β -subunit regulation in high conductance voltage-activated and Ca²⁺-sensitive K⁺ channels: An additional transmembrane region at the N-terminus, *Proceedings of the National Academy of Sciences of the United States of America*, **93**:14992-14927.
- Yellen, G., 1998, The moving parts of voltage-gated ion channels, *Quarterly Reviews of Biophysics*, **31**:239-295.

PEPTIDE TOXINS AS CONFORMATIONAL PROBES FOR K-CHANNELS

David Naranjo^{1*}

1. INTRODUCTION

During most of the last decade, peptide toxins from venomous animals were used as structural probes to unravel the architecture of K-channels. The structure of the external vestibule of the crystallized bacterial KcsA channel as representative of K-channels, was not only anticipated by such work, but also validated. Pore-plugging toxins are probes for the dynamic behavior of voltage-gated K-channels too: they bind with higher affinity to the closed channels and they appear to be insensitive to C-inactivation, a conformational change involving the toxin receptor area. Here, I revise possible mechanisms to account for these two findings.

Voltage-gated potassium channels are tetrameric membrane proteins. Each subunit carries six, probably α -helical, transmembrane segments. The first four transmembrane segments form the so-called voltage-sensing domain, containing the characteristic sequences that identify them as members of the family of voltage-gated ion channels (Noda *et al.*, 1984). Upon changes in voltage across the membrane, charged groups in this domain move to somehow enable the physical opening of a K⁺ permeation pathway in a separate domain of the protein. The permeation pathway is located in the so-called pore domain, made up of the fifth and sixth transmembrane segments. This domain has as its structural template the KcsA bacterial potassium channel (Doyle *et al.*, 1998).

In addition to the main gate, voltage gated potassium channels have several other gates that control the ion conduction process. After the channel opens, two other inactivating gates can interrupt the ion conduction; the N-inactivation and the usually slower C-inactivation (Hoshi *et al.*, 1991). There is a large body of evidence indicating that a segment in the amino terminus that enters the pore from the internal side produces the N-inactivation, occluding it (Zhou *et al.*, 2001). However, the slow inactivation is less well understood. It appears to be a concerted conformational change in the external pore entrance that renders the channels significantly less conductive to K⁺ (see for example: Yellen *et al.*, 1994; Liu *et al.*, 1996; Panyi *et al.*, 1995; Ogielska *et al.*, 1995; Larsson and Elinder, 2000).

¹ Centro de Neurociencia de Valparaíso, Universidad de Valparaíso, Gran Bretaña 1111, Playa Ancha, Valparaíso, Chile.

* corresponding author: David.Naranjo@uv.cl

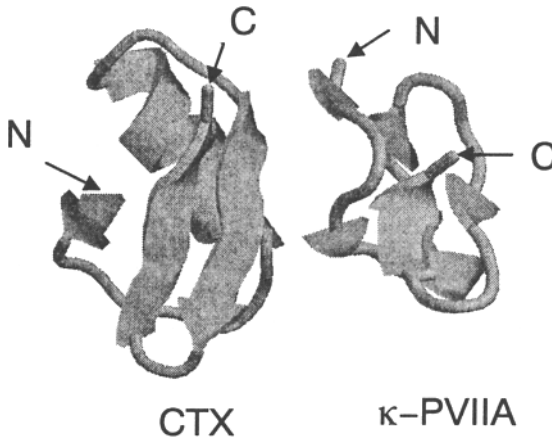


Figure 1. Rasmol renditions of charybdotoxin (CTX) and κ -conotoxin-PVIIA (κ -PVIIA) show that they share similar topological features. For CTX, the face that interacts with the K-channels pore is facing the viewer. This face forms an antiparallel β -sheet that put in close proximity the amino (N) and carboxyl (C) ends of the protein. To the back of the proteins, an α -helical structure connects the first and the β -strands. κ -PVIIA shows the same basic topology. It has a very short antiparallel β -sheet that put C-terminus nearby the N-terminus. The first β -strand is connected to the second by a short extended loop. However, for this toxin it is not clear that the face towards the viewer is the one that interact with the K-channel pore.

Peptide toxins from venomous animals have been widely used as structural probes for membrane proteins, particularly ion channels. Due to intramolecular disulfide bonds, they are generally short, structurally constrained, proteins. A subclass of K-channel specific toxin has evolutionary converged to a common mechanism of action; they occlude the ion conduction pore, the most conserved structure among K-channels. It is then expected that these toxins would interact with the pore-opening gates. Some interactions are expected to be stronger as, for example, with the pore constricting slow inactivation. Other interactions are expected to be weaker as, for example, with the voltage sensor. Here, I document the interaction, or rather the lack of it, of pore blocker toxins with the voltage-dependent activation and the slow-inactivation gates.

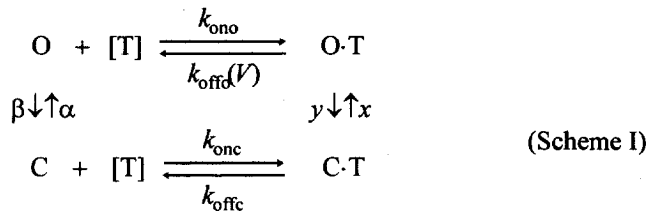
3. PORE-SPECIFIC TOXINS FOR POTASSIUM CHANNELS

Scorpion toxins of the α -KTx family, charybdotoxin (CTX), agitoxins (AgTx I and AgTx II), and iberiotoxin (IbTx) are the best characterized group in structural and functional terms (see Figure 1). They have provided the most important elements of our current view of the interaction with the pore of potassium channels (MacKinnon and Miller, 1988; Ranganathan *et al.*, 1996). Other venomous animals also supply toxins of this group; κ -conotoxin-PVIIA (κ -VIIA) come from marine cone snails; BgK from the sea anemone, and the Mamba snake, δ -dendrotoxin, which partially occludes the pore of Others have contributed more indirectly, as the pore-blocker toxins for sodium channels (French *et al.*, 1996). They share a number of important structural features:

- a) Intramolecular disulfide bounds. b) Abundant basic residues in the surface. c) Three antiparallel β -strands linked by a variable-length loop.

3. PEPTIDE TOXINS BIND TO OPEN AND CLOSED CHANNELS

Most of our current knowledge of the mechanism of pore blockade stems from work with the α -KTx family and with κ -PVIIA. The same three principles can be summarized as: *i*) toxin binds in a simple bimolecular fashion; *ii*) open and closed channels are competent to bind toxin; *iii*) Block channel gates near normally. These observations are summarized in the following simplified scheme:



where [T] is the toxin concentration, C, O, C·T, and O·T correspond to the unblocked-closed, unblocked-open, blocked-closed, and blocked-open channels, respectively. The constants: $k_{\text{on}o}$, and $k_{\text{on}c}$, $k_{\text{off}o}$, and $k_{\text{off}c}$, correspond to the association rates of the open and closed channels, and to the dissociation rates of the open and closed channels respectively. Here, $k_{\text{off}o}$ is the only voltage-dependent rate constant. Rates α and β are the opening and closing of the unblocked channel, while x and y are the corresponding rates for the blocked channel. In principle, this scheme is valid for all mentioned toxins.

In comparison with most scorpion toxins, κ -PVIIA has a relatively lower affinity for *Shaker* K-channels (in the range of 50 to 500 nM). Such lower affinity, due mostly to a lower stability of the toxin-channel complex, becomes kinetically advantageous. With the toxin in the bath, the same 100 ms voltage pulse used to open the channels also uncovers a relaxation from the closed state to a voltage-dependent binding equilibrium (See Figure 2). Thus, for this toxin we can distinguish binding to the closed and open states.

3.1. Binding to the Open State

The curves in Figure 2C are point-by-point quotients made of traces in the presence of the toxin divided by their respective control traces. They represent toxin-binding relaxation from a higher-affinity equilibrium with the closed channels to a lower affinity, and voltage-dependent equilibrium with the open channels. The time constants (τ) and voltage-dependent steady-state inhibition, $(I_{\text{pviiia}}/I_{\text{control}})_{\text{ss}}$, can be estimated from single exponential fits to the relaxations. Because the opening gate is much faster than the toxin binding kinetics (Garcia *et al.*, 1999; Naranjo, 2002), and because the channel open probability is near maximal at voltages positive to -10 mV, from scheme I, the following

equations are approximately valid:

$$\tau^{-1} \cong k_{\text{offo}} + [\text{T}] k_{\text{ono}}$$

$$(I_{\text{pviii}}/I_{\text{control}})_{\infty} \cong k_{\text{offo}} / (k_{\text{offo}} + [\text{T}] k_{\text{ono}})$$

By solving this equation system, we obtain the kinetic constants governing the toxin binding equilibrium to open channels. The association-rate constant appears to be diffusion limited, and therefore is voltage-independent (Miller, 1990). However, the bound complex is destabilized by depolarization in the open channel. Such voltage dependency disappears, or is drastically reduced, when permeant ions are removed from the intracellular side of the channels (See MacKinnon and Miller, 1988; Goldstein and Miller, 1993, for α -Ktx; García *et al.*, 1999, for κ -PVIIA). These results suggest that the voltage dependence arises from the electrostatic repulsion between positively-charged residues of the toxin and permeant ions residing in the pore.

3.2. Binding to the Closed State

In voltage-gated potassium channels, the main gate is located at the intracellular end of the pore. Thus, consistent with the proposed mechanism for the origin of the voltage dependency of the toxin unbinding, the binding equilibrium of the closed channels is voltage-independent. However, as seen Figure 2C, the toxin binds with higher affinity to the closed channel. Both the association and dissociation rates are slower. For example: k_{onc} is $\sim 1/5$ of k_{ono} and k_{offc} is $\sim 1/50$ of k_{offo} at 0 mV (Terlau *et al.*, 1999).

4. POSSIBLE ORIGINS FOR THE CLOSED-OPEN STATE DEPENDENCY

How does the closed-open state dependency arise? The closed-open conformational change may extend largely into the pore vestibule, thus affecting the toxin receptor area. Although, this kind of explanation cannot be neglected, we will explore here, two very simplistic model explanations that assume very little, if any, conformational change in the toxin receptor. *The pore occupancy model*, shows how the differences in pore occupancy between open and closed channels can account for a state-dependent toxin affinity; *The dynamic charges model*, examines how the voltage sensor movement can perturb the binding affinity of the toxin.

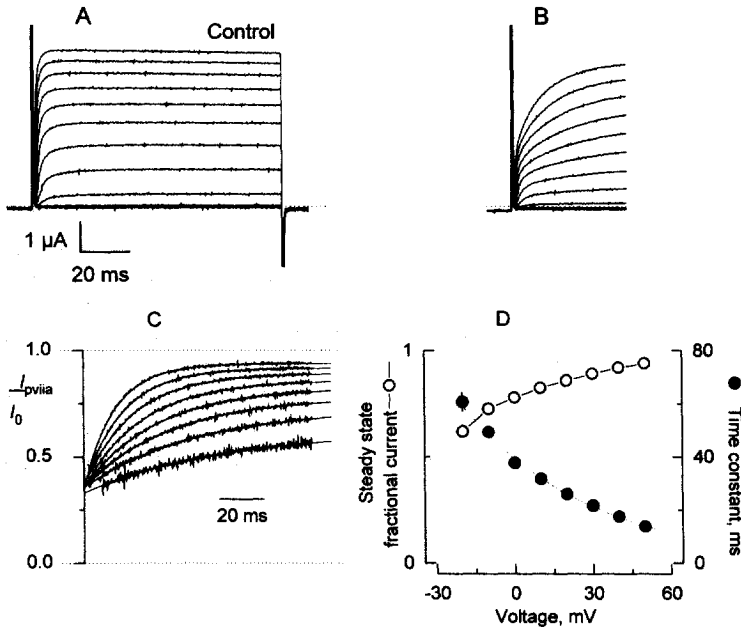


Figure 2. Effect of the κ -PVIIA on *Shaker* IR. Two-electrode voltage-clamp recordings of an oocyte expressing *Shaker* H4 $\Delta(6-46)$ in a control solution (A) and in the presence of 100 nM κ -PVIIA (B). Currents elicited from a holding voltage of -90 mV by activating pulses of -60 to +50 mV with intervals of 10 mV. Dotted lines indicate the zero current level. (C) After leak subtraction, records taken in the presence of 100 nM κ -PVIIA at each pulse voltage in B were divided point-by-point by leak-subtracted control records taken at corresponding voltages. Shown are the results of such an operation for -20 mV to +50 mV. Thin lines are fits of an exponential equation of the form: $f(t) = a \cdot b \cdot e^{-t/\tau}$, where a , b , and τ correspond to the steady state fractional current, the amplitude extrapolated to the beginning of the pulse, and the time constant, respectively. The $I_{pVIIA}/I_{control}$ curves converge to similar values when extrapolated to the beginning of the voltage pulse. The inhibition at resting was: 0.35 ± 0.004 for the -10 to +50 mV pulses corresponding to a $K_D = 54$ nM. (D) Results from single exponential fits to the traces in C. Plotted are the time constant and steady-state fractional current, $(I_{pVIIA}/I_{control})_{\infty}$, as a function of the pulse (a and τ in the equation above). Modified from Garcia *et al.*, (1999).

4.1. Pore Occupancy Modifies Toxin Binding

Toxin association to the closed channels is strongly dependent on the external K^+ . However, binding to the open channels is not (Terlau *et al.*, 1999). Such a result is nicely consistent with the idea that the pore occupancy is in equilibrium with the internal K^+ in the open channel and with the external K^+ in the closed channel. Terlau and coworkers proposed the existence of an externally-facing K^+ binding site in the pore that, when occupied, prevents the toxin from binding to the channel. Thus, toxin binding to the closed channels is slower because in normal physiological ionic conditions, this site is mostly occupied. But, closed channels, once blocked, cannot exchange permeant ions at both ends of the pore. Thus, they are unable to increase their state of occupancy. In a

reduced-ion occupancy state, the toxin-bound complex should be more stable (Figure 3A). The overall kinetics of toxin binding to the closed state (k_{onc} and k_{offc}) should be slower. In this view, the higher affinity for the closed state just results from the fact that k_{offc} is more affected than k_{onc} . However, there is something wrong with this picture; k_{offc} is voltage-independent. In the model, stability of the C·T complex should be strongly voltage-dependent (even more than in O·T complex), because it should follow the voltage dependence of the open probability. A single very brief opening event in the closed channel should equilibrate the pore occupancy with the internal solution.

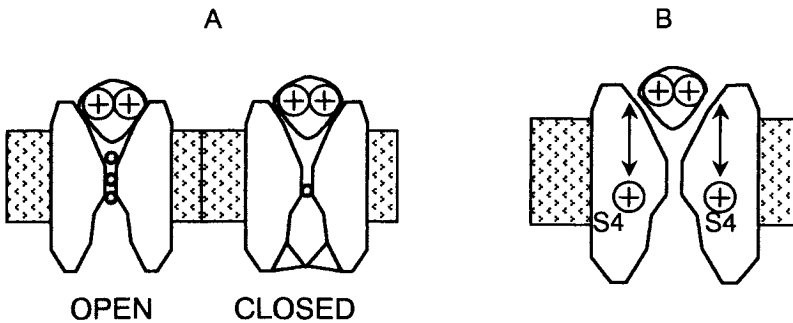


Figure 3. Models to explain closed-open state dependency of peptide toxin binding. (A) Occupancy model (B) Dynamic charges model.

5.2. The Voltage Sensor Interacts With the Toxin Bound to the Pore

μ -Conotoxin-GIIIA (μ -GIIA) is a relative of κ -PVIIA that blocks the sodium channel pore. A variant of this toxin, R13Q, incompletely blocks the channel pore. Thus, at single-channel level, it is possible to observe how the blocked channel gates between open and closed states (French *et al.*, 1996). French and coworkers observed that the activation curve for the blocked channels was shifted by +6 mV, as if stronger depolarization was necessary to open the channel. This additional electrical work to open the channel overcomes the electrostatic repulsion exerted by the positively-charged toxin (+5) on the outward movement of the gating charges (Figure 3B). Thus, the gating particles may make through-space electrostatic interaction with charges in the toxin. A more general statement would also include the "appearance" of a positive charge or the "disappearance" of a negative charge in the proximity of the bound toxin during gating (Gilly and Armstrong, 1982). Thus, the bound toxin should be destabilized by channel opening. This explanation may account for the increased stability of the C·T complex, but cannot explain the decrease in the association rate of the closed channel. In fact, the opposite is the expected result; increasing the number of negative charges in the proximity of the receptor increases the association rate for scorpion toxins (Escobar *et al.*, 1993; Stocker and Miller, 1994).

4.3. Ionic Strength Effects Could Distinguish Between Models.

To my knowledge, no systematic study of the effect of ionic strength on the pore occupancy of potassium channels has been performed. We do not expect pore occupancy to be dependent on ionic strength, because it is dominated by close-range interactions of K^+ with the pore linings (Doyle *et al.*, 1998). Thus, we would expect that the effects of ionic strength on the toxin binding to open or closed channels would be similar. However, if the toxin interacts electrostatically with dynamically located charges in the protein, the ionic-strength effects on the toxin binding should mirror that dynamic. In fact, when the ionic strength is changed from 60 to 160 mM, the dissociation constant for κ -PVIIA binding to closed channels increases 16-fold, while it grows only 5-fold for the open channels (Naranjo *et al.*, 2000). Kinetic analysis showed that the effects of the ionic strength on k_{ono} and k_{onc} were identical, in agreement with the occupancy model, but in disagreement with the dynamic charges model. In the opposing direction, k_{offc} but not k_{offo} were dependent on the ionic strength, in disagreement with the occupancy model, but in agreement with the dynamic charges model.

Thus, the explanation for the open-closed state dependency could lie in a synthesis of both models. Titration experiments of the external K^+ binding site and its relation to ionic strength are still to be performed. External divalent metals that trap channels in the closed conformation may disrupt the closed-open state dependency of the toxin binding (Gilly and Armstrong, 1982).

5. TOXINS BLOCK C-INACTIVATED AND CLOSED CHANNELS EQUALLY

Slow inactivation in *Shaker* K-channels involves a large number of residues spread from the C-terminus of S5 to the C-terminus of S6 in the pore domain. Interestingly, a large number of residues involved in the slow inactivation are also part of the peptide toxin receptor. This process probably involves a constriction of the external exit of the potassium permeation pathway produced by a concerted rearrangement of residues flanking the external entrance of the pore (Yellen *et al.*, 1994; Liu *et al.*, 1996; Panyi *et al.*, 1995; Ogielska *et al.*, 1995; Larsson and Elinder, 2000). At least three residues involved in such reorientation; 425, 448, and 449 (López-Barneo *et al.*, 1993; Liu *et al.*, 1996; Pérez-Cornejo, 1999) are also important for κ -PVIIA binding; (Scanlon *et al.*, 1997; Shon *et al.*, 1998; Jacobsen *et al.*, 2000).

Saturating applications of κ -PVIIA make a negligible effect on the macroscopic inactivation (Naranjo, 2002), and on the proportion of null traces in single channel studies (Figure 4A and B). This result suggests that the toxin binds equally well to inactivated and non-inactivated channels (Naranjo, 2002). Although we cannot be certain that single channel the null traces are due exclusively to visits to the slow-inactivated state, the lack of interaction of this pore-occluding toxin with the slow-inactivation gate falls within a more general scheme. In beautifully crafted experiments Liu and coworkers

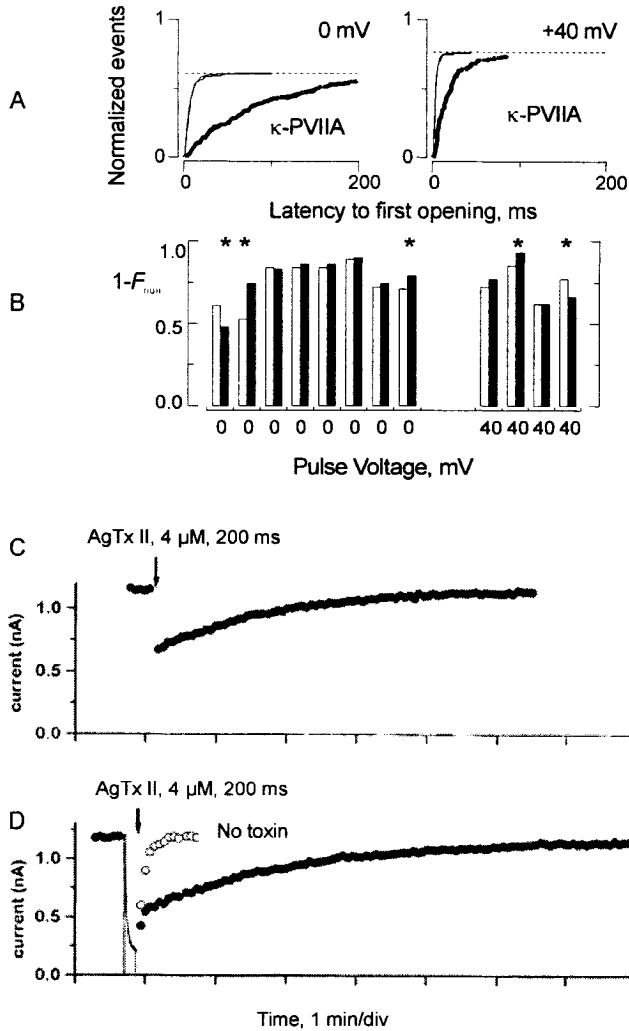


Figure 4. Slow inactivation does not interact with toxin binding. **A.** First latency analysis of single-channel traces with or without saturating toxin concentrations at 0 and 40 mV. Thick traces are in the presence of κ -PVIIA. **B.** κ -PVIIA does not modify the proportion of null traces. Comparisons for 0 and 40 mV. Asterisks indicate significantly different comparisons in a 2x2 contingency table with null hypothesis that the toxin does not modify the fraction of null traces. Each comparison had 140 to 480 control traces, and 120 to 540 toxin traces. **A** and **B** modified from Naranjo (2002). **C** and **D.** AgTx II binds equally rapidly to closed and inactivated channels. **C.** Binding of AgTx II to the closed state of T449C-Shaker. Circles represent the currents in the second half of a 10 ms voltage pulse (applied every 4 s). At the time indicated by the arrow, toxin (4 μ M) was applied for 200 ms at resting. The first test pulse after toxin application showed that 42% of the current was blocked. **D.** Binding of AgTx II to the inactivated T449C-Shaker. The trace represents currents during a 10 s depolarization to 0 mV. At the time indicated by the arrow (immediately after repolarization to -80 mV), 4 μ M of toxin was applied for 200 ms. Currents recovered with two phases: A fast phase characteristic of normal recovery from C-type inactivation, and a slow phase characteristic of toxin dissociation. The amplitude of the slow component is 53% of the current before toxin binding. Open circles represent recovery from inactivation without toxin application (**C** and **D** are modified from Liu *et al.*, 1996).

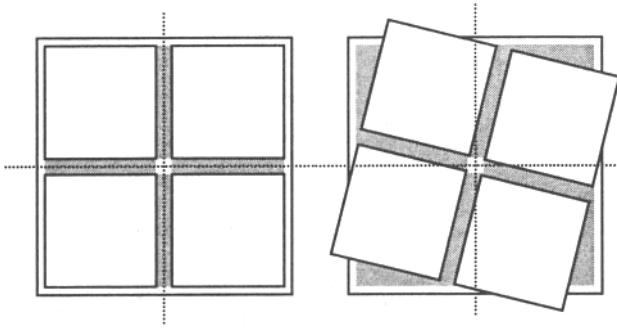


Figure 5. Rotational movement of the vestibule during slow inactivation. Representation of the *Shaker* K-channel toxin receptor from the extracellular side perpendicular to the plane of the membrane. During C-

(1996) found that, AgTx II, a well-known pore-occluding α -KTx scorpion toxin, binds equally well to either closed or slow inactivated channels (Figure 4C and D):

Given the large set of channel residues shared by the toxin receptor and slow inactivation, the lack of a visible interaction between the slow inactivation and the toxin binding is somehow surprising (Naranjo, 2002).

Cysteine substitution experiments show that a large set of residues changes solvent exposure considerably during slow inactivation. For example, Cd^{2+} binds 45,000-fold faster to slow inactivated T449C channels (Yellen *et al.*, 1994). Also, at positions 448, 449, and 450 of *Shaker*, Liu *et al.* (1996) measured increments of 100, 1000, and 10,000-fold respectively in the rate of cysteine modification by methanethiosulfonate derivatives in the slow-inactivated channel. The rates reached $10\text{-}50 \times 10^3 \mu\text{M}^{-1}\text{s}^{-1}$, close to sulfhydryl modification rates in solution (Stauffer and Karlin, 1994). The larger the change in the modification rate, the farther away from the pore is the α carbon of the equivalent residue in the KcsA K-channel crystal structure (Doyle *et al.*, 1998). Thus, while we cannot estimate the total movement in the vestibule of *Shaker* K-channel during the slow inactivation, we can say that that movement must be large; it appears to be larger for those residues away from the pore, and surprisingly, it does not get noticed by the bound toxin.

5.1. A Planar Rotation of the Vestibule During Slow Inactivation

A possible, although speculative, explanation for the lack of effect of slow inactivation on toxin binding would imply a rearrangement in which the relative positions of at least 425, 448, and 449 do not change drastically. Because, at least two, and possibly four, 449 residues simultaneously touch α KTx scorpion toxins, a geometrical constraint must be imposed on such a rearrangement (Naranjo and Miller, 1996; Gross and MacKinnon, 1996). This constraint would be satisfied by a concerted planar rotation of the vestibule around the pore (Figure 5), as has been proposed for the Pore-S6 loop (Larsson and Elinder, 2000). This rotational movement of the vestibule would twist the pore linings as in other ion channel gates, such as the gap-junction hemichannel, the nicotinic acetylcholine receptor, and the KcsA K-channel (Unwin and Zampighi, 1980; Unwin, 1995; Perozo *et al.*, 1999). This proposal might explain why when aromatic residues are present in position 449, TEA blocks in a nearly voltage-independent fashion

and does not interfere with the slow inactivation. But, in the wild-type 449T-*Shaker*, TEA blockade is voltage-dependent and interferes competitively with the slow inactivation gate, as if TEA was going deeper into the pore (Molina *et al.*, 1998).

6. CONCLUDING REMARKS

Until recently, before the structure of the KcsA channel was known, K-pore blocker peptide toxins were used successfully as structural probes for the most conserved structural locus of K-channels. A large part of the structural features of the external vestibule of the KcsA channel were precisely anticipated in voltage-gated K-channels. Now, pore-occluding peptide toxins have become probes for conformational changes, and, somehow unexpectedly, because of their size, probes for pore occupancy. Thus, the concurrence of a solid structural paradigm with a sensitive structural probe could be a valuable tool in protein dynamics.

7. ACKNOWLEDGMENTS

I thank L. Ruiz, B. Aguirre, and M.A. Hernández for technical help, Alan Neely, Miguel Holmgren, and Armando Gómez-Puyou for discussion. I thank Chris Miller, Irwin Levitan and Paul Brehm for providing essential equipment. DGAPA-UNAM, CONACyT-México 25247-N, and ICM-Chile P99037F funded this work.

8. REFERENCES

- Doyle, D.A., J. Morais-Cabral, R.A. Pfuetzner, A. Kuo, J.M. Gulbis, S.L. Cohen, B.T. Chait, and R. MacKinnon. 1998, The structure of the potassium channel: molecular basis of K⁺ conduction and selectivity, *Science*. **280**:69-77.
- Escobar L., Root, M. J., and Mackinnon, R., 1993, Influence of protein surface charge on the biomolecular kinetics of a potassium channel peptide inhibitor, *Biochemistry*, **32**:6982-6987.
- French, R.J., Prusak-Sochaczewski, E., Zamponi, G.W., Becker S., Kularatna A.S., Horn R. 1996, Interactions between a pore-blocking peptide and the voltage sensor of the sodium channel: an electrostatic approach to channel geometry, *Neuron*. **16**:407-413.
- García, E., M. Scanlon, and D. Naranjo. 1999, A marine snail neurotoxin shares with scorpion toxins a convergent mechanism of blockade on the pore of voltage gated K-channels, *J. Gen. Physiol* **114**:141-157.
- Gilly, W.F., Armstrong C.M. 1982, Slowing of sodium channel opening kinetics in squid axon by extracellular zinc, *J Gen Physiol*. **79**:935-964.
- Goldstein, S.A.N., and C. Miller. 1993, Mechanism of charybdotoxin block of a voltage-gated K⁺ channel, *Biophys. J*. **5**: 1613-1619
- Gross, A. and R. MacKinnon 1996, Agitoxin footprinting on the *Shaker* potassium channel pore, *Neuron* **16**:399-406.
- Hoshi, T., W.N. Zagotta, and R.W. Aldrich. 1991, Two types of inactivation in *Shaker* K⁺ channels: Effects of alterations in the carboxy-terminal region, *Neuron* **7**:547-556.
- Imredy, J.P., and R. MacKinnon 2000, Energetic and structural interactions between delta-dendrotoxin and a voltage-gated potassium channel, *J. Mol. Biol.* **296**: 1283-1294.
- Jacobsen R.B., E.D. Koch, B. Lange-Malecki, M. Stocker, J. Verhey, R.M. Van Wagoner, A. Vyazovkina, B.M. Olivera and H. Terlau, 2000, Single amino acid substitutions in κ -conotoxin PVIIA disrupt interaction with the *Shaker* K⁺ channel, *J. Biol. Chem.* **275**:24639-24644
- Larsson, H.P., and F. Elinder, 2000, A conserved glutamate is important for slow inactivation in K⁺ channels, *Neuron*, **27**: 573-583.
- Liu, Y., M. Jurman, and G. Yellen, 1996, Dynamic rearrangement of the outer mouth of a potassium channel

- during gating, *Neuron*, **16**: 859–867.
- López-Barneo, J., T. Hoshi, S. Heinemann, and R.W. Aldrich, 1993, Effects of external cations and mutations in the pore region on C-type inactivation of Shaker potassium channels, *Receptor Channels*, **1**:61-71.
- MacKinnon, R., and C. Miller, 1988, Mechanism of charybdotoxin block of Ca^{2+} -activated K^+ channels, *J. Gen. Physiol.* **91**: 335-349.
- Miller C., 1990, Diffusion-controlled binding of a peptide neurotoxin to its K^+ channel receptor, *Biochemistry*, **29**:5320-5325.
- Molina, A., P. Ortega-Sáenz, and J. López-Barneo, 1998, Pore mutations alter closing and opening kinetics in Shaker K^+ channels, *J. Physiol.* **509**:327–337.
- Naranjo, D., Hernández, C., and García, E., 2000, Ionic strength affects differentially the binding of κ -conotoxin-PVIIA to open and closed Shaker K^+ channels, *Biophysical Journal*, **78**:97A.
- Naranjo, D, 2002, κ -conotoxin PVIIA blockade of single Shaker K^+ channels, *Biophys. J.*, **82**:3003-3011.
- Naranjo, D. and C. Miller, 1996, A strongly interacting pair of residues on the contact surface of charybdotoxin and a Shaker K^+ channel, *Neuron*, **16**:123-130.
- Noda, M., S. Shimizu, T. Tanabe, T. Takai, T. Kayano, T. Ikeda, H. Takahashi, H. Nakayama, Y. Kanoaka, N. Minamino, K. Kangawa, H. Matsuo, M.A. Raftery, T. Hirose, S. Inayama, H. Hayashida, T. Miyata, and S. Numa, 1984, Primary structure of *Electrophorus electricus* sodium channel deduced from cDNA sequence, *Nature* **312**: 121-127.
- Ogielska, E.M., W.N. Zagotta, T. Hoshi, S.H. Heinemann, J. Haab, and R.W. Aldrich, 1995, Cooperative subunit interactions in C-type inactivation of K channels, *Biophys J.* **69**:2449-2457.
- Panyi, G., Z. Sheng, and C. Deutsch, 1995, C-type inactivation of a voltage-gated K^+ channel occurs by a cooperative mechanism, *Biophys J.* **69**:896-903.
- Pérez-Cornejo P., 1999, H^+ ion modulation of C-type inactivation of Shaker K^+ channels, *Pflugers Arch.* **437**:865-870
- Perozo E, D.M., Cortés, and L.G. Cuello, 1999, Structural rearrangements underlying K^+ -channel activation gating, *Science* **285**:73-78.
- Ranganathan. R., J.H. Lewis, and R. MacKinnon, 1996, Spatial localization of the K^+ channel selectivity filter by mutant cycle-based structure analysis, *Neuron*, **16**:131-9.
- Scanlon M., D. Naranjo, L. Thomas, P. Alewood, R. Lewis y D. Craik, 1997, Solution structure and proposed binding mechanism of a novel potassium channel toxin κ -conotoxin PVIIA, *Structure*, **5**: 1585-1597.
- Shon, K-J., M. Stocker, H. Terlau, W. Stühmer, R. Jacobsen, C. Walker, M. Grilley, M. Watkins, D.R. Hillyard, W.R. Gray, and B.M. Olivera, 1998, κ -conotoxin pviia is a peptide inhibiting the Shaker K^+ channel, *J. Biol. Chem.* **273**:33-38
- Stauffer, D.A., and A. Karlin, 1994, Electrostatic potential of the acetylcholine binding sites in the nicotinic receptor probed by reactions of binding-site cysteines with charged methanethiosulfonates, *Biochemistry*, **33**:6840-6849.
- Stocker, M. and Miller, C., 1994, Electrostatic distance geometry in a K^+ channel vestibule, *Proceedings of the National Academy of Sciences U.S.A.*, **91**:9509-9513.
- Terlau, H., A. Boccaccio, B.M. Olivera, and F. Conti, 1999, The block of Shaker K^+ channels by κ -conotoxin PVIIA is state dependent, *J. Gen. Physiol.* **114**:125-140.
- Unwin, N., 1995, Acetylcholine receptor channel imaged in the open state, *Nature*, **373**:37-43.
- Unwin, N., and G. Zampighi, 1980, Structure of the junction between communicating cells, *Nature*, **283**:545-549.
- Yellen, G., D. Sodickson, T.Y. Chen, and M.E. Jurman, 1994, An engineered cysteine in the external mouth of a K^+ channel allows inactivation to be modulated by metal binding, *Biophys J.* **66**:1068-1075.
- Zhou M, Morais-Cabral JH, Mann S, MacKinnon R., 2001, Potassium channel receptor site for the inactivation gate and quaternary amine inhibitors, *Nature*, **411**:657-661.

MOLECULAR PARTICIPANTS IN VOLTAGE-DEPENDENT GATING

Shinghua Ding¹, Thao P. Nguyen^{1,2}, and Richard Horn^{1*}

1. INTRODUCTION

The ion channels underlying action potentials in excitable cells have an approximate four-fold symmetry with each subunit, or homologous domain, surrounding a central permeation pathway (pore) that extends across the lipid bilayer membrane. Each subunit or domain contains a positively charged transmembrane segment, designated the S4 segment, that acts as a sensor of the membrane potential. The pore is lined by a selectivity filter at its external end and the four S6 transmembrane segments over most of its length. The S6 segments converge at their cytoplasmic ends to form the activation gate that opens and closes the pore. In the present work, we discuss the possible role of other putative voltage sensors in the channel, especially the S2 segment, and mechanisms for coupling S4 and S6 movement.

Voltage-gated ion channels are responsible for generating action potentials in excitable cells. Understanding how they accomplish this feat has occupied scientists worldwide for the last half century. This quest has been aided by many technological breakthroughs, including the cloning and sequencing of many members of the superfamily of voltage-gated ion channels, which include sodium, potassium, and calcium channels. As a result of a deluge of 'structure-function' studies the main molecular participants in voltage-dependent gating are now established.

An ion channel capable of voltage-dependent gating requires three molecular components: a selective permeation pathway (pore) through which privileged ions can diffuse across the membrane, a gate that permits or denies access to this pore, and a voltage sensor that moves in response to changes of membrane potential. A further requirement is that the voltage sensors and gates of the channel must be coupled, so that gates ultimately respond to changes of membrane potential by opening or closing. This article will describe these three molecular participants in voltage-dependent gating and

¹ Department of Physiology, Institute of Hyperexcitability, Jefferson Medical College, 1020 Locust Street, Philadelphia, PA 19119, U.S.A.

² Neurosciences Department, University of Pennsylvania, Philadelphia, PA 19104, U.S.A.

* corresponding author: richard.horn@tju.edu

consider other constituents of voltage-gated ion channels that also contribute to the gating process.

Voltage-gated ion channels form a superfamily that includes members selective for either sodium, calcium, or potassium ions. The central aqueous pore of these channels is surrounded by four subunits, in the case of potassium channels, or four homologous domains in the case of sodium and calcium channels. A recently discovered prokaryotic sodium channel, like some potassium channels, is made of four identical subunits (Ren *et al.*, 2001). Each subunit or domain typically has six transmembrane segments, S1-S6, with both amino and carboxy termini situated in the cytoplasmic compartment. An exception to this rule is seen in some members of calcium-activated potassium channels that have subunits with seven transmembrane segments, S0-S6, with an extracellular amino terminus (Meera *et al.*, 1997). The S4 segment is the main voltage sensor in this superfamily of ion channels (Bezannilla, 2000). It typically has 4 - 8 basic residues. Although charged residues are found in other transmembrane segments, there are rarely more than two charges in any transmembrane segment other than the S4 segment.

With the identities of some of the main molecular participants of voltage-dependent gating in hand, we will address two questions. The first is whether an S2 segment of sodium channels could, like S4, be a voltage sensor. The second concerns mechanisms for coupling S4's movement with the opening and closing of the activation gate.

2. RESULTS

The S2 segments of voltage-gated ion channels contain an absolutely conserved glutamate residue, about two-thirds of the distance from the extracellular to intracellular ends (Keynes and Elinder, 1999). This negatively charged residue has been implicated in electrostatic interactions with basic S4 residues in *Shaker* potassium channels (Papazian *et al.*, 1995; Tiwari-Woodruff *et al.*, 1997). It may also confer a voltage sensing role to the S2 segment in *Shaker* (Seoh *et al.*, 1996). To explore the role of this glutamate residue in sodium channels, we mutated it to positively charged lysine in the S2 segment of the second homologous domain of the human skeletal muscle sodium channel. Unlike the studies in potassium channels, in which a point mutation is expressed in each of four identical subunits, in our construct only one of the four S2 glutamates has been mutated. We expressed the mutant channel (E618K) in *Xenopus* oocytes and examined the effects on sodium currents in cell-attached patches. Figures 1 and 2 show the biophysical consequences of this charge-reversing mutation.

Superimposed currents elicited by a depolarization from -140 mV to -30 mV are shown in Figure 1B. The E618K mutant has dramatically slower kinetics of activation and inactivation than seen in wild type (WT) channels. However the data in Figures 1A, 1C and 1D suggest that this is a consequence largely of a ~26-mV depolarizing

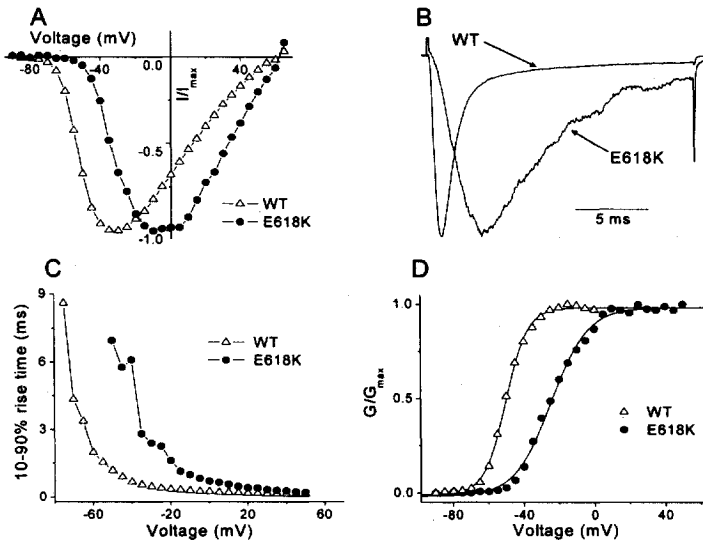


Figure 1. WT versus E618K mutant in cell-attached oocyte patches. Bath and pipette solution (in mM): 150 NaCl, 2 KCl, 1.5 CaCl₂, 1 MgCl₂, 10 Cs-Hepes, pH 7.4. A. Normalized peak *I-V*. B. Na⁺ currents at -30 mV. C. Activation rise time. D. Peak *G-V* relation with Boltzmann fits ($V_{mid} = -50.1, -24.5$ mV; $\delta = 6.2, 2.4 e_0$).

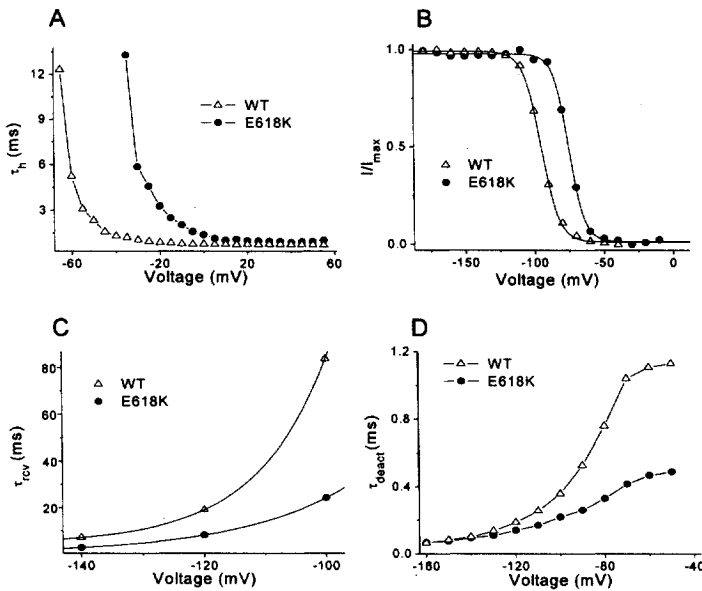


Figure 2. WT versus E618K mutant in cell-attached oocyte patches. A. τ_h from single exponential fits. B. Steady state inactivation. ($V_{mid} = -95.0, -75.1$ mV; $\delta = 4.0, 4.6 e_0$, for WT & E618K, respectively). C. Recovery from inactivation, time constants from single exponential fits. D. Fitted time constants of tail currents.

shift of activation, a more dramatic consequence than the homologous mutation (E293K) in *Shaker*, in which all four subunits carry the mutation (Tiwari-Woodruff *et al.*, 1997). The depolarizing shifts in activation may be responsible for similar shifts in parameters for inactivation (Figures 2A, 2B, and 2C), due to the coupling between these two gating processes (Armstrong and Bezanilla, 1977; Bezanilla and Armstrong, 1977).

These results show the importance of a conserved residue in an S2 segment. However, as in previous studies of S2 segments, they shed little light on whether S2 segments are voltage sensors. We attempted to test this hypothesis directly by measuring the voltage-dependent accessibility of a cysteine mutant of the homologous glutamate in the S2 segment of the fourth domain of the same isoform of sodium channel. Although this mutant was functional, the substituted cysteine showed no evidence of being accessible to hydrophilic cysteine reagents, leaving the question of S2's voltage-dependent movement open (T. P. Nguyen and R. Horn, unpublished).

We now turn to the question of coupling. Three mechanisms have been proposed to account for S4's interaction with the activation gate formed at the cytoplasmic end of the S6 segments (Horn, 2000). S4 might pull or twist either or both of the linkers at its extracellular or intracellular ends, or it might interact directly with the S6 segment within the transmembrane region. To explore the last possibility, we made cysteine mutations of four S6 residues, between I470 and V478 in *Shaker* potassium channels; these residues extend from approximately the middle to the bottom of the S6 segment. We examined the consequences of these mutations on the channel's gating currents, which are primarily produced by movement of the S4 segment (Bezanilla, 2000). The gating currents were measured in nonconducting mutants, using methods described previously (Ding and Horn, 2001). An effect of S6 mutations on gating currents would suggest the possibility of a direct communication between these two transmembrane segments, and therefore between voltage sensor and gate movement.

Figure 3 shows gating currents of WT (*Shaker*-IR in the background of T449V and W434F; Ding and Horn, 2001) and four cysteine mutants: I470C, V474C, V476C, V478C. Although the ON gating currents in response to depolarizations are rather comparable among the mutant and WT channels, the kinetics of OFF gating currents at -120 mV are significantly different from WT for all the mutants. The OFF gating currents after a depolarization to +40 mV are significantly slower for V476C and significantly faster for the other three mutants (Figure 3 and Table 1). The integrated charge-voltage ($Q-V$) relationships for these mutants are, by contrast, rather comparable to those of WT channels (Table 1).

Although these results suggest a direct S4-S6 interaction, further evidence will be needed to confirm this idea. An alternative possibility, for example, is that the S6 mutations have an allosteric effect on the downstream activation gate or its environs, and that this is the region that communicates with the S4 segment (Ding and Horn, 2002).

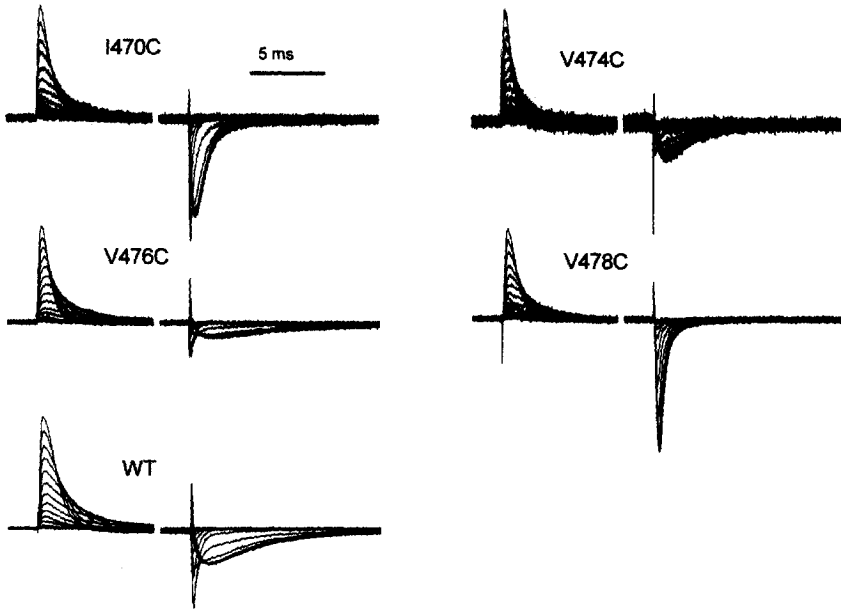


Figure 3. Gating currents for nonconducting variants of *Shaker* channels (WT) and four cysteine mutants. Depolarizations from -120 to +40 mV in 10-mV increments are shown. The holding potential was -120 mV.

Table 1. Q - V and OFF gating current kinetics of cysteine mutants in S6. Values of V_{mid} and q are from fits to single Boltzmann functions of the Q - V curve. τ is the time constant of OFF gating current decay at -120 mV from a depolarized voltage of +40 mV.

* indicates the estimated parameter is significantly different from WT.

	Q - V		τ (ms)	
	V_{mid} (mV)	q (e_0)		
WT	-51.3±2.4;	2.9±0.4	3.50±0.46	($n=4$)
I470C	-46.7±0.9;	3.2±0.1	1.01±0.07*	($n=5$)
V474C	-45.2±1.4;	3.0±0.3	1.44±0.19*	($n=3$)
V476C	-58.1±0.6;	5.6±0.1*	6.18±0.34*	($n=3$)
V478C	-42.5±1.5*;	2.5±0.1	0.49±0.03*	($n=5$)

3. CONCLUSIONS

The molecular participants involved in voltage sensing, gating, and coupling are under active investigation. Data from our and other laboratories suggest that voltage-dependent gating involves a coordinated, allosteric interplay among all regions of these transmembrane proteins. A major challenge is not only to uncover the details of these conformational changes, including the relevant energetics, but to fashion a coherent description that captures the essential features depicted in the crude cartoons of the last half century.

4. REFERENCES

- Armstrong, C. M., and Bezanilla, F. 1977, Inactivation of the sodium channel. II. Gating current experiments. *Journal of General Physiology* **70**:567-590.
- Bezanilla, F. 2000, The voltage sensor in voltage dependent ion channels. *Physiological Reviews* **80**:555-592.
- Bezanilla, F., and Armstrong, C. M. 1977, Inactivation of the sodium channel. I. Sodium current experiments. *Journal of General Physiology* **70**:549-566.
- Ding, S., and Horn, R. 2001, Slow photo-cross-linking kinetics of benzophenone-labeled voltage sensors of ion channels. *Biochemistry* **40**:10707-10716.
- Ding, S., and Horn, R. 2002, Pivotal role of the tail end of the S6 segment in coupling the voltage sensor and activation gate of *Shaker* K channels. *Biophysical Journal* **82**:174a.
- Horn, R. 2000, Conversation between voltage sensors and gates of ion channels. *Biochemistry* **39**:15653-15658.
- Keynes, R. D., and Elinder, F. 1999, The screw-helical voltage gating of ion channels. *Proceedings of the Royal Society of London. B: Biological Sciences* **266**:843-852.
- Meera, P., Wallner M., Song M., and Toro, L. 1997, Large conductance voltage- and calcium-dependent K⁺ channel, a distinct member of voltage-dependent ion channels with seven N-terminal transmembrane segments (S0-S6), an extracellular N terminus, and an intracellular (S9-S10) C terminus. *Proceedings of the National Academy of Sciences USA* **94**:14066-14071.
- Papazian, D. M., Shao, X. M., Seoh, S.-A., Mock, A. F., Huang, Y., and Wainstock D. H. 1995, Electrostatic interactions of S4 voltage sensor in *Shaker* K⁺ channel. *Neuron* **14**:1293-1301.
- Ren, D. J., Navarro, B., Xu, H. X., Yue, L. X., Shi, Q., and Clapham, D. E. 2001, A prokaryotic voltage-gated sodium channel. *Science* **294**:2372-2375.
- Seoh, S. A., Sigg, D., Papazian, D. M., and Bezanilla, F. 1996, Voltage-sensing residues in the S2 and S4 segments of the *Shaker* K⁺ channel. *Neuron* **16**:1159-1167.
- Tiwari-Woodruff, S. K., Schulteis, C. T., Mock, A. F., and Papazian, D. M. 1997, Electrostatic interactions between transmembrane segments mediate folding of *Shaker* K⁺ channel subunits. *Biophysical Journal* **72**:1489-1500.

CA²⁺ DYNAMICS AT NERVE-TERMINAL ACTIVE ZONES MONITORED BY ENDOGENOUS K_{Ca} CHANNELS

Alan D. Grinnell^{1*}, Bruce Yazejian¹, Xiaoping Sun¹, and Bo-Ming Chen¹

1. INTRODUCTION

Endogenous high-conductance calcium-activated K⁺ channels that co-localize with Ca²⁺ channels at presynaptic active zones in *Xenopus* nerve-muscle cultures have been characterized and used to quantify the rapid, dynamic changes in Ca²⁺ concentration during synaptic activity. Based upon calibrations of single-channel sensitivity to Ca²⁺ and voltage, the K(Ca) channels report Ca²⁺ concentrations of 100 μM or more at the inner membrane surface during action potentials or Ca²⁺-tail currents, and much faster kinetics of decay of calcium microdomains than has been shown by other methods.

The entry of Ca²⁺ at nerve terminal active zones (AZs) triggers neurotransmitter release. Although in several terminal preparations it is possible to quantify Ca²⁺ influx by measuring Ca²⁺ currents, an understanding of the role of Ca²⁺ requires a correlation of release with an accurate knowledge of the dynamics of Ca²⁺ buildup and decay at the sites of the Ca²⁺ sensors that trigger release. Because of the short latency between I_{Ca} and release (≤100 μsec in some preparations; Sabatini and Regehr, 1996), the rapid termination of release, and the fact that the time course of release to an action potential (AP) is the same over a very wide range of [Ca²⁺]_o (Andreu and Barrett, 1980), it is now widely believed that in most synapses the Ca²⁺-sensing molecules that trigger release require the high concentrations of Ca²⁺ found in the “Ca²⁺ microdomains” built up near clusters of open Ca²⁺ channels (Simon and Llinás, 1985; Zucker and Fogelson, 1986; Roberts, 1994; Llinás *et al.*, 1995; Zucker, 1996; Klingauf and Neher, 1997; Meir *et al.*, 1999). This also requires that the sensors be located close to Ca²⁺ channels and have a relatively low Ca²⁺ binding affinity. Consistent with these requirements is the observation that synaptic vesicles are clustered at active zones (AZs) on the presynaptic membrane where there are organized arrays of intramembranous particles (IMPs) probably representing Ca²⁺ and Ca²⁺-sensitive K⁺ (K_{Ca}) channels (Couteaux and Pecot-Dechavassine, 1970; Pumplin *et al.*, 1981; Roberts *et al.*, 1990). At least one of the vesicle-docking membrane proteins, syntaxin, is bound to Ca²⁺ channels (Sheng *et al.*,

¹ Department of Physiology, School of Medicine, University of California Los Angeles, CA 90095, U.S.A.

* corresponding author: adg@ucla.edu

1994), and docked vesicles appear to be indirectly attached to the IMPs thought to be Ca^{2+} channels (Harlow *et al.*, 2001.).

The difficulty in establishing the true relationship between Ca^{2+} and release is that the Ca^{2+} responsible for release enters through highly localized clusters of Ca^{2+} channels at AZs, which represent only a tiny fraction of the surface area of the nerve terminal. The I_{Ca} reveals how many Ca^{2+} ions have entered the terminal, but an unknown fraction enter through the membrane at regions other than the AZs. Without accurate knowledge of the geometry of Ca^{2+} channels and properties of local fixed and mobile buffers and Ca^{2+} sequestering/pumping systems, even knowledge of how much Ca^{2+} has entered at the AZ does not allow one to draw conclusions about the $[\text{Ca}^{2+}]_i$ at that point, or its time course of buildup, decay, and rate of removal.

Attempts to study Ca^{2+} dynamics in terminals have mostly employed Ca^{2+} -sensitive molecules and optical imaging techniques, even the best of which (DiGregorio *et al.*, 1997, 1999) have the drawbacks that they measure $[\text{Ca}^{2+}]$ from a relatively large volume within the terminal, extending far from the AZ, and require the introduction of an extrinsic buffer, which usually entails dialysis of the terminal and loss of intrinsic buffers.

We have sought to avoid these problems by using endogenous large conductance Ca^{2+} -sensitive K^+ channels (K_{Ca} or maxi-K channels) as monitors of the $[\text{Ca}^{2+}]_i$ at the inner-membrane surface at AZs. The I_{KCa} has been used in frog (Hudspeth and Lewis, 1988; Roberts *et al.*, 1990; Roberts, 1993), goldfish (Sugihara, 1994), and turtle hair cells (Art *et al.*, 1995) and goldfish bipolar nerve terminals (Sakaba *et al.*, 1997; Burrone *et al.*, 2002) to compare I_{Ca} -induced responses to those obtained by break-in with known concentrations of Ca^{2+} ; but Ca^{2+} dynamics during the Ca^{2+} transients were not studied. Dynamic changes in K_{Ca} channel conductance have been used in crayfish neuromuscular junctions to demonstrate the decay of $[\text{Ca}^{2+}]_i$ within 1-4 msec following a test depolarization (Blundon *et al.*, 1993, 1995), but the time course of these changes and the absolute level of $[\text{Ca}^{2+}]_i$ and the properties of microdomains were not studied. For K_{Ca} channels to serve as accurate reporters of local $[\text{Ca}^{2+}]_{\text{AZ}}$ during Ca^{2+} transients it is essential that they be co-localized with the Ca^{2+} channels that trigger release, that their Ca^{2+} -binding affinity be appropriate to reflect Ca^{2+} concentration levels that occur in Ca^{2+} domains near open Ca^{2+} channels, and that activation and inactivation kinetics be sufficiently rapid to follow transient changes in $[\text{Ca}^{2+}]_i$. In this communication, we summarize evidence that these conditions are met in the varicosity synapses formed by motoneuron neurites on muscle cells in embryonic *Xenopus* nerve-muscle cell cultures (Yazajian *et al.*, 1997, 2000; Sand *et al.*, 2001; Pattillo *et al.*, 2001).

2. METHODS

Fertilized eggs of *Xenopus laevis* are allowed to develop to stages 17-23 (Nieuwkoop and Fabre, 1967). The embryos are briefly rinsed in 70% ethanol, and the jelly coat and outer membranes of the eggs removed. The embryos are rinsed in sterile 10% normal frog Ringer (NFR) and the cranial and abdominal portions of the embryo are removed. The remaining spinal cord and somites are allowed to disaggregate in a Ca^{2+} - and Mg^{2+} -free solution (67 mM NaCl, 1.6 mM KCl, 2 mM EDTA, and 8 mM HEPES-NaOH at pH 7.4) for 30-60 minutes. The cells are then plated on to clean, uncoated glass coverslips. The cultures are maintained in a medium containing 50% L-15 (Gibco) and 50% NFR,

supplemented with 3 $\mu\text{g/ml}$ glutamine, 0.1 $\mu\text{g/ml}$ insulin, 0.7 $\mu\text{g/ml}$ sodium selenite, 0.6 $\mu\text{g/ml}$ transferrin, 1 $\mu\text{g/ml}$ sodium pyruvate and 50 units/ml penicillin-streptomycin. Within 24 hours, neurons have extended neurites that possess occasional varicose processes. Neurons continue to extend varicosity-studded neurites, and will readily grow *in vitro* for more than one week if the medium is changed every third day. We add 5 ng/ml BDNF and 5 ng/ml neurotrophin-3 (kindly provided by Neurogen) to the cultures, having found that this increases the survival rate of neurons in the cultures and promotes neurite outgrowth and synaptic maturation. These intact varicosities, in contact with muscle cells or not, are amenable to cell-attached and whole cell patch recording.

Since varicosities are small (about 5 μm in diameter), and Ca²⁺ channels are known to be sensitive to “wash-out” (Armstrong and Eckert, 1987) we use a modification of the “perforated” patch” technique described by Horn and Marty (1988) to gain electrical access to the motoneuron varicosity. Pipettes are made by multiple step pulling to a tip diameter that has an electrode resistance of 3-10 M Ω . The cells are typically bathed in a normal frog Ringer’s solution containing (in mM): 116 NaCl, 2 KCl, 1.8 CaCl₂, 1 MgCl₂, 5 HEPES, pH 7.3 with 1 mM 3,4, diaminopyridine (DAP) and 300 nM TTX to eliminate most of the voltage-sensitive K⁺ and all of the voltage-sensitive Na⁺ currents. The postsynaptic pipette contains 116 KCl, 1 NaCl, 1 MgCl₂, 10 EGTA, 5 HEPES, pH 7.3. The presynaptic pipette is filled with an internal solution containing 52 K₂SO₄, 38 KCl, 5 HEPES, 1 EGTA, and 1 DAP plus 400-600 $\mu\text{g/ml}$ amphotericin B (Rae *et al.*, 1991). Within about 1-5 minutes of seal formation, the amphotericin-B has made a low-resistance pathway with a series resistance of \sim 100 M Ω or less. At this point, after series resistance compensation, stable “whole-cell” recordings of varicosity current can be made for long periods of time (more than an hour). Recording is done with Axopatch 200A and 200B patch-clamp amplifiers (Axon Instruments). In all cases, voltage steps are generated and current traces digitized at 10-100 kHz, stored, and analyzed using pClamp software (Axon Instruments) on a Pentium III microprocessor. When necessary, whole-cell currents are 8-pole Bessel filtered at 1-3 kHz. Voltage-dependent Ca²⁺ current IV curves are typically made with 20 ms steps from -70 through $+80$ mV in 10 mV steps, enabling P/-2 or P/-4 subtraction.

3. RESULTS

3.1. K_{Ca} Currents Track Ambient [Ca²⁺]_{AZ}.

To study the temporal resolution with which K_{Ca} currents can track Ca²⁺ transients, we generated Ca²⁺-tail currents in varicosities in the presence of TTX and DAP to block voltage-sensitive Na⁺ and K⁺ currents. Figure 1 illustrates the procedure used to quantify the I_{KCa}, and thereby [Ca²⁺]_{AZ}, as a function of I_{Ca} during a Ca²⁺-tail current (from Yazejian *et al.*, 2000). A large step depolarization to near E_{Ca} ($+80$ mV or higher) was imposed on the presynaptic varicosity, opening Ca²⁺ channels without permitting significant Ca²⁺ entry. After 5-10 msec, the potential was stepped back to the holding potential of -70 mV for various lengths of time, producing a Ca²⁺ current as Ca²⁺ flowed in synchronously through all open Ca²⁺ channels (Figure 1). In the panels shown, the potential was held at -70 mV for 240 and 500 μsec before being stepped again to $+80$ mV or higher (the test pulse), terminating Ca²⁺ entry and imposing a large driving force

for K^+ through open K_{Ca} channels. At the same time, a postsynaptic patch electrode was used to monitor the release triggered by that fraction of the Ca^{2+} -tail current.

In order to compare the Ca^{2+} current, K_{Ca} current, and release, it was necessary to measure each accurately. This was done as shown in Figure 1 by blocking the K_{Ca} current selectively with ibertoxin (IbTX, **d**) and then subtracting **d** from **c**, yielding I_{KCa} (**e**). When the I_{Ca} was then blocked with ω -CgTX GVIA (**f**), the I_{Ca} (**g**) could be obtained by subtraction of **f** from **d**.

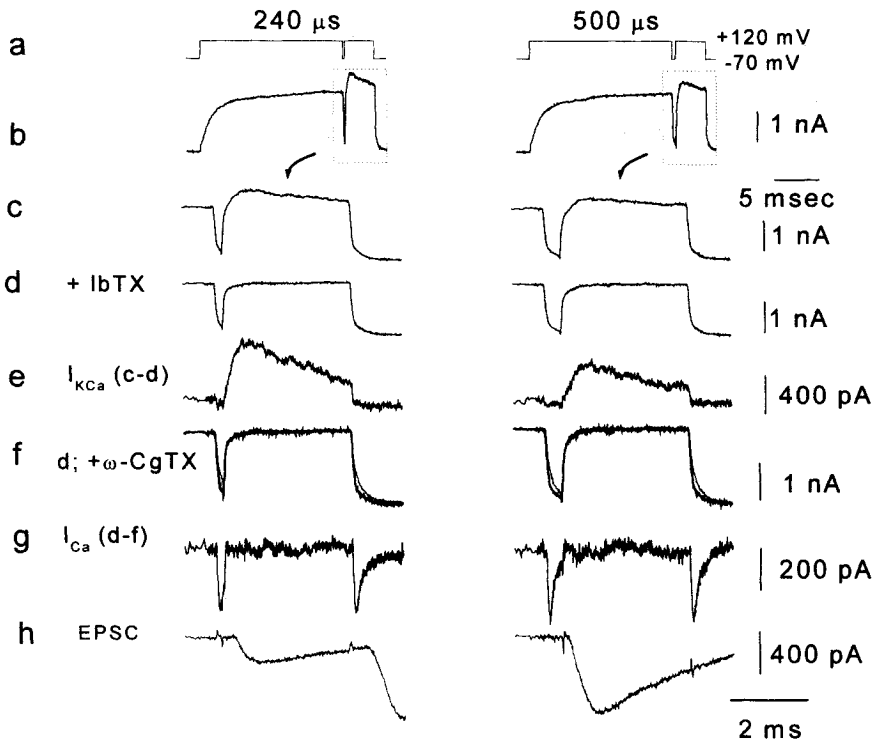


Figure 1. Experimental procedure for correlating I_{KCa} and release with I_{Ca} . A step depolarization to $\sim E_{Ca}$ (120 mV) was stepped back to -70 mV to produce a Ca^{2+} -tail current which was truncated after varying lengths of time (240 and 500 μ sec shown) by re-depolarization to $+120$ mV (the test pulse). The test pulse produced an I_{KCa} (**b** and **e**), which could be isolated (**e**) by subtracting records after block with IbTX (**d**) from those before (**c**). Further block of Ca^{2+} channels with ω -CgTX GVIA (**f**) and subtraction from (**d**) yielded the I_{Ca} (**g**). Note that release (**h**) was greater to 500 μ sec Ca^{2+} entry than to the 240 μ sec fraction of the tail current, whereas the I_{KCa} was larger to the 240 μ sec window of Ca^{2+} entry, in which the rate of Ca^{2+} entry was greater at the time of the test pulse. Modified from Yazejian *et al.*, 2000, *Nature Neuroscience*, 3:566-571 and reprinted with permission from Nature Neuroscience.

Note that with a 240 μ sec window of repolarization to -70 mV the truncated Ca^{2+} tail current yielded a larger I_{KCa} than the almost complete Ca^{2+} -tail current within a 500 μ sec window at -70 mV. The K_{Ca} channel open probability decreased as the rate of Ca^{2+} entry

decreased, even though more total Ca²⁺ had entered during the ensuing 250 μsec. Release, on the other hand, increased in proportion to the integral of I_{Ca}.

Figure 2 shows the time course of a representative Ca²⁺-tail current, plotted with the peak I_{KCa} that could be elicited as a function of the duration at -70 mV before stepping again to ~ E_{Ca} (mean of 6 experiments, normalized). Note that, on average, the peak elicitable I_{KCa} tracked the I_{Ca} quite closely. It increased with only a 20-35 μsec delay as I_{Ca} increased, peaked within 40 to 50 μsec of the peak I_{Ca}, and declined as I_{Ca} declined with a delay of no more than 100-200 μsec, even though Ca²⁺ continued to enter. Thus the I_{KCa} reflects the ambient [Ca²⁺]_{AZ} at the time of the second depolarizing step, or at most a few tens of μsec before. Release, on the other hand, integrates Ca²⁺ entry, at least on the time scale of a Ca²⁺-tail current. It is important to note that the graph does not show the time course of the I_{KCa} itself. Rather it is a plot of the peak amplitude of the I_{KCa} that could be elicited by the test pulse after each duration of Ca²⁺ entry.

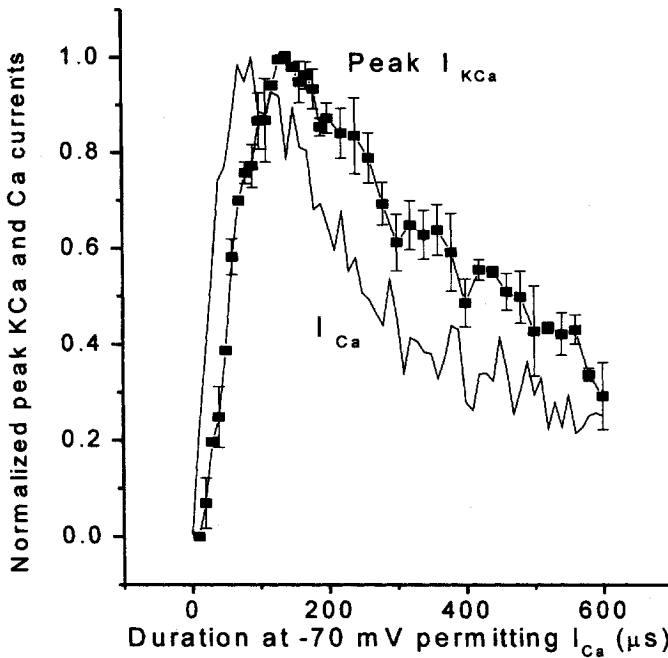


Figure 2. Comparison of time course of Ca²⁺-tail current and peak I_{KCa} that could be elicited by a large step depolarization at various times during the tail current. The representative I_{Ca} is from the experiment of Figure 1; the peak magnitude of the I_{KCa} that could be elicited by the test pulse, the mean of 6 experiments, is plotted against the duration of the time at -70 mV (fraction of the tail current permitted to enter). Modified from Yazejian *et al.*, 2000, *Nature Neuroscience*, 3:566-571 and reprinted with permission from Nature Neuroscience.

3.2. K_{Ca} Channel Properties and I_{KCa} Calibration

Our objective was to be able to quantify the absolute $[Ca^{2+}]$ at the AZ during waveforms such as Ca^{2+} tail currents or action potentials. Thus it was necessary to calibrate the K_{Ca} signals. In principle, this might be done by calibrating the percentage of K_{Ca} channels that open in response to a known $[Ca^{2+}]_i$ and membrane potential. However, it is not easy to know how many channels are present, and if a significant number are not at the AZ, even knowledge of the total number would be misleading. Thus another means of calibrating the Ca^{2+} -dependence of K_{Ca} channels was needed.

A careful study of K_{Ca} channels in this preparation shows that in most respects they resemble K_{Ca} channels studied in other preparations. They have a high conductance (mean 244 ± 5 pS) in 120 mM symmetrical K^+ , are highly selective for K^+ , and are blocked by charybotoxin and iberiotoxin (IbTX) (Figure 3). Single-channel properties could be maintained stably for periods of several minutes. The channels differed from K_{Ca} channels studied in other synaptic terminals (Bielefeldt and Jackson, 1993; Dopico *et al.*, 1999; Sun *et al.*, 1999) in showing a much lower Ca^{2+} affinity ($K_D \sim 7.7$ μM at +20 mV; Sun, Yazejian, and Grinnell, unpublished).

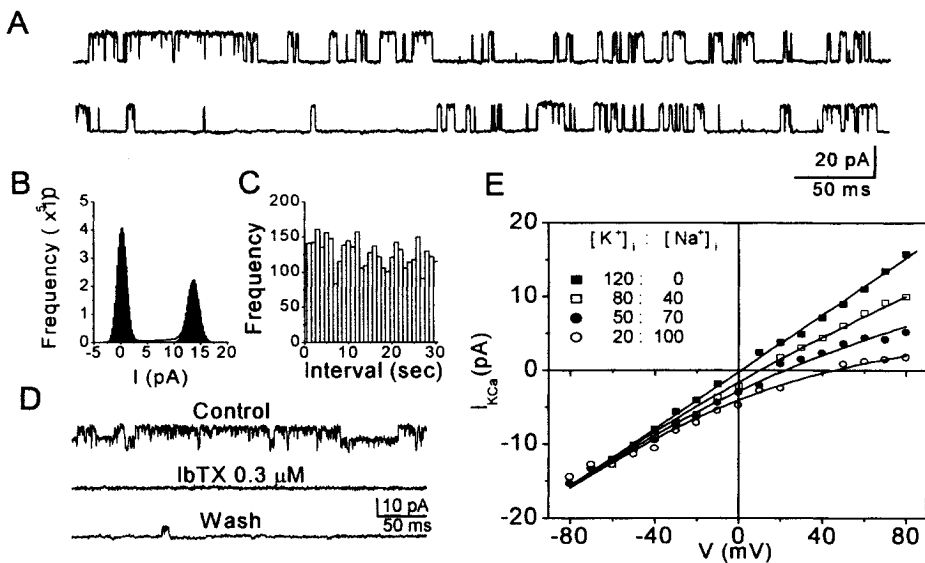


Figure 3. Characteristics of single K_{Ca} channels in the *Xenopus* varicosity synapses. **A:** traces showing sample single channel behavior in a detached patch at +60 mV and 5 μM $[Ca^{2+}]_i$, with symmetrical 120 mM K^+ across the membrane. **B:** Amplitude histogram for the channel in A. The mean channel conductance was 211 pS. **C:** Stability of the opening frequency of this channel over a period of 30 sec. **D:** Records for a different patch at 0 mV, with NFR in the patch pipette, 116 mM KCl on the inside surface, showing that IbTX irreversibly blocks the channel. **E:** Plot of I_{KCa} vs. membrane potential in symmetrical 120 mM K^+ , and as a function of K^+ : Na^+ concentration ratios ($n=6-8$ for each point.) The K_{Ca} channels are ~ 45 times more permeable to K^+ than to Na^+ .

Of greatest interest from the point of view of [Ca²⁺]_{AZ} measurement was the observation that, although the K_{Ca} channels opened over a wide range of [Ca²⁺]_i, from ~ 1 μM up, the time constant of activation differed systematically as a function of [Ca²⁺]_i. Indeed, we find that the most sensitive criterion of [Ca²⁺]_i is the K_{Ca} current activation time constant, which does not saturate even up to 100-200 μM.

Figure 4A includes sample traces showing the behavior of a single K_{Ca} channel in an isolated inside-out patch with 1, 5, 10, and 100 μM Ca²⁺ on the inside surface. In each case the patch, which was held initially at zero mV in symmetrical KCl solutions, was stepped from zero mV to -70 mV, causing open channels to close, and then stepped to +20 mV. Above the single traces are ensemble curves built up by averaging 200 traces at each [Ca²⁺]_i. The differences in activation time at those four Ca²⁺ concentrations are quite clear. At 1 μM, there was no channel opening. At 5 μM and higher concentrations, the channel eventually reached nearly full open state, but with very different rise times. When many such records were averaged at different Ca²⁺ concentrations and membrane potentials, the Ca²⁺-calibration curves of Figure 4B resulted. Over the broad range of voltages between +20 and +130 mV, K_{Ca} channel activation time constants were relatively insensitive to voltage, but highly sensitive to [Ca²⁺]_i. When these values were used to translate the time constants of activation of I_{KCa} evoked by Ca²⁺-tail currents into Ca²⁺ concentrations, data such as those shown in Figure 5 resulted.

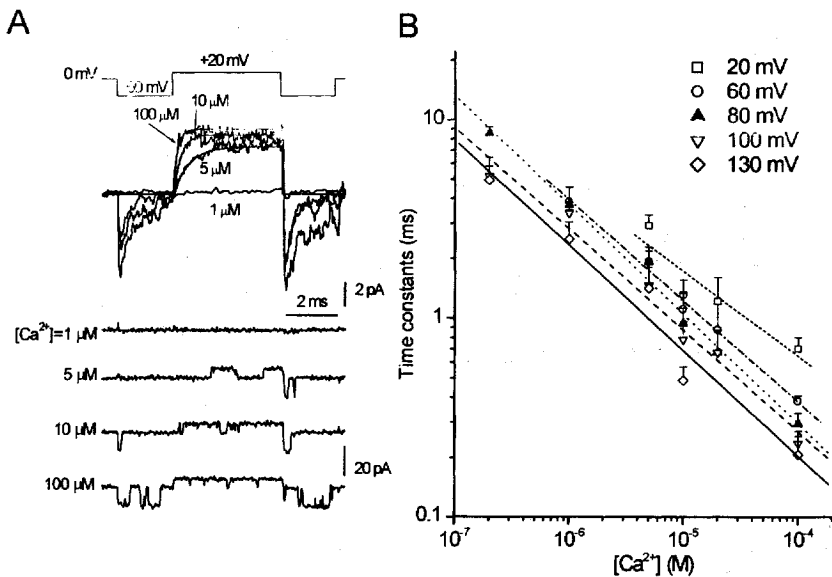


Figure 4. Calibration of Ca²⁺ sensitivity of K_{Ca} channels. A: Ensemble currents constructed from 200 traces like those shown below at 1, 5, 10, and 100 μM [Ca²⁺]_i in response to the waveform shown at the top. The patch, with a single K_{Ca} channel, was stepped from a holding potential of 0 mV to -60 mV, closing the K_{Ca} channel. A step to +20 mV then opened the channel with the activation kinetics shown for each concentration. B: Calibration curves derived from experiments like those of A, showing I_{KCa} activation time constants at different [Ca²⁺]_i and membrane potential (n = 3-11 for each point).

The calibration curves of Figure 4B were obtained for single channels studied with symmetrical K^+ -rich solutions across the membrane patch. This configuration, which is used routinely by virtually all investigators in the study of single K^+ channels, is highly artificial, and moreover involves loss of the normal soluble cytoplasmic components of the terminal. Consequently, we have sought also to calibrate K_{Ca} channel behavior in the more intact terminal. We have done this by characterizing single K_{Ca} channels in cell-attached configuration with normal frog Ringer in the patch pipette and Ca^{2+} entering only through the Ca^{2+} channels in the patch (no Ca^{2+} in the bathing Ringer), then detaching the patch and measuring time constants of activation with known $[Ca^{2+}]_i$ in a KCl solution facing the inside surface. Analysis of activation time constants of channels in such isolated patches, with normal frog Ringer (containing 1.8 mM Ca^{2+}) in the patch pipette and zero Ca^{2+} Ringer outside the rest of the cell, yielded calibrated curves very close to those of Figure 4B. Moreover, if one factors in a minimal delay for activation of the Ca^{2+} channels necessary for Ca^{2+} entry, ensembled K_{Ca} channel currents from channels recorded in the on-cell configuration, before patch excision, suggested that $[Ca^{2+}]_i$ can reach levels of at least as high as 100 μM during depolarizations to +20 to +40 mV (Sun and Grinnell, unpublished). Interestingly, both L-type and N-type Ca^{2+} channels can trigger release in this preparation, but their mean time constants of activation are quite different: 0.46 msec for L-type and 1.44 msec for N-type, at +20 mV (Sand *et al.*, 2001).

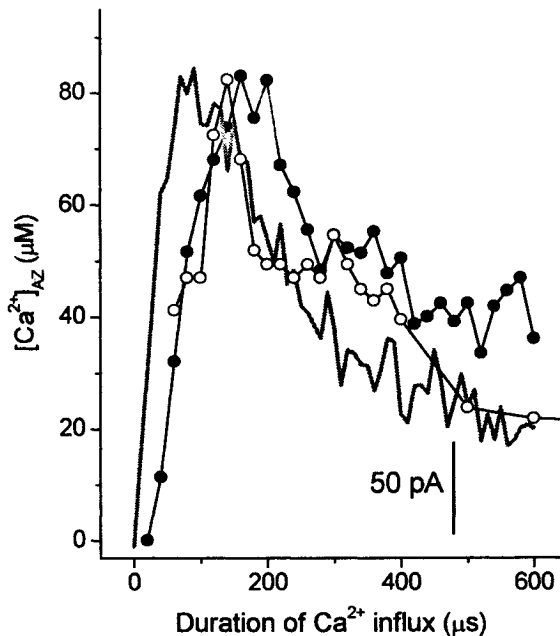


Figure 5. $[Ca^{2+}]_{AZ}$ as a function of rate of Ca^{2+} influx during a Ca^{2+} -tail current. The time course and amplitude of a typical Ca^{2+} -tail current (gray, from Figure 1) are shown along with the $[Ca^{2+}]_{AZ}$ derived from I_{KCa} activation time constants in two representative experiments (solid dots from data of Figure 1).

Thus the results of calibration of I_{KCa} activation time constants under these different conditions were consistent with each other and with the conclusion that K_{Ca} channels at the AZ see Ca²⁺ concentrations approaching 100 μM during Ca²⁺-tail currents. The [Ca²⁺]_{AZ} during an action potential waveform is larger still, revealing a peak, at the site of K_{Ca} channels, of up to ~ 175 μM (Yazejian *et al.*, 2000).

3.3. Titration of [Ca²⁺]_{AZ} for Study of Release

The K_{Ca} channels in the *Xenopus* motoneuron varicosities are ideally suited to allow a careful, quantitative analysis of the release-triggering effectiveness of different Ca²⁺ concentrations for different lengths of time. By altering the Ca²⁺-driving force, it is possible to titrate [Ca²⁺]_{AZ} over a wide range. Figure 6 shows the range of [Ca²⁺]_{AZ} that was obtained and maintained for periods of several msec in a representative experiment - from approximately 1 μM to nearly 200 μM.

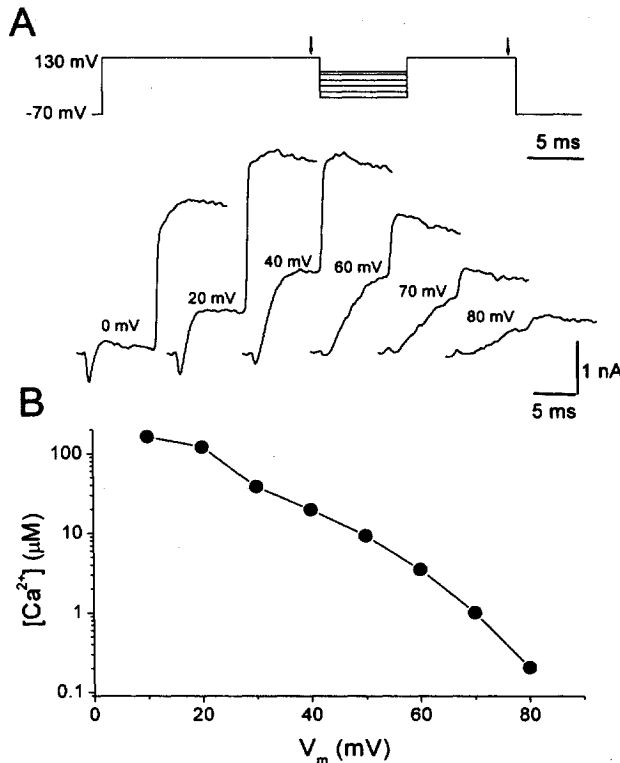


Figure 6. Titration of [Ca²⁺]_{AZ} by varying Ca²⁺-driving force. A: Ca²⁺ channels were opened by depolarization to +130 mV; then the potential was stepped back to different intermediate potentials between 0 and +80 mV, with different driving force for both Ca²⁺ and K⁺ at each potential. After 8 msec, the potential was again stepped to +130 mV, terminating Ca²⁺ entry and imposing a large uniform driving force for K⁺. Below are whole-cell K_{Ca} currents generated by this waveform, when the intermediate potential was the value shown. These traces (each the average of 3) show the portion of the response between the arrows, obtained by subtraction of records after IBTX block from those before. B: Calculated [Ca²⁺]_{AZ} at each intermediate potential, determined by the activation time constant of the I_{KCa}.

In the stimulus the varicosity was depolarized to +130 mV for several msec to open a maximum number of Ca^{2+} channels. Then the terminal was repolarized for 8 msec to different intermediate potentials between +40 and -40 mV, allowing Ca^{2+} entry with different driving force, generating K_{Ca} currents in proportion to the $[\text{Ca}^{2+}]_{\text{AZ}}$ and potential. Repolarization to +130 mV terminated Ca^{2+} entry, but added a uniform driving force for K^+ through all open K_{Ca} channels at that time. Experiments of this sort show that in this preparation 100-200 μsec exposure to $[\text{Ca}^{2+}]_{\text{AZ}}$ of 50 μM is sufficient to evoke substantial release, while at 20-30 μM $[\text{Ca}^{2+}]_{\text{AZ}}$, integration over a period of 0.5 – 1 msec may be required to evoke any release (Yazejian *et al.*, 2000 and unpublished).

4. DISCUSSION

If one accepts that the K_{Ca} channels are seeing at least 100 μM $[\text{Ca}^{2+}]_{\text{AZ}}$, it is possible to estimate the effective distance of the K_{Ca} channels from open Ca^{2+} channels. With standard models of Ca^{2+} diffusion from an array of open Ca^{2+} channels, and employing widely used values for Ca^{2+} -channel current, Ca^{2+} -diffusion constant, and amounts and properties of local fixed and mobile Ca^{2+} -buffering molecules (Roberts, 1994; DiGregorio *et al.*, 1999; Hille, 1992), it can be calculated that K_{Ca} channels, on average, must be no more than 8 nm from a single open Ca^{2+} channel or 20 nm from an equidistant array of four (Yazejian *et al.*, 2000). Consistent with this estimate is the observation that 5 mM EGTA introduced into the terminal via a patch pipette on the soma has no effect on release (or may even increase it, perhaps due to washout of endogenous buffer), while 2 mM BAPTA, a much faster binding Ca^{2+} buffer with approximately the same Ca^{2+} binding affinity as EGTA, severely reduces release (X.-P. Sun and A.D. Grinnell, unpublished). Thus K_{Ca} channels are closely localized with Ca^{2+} channels, do not saturate over the range of $[\text{Ca}^{2+}]_{\text{AZ}}$ expressed during different forms of activation, bind/unbind Ca^{2+} rapidly enough to track changes in $[\text{Ca}^{2+}]_{\text{AZ}}$ during Ca^{2+} transients, and show activation kinetics sufficiently fast to play a functional role in transmitter release. The nature of that functional role requires further investigation. K_{Ca} channels clearly are not necessary for neurotransmitter release, since many varicosity synapses do not have a detectable I_{KCa} , yet show good release. The extent of their expression may be a function of the developmental stage of the synapse. K_{Ca} currents tend to be more prominent in synaptic varicosities in two- and three-day cultures than in one-day cultures. However, the correlation is not strong, and K_{Ca} currents can be found even in non-synaptic varicosities of one-day cultures. Alternatively, there may be sub-categories of motoneurons that express, or do not express, K_{Ca} channels. Curiously, in contrast to their role in mature frog neuromuscular junctions (Robitaille and Charlton, 1992; Robitaille *et al.*, 1993) and many other synapses (Storm, 1987; Roberts *et al.*, 1990; Sah, 1996), where they truncate release by accelerating repolarization, in the *Xenopus* varicosities these channels appear to enhance release (Pattillo *et al.*, 2001).

5. ACKNOWLEDGMENTS

We thank Dr. Art Peskoff for his mathematical/modeling expertise, and Brad Smith for many helpful discussions and unfailing technical assistance. Supported by grants from NIH and NSF.

6. REFERENCES

- Andreu, R. and Barrett, E.F., 1980, Calcium dependence of evoked transmitter release at very low quantal contents at the frog neuromuscular junction. *Journal of Physiology*, **308**: 79-97.
- Armstrong, D. and Eckert, R., 1987, Voltage-activated calcium channels that must be phosphorylated to respond to membrane depolarization. *Proceedings of the National Academy of Sciences USA*, **84**: 2518-2522.
- Art, J.J., Wu, Y.-C. and Fettiplace, R., 1995, The calcium-activated potassium channels of turtle hair cells, *Journal of General Physiology*, **105**: 49-72.
- Bielefeldt, K. and Jackson, M.B., 1993, A calcium-activated potassium channel causes frequency-dependent action-potential failures in a mammalian nerve terminal. *Journal of Neurophysiology*, **70**: 284-298.
- Blundon, J.A., Wright, S.N., Brodwick, M.S., and Bittner, G.D., 1993, Residual free calcium is not responsible for facilitation of neurotransmitter release. *Proceedings of the National Academy of Sciences USA*, **90**:9388-9392.
- Blundon, J.A., Wright, S.N., Brodwick, M.S., and Bittner, G.D., 1995, Presynaptic calcium-activated potassium channels and calcium channels at a crayfish neuromuscular junction. *Journal of Neurophysiology*, **73**:178-189.
- Burrone, J., Neves, G., Gomis, A., Cooke, A., and Lagnado, L., 2002, Endogenous calcium buffers regulate fast exocytosis in the synaptic terminal of retinal bipolar cells. *Neuron*, **3**:33(1): 101-12.
- Couteaux, R. and Pécot-Dechavassine, M., 1970, Vésicules synaptiques et poches au niveau des zones actives de la jonction neuromusculaire. *C.R. Academy of Science (Paris)*, **271**: 2346-2349 (in French).
- DiGregorio, D. A. and Vergara, J. L., 1997, Localized detection of action potential-induced presynaptic calcium transients at a *Xenopus* neuromuscular junction. *Journal of Physiology*, **505.3**: 585-592.
- DiGregorio, D.A., Peskoff, A., and Vergara, J.L., 1999, Measurement of action potential-induced presynaptic calcium domains at a cultured neuromuscular junction. *Journal of Neuroscience*, **19**: 7846-7859.
- Dopico, A.M., Widmer, H., Wang, G., Lemos, J.R. and Treisman, S.N., 1999, Rat supraoptic magnocellular neurones show distinct large conductance, Ca²⁺-activated K⁺ channel subtypes in cell bodies versus nerve endings. *Journal of Physiology*, **519**: Pt 1, 101-114.
- Harlow, M.L., Ress, D., Stoschek, A., Marshall, R.M., and McMahan, U.J., 2001, The architecture of active zone material at the frog's neuromuscular junction. *Nature*, **409**: 479-84.
- Hille, B., 1992, *Ionic Channels of Excitable Membranes*, Sinauer, Sunderland, Massachusetts, 2nd edition, pp. 83-114.
- Horn, R. and Marty, A., 1988, Muscarinic activation of ionic currents measured by a new whole-cell recording method. *Journal of General Physiology*, **92**: 145-159
- Hudspeth, A.J. and Lewis, R.S., 1988, Kinetic analysis of voltage- and ion-dependent conductances in saccular hair cells of the bullfrog, *Rana catesbeiana*. *Journal of Physiology*, **400**: 237-274.
- Klingauf, J. and Neher, E., 1997, Modeling buffered Ca²⁺ diffusion near the membrane: implications for secretion in neuroendocrine cells. *Biophysical Journal*, **72**: 674-690.
- Llinás, R.R., Sugimori, M., and Silver, R.B., 1995, The concept of calcium concentration microdomains in synaptic transmission. *Neuropharmacology*, **34**: 1443-1451.
- Meir, A., Ginsburg, S., Butkevich, A., Kachalsky, S.G., Kaiserman, I., Ahdut, R., Demigoren, S., and Rahamimoff, R., 1999, Ion channels in presynaptic nerve terminals and control of transmitter release. *Physiological Reviews*, **79**: 1019-1088.
- Nieuwkoop, P.D. and Faber, J., 1967, *Normal table of Xenopus laevis*. 2nd Edition Amsterdam: North Holland.
- Pattillo, J.M., Yazejian, B., DiGregorio, D.A., Vergara, J.L., Grinnell, A.D., and Meriney, S.D., 2001, Contribution of presynaptic calcium-activated potassium currents to transmitter release regulation in cultured *Xenopus* nerve-muscle synapses. *Neuroscience*, **102**: 229-240.
- Pumplin, D. W., Reese, T. S. and Llinás, R., 1981, Are the presynaptic membrane particles the calcium channels? *Proceedings of the National Academy of Sciences USA*, **78**: 7210-7213.

- Rae, J., Cooper, K., Gates, P., and Warsky, M., 1991, Low access resistance perforated patch recordings using amphotericin B. *Journal of Neuroscience Methods*, **37**: 15-26.
- Roberts, W.M., 1993, Spatial calcium buffering in saccular hair cells. *Nature*, **363**: 74-76.
- Roberts, W.M., 1994, Localization of calcium signals by a mobile calcium buffer in frog saccular hair cells. *Journal of Neuroscience*, **14**(5): 3246-3262.
- Roberts, W.M., Jacobs, R.A., and Hudspeth, A.J., 1990, Co-localization of ion channels involved in frequency selectivity and synaptic transmission at presynaptic active zones of hair cells. *Journal of Neuroscience*, **10**: 3664-3684.
- Robitaille, R. and Charlton, M.P., 1992, Presynaptic calcium signals and transmitter release are modulated by calcium-activated potassium channels. *Journal of Neuroscience*, **12**: 297-305.
- Robitaille, R., Garcia, M.L., Kaczorowski, G.J., and Charlton, M.P., 1993, Functional co-localization of calcium and calcium-gated potassium channels in control of transmitter release. *Neuron*, **11**: 645-655.
- Sabatini, B.L. and Regehr, W.G., 1996, Timing of neurotransmission at fast synapse in the mammalian brain. *Nature*, **384**: 170-172.
- Sah, P., 1996, Ca²⁺-activated K⁺ currents in neurones: types, physiological roles and modulation. *Trends in Neuroscience*, **19**: 150-154.
- Sakaba, T., Ishikane, H., and Tachibana, M., 1997, Ca²⁺-activated K⁺ current at presynaptic terminals of goldfish retinal bipolar cells. *Neuroscience Research*, **27**: 219-228.
- Sand, O., Chen, B.-M., and Grinnell, A.D., 2001, Contribution of L-type Ca²⁺ channels to evoked transmitter release in cultured *Xenopus* nerve-muscle synapses. *Journal of Physiology*, **536**: 21-33.
- Sheng, M., Tsaur, M.L., Jan, Y.N., and Jan, L.Y., 1994, Contrasting sub-cellular localization of the Kv1.2 K⁺ channel subunit in different neurons of rat brain. *Journal of Neuroscience*, **14**: 2408-2417.
- Simon, S.M. and Llinás, R.R., 1985, Compartmentalization of the sub-membrane calcium activity during calcium influx and its significance in transmitter release. *Biophysical Journal*, **48**: 485-498.
- Storm, J.F., 1987, Action potential depolarization and a fast after-hyperpolarization in rat hippocampal pyramidal cells. *Journal of Physiology*, **385**: 733-759.
- Sugihara, I., 1994, Calcium-activated potassium channels in goldfish hair cells. *Journal of Physiology*, **476**: 373-390.
- Sun, X.-P., Schlichter, L.C., and Stanley, E.F., 1999, Single-channel properties of BK-type calcium-activated potassium channels at a cholinergic presynaptic nerve terminal. *Journal of Physiology*, **518**: 639-651.
- Yazajian, B., DiGregorio, D., Vergara, J.L., Poage, R., Meriney, S.D., and Grinnell, A.D., 1997, Direct measurements of presynaptic calcium and calcium-activated potassium currents regulating neurotransmitter release at cultured *Xenopus* nerve-muscle synapses. *Journal of Neuroscience*, **17**: 2990-3001.
- Yazajian, B.M., Sun, X.-P., and Grinnell, A.D., 2000, Tracking presynaptic Ca²⁺ dynamics during neurotransmitter release with Ca²⁺-activated K⁺ channels. *Nature Neuroscience*, **3**: 566-571.
- Zucker, R.S. and Fogelson, A.L., 1986, Relationship between transmitter release and presynaptic calcium influx when calcium enters through discrete channels. *Proceedings of the National Academy of Sciences USA*, **83**: 3032-3036.
- Zucker, R.S., 1996, Exocytosis: a molecular and physiological perspective. *Neuron* **17**: 1049-1055.

FINE TUNING OF EXCITABILITY BY K_{Ca} CHANNELS IN MUDPUPPY PARASYMPATHETIC NEURONS

Fabiana S. Scornik^{1*}

1. INTRODUCTION

Mudpuppy parasympathetic cardiac neurons generate spontaneous miniature outward currents (SMOCs) that result from the simultaneous activation of large conductance calcium activated (K_{Ca}) channels by Ca^{2+} released from caffeine- and ryanodine-sensitive intracellular stores (Satin and Adams 1987; Merriam *et al.*, 1999; Scornik *et al.*, 2001).

The present article summarizes recent findings on SMOC regulation and on the role of these currents on action potential (AP) generation. The data presented in this article suggest that spatial distribution determines differential roles of K_{Ca} channels, in the generation and repolarization of AP in parasympathetic neurons from the mudpuppy cardiac ganglia.

Parasympathetic cardiac neurons, like other autonomic neurons, express a number of different voltage- and ligand-gated potassium channels in their plasma membranes that are important determinants of membrane potential and neuronal excitability (Brown 1988; Rudy 1988; Adams and Harper 1995). Among these different potassium conductances, K_{Ca} channels have been shown particularly, to play a key role in determining resting membrane potential, action potential repolarization and post action potential hyperpolarizations (Rudy 1988; Kaczorowski *et al.*, 1996; Sah 1996).

Activation of K_{Ca} channels is very dynamic because it is gated by elevation of the Ca^{2+} concentration at the intracellular side of the channel. Very localized elevations of Ca^{2+} , which do not significantly elevate global intracellular Ca^{2+} , can activate K_{Ca} channels. Thus, physiological activation of K_{Ca} channels may be coupled to highly localized changes of cell Ca^{2+} .

Although spontaneous miniature outward currents (SMOCs) were described in neurons over two decades ago, their physiological role remained unclear.

¹ Masonic Medical Research Laboratory, 2150 Bleecker St. Utica, NY 13501, USA

* corresponding author fscornik@mml.edu

The first evidence for these spontaneous changes in membrane activity was presented in 1977 by Hartzell *et al.* These authors reported the presence of spontaneous hyperpolarizations in the parasympathetic cardiac ganglion of the mudpuppy. The observed hyperpolarizations were sensitive to membrane potential, being smaller at voltages closer to E_K . Later, Mathers and Barker (1981) described spontaneous fluctuations in membrane activity in both, I_{clamp} (hyperpolarizations) and V_{clamp} (outward currents) in mouse DRG neurons. These spontaneous currents were sensitive to TEA and to calcium changes in the external solution. Satin and Adams (1987) reported a detailed study of SMOCs from cultured bullfrog sympathetic neurons and acutely dissociated neurons from the mudpuppy cardiac ganglion. In this study, the authors proposed that SMOCs resulted from the activation of a calcium sensitive potassium conductance by calcium released from the endoplasmic reticulum. They hypothesized that membrane depolarization was coupled to calcium release from the stores but, because they observed SMOCs in the presence of $100 \mu\text{M Cd}^{2+}$ in the external solution, they did not correlate this membrane potential modulation with calcium influx. The involvement of K_{Ca} channels in SMOCs was also proposed for presynaptic nerve terminals in the chick ciliary ganglion since spontaneous hyperpolarizations in this preparation, were inhibited by TEA and Ba^{2+} and activated by caffeine (Fletcher and Chiappinelli, 1992). Recent studies of SMOCs in a mammalian preparation showed that calcium release from internal stores could also activate spontaneous outward currents through small conductance calcium dependent potassium channels (SK) (Arima *et al.*, 2001).

The data presented in this article, summarizes the most recent findings on SMOC regulation, from the single channel level to their role in membrane excitability (Merriam *et al.*, 1999; Scornik *et al.*, 2001; Parsons *et al.*, 2002).

2. RESULTS

2.1. Basic Characteristics of SMOCs and K_{Ca} Channels Underlying SMOCs

Whole cell voltage clamp recordings from parasympathetic mudpuppy's neurons, evidence spontaneous, fast outward deflections of the current that remain constant at each given holding potential (Merriam *et al.*, 1999). In the presence of $200 \mu\text{M Cd}^{2+}$ in the bath solution, SMOC spike-like activity decreases quickly, but it is maintained for prolonged periods at a greatly reduced frequency (Figure 1A). Under these conditions, it is possible to resolve individual events to find the fast onset and a slower decay signal that characterizes SMOCs. The amplitude and decay time of these signals are voltage-dependent, both increasing at positive holding potentials (Figure 1B). SMOC frequency is also voltage dependent; its current-voltage relationship is bell-shaped with the maximum frequency occurring near -10 mV (Figure 1C).

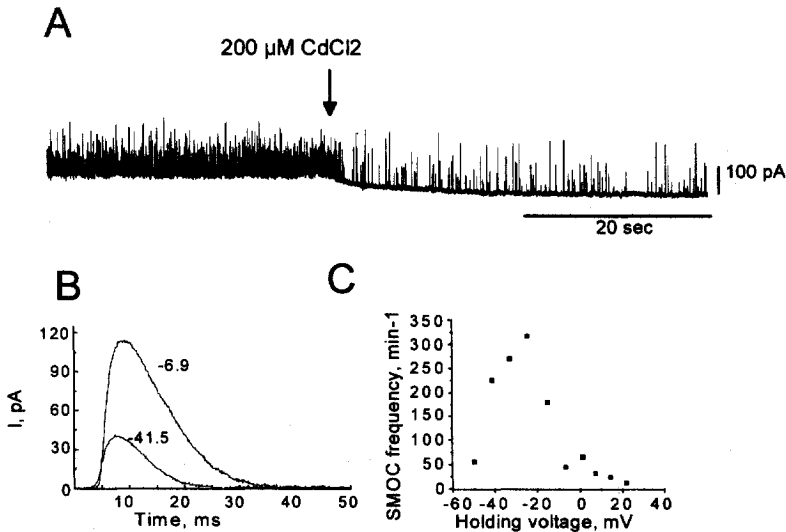


Figure 1. Basic characteristics of SMOCs. Whole cell currents studied in the absence and after addition of cadmium. **A:** Example of a continuous recording of SMOCs showing typical spike-like activity. Frequency of SMOCs decreases upon addition of 200 μM CdCl₂ to the bath (arrow). $V_h = -10$ mV. **B:** SMOCs recorded at two different holding potentials plotted in an expanded scale to show SMOC kinetics. **C:** voltage dependence of SMOC frequency in the presence of 200 μM CdCl₂.

Different pharmacological studies of SMOCs, in mudpuppy parasympathetic neurons, have shown that these currents result from the activation of clusters of K_{Ca} channels (Satin and Adams, 1987; Merriam et al, 1999). The reported number of channels involved in these clusters varied in a wide range from a few to many thousands of channels (Satin and Adams 1987; Fletcher and Chiappinelli 1992). Recently, it was established that an average SMOC involves the simultaneous activation of 18 to 23 channels with an opening probability approaching the unit (Scornik et al, 2001). This calculation comes from analyzing the ratio between the average peak amplitude of SMOCs and the amplitude of the single channels. Current-voltage relationship for both, SMOCs recorded in whole cell configuration, and K_{Ca} single channel current recorded in a cell attached patch, in the same external solution are shown in Figure 2. *NPo* values, obtained from the ratio between average peak amplitude of SMOCs and single channel values, do not change appreciably over the voltage range from -20 to +37 mV, ranging from 16 at -20 mV to 18 at +37 mV. The apparent insensitivity to membrane voltage suggests that the rise in Ca²⁺ concentration near the channel, during a SMOC, must approach values that shift the voltage activation curve close to saturation in this voltage range. For K_{Ca} channels from mudpuppy parasympathetic neurons, this value must be above 40 μM (Scornik *et al.*, 2001).

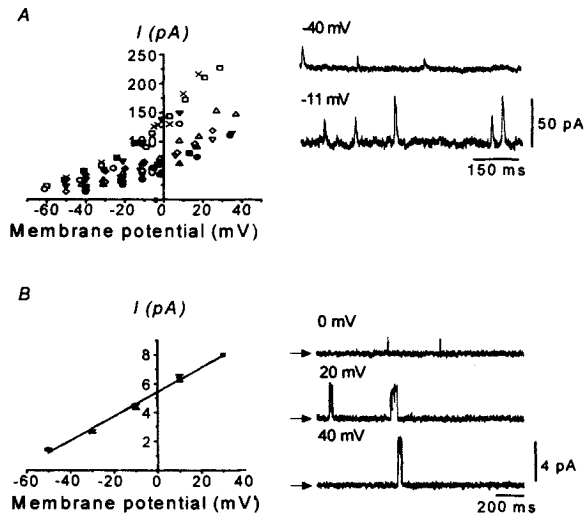


Figure 2. Current-Voltage relationship of SMOCs (A) and single K_{Ca} channels (B) studied in perforated whole cell and cell attached patch, respectively, using the same ionic composition for the bath solution. Arrows in B mark the close state of the channel.

2.2. SMOCs are Triggered by Calcium Released From Internal Stores

Cytoplasmic Ca^{2+} concentration is generally maintained at very low levels. However, Ca^{2+} levels can be elevated locally for a brief period following Ca^{2+} influx or following Ca^{2+} release from internal stores. Neurons, like most cell types, exhibit IP_3 - or ryanodine and caffeine-sensitive Ca^{2+} pools that are involved in the release of Ca^{2+} from intracellular stores (Berridge 1993; Verkhratsky and Shmigol 1996; Henzi and MacDermott 1992; Kuba 1994). It has been hypothesized for neurons that the release of Ca^{2+} from ryanodine-sensitive stores may amplify and prolong intracellular Ca^{2+} signaling by the process of Ca^{2+} induced Ca^{2+} release (CICR) (Hua *et al.*, 1993).

Merriam *et al.*, (1999) demonstrated that, in mudpuppy neurons, SMOCs are generated by the release of intracellular calcium from ryanodine and caffeine sensitive stores.

Caffeine stimulates Ca^{2+} release from ryanodine-sensitive internal Ca^{2+} stores by sensitizing the release receptor to Ca^{2+} . In cells voltage-clamped to membrane potentials between -10 and +10 mV, addition of 2- 3 mM caffeine to the bath solution increases the frequency of SMOCs without affecting their amplitude (Merriam *et al.*, 1999). The increase in SMOC activity is exemplified in Figure 3A. Because SMOCs result from the activation of K_{Ca} channels, it would be expected that in cell-attached patch, addition of caffeine to the bath, induced activation of single K_{Ca} channels. The increase of single K_{Ca} channel activity in cell attached patches of mudpuppy parasympathetic neurons was reported by Scornik *et al.* (2001), and is shown in 3B. In some patches, single channel activity increases homogeneously. Nevertheless, addition of caffeine to the bath solution may cause clustered activation of K_{Ca} channels in the patch (Figure 3B, bottom trace).

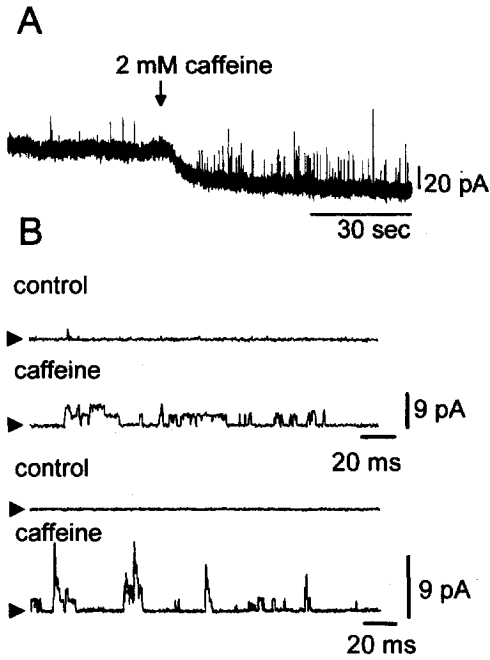


Figure 3. Effect of caffeine on K_{Ca} channels underlying SMOCs. **A:** addition of 2 mM caffeine to the bath (arrow) increases SMOC frequency. V_h = 0 mV. **B:** Single channel activity from 2 different cell attached patch recordings. 3 mM caffeine increases single channel activity homogeneously (upper two traces, V_h = -30 mV) or by inducing burst of activities (lower two traces, V_h = -40). Arrows in B mark the close state of the channel.

A different approach to studying the role of calcium released from internal stores in SMOC generation is the use of Ca-ATPase inhibitors such as cyclopiazonic acid (CPA) or thapsigargin. In the presence of these inhibitors, the refill of calcium stores is impaired and the stores get eventually empty of releasable calcium.

The decrease of SMOC activity caused by addition of CPA to the bath solution is shown in Figure 4. In this type of experiment, SMOCs were recorded at a constant voltage before and after addition of CPA to the bath solution. In this condition, the frequency of SMOCs decreases gradually to get almost vanished after 18 minutes of exposure to the drug (Merriam *et al.*, 1999). Merriam *et al.* (1999) demonstrated that, in mudpuppy neurons held a constant voltage, high concentrations of caffeine, provoke a large outward K_{Ca} current. In control conditions, the same large outward current is observed upon subsequent applications of 30 mM caffeine to the bath. When caffeine is added to the bath together with CPA, a first large outward current occurs. However, after washing out caffeine with a CPA containing solution, a second application of caffeine is unable to produce any large outward current indicating that intracellular calcium pools are exhausted. It was also shown in this study that SMOC activity disappears, and it is not recovered for all the time that CPA is present in the bath.

This observation demonstrates that SMOCs do not occur when intracellular stores are empty of releasable calcium.

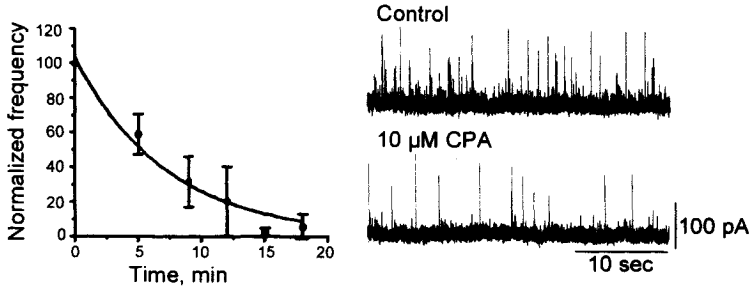


Figure 4. CPA-induced depletion of intracellular stores decreases SMOC frequency. Plot shows SMOC frequency measured at different times upon addition of 10 μM CPA to the bath solution. Records on the right are examples of SMOC activity before and after addition of CPA. $V_h = -10$ mV.

2.3. Calcium Influx Modulates SMOC Activity

The fact that SMOC frequency is diminished in the presence of CdCl_2 indicates that calcium influx affects SMOC activation. Although CdCl_2 inhibits most of the voltage dependent calcium current, little remaining calcium channel activity would be sufficient for triggering membrane localized events. The demonstration of the role of calcium influx on SMOC activity was done by studying SMOCs in the absence of calcium in the bath solution (Merriam et al, 1999), as illustrated in Fig. 5. This figure shows SMOCs recorded at a constant voltage, in a normal bath solution (3.6 mM CaCl_2), and after replacement by a solution without CaCl_2 (arrow in Fig. 5). It is clear that SMOC activity dramatically decreases after exposing the cell to the 0 calcium solution. In addition, Merriam *et al.*, (1999) demonstrated that SMOC activity diminishes considerably in the presence of the N-type calcium channel blocker, ω -conotoxin GVIA, which blocks most of the total calcium current in mudpuppy parasympathetic neurons (Merriam and Parsons, 1995). On the other hand, the L-type channel blocker, nifedipine, which blocks only 10-15% of the total calcium current in these cells (Merriam and Parsons, 1995), slightly affects SMOC activity (Merriam et al, 1999).

Interestingly, when SMOCs are inhibited by either, replacing the bath with a free calcium solution, or by block of N-type channels, channel activity can be recovered by addition of 2-3 mM caffeine to the external solution. In addition, SMOCs can be abolished by the fast calcium chelator BAPTA added to the bath solution in its AM form. Again, SMOC activity is recovered upon subsequent addition of 3 mM caffeine to the bath (Figure 5), suggesting that although BAPTA is fast enough to interrupt the CICR process, it is not sufficient to interfere with the activation of K_{Ca} channels by calcium release from the intracellular stores.

The results presented in the previous sections demonstrate that both, calcium influx through voltage activated calcium channels and calcium release from internal stores affect SMOCs. Recovery of SMOC activity after addition of caffeine makes clear that

calcium release from internal stores can generate SMOCs, even in the absence of calcium influx. However, calcium influx alone is not sufficient to trigger SMOCs if the internal stores are empty (Merriam *et al.*, 1999).

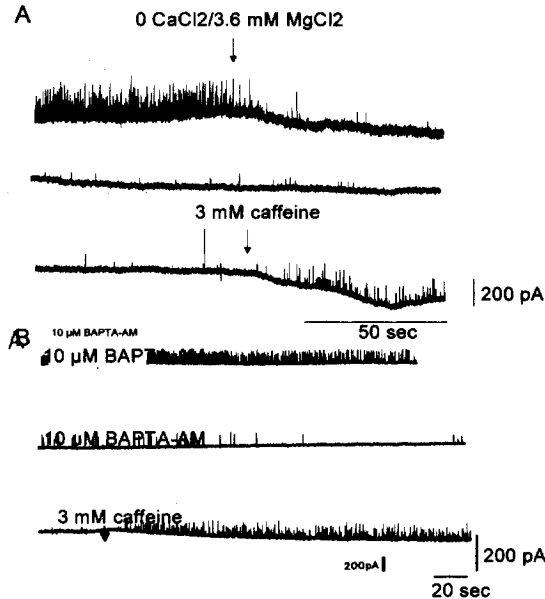


Figure 5. Calcium influx modulates SMOC activity. **A:** Continuous recording, at -10 mV, of SMOC activity before and after replacement of normal calcium containing solution by a 0 calcium solution (arrow), and after subsequent addition of 3 mM caffeine to the 0 calcium solution. **B:** Continuous recording, at -10 mV, of SMOC activity in the presence of BAPTA-AM in the bath solution, SMOC activity starts decreasing within 3 minutes after addition of BAPTA to the bath. Middle trace shows SMOC activity 20 minutes after addition of BAPTA-AM to the bath. Bottom trace shows recovery of activity upon addition of 3 mM caffeine, 30 minutes after BAPTA-AM was added to the bath.

2.4. Physiological Role of SMOCs in Mudpuppy Parasympathetic Neurons

Because K_{Ca} channel activation plays an important role in AP repolarization (Adams and Harper, 1995; Clark *et al.*, 1990), it would be possible that SMOCs also played a role in this face of the AP. However, the maximum frequency of SMOCs, from mudpuppy parasympathetic neurons, was observed at voltages near the threshold for spike generation. This opened the question of whether SMOCs played a role on setting off the AP in parasympathetic mudpuppy neurons.

Since SMOCs result from the opening of K_{Ca} channels induced by CICR, the physiological role of SMOCs on AP repolarization and generation should be evidenced by blocking of K_{Ca} channels directly, or by interfering with the CICR process.

These types of experiments are exemplified in figure 6 and table 1. Figure 6 shows the voltage response to the application of a ramp of current to a mudpuppy neuron with a resting potential of near -55 mV. It is evident, in the control trace, that when membrane

voltage approaches -20 mV, hyperpolarizing deflections, resembling SMHs become apparent and only a couple of action potentials appear at the end of the ramp.

Interestingly, when iberiotoxin is added to the bath solution, the small hyperpolarizations disappear and APs start earlier on the time course of the ramp. In contrast, when nifedipine, is added to the bath solution, the hyperpolarizations are still marked and the latency to the first action potential in the presence of the drug remains the same as in the control (lower trace).

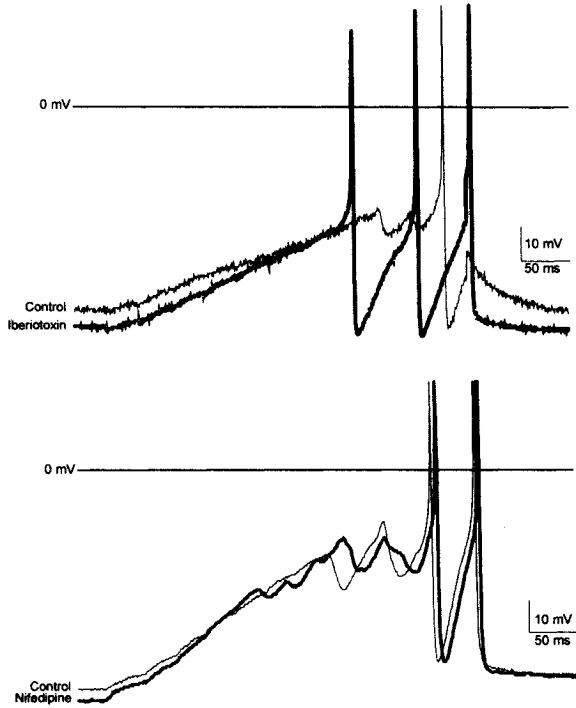


Figure 6. Lock of K_{Ca} channels changes the latency to action potential generation. Voltage response to a 400 msec depolarizing current ramp before, and after addition of iberiotoxin (upper traces), or nifedipine (lower traces). Thin trace represents voltage response to the current ramp in control conditions and thick trace shows response to the ramp after treatment.

Table 1 summarizes the experimental results of the effect of different pharmacological agents on AP duration, maximum rate of fall (MRF) and latency to AP (Scornik et al, 2001a, Parsons *et al.*, in press). A striking point from the table is that block of K_{Ca} channels by the specific channel blocker, iberiotoxin, affects both, AP properties and firing latency. However, inhibition of calcium release from internal stores by thapsigargin decreases the latency to the first AP without affecting the AP properties.

In addition, the results reported in Table 1 show that although calcium influx through L- and N-type calcium channels affects AP characteristics, only calcium influx through N-type calcium channels, which were shown to inhibit SMOCs, produces a change of the latency to the first AP. This evidence indicates that, in parasympathetic mudpuppy neurons, K_{Ca} channels activated by calcium release from internal stores modulate the initiation of APs, while K_{Ca} channels activated directly by calcium influx through voltage activated calcium channels, affect the repolarization face of the AP.

Table 1. Effect of channel blockers and calcium release inhibitors on AP duration, MRF and latency to AP. Values are expressed as mean \pm S.E. Numbers in parenthesis are n values for each control and treatment. * Difference is significant at $p \leq 0.05$.

	AP duration ms		MRF mV/ms		Latency to 0 mV/ms	
Control	3.46 \pm 0.03		45.1 \pm 1.9		311.3 \pm 22.6	
Iberiotoxin	5.70 \pm 0.17*	(8)	25.6 \pm 1.7*	(8)	258.8 \pm 13.0*	(5)
Control	3.33 \pm 0.25		53.0 \pm 5.9		279.6 \pm 8.2	
ω -Ctx GVIA	4.69 \pm 0.57*	(6)	32.5 \pm 4.6*	(6)	234.0 \pm 8.6*	(6)
Control	3.47 \pm 0.35		46.6 \pm 4		336.6 \pm 33.5	
Nifedipine	4.10 \pm 0.40*	(4)	36.6 \pm 3.6*	(4)	306.8 \pm 23.6	(4)
Control	3.21 \pm 0.17		55.2 \pm 3.8		307.5 \pm 12.2	
Thapsigargin	3.26 \pm 0.24	(5)	51.9 \pm 4.2	(5)	209.2 \pm 21.7*	(12)
Control	2.49 \pm 0.17		54.5 \pm 4.3		255.6 \pm 26.4	
Ryanodine	3.31 \pm 0.1	(3)	44.8 \pm 1.7	(3)	200.3 \pm 21.3	(6)
Control	3.1 \pm 0.13		56.6 \pm 6.8		290.4 \pm 26.2	
Apamine	2.98 \pm 0.16	(3)	56.5 \pm 7	(3)	303.2 \pm 29.6	(7)

3. CONCLUDING REMARKS

An interesting point that arises from the data presented in this chapter is that depolarizations of the plasma membrane to near threshold potentials would induce, via a CICR mechanism, activation of K_{Ca} channels that will result in a decrease of membrane excitability. Mudpuppy parasympathetic cardiac neurons receive inputs from many different neurons (Parsons *et al.*, 1987). This negative feedback mechanism of AP triggering may play an important role in the integration of different input signals to these neurons.

Perhaps the most remarkable point of this chapter emerges from the evidence shown for different physiological roles of K_{Ca} channels, depending on the source of calcium that activates them.

Single channel studies of K_{Ca} channels from mudpuppy parasympathetic neurons did not show channel populations with different functional properties. However, when APs were studied, different physiological populations of K_{Ca} channels become evident. The difference appears to be determined by K_{Ca} channel activation by calcium coming from different, intracellular or extracellular, sources. It is important to remark that not only calcium, but also voltage determine K_{Ca} channel opening. When the plasma membrane is only slightly depolarized, the increase in the intracellular calcium concentration by calcium influx will not be sufficient to activate K_{Ca} channels. Nevertheless, calcium

influx will activate calcium release that will result in activation of K_{Ca} channels in proximity with the intracellular stores. On the other hand, K_{Ca} channel activity will increase due to the change in voltage during an AP. In this condition, the increase in the intracellular calcium concentration due to calcium influx will be enough to increase K_{Ca} activity, resulting in a shortening of the AP.

Whether these different behaviors of K_{Ca} channels respond to differential distribution of the channels in the cell remains to be clarified.

4. ACKNOWLEDGMENTS

Thanks to Dr. Rodney Parsons in whose laboratory at the University of Vermont these experiments were completed. I also acknowledge that the results presented in this chapter represent work done in collaboration with Ms. Laura Merriam and Dr. Karen Barstow. The studies were supported by NIH Grant NS 23978, NSF Grant IBN-0076741 and AHA Grant 9820031T. Special thanks to Drs. Sepúlveda and Bezanilla for giving me the opportunity of writing this chapter that is the best way of making public my gratefulness to Drs. Ramón Latorre and Enrico Stefani for all those, not always easy, hours we shared.

5. REFERENCES

- Adams, D. J. and Harper, A. A., 1995, Electrophysiological properties of autonomic ganglion neurons, In: *The Autonomic Nervous System*, edited by Burnstock G. Reading, UK, Harwood, p. 153-212.
- Arima, J., Matsumoto, N., Kishimoto, K. and Akaike, N., 2001, Spontaneous miniature outward currents in mechanically dissociated rat Meynert neurons, *J. Physiol.* **534**:99-107.
- Berridge, M. J., 1993, Inositol tris-phosphate and calcium signaling, *Nature* **36**:315-325.
- Brown, D., 1988, M-currents: an update, *Trends Neurosci.* **11**:294-299.
- Clark, R. B., Tse, A. and Giles W. R., 1990, Electrophysiology of parasympathetic neurons isolated from interatrial septum of bull-frog heart, *J. Physiol. (Lond.)* **427**:89-125.
- Fletcher, G. H. and Chiappinelli, V. A., 1992, Spontaneous miniature hyperpolarizations of presynaptic nerve terminals in the chick ciliary ganglion, *Brain Res.* **579**:165-168.
- Hartzell, H. C., Kuffler, S. W., Stickgold, R. and Yoshikami, D., 1977, Synaptic excitation and inhibition resulting from direct action of acetylcholine on two types of chemoreceptors on individual amphibian parasympathetic neurons, *J. Physiol. (Lond.)* **271**:817-846.
- Henzi, V. and MacDermott, A. B., 1992, Characteristics and function of Ca^{2+} - and inositol 1,4,5-trisphosphate-releasable stores of Ca^{2+} in neurons, *Neuroscience* **46**:251-273.
- Hua, S-Y., Nohmi, M. and Kuba, K., 1993, Characteristics of Ca^{2+} release induced by Ca^{2+} influx in cultured bullfrog sympathetic neurons, *J Physiol. (Lond.)* **464**:245-272.
- Kaczorowski, G. J., Knaus, H-G., Leonard, R. J., Mcmanus, O. B. and Garcia, M. L., 1996, High-conductance calcium-activated potassium channels: structure, pharmacology, and function, *J. Bioenerg. Biomembr.* **28**:255-267.
- Kuba, K., 1994, Ca^{2+} -induced Ca^{2+} release in neurons, *Jpn. J. Physiol.* **44**:613-650.
- Mathers, D. A. and Barker, J. L., 1981, Spontaneous voltage and current fluctuations in tissue cultured mouse dorsal root ganglion cells, *Brain Res.* **293**:35-47.
- Merriam, L. A. and Parsons, R. L., 1995, Neuropeptide galanin inhibits ω -conotoxin GVIA-sensitive calcium channels in parasympathetic neurons, *J. Neurophysiol.* **73**:1374-1382.
- Merriam, L. A., Scornik, F. S., and Parsons, R. L., 1999, Ca^{2+} -induced Ca^{2+} release activates spontaneous miniature outward currents (SMOCs) in parasympathetic cardiac neurons, *J Neurophysiol* **82**:540-550.
- Parsons, R. L., Neel, D. S., McKeon, T. W. and Carraway, R. E., 1987, Organization of a vertebrate cardiac ganglion: a correlated biochemical and histochemical study, *J. Neurosci.* **7**:837-846
- Parsons, R. L., Barstow, K. L. and Scornik, F. S., 2002, Spontaneous miniature hyperpolarizations affect threshold for action potential generation in mudpuppy cardiac neurons, *J. Neurophysiology*, **88**:1119-1127.

- Rudy, B., 1988, Diversity and ubiquity of K channels, *Neuroscience* **25**:729-749.
- Sah, P., 1996, Ca⁺-activated K⁺ currents in neurons: types, physiological roles and modulation, *Trends Neurosci.* **19**:150-154.
- Satin, L. S. and Adams, P. R., 1987, Spontaneous miniature outward currents in cultured bullfrog neurons, *Brain Res* **401**:331-339.
- Scornik, F. S., Merriam, L. A. and Parsons, R. L., 2001, Number of K_{Ca} channels underlying spontaneous miniature outward currents (SMOCs) in mudpuppy cardiac neurons, *J Neurophysiol.* **85**:54-60.
- Scornik, F. S., Barstow, K. L. and Parsons, R. L., 2001, SMOCs modulate excitability of mudpuppy parasympathetic neurons, *Soc. Neurosci. Abstr.* **27**, Program N° 572.14.
- Verkhatsky, A. and Shmigol, A., 1996, Calcium-induced calcium release in neurons, *Cell Calcium* **19**:1-14.

TWINKLE TWINKLE LITTLE SPARK: OUT OF TUNE POTASSIUM CHANNELS

Guillermo J. Pérez^{1*}

1. INTRODUCTION

In arterial smooth muscle, large conductance calcium-activated potassium channels (K_{Ca} channels) are central to the regulation of myogenic tone (Brayden and Nelson, 1992). In this tissue, and also in other smooth muscle preparations, K_{Ca} channels are activated by the localized release of Ca^{2+} (Ca^{2+} sparks) from the sarcoplasmic reticulum (SR) resulting in a transient potassium efflux that causes hyperpolarization and, in turn, vaso-relaxation (Nelson *et al.*, 1995; Knot *et al.*, 1998; Pérez *et al.*, 1999). The K_{Ca} channel is the only member of the large family of voltage-gated K^+ channels that are activated by Ca^{2+} , which makes the channel uniquely suited to integrate Ca^{2+} and voltage signals to modulate membrane potential and excitability. In smooth muscle, the K_{Ca} channel is composed of two different subunits, an α pore forming subunit, and a $\beta 1$ -regulatory subunit. We created “out of tune” K_{Ca} channels by removing the $\beta 1$ subunit in transgenic mice ($\beta 1$ -knockout mice (KO)). We demonstrate that the $\beta 1$ subunit is crucial for tuning K_{Ca} channels to their “native” Ca^{2+} waveform (Ca^{2+} sparks) to maintain normal arterial function. Furthermore, the altered K_{Ca} channels channel properties produced by removal of the $\beta 1$ subunit promote severe physiological consequences that include elevated arterial tone, elevated blood pressure and consequently increased heart size (Brenner *et al.*, 2000; Standen, 2000).

More than twenty years ago, at the very onset of the single-channel and patch-clamp recording era, Ramón Latorre and his colleagues reported, for the first time, the single-channel characteristics of K_{Ca} channels from skeletal muscle, reconstituted into lipid bilayers (Latorre *et al.*, 1982). This pioneering work depicted the very hallmarks of K_{Ca} channels, namely, high conductance, high potassium selectivity, and Ca^{2+} and voltage dependence. A few years later, K_{Ca} channels were also reconstituted from smooth muscle preparations displaying similar characteristics (Cecchi *et al.*, 1986). Using channel reconstitution into lipid bilayers, Enrico Stefani’s laboratory was the first to propose that smooth muscle K_{Ca} channels could be modulated by closely-associated (G)

¹ Department of Experimental Cardiology, Masonic Medical Research Laboratory, 2150 Bleecker St. Utica, NY 13501, USA.

* corresponding author: gperez@mmrl.edu

proteins (Toro *et al.*, 1990). Indeed, an even “more than closely” associated protein was later discovered in smooth muscle and identified as an integral part of the K_{Ca} channel itself - the β subunit, now termed $\beta 1$ subunit (García-Calvo *et al.*, 1994). The extensive work on the molecular biology of K_{Ca} channels revealed that these channels exist, in most tissues, as heterodimers formed by two different subunits termed α and β . The α subunit contains the pore-forming region, the voltage sensor, and the Ca^{2+} -binding site, while the β subunit, first discovered in smooth muscle, has regulatory functions.

Studies on expressed K_{Ca} channels have shown that the smooth muscle specific $\beta 1$ subunit subtype increases the apparent Ca^{2+} sensitivity of the channel, slows the activation and deactivation kinetics, and increases the sensitivity to DHS-1, a soyasaponin derivative that activates the channel (McManus *et al.*, 1995; Meera *et al.*, 1996, Dworetzky *et al.*, 1996). In a detailed biophysical study using expression systems Cox and Aldrich (2000), developed an allosteric model to explain how the $\beta 1$ subunit exerts its activator effects. These authors suggest that the $\beta 1$ subunit steady-state effects are due to a decrease in the intrinsic energy difference between the closed and open conformation. This allosteric interaction can account for changes in Ca^{2+} sensitivity and voltage sensitivity between α and $\alpha+\beta 1$ K_{Ca} channels. Along these lines, Nimigean and Magleby (2000) working with expressed single channels in HEK 293 cells, suggested that the $\beta 1$ subunit acts as a gain control on bursting kinetics, independent of whether the channel is activated by Ca^{2+} or voltage. $\beta 1$ -subunit modulation of K_{Ca} channels is also present in humans. With the contribution, among other notorious scientists, of Ramón and Enrico, Wallner *et al.*, (1995) first cloned the human α subunit of the K_{Ca} channel and also demonstrated that its co expression with the $\beta 1$ subunit (cloned from bovine smooth muscle) regulated the human K_{Ca} channel. Soon after, the “more than closely” related laboratory, headed by Dr. Ligia Toro, showed that in human coronary arteries, native K_{Ca} channels were, indeed, formed by complexes of $\alpha + \beta 1$ (Tanaka *et al.*, 1997). Thus $\beta 1$ subunit modulation appeared to be conserved among species, suggesting an essential role in controlling vital physiological functions. Moreover, recently, a completely different new role for the $\beta 1$ subunit was suggested by Ramón’s laboratory. In this recent work, Valverde *et al.*, (1999) discovered that the $\beta 1$ subunit can act as a non-genomic estrogen receptor that modulates K_{Ca} channels activity in expression systems.

Despite the tremendous progress in understanding the modulation exerted by the $\beta 1$ on K_{Ca} -channel activity, until recently, there was no direct demonstration for the modulatory role of the $\beta 1$ subunit in native K_{Ca} channels.

1.1. Activation of K_{Ca} Channels by Ca^{2+} Sparks

The voltage and Ca^{2+} dependency of K_{Ca} channels described early on by Ramón in skeletal muscle was always thought to represent an exquisitely equipped feedback mechanism for smooth muscle relaxation. Thus, whenever intracellular Ca^{2+} and/or membrane potential increased, K_{Ca} channels should activate and promote hyperpolarization. However, at physiological membrane potentials of smooth muscle cells, (around -40 mV) K_{Ca} channels can only sense elevations in intracellular Ca^{2+} in the micromolar range, a level that is too high for global intracellular Ca^{2+} concentrations compatible with normal cell functioning. This apparent paradox suggests that K_{Ca}

channels must experience high local Ca^{2+} concentrations in order to be activated. Indeed, Nelson *et al.*, (1995), first demonstrated the existence of Ca^{2+} sparks in vascular smooth muscle, which represent high local Ca^{2+} transient elevations arising from the release of Ca^{2+} from intracellular Ca^{2+} stores. Ca^{2+} sparks in smooth muscle are largely due to the concerted opening of a number of ryanodine receptor release channels (RyRs) located in the SR membrane. In this way, Ca^{2+} sparks are now thought to be one of the main activators of K_{Ca} channels, with little impact on global Ca^{2+} concentration but with a tremendous impact on nearby K_{Ca} channels. The concept of Ca^{2+} sparks having a role in vasorelaxation through the local activation of K_{Ca} channels, was also proposed by Nelson *et al.* (1995) (see Fay, 1995) and further supported by Pérez *et al.* (1999) in the same tissue. When Ca^{2+} sparks stimulate K_{Ca} channels, a transient outward current can be recorded in voltage-clamped myocytes. Transient K_{Ca} currents, in isolated smooth muscle cells, were originally described by Benham and Bolton (1986), and were thought to be caused by sudden discharges of Ca^{2+} stores near the membrane. Increasing evidence for this local control of K_{Ca} channels by Ca^{2+} sparks in other vascular and non-vascular smooth muscle (see Jaggar *et al.*, 2000 for a review) supports the idea that this relationship may be finely tuned by specific molecular components. The coding of Ca^{2+} sparks to cellular processes depends on a number of factors, including the amount of Ca^{2+} release during a spark, the proximity of the Ca^{2+} spark site to a target protein, and the Ca^{2+} sensitivity of the target (i.e., K_{Ca} channels).

Thus, when visualized in high-speed confocal microscopy, fluo 3- (or fluo 4-) loaded intact arteries, display a vivid “twinkling” Ca^{2+} spark symphony that has to be correctly interpreted by K_{Ca} channels in order to maintain normal arterial function.

2. RESULTS

To study the functional role of the $\beta 1$ subunit in native tissues we created transgenic mice lacking the $\beta 1$ subunit by gene-targeting disruption (Brenner *et al.*, 2000). The gene targeting vector was constructed to delete the first coding exon (exon 2) of the gene. The targeting vector was also designed to insert a β -galactosidase reporter (*lacZ* gene) in translational frame with the $\beta 1$ -subunit translation-initiation site and thus report transcription from the $\beta 1$ gene promoter (Brenner *et al.*, 2000). Having the *lacZ* gene targeted to the $\beta 1$ locus afforded us the opportunity to examine directly which cell types normally express the $\beta 1$ subunit. The tissue specificity of the K_{Ca} -channel $\beta 1$ subunit was evaluated by *lacZ* staining of the samples. Figure 1 shows positive *lacZ* staining (originally blue stains) in a dissected basilar cerebral artery from a KO mouse. This assay was also tested in a variety of tissues (bladder, heart, brain, gastrointestinal tract, and airway tract) with positive results obtained only in smooth muscle from KO animals. In contrast, no blue staining was detected in wild type (WT) animal tissue or in non smooth muscle tissue from KO mice (Brenner *et al.*, 2000). Thus, the $\beta 1$ subunit expression seems to be specifically distributed in smooth muscle myocytes.

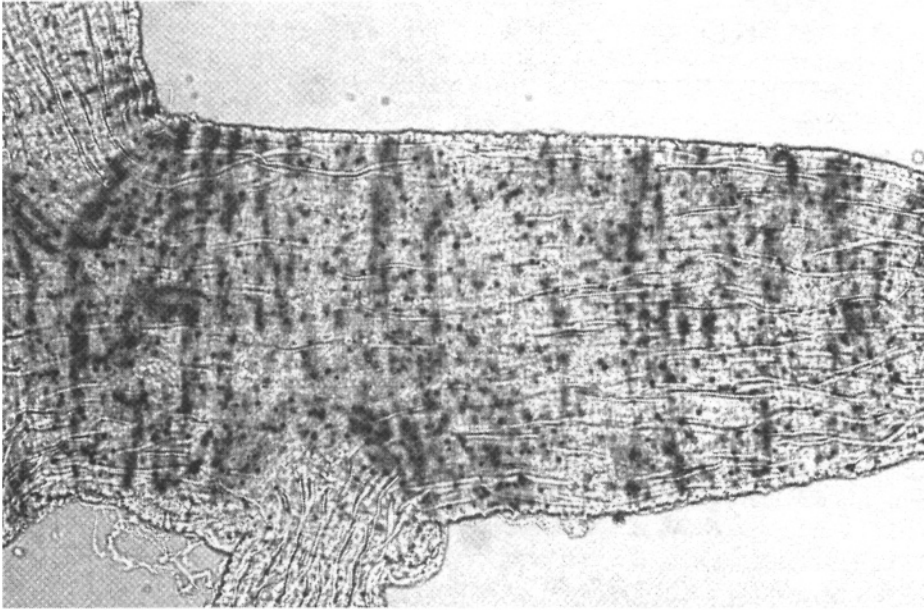


Figure 1. A dissected cerebral basilar artery from KO mouse positively stained for β -galactosidase activity (dark staining). Image was taken with a 20X objective.

2.2. Out of Tune

At the functional level, single K_{Ca} channel activity was evaluated in excised inside-out membrane patches from isolated arterial smooth muscle cells. Consistent with previous reports in expression systems, K_{Ca} channel activity was dramatically diminished in the absence of the $\beta 1$ subunit. However, single-channel conductance remained unaltered (~ 215 pS, in 140/140 KCl, not shown). In addition, the lack of the $\beta 1$ subunit seems not to alter channel density as evaluated by the number of channels present per patch pipette (about 2 to 3 channels in either condition). Figure 2 illustrates single-channel recordings at the same Ca^{2+} concentration ($10 \mu M$) and at the same holding potential (± 40 mV) for both KO and WT. Despite having two K_{Ca} channels present in the membrane patch from the KO, the record in Figure 2 shows only brief channel openings at -40 mV (top left) whereas in the WT case, the channels have a more pronounced activity (top right). Differences in activity were also present at depolarized potentials (bottom traces).

Figure 3 (left panels) shows the Ca^{2+} dose response of single excised patches (from 2-11 patches at each concentration) at -40 mV and $+40$ mV in WT and KO conditions. At -40 mV, the K_d values obtained from a fitted Hill equation (solid line) were $1.9 \mu M$ for WT and KO, respectively. At a very high depolarizing voltage ($+80$ mV, top right)

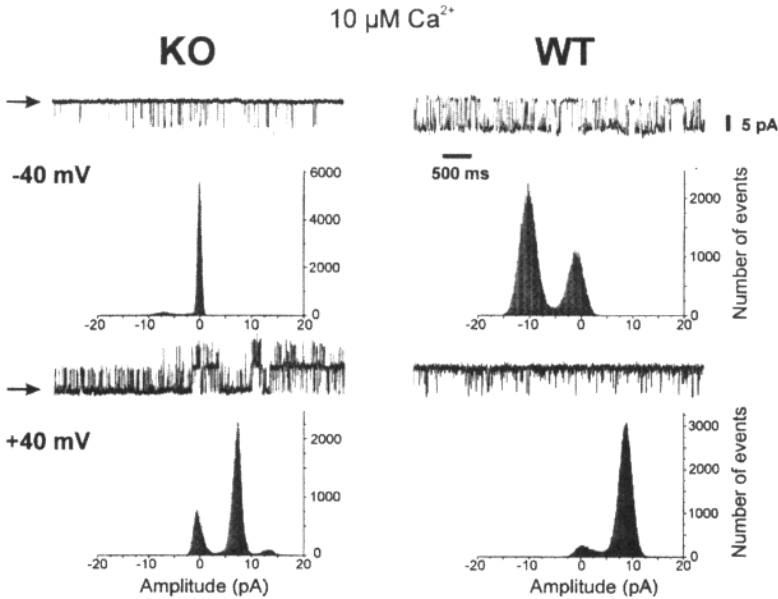


Figure 2. Single K_{Ca} channel records from KO and WT cerebral artery myocytes. Corresponding all point histograms, illustrating the difference in activity at the same Ca^{2+} concentration and indicated membrane potential. Arrows mark the closed state of the channel

the K_d for KO was $3.8 \mu M$. The open probability of channels from WT animals was near 1 over the range of Ca^{2+} concentrations studied in figure 3 (not shown).

In addition, Figure 3 (bottom right panel) also shows that the voltage dependence of these channels, at $10 \mu M Ca^{2+}$, is shifted towards more depolarized potentials in the absence of the $\beta 1$ subunit. The curves were fitted to a Boltzmann equation (solid line WT, dotted line KO), with half-activation voltages around $-30 mV$ for WT and $+60 mV$ for KO. These results are in good agreement with previously reported experiments done in the presence or absence of the $\beta 1$ subunit using expression systems (Meera *et al.*, 1996). Moreover, the soyasaponin derivative DHS-1 failed to activate K_{Ca} channel from KO animals (Brenner *et al.*, 2000). We conclude that the modulatory effects exerted by the $\beta 1$ subunit on expressed K_{Ca} channels is also observed in native channels recorded from freshly dissociated arterial myocytes.

K_{Ca} channel activity was further evaluated in a wider range of Ca^{2+} concentrations and holding potentials, in the presence and absence of the $\beta 1$ subunit. Figure 3 shows that Ca^{2+} dependence at different voltages is seriously compromised when the $\beta 1$ subunit is not present.

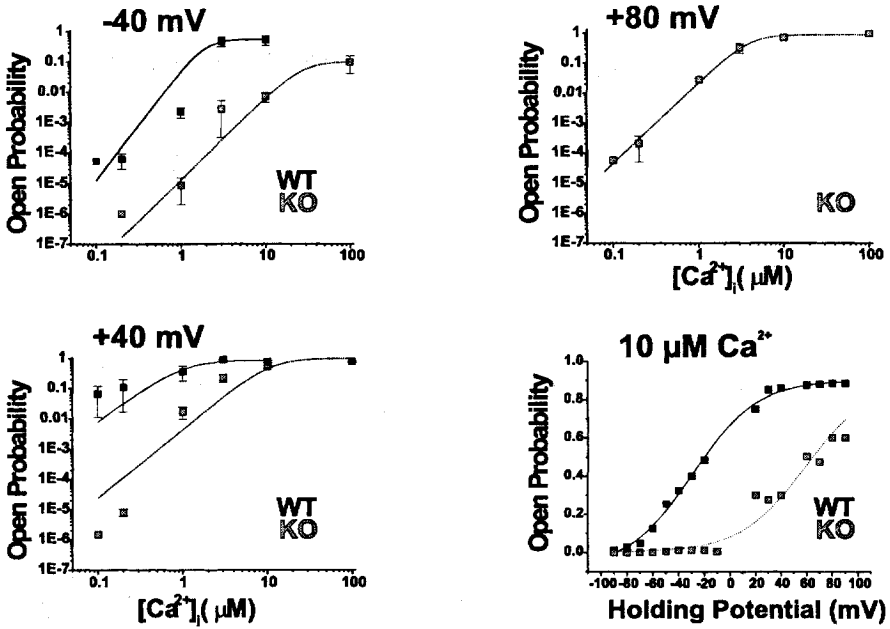


Figure 3. Ca²⁺ and voltage dependence of K_{Ca} channels from WT and KO animals. Left panels show the Ca²⁺ dose response of single excised patches (from 2-11 patches at each concentration) at the indicated holding potential. Bottom right panel shows the voltage dependence of single K_{Ca} channel activity from WT and KO animals, at 10 μM Ca²⁺.

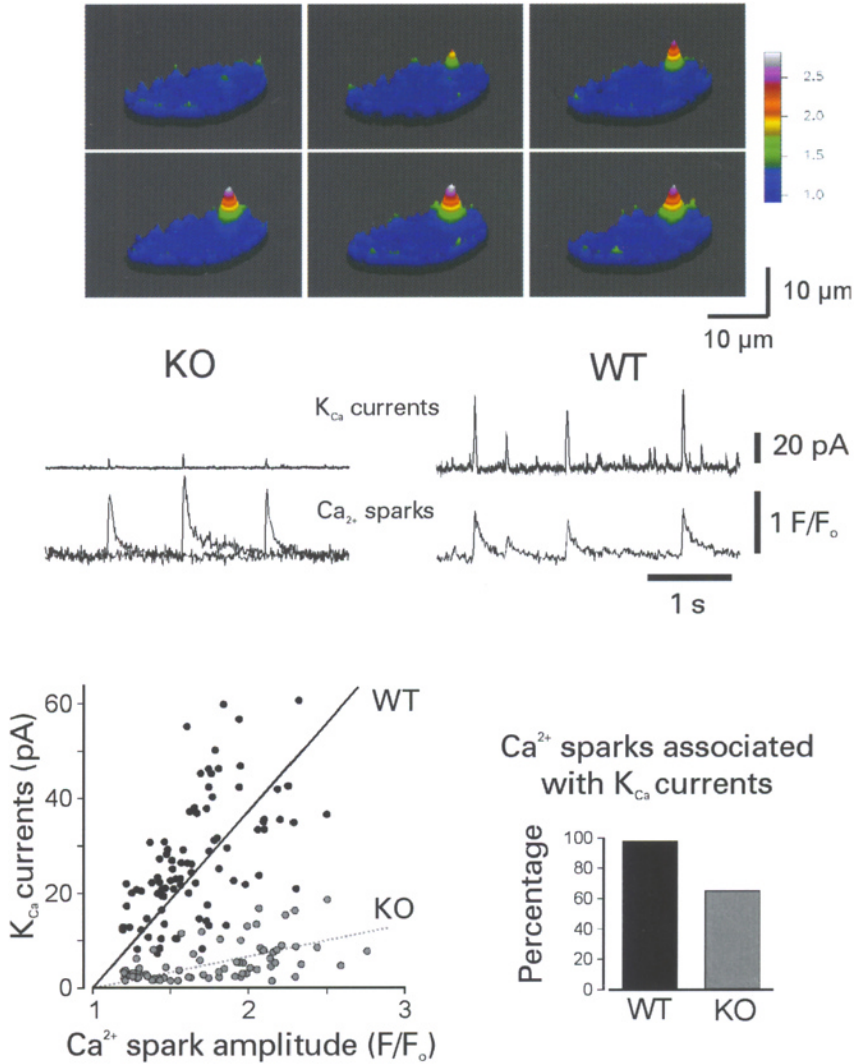


Figure 4. Simultaneous recording of Ca^{2+} sparks and K_{Ca} currents in cerebral artery myocytes. Top, Consecutive 3D images of a Ca^{2+} sparks from a $\beta 1$ KO myocytes obtained every 8.33 ms. No significant differences were found in Ca^{2+} spark frequency and amplitude between control and KO myocytes. Control frequency = 1.41 ± 0.2 Hz ($n = 6$ cells), and KO frequency = 1.35 ± 0.3 ($n = 7$ cells). Control amplitude = 1.65 ± 0.03 in control ($n = 94$ from 6 cells). Middle, Simultaneous K_{Ca} current Ca^{2+} spark measurements (fractional fluorescence, F/F_0) recorded at -40 mV. Fractional fluorescence traces originate from average F/F_0 of $2.2 \times 2.2 \mu\text{m}$ box regions centered in Ca^{2+} spark sites. WT cell had one Ca^{2+} spark site and KO cell had two spark sites. Bottom left, K_{Ca} current as a function of Ca^{2+} spark amplitude in WT cells (black, 94 sparks from 6 cells) and KO cells (gray, 71 sparks from 7 cells). Lines represent linear regression fit (slope_{WT} = 37.8 ± 1.6 vs. slope _{$\beta 1$ -KO} = 6.7 ± 0.5 , $p < 0.001$). Bottom right, percentage of Ca^{2+} sparks causing transient K_{Ca} current in WT vs. KO amplitude 1.77 ± 0.05 ($n = 71$ from 7 cells). Reprinted by permission from Nature (407: 870-876, 2000) copyright (2000) Macmillan Publishers Ltd.

2.3 Twinkle Twinkle

As mentioned above, in arterial smooth muscle, “twinkling” Ca^{2+} sparks arising from the spontaneous release of Ca^{2+} from the SR through RyRs, are K_{Ca} -channel activators in the sarcolemma, promoting transient K_{Ca} currents.

The characteristics of Ca^{2+} sparks were not affected by the absence of the K_{Ca} channel $\beta 1$ subunit. No obvious differences were found between Ca^{2+} sparks in isolated myocytes from WT and KO animals. Figure 4 (top) illustrates this with a 3D representation of the life cycle of a Ca^{2+} spark recorded with confocal microscopy at 8.33 ms/frame in an isolated arterial myocyte from a KO animal. Despite the similarity between Ca^{2+} sparks recorded from WT or KO, functional coupling between Ca^{2+} sparks and the activation of transient K_{Ca} current was seriously disrupted. Figure 4 (middle panel) shows traces of whole-cell currents and fluorescence over time, obtained in simultaneous patch-clamp and confocal-imaging recordings. This example shows that, in isolated arterial myocytes, big Ca^{2+} sparks (middle left traces) elicit very small currents when the $\beta 1$ subunit is not present. In contrast, the channels from WT animals produced conspicuous transient outward K_{Ca} currents upon Ca^{2+} - spark stimulation (middle right traces). This indicates that the coupling efficiency between Ca^{2+} sparks and K_{Ca} channels is severely distorted when the $\beta 1$ subunit is absent. This can be better viewed in a scatter plot that shows the relationship between Ca^{2+} spark amplitudes and K_{Ca} current amplitude from several experiments (Figure 4, bottom left). The absence of the $\beta 1$ subunit reduces the tuning of K_{Ca} channels to Ca^{2+} sparks approximately six-fold (Brenner, *et al.*, 2000). Furthermore, the ability of Ca^{2+} sparks to activate transient K_{Ca} currents was seriously compromised in the absence of the $\beta 1$ subunit. In the WT, essentially every Ca^{2+} spark evoked a transient at -40 mV. However, in the KO, 35% of the sparks failed to evoke a detectable K_{Ca} current (Figure 4, bottom right). Since K_{Ca} channel density and Ca^{2+} spark amplitude were unaltered in the KO, these results suggest that the overall K_{Ca} channel activity during Ca^{2+} sparks is reduced by at least 12- fold in the KO, consistent with the diminished Ca^{2+} sensitivity of K_{Ca} channels (Figure 4).

Thus, we showed that native K_{Ca} channels lacking the $\beta 1$ subunit behave “out of tune” and cannot correctly interpret the Ca^{2+} sparks symphony. This also holds true in intact artery experiments where the effect pressure on arterial diameter was evaluated. Elevation of intravascular pressure constricts small arteries, including cerebral arteries. Cerebral arteries which lack the $\beta 1$ subunit are significantly more constricted in response to increased pressure than are control arteries (Brenner *et al.*, 2000). These results indicate that the lack of the $\beta 1$ subunit leads to an elevation in arterial tone. The actual contribution of the impaired K_{Ca} channels that lack the $\beta 1$ subunit seems to be very small. Iberitoxin (a potent K_{Ca} channel blocker) had no effect on KO cerebral arteries, while it caused a 74 % increase in arterial tone in the WT (Brenner *et al.*, 2000). If no systemic physiological control mechanisms can compensate for the increased arterial tone, arterial

blood pressure should be elevated in mice lacking the K_{Ca} channel $\beta 1$ subunit. The mean arterial blood pressure of the KO mice was indeed elevated and comparable to transgenic mice with compromised endothelial function. In WT animals, average blood pressure was 114 ± 6.0 mm Hg ($n = 6$) whilst KO average blood pressure was 134 ± 5.1 mm Hg ($n = 6$) ($p < 0.03$). Furthermore, $\beta 1$ knockout mice also show symptoms of hypertension as the hearts in KO animals tend to be significantly larger than in WT animals (Brenner *et al.*, 2000).

3. CONCLUDING REMARKS

Our results support the concept that the $\beta 1$ subunit is required for specific tuning of K_{Ca} channel properties to the needs of an arterial smooth muscle cell. This is illustrated in the cartoon model in Figure 5.

A number of K_{Ca} channels are activated by Ca^{2+} sparks in the presence of the $\beta 1$ subunit. In contrast, only a few channels facing really high Ca^{2+} concentrations can be activated when the $\beta 1$ subunit is not present.

The increased sensitivity to Ca^{2+} conferred by the $\beta 1$ subunit is required for the K_{Ca} channel to translate Ca^{2+} sparks to membrane potential hyperpolarization. The decreased coupling of Ca^{2+} to channel activity extrapolated well to the functional defects observed in the intact artery and whole animal. Moreover, end organ pathology, such as myocardial hypertrophy, observed in chronic hypertension was also observed in the K_{Ca} channel $\beta 1$ KO mice.

The K_{Ca} channel $\beta 1$ KO mouse therefore presents a unique model, wherein a clearly defined molecular defect could be used to study the secondary effects of hypertension (Brenner *et al.*, 2000). This animal model also constitutes an invaluable tool to study the role of the $\beta 1$ subunit in native K_{Ca} channels. For instance, using this model, Dick and Sanders (2001) recently corroborated Ramón's group's hypothesis that the $\beta 1$ subunit can act as a non-genomic estrogen receptor.

5. ACKNOWLEDGMENTS

Special thanks to Dr. Nelson and Dr. Aldrich in whose laboratories most of the data was obtained. Thanks to all colleagues who have worked on this project: Mark Nelson, Adrian Bonev, Del Eckman, R. Brenner, J. Kosek, S. Wiler, A. Patterson, and Rick Aldrich. This work was supported by an award from the American Heart Association (GP). This work was also supported by NIH and NSF. Reprinted by permission from Nature (407: 870-876, 2000) copyright (2000) Macmillan Publishers Ltd.

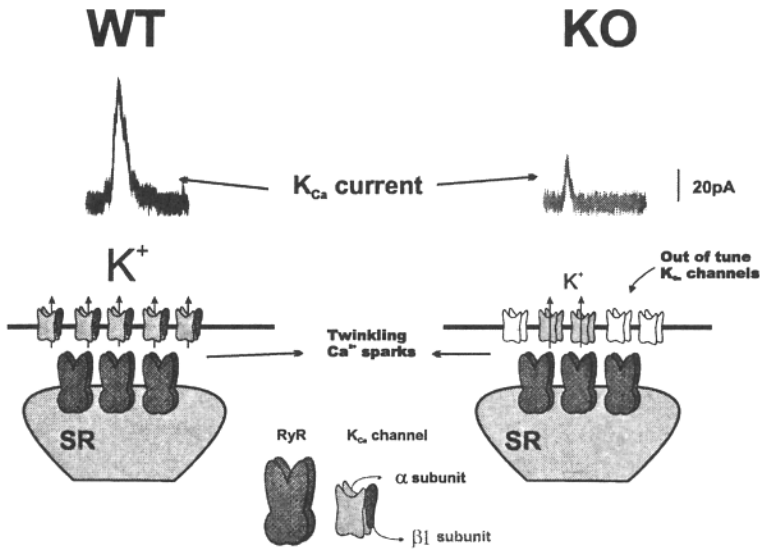


Figure 5. Schematic representation of the functional coupling between K_{Ca} channels and RyRs in arterial myocytes from WT and KO animals. Within a cluster of RyRs produces the local release of Ca^{2+} (Ca^{2+} sparks) K_{Ca} channels in the sarcolemma are activated producing a transient outward K_{Ca} current (left trace). If the $\beta 1$ subunit is absent (KO), only a few channels are able to respond to the high local Ca^{2+} elevation produced by the same sized Ca^{2+} spark.

5. REFERENCES

- Benham, C. D. and Bolton T. B., 1986, Spontaneous transient outward currents in single visceral and vascular smooth muscle cells of the rabbit, *Journal of Physiology (Lond)*, **381**:385-406.
- Brayden, J.E. and Nelson, M.T., 1992, Regulation of arterial tone by activation of calcium-dependent potassium channels, *Science*, **256**:532-535.
- Brenner R., Perez G.J., Bonev A.D., Eckman D.M., Kosek J.C., Wiler S.W., Patterson A.J., Nelson M.T., and Aldrich R.W., 2000, Vasoregulation by the beta1 subunit of the calcium-activated potassium channel, *Nature*, **407**:870-876.
- Cecchi, X., Alvarez, O., & Wolff, D., 1986, Characterization of a calcium-activated potassium channel from rabbit intestinal smooth muscle incorporated into planar bilayers, *Journal of Membrane Biology*, **91**:11-18.
- Cox, D. H. and Aldrich, R. W., 2000, Role of the $\beta 1$ subunit in large-conductance Ca^{2+} -activated K^+ channel gating energetics, Mechanisms of enhanced Ca^{2+} sensitivity, *Journal of General Physiology* **116**:411-432.
- Dick, G. M., and Sanders, K. M., 2001, (Xeno) estrogen sensitivity of smooth muscle BK channels conferred by the regulatory beta 1 subunit: a study of beta 1 knockout mice, *Journal of Biological Chemistry*, **276**:44835-44840.
- Dworetzky, S.I., Boissard C.G., Lum-Ragan J.T., McKay M.C., Post-Munson D.J., Trojnecki J.T., Chang C.P., and Gribkoff V.K., 1996, Phenotypic Alteration of a Human BK (hSlo) Channel by hSlobeta Subunit Coexpression: Changes in Blocker Sensitivity, Activation/Relaxation and Inactivation Kinetics, and Protein Kinase A Modulation, *Journal of Neuroscience*, **16**:4543-4550.
- Fay F.S. 1995, Calcium sparks in vascular smooth muscle: relaxation regulators, *Science*, **270**:588-589.
- Garcia-Calvo, M., Knaus H. G., McManus O. B., Giangiacomo K. M., Kaczorowski G. J., and Garcia M. L., 1994, Purification and reconstitution of the high-conductance, calcium- activated potassium channel from tracheal smooth muscle, *Journal of Biological Chemistry*, **269**:676-682.
- Jaggar, J. H., Porter V. A., Lederer W. J., and Nelson M. T., 2000, Calcium sparks in smooth muscle, *American Journal of Physiology, Cell Physiology*, **278**: C235-C256.
- Knot, H.J., Standen, N.B., and Nelson, M.T., 1998, Ryanodine receptors regulate arterial diameter and wall $[\text{Ca}^{2+}]$ in cerebral arteries of rat via Ca^{2+} -dependent K^+ channels, *Journal of Physiology (Lond)* **508**:211-221.
- Latorre, R., Vergara, C., & Hidalgo, C., 1982, Reconstitution in planar lipid bilayers of a Ca^{2+} -dependent K^+ channel from transverse tubule membranes isolated from rabbit skeletal muscle, *Proceedings of the National Academy of Science U.S.A.*, **79**:805-809.
- McManus, O.B. Helms, L. M., Pallanck, L., Ganetzky, B., Swanson, R., and Leonard, R. J., 1995, Functional role of the beta subunit of high conductance calcium-activated potassium channels, *Neuron*, **14**:645-650.
- Meera, P., Wallner, M., Jiang, Z. and Toro, L., 1996, A calcium switch for the functional coupling between alpha (hSlo) and beta subunits (KV,Ca beta) of maxi K channels, *FEBS Letters*, **382**:84-88.
- Nelson M.T., Cheng H., Rubart M., Santana L.F., Bonev A.D., Knot H.J., Lederer W.J., 1995, Relaxation of arterial smooth muscle by calcium sparks, *Science*, **270**:633-7.
- Nimigeon, C. M. and Magleby K.L., 2000, Functional coupling of the β subunit to the large conductance Ca^{2+} -activated K^+ channel in the absence of Ca^{2+} , Increased Ca^{2+} sensitivity from a Ca^{2+} independent mechanism, *Journal of General Physiology*, **115**:719-734.
- Perez, G.J., Bonev, A.D., Patlak, J.B. and Nelson, M.T., 1999, Functional coupling of ryanodine receptors to K_{Ca} channels in smooth muscle cells from rat cerebral arteries, *Journal of General Physiology*, **113**:229-238.
- Standen, N. Cardiovascular biology: Tuning channels for blood pressure, *Nature* **407**, 845 - 848 (2000).
- Tanaka, Y., Meera, P., Song, M., Knaus, H.G. and Toro, L. Molecular constituents of maxi KCa channels in human coronary smooth muscle: predominant alpha + beta subunit complexes, *J Physiol (Lond)* **502**, 545-557 (1997).
- Toro, L., Ramos-Franco, J., & Stefani, E., 1990, GTP-dependent regulation of myometrial KCa channels incorporated into lipid bilayers, *Journal of General Physiology* **96**, 373-394.
- Tseng-Crank, J., N. Godinot, T. E. Johansen, P. K. Ahring, D. Strobaek, R. Mertz, C. D. Foster, S. P. Olesen, and P. H. Reinhart. Cloning, expression, and distribution of a Ca^{2+} -activated K^+ channel beta-subunit from human brain, *Proc.Natl.Acad.Sci.* **93**, 9200-9205 (1996).

- Valverde M., Rojas. P. Amigo, J. Cosmelli, D. Orio, P., Bahamonde M. I., Mann, G. E., Vergara, C. and Latorre, R., Acute Activation of Maxi-K channels (*hSlo*) by estradiol binding to the β subunit, *Science* **285**, 1929-1931 (1999).
- Wallner, M., P. Meera, M. Ottolia, G. J. Kaczorowski, R. Latorre, M. L. Garcia, E. Stefani, and L. Toro. Characterization of and modulation by a beta-subunit of a human maxi KCa channel cloned from myometrium, *Receptors.Channels* **3**, 185-199 (1995).

A CLC-2-LIKE CHLORIDE CONDUCTANCE IN *DROSOPHILA* PHOTORECEPTORS

Gonzalo Ugarte^{1,2}, Peter M. O'Day³, Juan Bacigalupo^{1,2} and Cecilia Vergara^{1*}.

1. INTRODUCTION

A chloride channel with electrophysiological characteristics resembling those described for the mammalian CIC-2 protein was identified in *Drosophila* photoreceptors. The channel has a unitary conductance of ~4.4 pS, it is activated at hyperpolarizing potentials, it is independent of Ca²⁺ and it is blocked by 1mM Zn²⁺ and anthracene, but not by DIDS. Its selectivity sequence is Cl⁻ = SCN⁻>Br⁻>>I⁻. This channel is modulated by linolenic acid (LNA), a molecule recently proposed as the endogenous agonist of the light-dependent channels TRP and TRPL in these cells. At a macroscopic level, the chloride currents recorded from the *trp/trpl* mutant that lacks both light-sensitive channels, are also activated by LNA and blocked by anthracene.

2. OVERVIEW OF CIC CHANNELS WITH EMPHASIS ON CIC-2.

Chloride-selective channels are present in prokaryotic and eukaryotic cells. In many cell types their functional role has not yet been determined, but some of their known functions include the modulation of cellular excitability by stabilizing the membrane potential, control of cellular volume, electrolyte and fluid transport in epithelia, or mediation of cellular acidification of intracellular organelles by carrying countercharges. Based on primary-sequence homology, chloride channels have been classified into three different groups: ligand-gated channels, the voltage-activated CIC family and the cAMP-activated cystic fibrosis transmembrane conductance regulator (CFTR) that belongs to the family of ABC transporters. The CIC is a large gene family that apparently evolved very early, since such genes have been found in *E. Coli*, yeast, plants and mammals. In mammals, nine different members of the family have been identified so far. The nine products of these genes show differences in their selectivity, single-channel conductance,

¹ Biology Department, Faculty of Sciences, University of Chile, Santiago, Chile.

² Millennium Science Institute for Advanced Studies in Cell Biology and Biotechnology, Santiago, Chile.

³ Institute of Neuroscience, University of Oregon, Eugene, Oregon, USA.

* corresponding author: cvergara@uchile.cl

voltage-dependence, and sensitivity to blockers (Jentsch and Gunther 1997, Jentsch *et al.* 1999, Dutzler *et al.* 2002).

CIC-0 from the electric organ of *Torpedo* was the first member of the CIC family from which single-channel recordings were obtained (White and Miller, 1979), and also the first to be cloned (Jentsch *et al.* 1990). From the analysis of single-channel currents, Miller and White proposed that CIC-0 contains two parallel and independent pores (Miller 1982, Miller and White 1984), an idea that was confirmed once the X-ray structure of two bacterial CIC channels was obtained (Dutzler *et al.*, 2002). The sequence alignment of four of the CIC channel family members with that of the two bacterial channels from which the structure was resolved, together with the rather high sequence similarity to the other CIC channels, strongly suggests that the whole family shares the same general three-dimensional structure (Dutzler *et al.* 2002).

CIC-1 channels from rat skeletal muscle were cloned by homology screening of the CIC-0 from *Torpedo* (Steinmeyer *et al.*, 1991a). They are mainly expressed in skeletal muscle, they open in response to depolarization, have a very low single-channel conductance (~ 1 pS) and exhibit the same "double-barrel" behavior shown by CIC-0 channels (Saviane *et al.*, 1999). Their expression is developmentally regulated in muscle and mutations in CIC-1 channels are the cause of the myotonia associated with Becker and Thomsen's diseases (Steinmeyer *et al.* 1991a, b).

CIC-2 channels were first described by Thiemann *et al.* (1992) after the screening of cDNA libraries of rat heart and brain using cDNA from the rat CIC-1 channel. Northern blot analysis showed that CIC-2 is also expressed in skeletal muscle, lungs, kidney, pancreas, stomach, intestine, liver and also in cell lines of neuronal, fibroblastic or epithelial origin. When expressed in *Xenopus* oocytes, a slowly activating Cl^- current was recorded in response to hyperpolarization. The wide range of tissues and cell types that express these channels suggests that they have an important house-keeping role and, considering that under resting conditions the channels are closed, these authors proposed that "perhaps some other mechanism of activation, in addition to hyperpolarization, exists *in vivo*". They later showed that extracellular hypotonicity and acidic pH are also stimuli for activation of these channels, when are expressed in *Xenopus* oocytes (Gründer *et al.* 1992, Jordt and Jentsch 1997).

The distribution of CIC-2 channels in rat brain was investigated by Smith *et al.* (1995) by *in situ* hybridization. The mRNA for this channel was differentially expressed in neurons and undetectable in glia. With a few exceptions, this group found a high correlation between CIC-2 mRNA expression levels and neuronal size, with expression high in the largest neurons of different regions of the brain. This correlation led them to propose that CIC-2 channels participate in the control of Cl^- homeostasis and neuronal excitability in the CNS by maintaining, or not, the Cl^- reversal potential positive with respect to the membrane potential. This proposal has been supported by studies involving gene transfer of CIC-2 channels in neurons that express GABA receptors, demonstrating that CIC-2 expression can modify the Cl^- equilibrium potential, reversing GABA-receptors function from excitation to inhibition (Staley *et al.*, 1996)

CIC-2 channels are expressed in airways epithelium and their expression is developmentally regulated; it is high in the fetus and decreases to low levels in the adult. Because channel distribution in rat lungs overlaps with that of CFTR channels, which are defective in cystic fibrosis, and also because CIC-2 channels share several biophysical properties with CFTR channels, they are considered as possible therapeutic targets for

this disease. Cloned human hCIC-2 channels expressed in an airway epithelial cell line derived from a CFTR patient, display activation by low extracellular pH. There is interest in unraveling the mechanism of pH activation, because this could aid selection of pharmacological agents that could mimic the effect of low pH, and also help to understand the mechanisms that control their expression (Schwiebert *et al.*, 1998).

CIC-2 channels were identified in rod bipolar cells of the rat retina by immunohistochemistry. Patch-clamp recordings on individual cells showed an inwardly-rectifying current with properties that indicate the functional expression of CIC-2 channels in these cells, and it was proposed that their role was to clamp the chloride reversal potential close to the resting membrane potential (Enz *et al.*, 1999).

Recently developed knockout mice for CIC-2 presented two defects, male infertility and retinal degeneration (Böls *et al.*, 2001), suggesting a crucial role of these channels in the control of ionic environment in the germinal and retinal epithelia.

The heterologous expression of hCIC-2 in HEK cells allowed identification of several other activators of these channels, among them, protein kinase A, arachidonic acid, the *cis*-unsaturated C:18 oleic acid and the *trans*-unsaturated C:18 elaidic acid (Tewari *et al.*, 2000). In *Drosophila* photoreceptors, the polyunsaturated fatty acid (PUFA), linolenic acid C:18:3 (LNA), is thought to be produced by light activation of the enzymatic cascade that leads to activation of the light-dependent channels TRP and TRPL. Chyb *et al.*, (1999) have proposed that PUFA is the endogenous activator of these channels. We found that LNA also modulates a CIC-2-like channel present in *Drosophila* photoreceptors (see below).

Other members of the same family are CIC-K_a and CIC-K_b, present almost exclusively in kidney and in the inner ear, and CIC-3 to CIC-7, which are present in intracellular organelles (Jentsch *et al.*, 1999).

The analysis of CIC-0 and CIC-1 gating and permeation properties as a function of the permeating ion led to the conclusion that the two processes are coupled in these channels. To explain this phenomenon, the existence of two anionic binding sites in the pore, one closer to the internal solution modulating conduction selectivity and another closer to the external solution controlling gating selectivity, was proposed (Pusch *et al.*, 1995, Chen and Miller, 1996, Rychkov *et al.*, 1998). The recently obtained structure for two bacterial CIC channels shows that there are effectively two anions lining the conduction pore. On the inner site, there is a Cl⁻ ion specifically coordinated, and on the outer site there is a carboxylate anion given by the side chain of a glutamate residue (very well conserved across voltage-dependent Cl⁻ channels) that projects into the pore and “blocks” it. For Cl⁻ ions to permeate, they must induce a conformational change that displaces the glutamate side chain from the pore, a fact that could explain the coupling between conduction and gating (Dutzler *et al.*, 2002). Site-directed mutagenesis has provided support for this view (Dutzler *et al.*, 2003).

3. RESULTS

Patch-clamp single-channel recordings from inside-out plasma membrane patches and whole-cell currents from voltage-clamped *Drosophila* photoreceptors were obtained from wild-type flies and the double mutant *trp;trpl*. This mutant lacks the light-dependent channels TRP and TRPL.

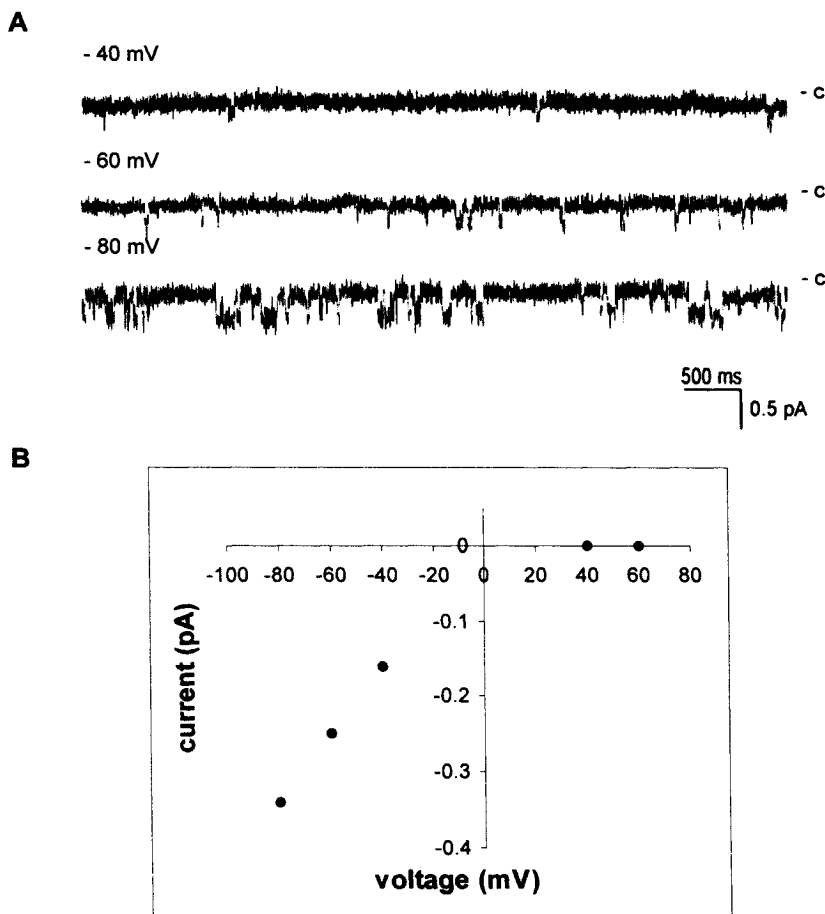


Figure 1. Unitary chloride currents in plasma membrane of *Drosophila* photoreceptors. **A.** Unitary currents recorded in an excised patch (inside-out) from plasma membrane of a *Drosophila* photoreceptor, in symmetrical NaCl-containing solutions. Membrane potentials and closed-state level of the channel (-c) are indicated. Single-channel events were observed when the membrane patch was hyperpolarized, but no outward transitions were recorded at depolarizing voltages. **B.** Current-voltage plot for unitary currents from the same patch. The slope conductance corresponds to 4.5 pS. The average single-channel conductance was 4.4 pS (average \pm 0.2 s.d., $n=4$).

Figure 1A shows single-channel currents recorded in symmetric NaCl from inside-out membrane patches of photoreceptors at various hyperpolarizing potentials. Figure 1B illustrates the current-voltage (I-V) curve for the transitions shown in A. No currents were seen at depolarizing potentials and the slope of the curve indicates a unitary conductance of 4.5 pS (4.4 ± 0.2 pS, average \pm s.d.; $n = 4$). When sodium was replaced by the impermeant cation N-methyl-D-glucamine in the bath, no changes were observed in the measured currents, indicating that this channel is anion selective.

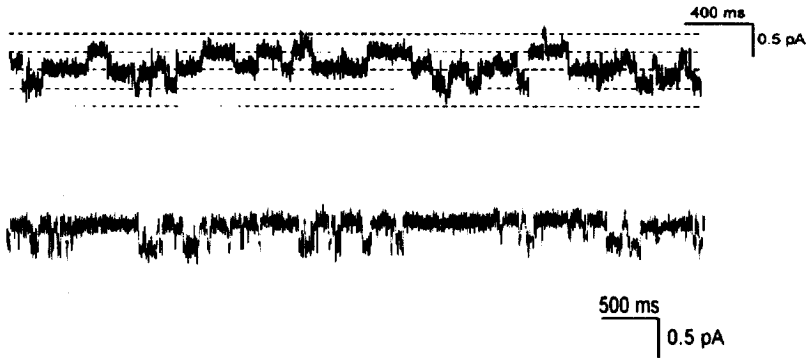


Figure 2. Unitary chloride currents observed in *Drosophila* retina resemble CIC-2 unitary currents. The upper trace corresponds to unitary recording of CIC-2~CIC-2 concatemers expressed in *Xenopus* oocytes. The patch containing two channels was recorded at -120 mV (Modified from Weinreich and Jentsch, 2001). The lower trace corresponds to single-channel chloride currents recorded in an inside-out patch from a photoreceptor plasma membrane. $V_m = -80$ mV. Unitary conductance corresponds to ~ 2.6 pS and ~ 4.4 pS, respectively.

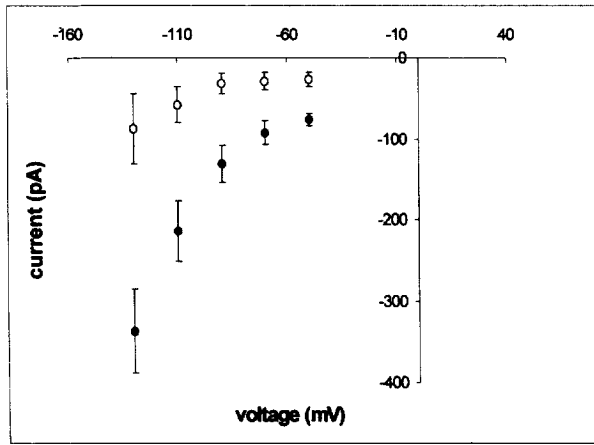


Figure 3. Hyperpolarization-activated chloride currents in *Drosophila* photoreceptors. Current-voltage (I-V) relations for whole-cell currents generated by hyperpolarizing voltages obtained in internal CsCl and corrected for remnant currents recorded in cesium aspartate. The graph includes amplitudes of currents obtained in 128 mM external Cl⁻ (open circles) and in 28 mM external Cl⁻ (closed circles). Data are average \pm s.d., $n = 5$.

Figure 2 compares the recordings of a CIC-2~CIC-2 concatemer expressed by Weinreich and Jentsch (2001) in *Xenopus* oocytes (upper trace) and the CIC-2-like channel from *Drosophila* photoreceptors (lower trace). The gating pattern and the single-channel conductance are similar in both cases.

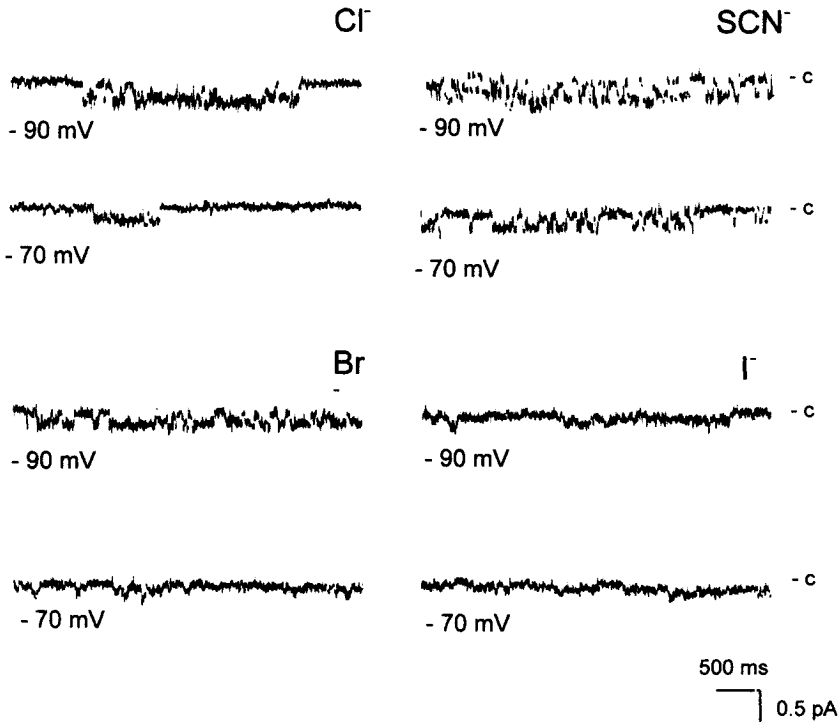


Figure 4. Gating properties of chloride channels present in *Drosophila*. Current traces were recorded from inside-out patches exhibiting channel activity obtained under symmetric and bi-ionic conditions, in which Cl^- was replaced by the indicated anion. Membrane potentials are indicated below traces

The chloride channel exhibited a pharmacological profile characteristic of Cl^- channels; Zn^{2+} and anthracene (9-AC) at 1 mM blocked the conductance reversibly, whereas the same concentration of DIDS did not affect channel activity.

We found that the hyperpolarization-activated currents in *Drosophila* photoreceptors are anion selective. Figure 3 shows I-V curves for whole-cell macroscopic currents activated by hyperpolarizing potential steps at 28 mM and 128 mM external Cl^- in voltage-clamped cells. Under these conditions there is a current through the K^+ conductance, due to incomplete blockade by cesium (Cs^+), that adds to the Cl^- current at voltages positive to -70 mV .

Because of this remnant current, it is not possible to determine a reversal potential by extrapolating the curve. However, it is clear that the current at very negative potentials increased significantly as the driving force for Cl^- increased. This suggests that the channel is selective for anions.

The hyperpolarization-activated macroscopic currents recorded in the *trp;trpl* mutant photoreceptors (lacking TRP and TRPL light-dependent channels), can be also activated by micromolar concentrations of linolenic acid (LNA) and blocked by 9-AC. LNA also induced a dose-dependent activation of the Cl^- channel recorded in excised patches. The

probability of the channel being open (P_o) increased 2.4 fold at 50 μ M LNA, the highest dose tested.

The relative anion permeability of the channel was determined from I-V curves of unitary currents obtained under bi-ionic conditions, with Cl^- as the reference ion. According to these results, the selectivity sequence corresponds to $\text{Cl}^- = \text{SCN}^- > \text{Br}^- \gg \text{I}^-$.

Figure 4 presents evidence for coupling between gating and ion permeation for hyperpolarization-activated chloride channels present in *Drosophila* photoreceptors. The Figure shows single-channel current traces obtained at -90 and -70 mV under symmetric conditions for Cl^- , and under bi-ionic conditions for SCN^- , Br^- or I^- . It is clear that the gating kinetics are different for these permeating anions.

Immunohistochemistry of whole *Drosophila* retinal slices probed with an anti-rat CIC-2 antibody, showed that reactive proteins are localized in the soma and in the synaptic terminal regions of the photoreceptors. In the soma, the immunoreactivity is mainly distributed in the plasma membrane and in a lower density in the rhabdomeres, the microvillar system that contains the light transduction machinery. This localization is consistent with a role for these channels in regulating the intracellular $[\text{Cl}^-]$, as has also been proposed for rod bipolar cells in the rat (Enz *et al.*, 1999).

5. ACKNOWLEDGMENTS

Supported by Fondecyt 2970006 and Mideplan ICM P99-031-F. Ceci dedicates this paper to Enrico and Ramón for “being there” and allowing her to celebrate with them, to “the Panchos” for organizing the details of the celebration.

6. REFERENCES

- Böls, M. R., Stein, V., Hübner, C., Zdebik, A. A., Jordt, S., Mukhopadhyay, A. K., Davidoff, M. S., Holstein, A., and Jentsch, T. J., 2002, Male germ cells and photoreceptors, both depend on close cell-cell interactions, degenerate upon CIC-2 channel disruption, *EMBO J.*, 20: 1289-1299.
- Chen, T. Y., and Miller, C., 1996, Nonequilibrium gating and voltage dependence of the CIC-0 Cl^- channel, *J. Gen. Physiol.*, 108: 237-250.
- Chyb, S., Raghu, P., and Hardie, R. C., 1999, Polyunsaturated fatty acids activate the *Drosophila* light-sensitive channels TRP and TRPL, *Nature*, 379: 255-259.
- Dutzler, R., Campbell, E. B., Cadene, M., Chait, B. T., and MacKinnon, R., 2002, X-ray structure of a CIC chloride channel at 3.0 Å reveals the molecular basis of anion selectivity, *Nature*, 415: 287-294.
- Dutzler, R., Campbell, E. B., & MacKinnon, R. (2003). Gating the selectivity filter in CIC chloride channels, *Science* 300: 108-112.
- Enz, R., Ross, B. J., and Cutting, G. R., 1999, Expression of the voltage-gated chloride channel CIC-2 in rod bipolar cells of the rat retina, *J. Neurosci.*, 19: 9841-9847.
- Gründer, S., Thiemann, A., Pusch, M., and Jentsch, T. J., 1992, Regions involved in the opening of CIC-2 chloride channel by voltage and cell volume, *Nature*, 360: 759-762.
- Jentsch, T. J., Steinmeyer, K., and Schwarz, G., 1990, Primary structure of *Torpedo marmorata* chloride channel isolated by expression cloning in *Xenopus* oocytes, *Nature*, 348: 519-514.
- Jentsch, T. J., and Günther, W., 1997, Chloride channels: an emerging molecular picture, *BioEssays*, 19: 117-126.
- Jentsch, T. J., Friedrich, T., Schriever, A., and Yamada, H., 1999, The CIC chloride channel family, *Pflügers Arch.*, 437: 783-795.
- Jordt, S. E., and Jentsch, T. J., 1997, Molecular dissection of gating in the CIC-2 chloride channel, *EMBO J.*, 16: 1582-1592.

- Miller, C., 1982, Open state substructure of single chloride channels from *Torpedo* electroplax, *Phil. Trans. R. Soc. Lond. B*, **299**: 401-411.
- Miller, C., and White, M. M., 1984, Dimeric structure of single chloride channels from *Torpedo* electroplax, *Proc. Natl. Acad. Sci. USA*, **81**: 2772-2775.
- Pusch, M., Ludewig, U., Rehfeldt, A., and Jentsch, T. J., 1995, Gating of the voltage-dependent chloride channel CIC-0 by the permeant anion, *Nature*, **373**: 527-531.
- Rychkov, G. Y., Pusch, M., Roberts, M. L., Jentsch, T. J., and Bretag, A. H., 1998, Permeation and block of the skeletal muscle chloride channel, CIC-1, by foreign anions, *J. Gen. Physiol.*, **111**: 653-665.
- Saviane, C., Conti, F., and Pusch, 1999, The muscular chloride channel CIC-1 has a double barreled appearance that is differentially affected in dominant and recessive myotonia, *J. Gen. Physiol.*, **113**: 457-467.
- Schwieber, E. M., Cid-Soto, L. P., Stafford, D., Carter, M., Blaisdell, C. J., Zeitlin, P. L., Guggino, W. B., and Cutting, G. R., 1998, Analysis of CIC-2 channels as an alternative pathway for chloride conduction in cystic fibrosis airway cells, *Proc. Natl. Acad. Sci. USA*, **95**: 3879-3884.
- Smith, R. L., Clayton, G. H., Wilcox, C. L., Escudero, K. W., and Staley, K. J., 1995, Differential expression of an inward rectifying chloride conductance in rat brain neurons: a potential mechanism for cell-specific modulation of postsynaptic inhibition, *J. Neurosci.*, **15**: 4057-4067.
- Staley, K., Smith, R., Schaack, J., Wilcox, C., and Jentsch, T. J. (1996). Alteration of GABA_A receptor function following gene transfer of the CIC-2 chloride channel. *Neuron* **17**: 543-551.
- Steinmeyer, K., Ortland, C., and Jentsch, T. J., 1991a, Primary structure and functional expression of a developmentally regulated chloride channel, *Nature*, **354**: 301-304.
- Steinmeyer, K., Kloche, R., Ortland, C., Gronemeier, M., Jockusch, H., Gründer, S., and Jentsch, T. J., 1991b, Inactivation of muscle chloride channel by transposon insertion in myotonic mice, *Nature*, **354**: 304-308.
- Tewari, K. P., Malinowska, D. H., Sherry, A. M., and Cuppoletti, J., 2000, PKA and arachidonic acid activation of human recombinant CIC-2 chloride channels, *Am. J. Physiol. Cell Physiol.*, **279**: C40-C50.
- Thiemann, A., Gründer, S., Pusch, M., and Jentsch, T. J., 1992, A chloride channel widely expressed in epithelial and non-epithelial cells, *Nature*, **356**: 57-60.
- Weinreich, F., and Jentsch, T. J., 2001, Pores formed by single subunits in mixed dimers of different CLC chloride channels, *J. Biol. Chem.*, **276**: 2347-2353.
- White, M. M., and Miller, C., 1979, A voltage-gated anion channel from the electric organ of *Torpedo californica*, *J. Biol. Chem.*, **254**:10161-10166.

EDITORS' NOTE

Since submission of this book to the press, two papers dealing with the crystal structure of a voltage dependent channel of a prokaryote have appeared which propose a novel configuration of the voltage sensor (Jiang et al., 2003, Nature vol. 423: 33-41 and 42-48). The generated model is quite different from the models proposed so far and has generated a large controversy as to how the voltage sensor operates. This controversy has not yet been resolved and it is important to keep in mind that much of the discussion of voltage sensing is still based on models such as those used in this volume.